

Manuscript Number:

Title: Numerical Studies on the Effect of Delta-Shaped Obstacles' Spacing on the Heat Transfer and Pressure Drop in V-Corrugated Channel of Solar Air Heater

Article Type: Regular Paper

Section/Category: Solar heating and cooling, buildings & other applications

Keywords: delta-shaped obstacle; v-corrugated channel; solar air heater; numerical study

Corresponding Author: Dr. Ekadewi Anggraini Handoyo, Dr

Corresponding Author's Institution: Petra Christian University

First Author: Ekadewi Anggraini Handoyo, Dr

Order of Authors: Ekadewi Anggraini Handoyo, Dr; Ichsani Djatmiko, Prof.; Prabowo Prabowo, Prof.; Sutardi Sutardi, Prof.

Abstract: Solar air heater (SAH) is simple in construction compared to solar water heater. Yet, it is very useful for drying or space heating. Unfortunately, the convective heat transfer between the absorber plate and the air inside the solar air heater is rather low. Some researchers reported that obstacles are able to enhance the heat transfer in a flat plate solar air collector and others found that a v-corrugated absorber plate gives better heat transfer than a flat plate. There was research combine these two in a SAH. Yet, the spacing between obstacles was not studied yet. Whereas, its spacing possibly will effect the heat transfer and pressure drop of the air flowing across the channel. The first step in numerical study is generating mesh or grid of the air flow inside a v-corrugated channel which was blocked by some delta-shaped obstacles. The mesh was designed three-dimension and not uniform. The mesh are made finer for area near obstacles and walls both for upper and bottom, and then gradually coarser. Grid independency is the next step to be conducted. When the mesh is already independent, the numerical study begins. To validate the numerical model, an indoor experiment was conducted. Turbulent model used was Shear Stress Transport $K-\omega$ (SSTK- ω) standard. Having a valid numerical model, the spacing between obstacles was studied numerically. Ratio spacing to height, S/H of obstacles investigated were 0.5; 1; 1.5; and 2. From numerical studies in a v-corrugated duct, it is found that backflow between obstacles and high velocity in the gap between obstacles and absorber plate causes the flow became more turbulent and enhanced the convection heat transfer between the air and the absorber plate. Obstacles placed in a small spacing increase air temperature difference and pressure drop. Air temperature difference and pressure drop increase from 15.81oC and 365.89 Pa, to 16.12oC and 408.90 Pa, to 16.53oC and 462.34 Pa, to 16.56oC and 544.12 Pa for ratio S/H decreases from 2 to 1 $\frac{1}{2}$ to 1, and to $\frac{1}{2}$, respectively. Efficiency of SAH and friction factor are

decreasing as ratio S/H is increasing. The best delta-shaped obstacles' spacing inserted in a v-corrugated duct is equal to its height or ratio $S/H = 1$. When ratio S/H used is 1 instead of 0.5, efficiency of SAH is decreasing 0.18% and friction factor is decreasing 15%. So, sacrificing a small amount of efficiency but reducing a significant friction factor is advantageous.

Suggested Reviewers: Ebru Kavak Akpınar

ebruakpinar@firat.edu.tr

He/she write the same topic with me, i.e. obstacles in Solar Air Heater.

Adisu Bekele

addisu2005@yahoo.com

He/she write the same topic with me, i.e. obstacles in Solar Air Heater.

Md Azharul Karim

makarim@mame.mu.oz.au

He/she write the same topic with me, i.e. v-corrugated air collector.

Numerical Studies on the Effect of Delta-Shaped Obstacles' Spacing on the Heat Transfer and Pressure Drop in V-Corrugated Channel of Solar Air Heater

The research was part of my previous doctoral study. This topic was chosen as an effort to enhance the heat transfer in a solar air heater (SAH) which is usually low. A numerical study was set up to investigate the effect of obstacles' spacing used in a v-corrugated SAH. An indoor model of a SAH was constructed for validation of the numerical study. After generating 3-D mesh or grid of the air flow inside a v-corrugated channel which was blocked by some delta-shaped obstacles, grid independency is the next step to be conducted. When the mesh is already independent, the numerical study begins. Having a valid numerical model, the spacing between obstacles was studied numerically. Ratio spacing to height, S/H of obstacles investigated were 0.5; 1; 1.5; and 2.

From numerical studies in a v-corrugated duct, it is found that backflow between obstacles and high velocity in the gap between obstacles and absorber plate causes the flow became more turbulent and enhanced the convection heat transfer between the air and the absorber plate. Efficiency of SAH and friction factor are decreasing as ratio S/H is increasing. The best delta-shaped obstacles' spacing inserted in a v-corrugated duct is equal to its height or ratio $S/H = 1$. When ratio S/H used is 1 instead of 0.5, efficiency of SAH is decreasing 0.18% and friction factor is decreasing 15%. So, sacrificing a small amount of efficiency but reducing a significant friction factor is advantageous.

The corresponding author is:
Ekadewi A. Handoyo.
Jl. Siwalankerto 121 – 131 Surabaya 60236, Indonesia
Tel.: 62-31-2983465; fax: 62-31-8491215.
E-mail address: ekadewi@petra.ac.id.

This research is certainly original and all of the data are obtained via the experiments done by the authors.

Highlights

This paper explains about how to improve a Solar air heater (SAH) performance. SAH is simple in construction compared to solar water heater. But, it is very useful for drying or space heating. Unfortunately, the convective heat transfer between the absorber plate and the air inside the solar air heater is rather low.

Improving heat transfer in SAH will improve its efficiency, too. Unfortunately, the pressure drop is usually also increasing. Some efforts, such as replacing the flat absorber plate with v-corrugated plate or inserting obstacles in the flow, are using widely. Yet, the spacing between obstacles was not studied yet. Whereas, its spacing possibly will effect the heat transfer and pressure drop of the air flowing across the channel.

This paper shows the velocity vector of the air flow around the obstacles in a v-corrugated channel. Further, it describes how the smaller ratio of spacing to obstacles' height, S/H , more heat is transfered to the air and higher pressure drop. In the end, the paper concludes that sacrificing a small amount of efficiency but reducing a significant friction factor is advantageous.

Numerical Studies on the Effect of Delta-Shaped Obstacles' Spacing on the Heat Transfer and Pressure Drop in V-Corrugated Channel of Solar Air Heater

Ekadewi A. Handoyo¹, Djatmiko Ichsani², Prabowo², Sutardi²

¹Mechanical Engineering Dept, Petra Christian University, Surabaya – Indonesia

²Mechanical Engineering Dept, Institut Teknologi Sepuluh Nopember, Surabaya – Indonesia

Corresponding author: ekadewi@petra.ac.id

Abstract

Solar air heater (SAH) is simple in construction compared to solar water heater. Yet, it is very useful for drying or space heating. Unfortunately, the convective heat transfer between the absorber plate and the air inside the solar air heater is rather low. Some researchers reported that obstacles are able to enhance the heat transfer in a flat plate solar air collector and others found that a v-corrugated absorber plate gives better heat transfer than a flat plate. There was research combine these two in a SAH. Yet, the spacing between obstacles was not studied yet. Whereas, its spacing possibly will effect the heat transfer and pressure drop of the air flowing across the channel.

The first step in numerical study is generating mesh or grid of the air flow inside a v-corrugated channel which was blocked by some delta-shaped obstacles. The mesh was designed three-dimension and not uniform. The mesh are made finer for area near obstacles and walls both for upper and bottom, and then gradually coarser. Grid independency is the next step to be conducted. When the mesh is already independent, the numerical study begins. To validate the numerical model, an indoor experiment was conducted. Turbulent model used was Shear Stress Transport K- ω (SSTK- ω) standard. Having a valid numerical model, the spacing between obstacles was studied numerically. Ratio spacing to height, S/H of obstacles investigated were 0.5; 1; 1.5; and 2.

From numerical studies in a v-corrugated duct, it is found that backflow between obstacles and high velocity in the gap between obstacles and absorber plate causes the flow became more turbulent and enhanced the convection heat transfer between the air and the absorber plate. Obstacles placed in a small spacing increase air temperature difference and pressure drop. Air temperature difference and pressure drop increase from 15.81°C and 365.89 Pa, to 16.12°C and 408.90 Pa, to 16.53°C and 462.34 Pa, to 16.56°C and 544.12 Pa for ratio S/H decreases from 2 to 1 ½ to 1, and to ½, respectively. Efficiency of SAH and friction factor are decreasing as ratio S/H is increasing. The best delta-shaped obstacles' spacing inserted in a v-corrugated duct is equal to its height or ratio S/H = 1. When ratio S/H used is 1 instead of 0.5, efficiency of SAH is decreasing 0.18% and friction factor is decreasing 15%. So, sacrificing a small amount of efficiency but reducing a significant friction factor is advantageous.

Keywords: delta-shaped obstacle; v-corrugated channel, solar air heater; numerical study.

1. Introduction

Solar energy can be converted into thermal energy in a solar collector. Solar collector basically is device used to trap solar energy to heat a plate and transfer the heat to a fluid flowing under or above the plate. When sun light falls onto a plate, solar radiation reaches the plate at lower wavelength and heat it up. Then, the heat is carried away by either water or air that flows under or above the plate. Solar collector used to

heat up air is called solar air heater (SAH) and solar water heater for water. Generally, the solar air heater is less efficient than the solar water heater, because air has less thermal capacity and less convection heat transfer coefficient. Yet, air is much lighter and less corrosive than water. The other benefit is that heated air can be used for moderate-temperature drying, such as harvested grains or fish. Since the solar air heater has less convective heat transfer coefficient than solar water heater, some researchers tried to increase this convective heat transfer coefficient.

A popular type of solar air heaters is the flat plate SAH, which has a cover glass on the top, insulation on the sides and bottom to prevent heat transferred to the surrounding, a flat absorber plate that makes a passage for the air flowing with sides and bottom plate. Usually, the passage or channel has a rectangular cross-section. The absorber plate will transfer the heat to the air via convection. Unfortunately, the convection coefficient is very low. To increase the convection coefficient from the absorber plate, a v-corrugated plate is used instead of a flat plate. Tao Liu et al. (Tao, Wen, Wen, & Chan, 2007) stated that a solar air heater with a v-grooved absorber plate could reach efficiency 18% higher than the flat plate on the same operation condition and dimension or configuration. Karim and Hawlader (Karim & Hawlader, 2006) found that a solar collector with a v-absorber plate gave the highest efficiency and the flat plate gave the least. The results showed that the v-corrugated collector is 10–15% and 5–11% more efficient in single pass and double pass modes, respectively, compared to the flat plate collectors. Choudhury and Garg (Choudhury & Garg, 1991) made a detailed analysis of corrugated and flat plate solar air heaters of five different configurations. For the same length, mass flow rate, and air velocity, it was found out that the corrugated and double cover glass collector gave the highest efficiency. According to Naphon (Naphon, 2007) the corrugated surfaces give a significant effect on the enhancement of heat transfer and pressure drop. The Nusselt number of flow in a v-corrugated channel can be 3.2 – 5.0 times higher than in a plane surfaces while the pressure drop 1.96 times higher than on the corresponding plane surface. Islamoglu and Parmaksizoglu (Islamoglu & Parmaksizoglu, 2003) reported that the corrugated channel gave the higher Nusselt number than the straight channel and the higher channel height gave higher Nusselt number for the flow with the same Reynolds number.

Besides changing the cross section area of the channel, some also give effort to increase turbulence inside the channel with fins or obstacles. The result of experimental study done by Promvonge (Promvonge, 2010) in turbulent flow regime (Reynolds number of 5000 to 25,000) showed that multiple 60° V-baffle turbulator fitted on a channel provides the drastic increase in Nusselt number, friction factor, and the thermal enhancement factor values over the smooth wall channel. Kurtbas and Turgut (Kurtbas & Turgut, 2006) investigated the effect of fins located on the absorber surface in free and fixed manners. They used two kinds of rectangular fins which dimension is different but total area is the same. The first type fin (I) has dimension 810 x 60 mm and the second (II) type 200 x 60 mm. To have the same total area, there are 8 fins and 32 fins for the first and second, respectively. The fins type II, both free and fixed, were more effective than type I and flat-plate collector. The fixed fin collector was more effective than free fin collector. Romdhane (Romdhane, 2007) created turbulence in the air channel using obstacles or baffles. The efficiency of collector and the air temperature was found increasing with the use of baffles. Baffles should be used to guide the flow toward the absorber plate. Ho et al. (Ho, Yeh, & Chen, 2011) inserted fins attached by baffles and external recycling to a solar air heater. The experiment and theoretical investigations gave result that heat transfer was improved by employing baffled double-pass with external recycling and fin attached over and under absorber plate. Abene et al. (Abene, Dubois, Le Ray, & Oagued, 2004) used obstacles on the flat plate of a solar air collector for drying grape. The obstacles ensure a good air flow over

the absorber plate, create the turbulence and reduce the dead zones in the collector. Esen (Esen, 2008) used a double-flow solar air heater to investigate three different type obstacles placed on absorber plates compare with the flat plate. The collector has three absorber plates to make three passages for the air flowing through. From the research done, it was found that type III obstacles with flow in middle passage gave the highest efficiency and all collectors with obstacles gave higher efficiency than the flat plate. Akpınar and Koçyiğit (Akpınar & Koçyiğit, 2010) had experimental investigation on solar air heater with several obstacles (Type I, Type II, and Type III) and without obstacles. The optimal value of efficiency was obtained for the solar air heater with Type II obstacles on absorber plate in flow channel duct for all operating conditions and the collector with obstacles appears significantly better than that without obstacles. Bekele et al. (Bekele, Mishra, & Dutta, 2011) investigated experimentally the effect of delta shaped obstacles mounted on the absorber surface of an air heater duct. They found that the obstacle mounted duct enhances the heat transfer to the air. The heat transfer got higher if the obstacle height was taller and its longitudinal pitch was smaller.

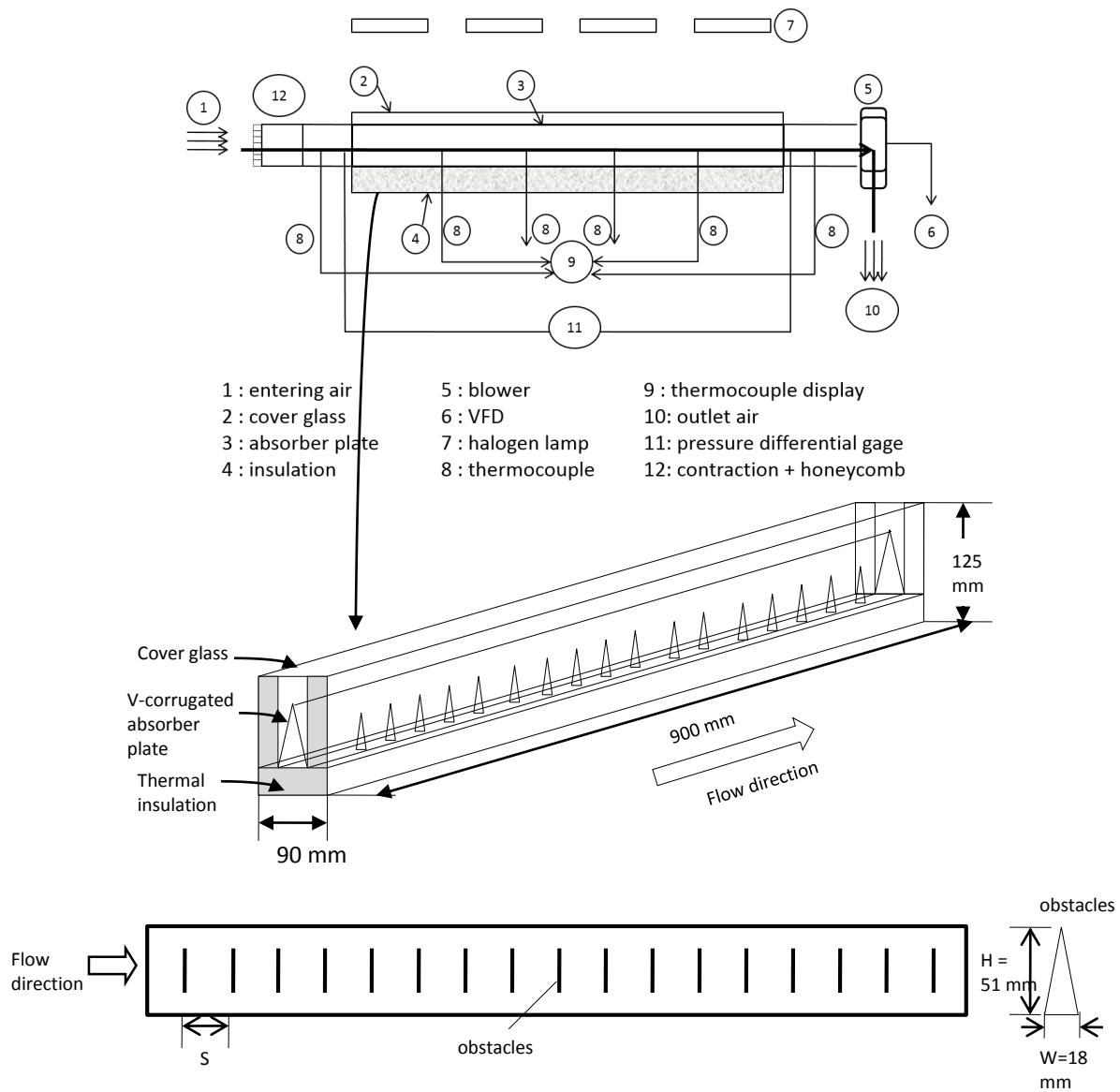
The combine of those two findings, i.e. obstacles and v-corrugated absorber plate are able to improve SAH are important to be studied. Handoyo et al. (Handoyo, Ichsan, Prabowo, & Sutardi, 2014) reported that the obstacles are able to enhance heat transfer in a v-corrugated SAH but increase the air pressure drop. To reduce the air pressure drop, the obstacles were bent vertically. The optimal bending angle is 30°. The SAH's efficiency was 5.3% lower when the obstacles bent 30° instead of straight (0°), but the pressure drop was 17.2% lower. The obstacles' spacing should also give contribution to the air pressure drop. When the spacing is large, the obstacles used is less and the air pressure drop will be reduced. What about the heat transfer? How will the spacing between obstacles effect the heat transfer from the absorber plate to the flowing air? Right now, there is no research investigating the effect of obstacles' spacing on a v-corrugated SAH performance.

This paper describes the result of the numerical studies of obstacles' spacing inserted in a v-corrugated channel of a SAH. The heat transfer from the v-corrugated absorber plate and the air pressure drop flowing the v-corrugated channel is to be discussed. The obstacles are delta-shaped and installed on bottom plate of the channel.

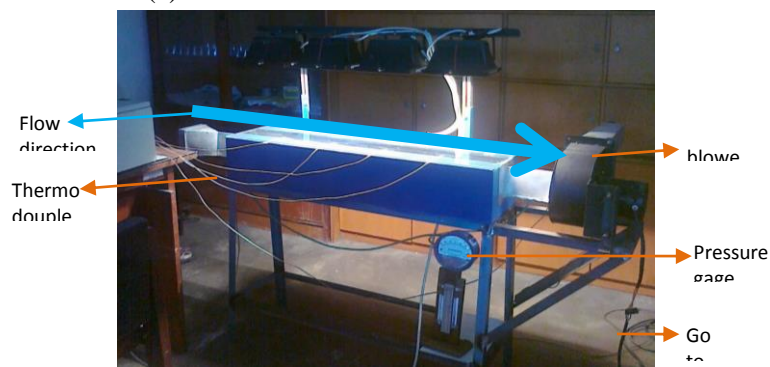
2. Experimental set-up

The studies began with choosing a solar collector model to be studied. The study will be conducted numerically. Thus, a validation is required to prove that the result is true. The validation is accomplished via experiment. An indoor experiment model was constructed to validate numerical result. It is a model of SAH using v-corrugated absorber plate. Its schematic view and photograph are shown in Fig. 1 (a) and (b), respectively. The experiment was conducted in a laboratory of Mechanical Engineering Dept of Petra Christian University, Surabaya, Indonesia.

The collector model's dimension was 900 mm long, 90 mm width, and 125 mm height. A single 3-mm transparent-tempered glass was used as the collector cover. The v-corrugated absorber plate was made of 0.8-mm-thick aluminum and painted black. The apex angle of the v-corrugated plate was 20°. The v-corrugated channel's cross section was 30 mm width and 85 mm height. To prevent heat loss, the left and right walls of collector are insulated with a 25-mm Styrofoam each and a 35-mm Styrofoam for the bottom. The delta-shaped obstacles were made congruent to the channel i.e. triangular and its dimension was 18 mm wide, 51 mm height.



(a) Schematic of the solar collector model



(b) Photograph of experimental set-up.

Fig 1. The SAH model used in experiment

The experiment was conducted indoor to maintain the radiation intensity, wind's velocity and temperature. So, a bias result caused by different outdoor condition could be avoided. The sunlight is replaced with four 500-Watt halogen lamps. The radiation intensity received on the collector was measured using a pyranometer (Kipp & Zonen, type SP Lite2) placed on top of the cover glass. To ensure the homogenous intensity and to generate a certain absorber plate's temperature, these lamps were equipped with adjustable turner individually. The surrounding air condition was controlled by an air conditioner installed in the room. Its temperature, humidity, and wind velocity are well controlled. The collector was equipped with T-type thermocouple which accuracy is 0.1°C for measuring the air temperature at inlet and outlet of the collector, temperature of the absorber plate (at four different locations), and ambient temperature. The pressure drop between inlet and outlet of the flowing air across the collector is also measured with a Magnehelic differential pressure gage which accuracy is ± 2 Pa. A centrifugal blower (1000 m³/h, 580 Pa, 0.2 kW, 380 Volt input) was used to induce the air flowing through the collector. The air flow was adjusted by means of a variable-frequency drive (VFD) to be 5.0 m/s (or Reynolds number = 10,000). The air flow is measured using digital anemometer which accuracy is ± 0.1 m/s. All of the measurement equipments such as pressure gages and thermocouples are installed according to ASHRAE requirement (ASHRAE, 1986).

3. Numerical set up

The discussion in this paper is on the heat transferred to the flowing air and its pressure drop, then the domain of numerical study is focused on the air flow inside the v-corrugated channel. The apex angle of the v-corrugated channel is 20°. Its dimension was 900 mm long, 30 mm width, and 85 mm height. The delta-shaped obstacles were made congruent to the channel i.e. triangular and its dimension was 18 mm wide, 51 mm height. The obstacles were installed in one line only, because there is no much space in the channel. Thus, the spacing to be discussed is actually longitudinal pitch. To specify the obstacles' spacing, a ratio of spacing to height S/H is used. In this study, the ratio S/H used were ½, 1, 1 ½, and 2.

The numerical model for this problem was developed under some assumptions, i.e. as steady three-dimensional turbulent, incompressible flow and constant fluid properties. The space of obstacles was taken equal to height of obstacles, thus ratio is 1. Then, there are 17 obstacles used in this flow. Body force and viscous dissipation are ignored and it was assumed no radiation heat transfer. With these assumptions, (Incropera & DeWitt, 2002) give the related governing equations as follow:

$$\frac{\partial u}{\partial x} + \frac{\partial v}{\partial y} + \frac{\partial w}{\partial z} = 0 \quad (1)$$

$$u \frac{\partial u}{\partial x} + v \frac{\partial u}{\partial y} + w \frac{\partial u}{\partial z} = -\frac{1}{\rho} \frac{\partial P}{\partial x} + \vartheta \left(\frac{\partial^2 u}{\partial x^2} + \frac{\partial^2 u}{\partial y^2} + \frac{\partial^2 u}{\partial z^2} \right) \quad (2)$$

$$u \frac{\partial v}{\partial x} + v \frac{\partial v}{\partial y} + w \frac{\partial v}{\partial z} = -\frac{1}{\rho} \frac{\partial P}{\partial y} + \vartheta \left(\frac{\partial^2 v}{\partial x^2} + \frac{\partial^2 v}{\partial y^2} + \frac{\partial^2 v}{\partial z^2} \right) \quad (3)$$

$$u \frac{\partial w}{\partial x} + v \frac{\partial w}{\partial y} + w \frac{\partial w}{\partial z} = -\frac{1}{\rho} \frac{\partial P}{\partial z} + \vartheta \left(\frac{\partial^2 w}{\partial x^2} + \frac{\partial^2 w}{\partial y^2} + \frac{\partial^2 w}{\partial z^2} \right) \quad (4)$$

$$u \frac{\partial T}{\partial x} + v \frac{\partial T}{\partial y} + w \frac{\partial T}{\partial z} = \alpha \left(\frac{\partial^2 T}{\partial x^2} + \frac{\partial^2 T}{\partial y^2} + \frac{\partial^2 T}{\partial z^2} \right) \quad (5)$$

In the above equations, ρ is the density of the air, p is the pressure, ϑ is the kinematic viscosity, α is the thermal diffusivity, and T is the temperature of the fluid. The boundary conditions of this problem were:

At the inlet: $u = 5.0$ m/s, $v = w = 0$, $T = 297.46$ K

At the upper wall which is the absorber plate: $u = v = w = 0$

At the bottom wall: $u = v = w = 0$

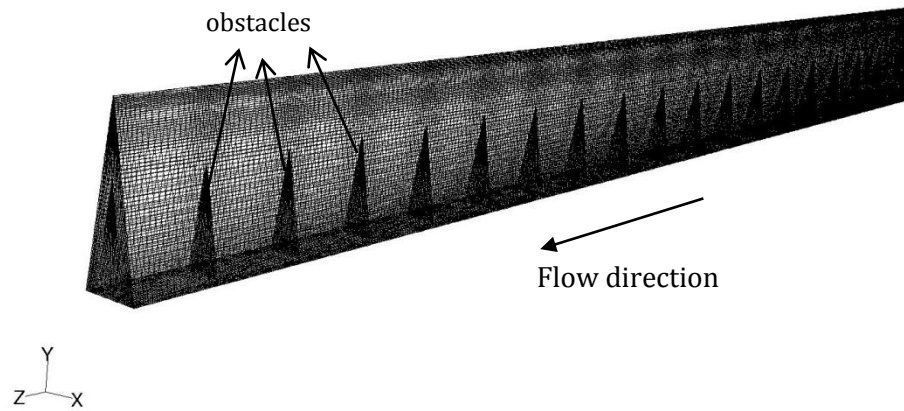
On the 17 obstacles: $u = v = w = 0$

Inlet Reynolds number was calculated with: $Re = \frac{uD_h}{\nu}$ (6)

In Eq. (6), D_h is hydraulic diameter and calculated with: $D_h = \frac{4A}{P}$ (7)

The area, A , in Eq. (7) is the channel cross section area, and P , is its perimeter.

The governing equations above with the boundary conditions were solved using a commercial CFD package, FLUENT 6.3.26 (FLUENT, 2003). The grids of the domain were generated using Gambit 2.4.6. The domain and meshing used in this numerical study were shown in Fig. 2. Since the geometry is a triangular channel, the numerical study should be conducted in three dimensions and all of the meshes were designed to have quality less than 0.7.

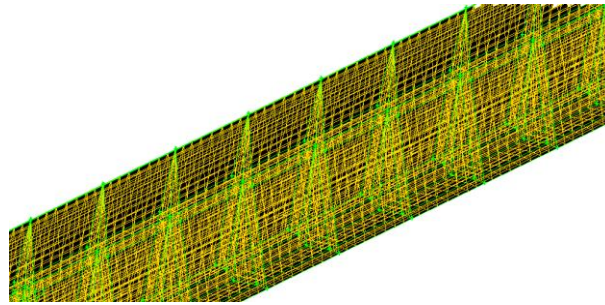


Grid

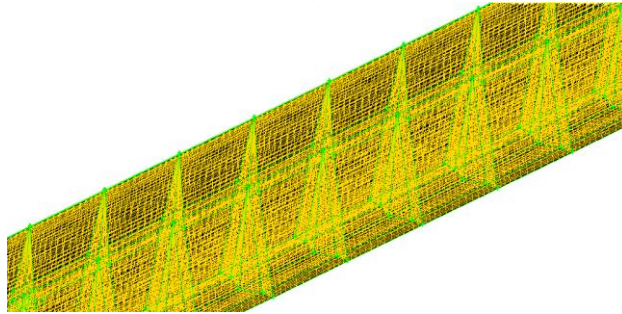
Feb 08, 2013
FLUENT 6.3 (3d, dp, pbns, ske)

Fig 2. The grid used in numerical studies

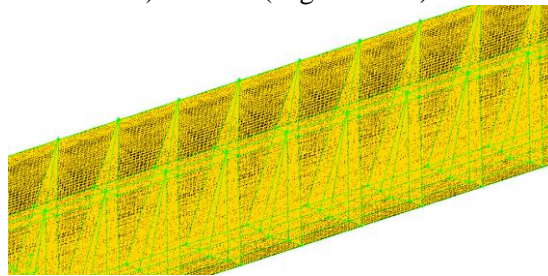
After having a good mesh, the next step is doing grid independency. The grid or mesh is made smaller to get more accurate and detailed result. But, when the mesh is too small, calculation which is done by iteration needs a very long time and might end up with diverge result. Therefore, in this study the mesh or grids were designed not uniform. The finer mesh are used for area near walls both for upper and bottom walls and then gradually the mesh are made coarser as shown in Fig 2. When there are obstacles in the flow, the mesh are designed to be finer not only near the walls but also around the obstacles in Fig 2. There are four meshes designs to be checked for independency as shown in Fig 3a), 3b), 3c), and 3d). The number of cells, faces, and nodes used in each design are shown in Table 1.



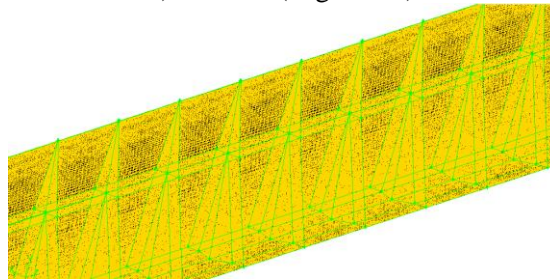
a) Mesh A (most coarse)



b) Mesh B (slight coarse)



c) Mesh C (slight fine)



d) Mesh D (most fine)

Fig 3. Mesh design checked for independency

Table 1. Number of cells, faces, and nodes of the four mesh design

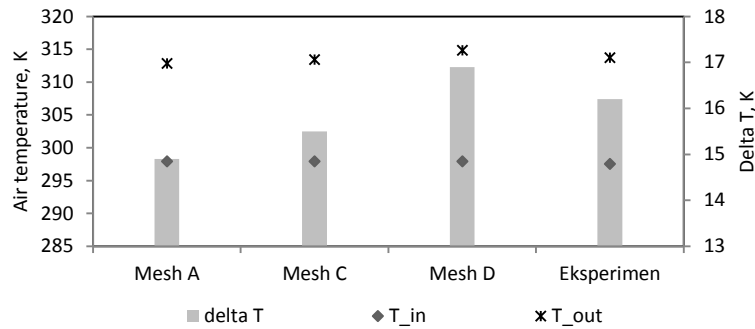
	Mesh A	Mesh B	Mesh C	Mesh D
cell	55,296	338,688	1,092,000	1,980,000
face	173,936	1,043,224	3,335,300	6,026,900
node	63,172	365,480	1,150,798	2,066,248

To check the grid independency, the result from numerical study will be compared to experiment result. The same boundary conditions and setting are used in each numerical study of the four grids design as in Fig 3. The boundary conditions are: inlet air velocity = 5.0 m/s, inlet air temperature = 297.46 K, and constant upper plate temperature. The settings in software used are: three dimension, double precision.

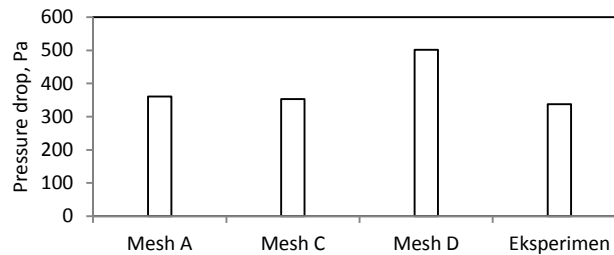
Shear Stress Transport K- ω (SSTK- ω) standard turbulent model was chosen to simulate the flow. The SIMPLEC algorithm was employed to deal with the problem of velocity and pressure coupling. Second-order upwind scheme were used to discretize the main governing equations. Velocity boundary condition was applied at the inlet section while outflow was employed for the outlet. The absorber plate was set to the value as obtained during experiments. Material of the absorber, bottom plate and the obstacles is aluminum. Fluid is air with inlet pressure 1 atm and its properties, such as density, viscosity, thermal conductivity are function of temperature.

Numerical studies were conducted for each of the four mesh: A, B, C, and D. Fig 4 shows global properties resulted from the numerical studies. They are the inlet and outlet temperature of air flowing through the channel and its pressure drop. Only Mesh B could not converge and the residual could not meet the criteria. So, there is no result of Mesh B in Fig 4.

The experiment result which will be discussed in Section 4 gives pressure drop as much as 265 Pa, air temperature outlet 40.5°C when the air inlet velocity is 5.0 m/s and inlet air temperature 24.3°C.



a. The air temperature from numerical studies compared to experiment



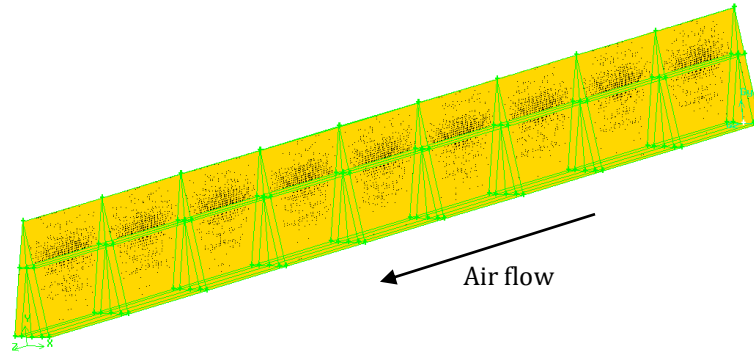
b. The pressure drop from numerical studies compared to experiment

Fig 4. The numerical studies of Mesh A, C, and D compared to the result of experiment

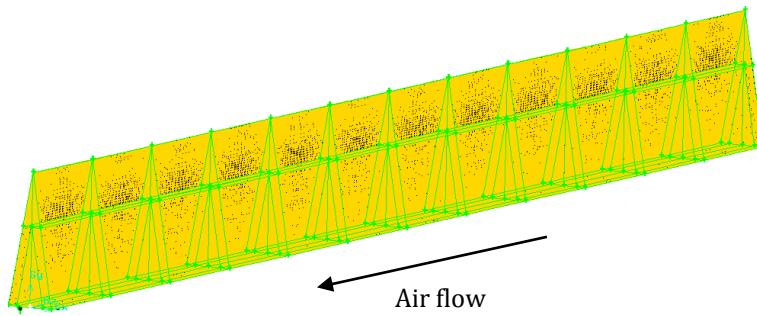
Fig. 4 shows that numerical study with Mesh C and D give better result of air temperature compare to experiment than Mesh A, but mesh D gives too high pressure drop result. Numerical studies using Mesh C give the most closely result to experiments. Thus, Mesh C was chosen for the numerical studies.

Using Mesh C pattern, some numerical studies were conducted to know the effect of obstacles' spacing. The ratio of spacing to height, S/H, studied numerically were 1/2, 1, 1 1/2, and 2. The Mesh used in this study

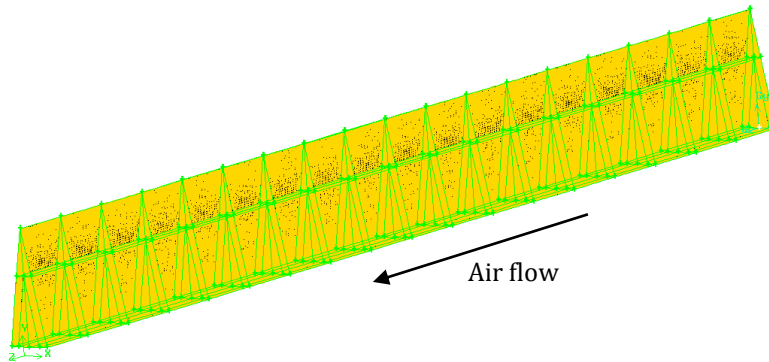
are in Fig. 5 a – 5 d. When the ratio S/H is bigger, then the number of obstacle is less. Number of obstacles are 8, 11, 17, and 35 for ratio S/H 2, $1\frac{1}{2}$, 1, and $\frac{1}{2}$, respectively.



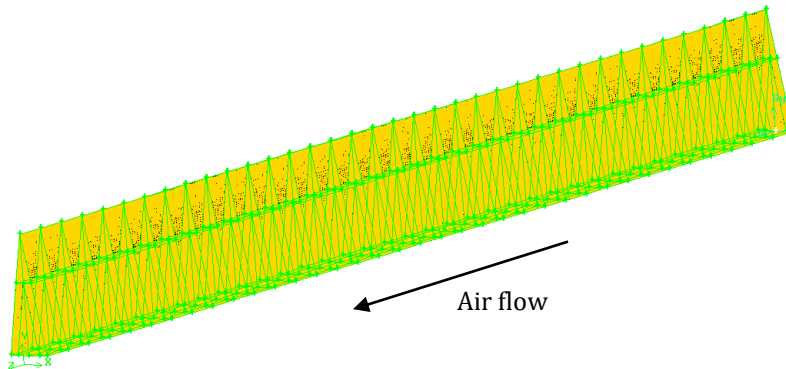
a. Ratio $S/H = 2$



b. Ratio $S/H = 1\frac{1}{2}$



c. Ratio $S/H = 1$



d. Ratio $S/H = \frac{1}{2}$

Fig. 5. The Mesh used for numerical studies of each spacing to height ratio, S/H

4. Results and discussion

Since the experiment is conducted to validate the numerical result, then it is not necessary to conduct experiments for all ratio S/H . The ratio S/H used in experiment equals to 1. Thus, there are 17 obstacles inserted and the percentage of air flow blockage in the channel was 36%. The experiment followed the numerical setting. The experiments were conducted at certain inlet air velocity and certain radiation intensity or absorber temperature. A VFD was used to get an inlet air velocity equals to 5.0 m/s. An adjustable turner was used to adjust the radiation intensity that make the absorber's temperature as high as 320 K or 47°C.

When the numerical result is close to the experimental result, then the numerical result is valid. Table 2 shows the comparison between numerical and experimental results at 5.0-m/s-inlet air velocity and 320 K absorber temperature. Temperature difference of numeric is very close to experiment, while pressure drop is higher about 16% than experiment. Thus, the numerical study using several setting discussed above is acceptable and valid.

Table 2. Comparison between numerical and experimental results

	Numeric	experiment
$T_{in}, ^\circ\text{C}$	297.9	297.5
$T_{out}, ^\circ\text{C}$	314.4	313.7
$\Delta T, ^\circ\text{C}$	16.5	16.2
$\Delta P, \text{Pa}$	462.3	397.7

Having a valid grids, setting, and viscous model, the numerical study was continued to investigate the spacing effect of obstacles on the bottom plate of air duct. Diagrams of velocity vector of air flow around the obstacles inserted at ratio S/H equals to 2, $1\frac{1}{2}$, 1, and $\frac{1}{2}$ are shown in Figure 6 a), 6 b), 6 c) and 6 d), respectively. All of the velocity vectors were taken at height $y = 10 \text{ mm}$ from the bottom plate. When the ratio $S/H = 2$, the spacing between obstacles = 100 mm. For ratio $S/H = 1\frac{1}{2}$, the spacing = 75 mm, and for ratio $S/H = \frac{1}{2}$, the spacing = 25 mm.

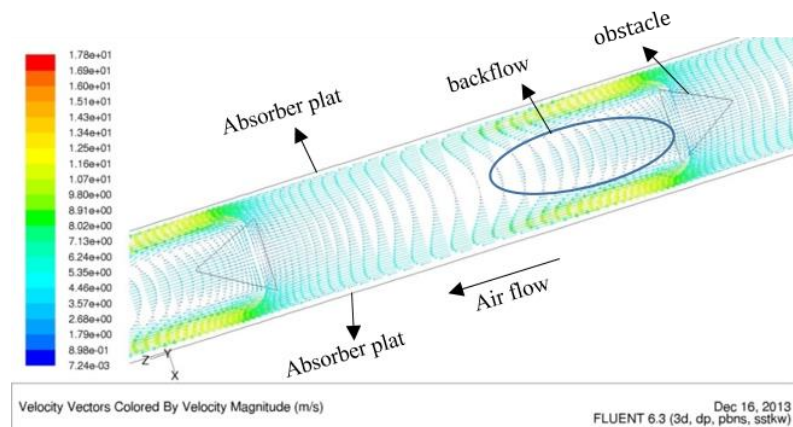


Figure 6 a) Velocity vector of air flow around *obstacle* with ratio $S/H = 2$

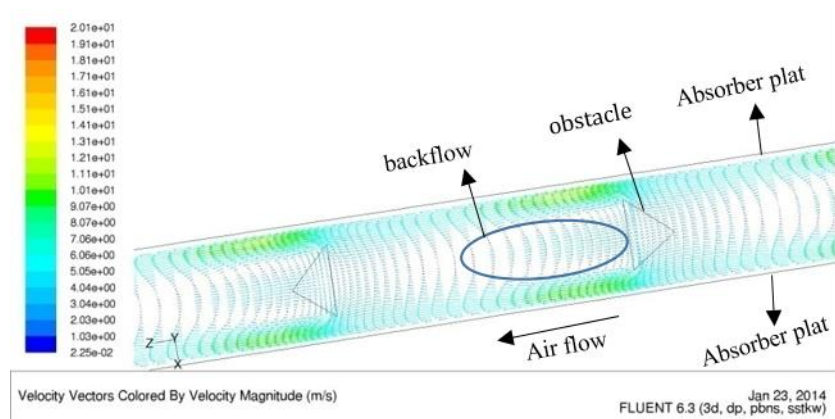


Figure 6 b) Velocity vector of air flow around *obstacle* with ratio $S/H = 1 \frac{1}{2}$

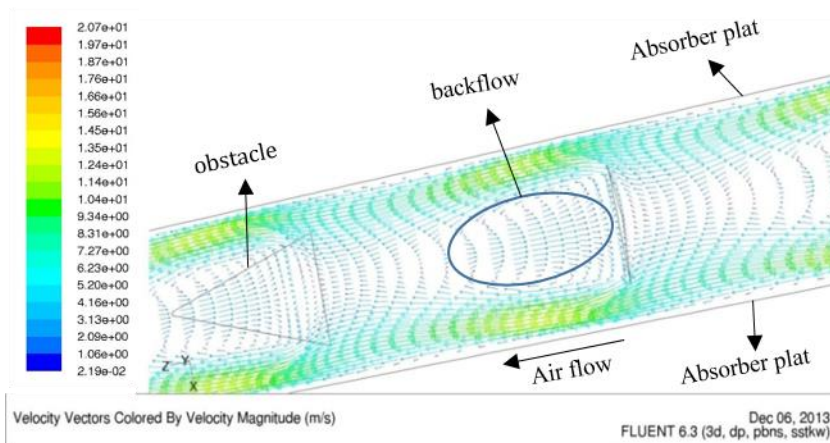


Figure 6 c) Velocity vector of air flow around *obstacle* with ratio $S/H = 1$

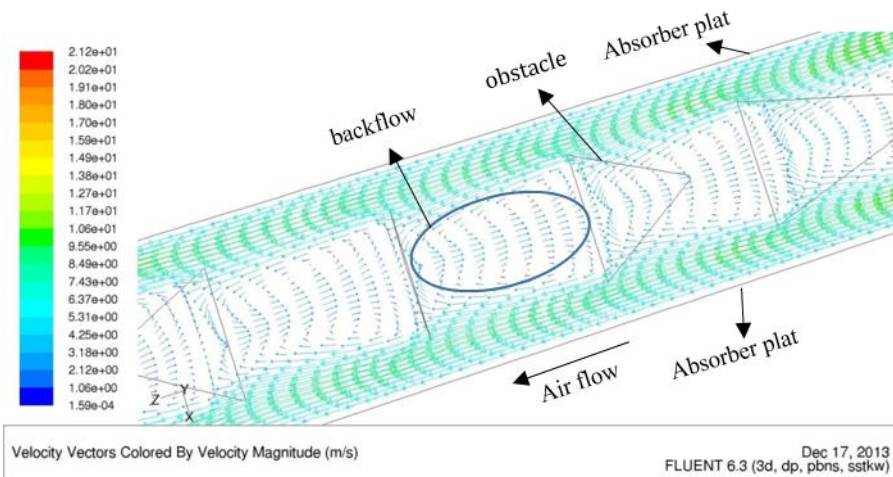


Figure 6 d) Velocity vector of air flow around *obstacle* with ratio $S/H = \frac{1}{2}$

Figure 6 a) – 6 d) show how the air flow encounters separation when flow through obstacles. The obstacles cause backflow between two consecutive obstacles in downstream. There are more backflows when the obstacles' spacing are closer and they cause a higher pressure drop. The air velocity looks higher near

absorber plate when there is backflow or swirl in the flow. This high air velocity makes flow become more turbulent and more heat transferred from the absorber plate to the air. This convection heat transfer to the air makes outlet air temperature higher. Thus, the closer the obstacles' spacing makes the higher pressure drop and higher convection heat transfer from the absorber plate to the air flow.

When the spacing between obstacles is twice its height (ratio $S/H = 2$), air flow is blocked by obstacles and causes backflow behind the obstacles. The backflow caused by separation gradually diminish between two obstacles in downstream as shown in Fig 6 a). Since the air is blocked, most of air is forced to flow in the gap between obstacles and absorber plate. It is shown by longer and higher vector of velocity in the gap. More air is heated by absorber plate. Furthermore, higher velocity increases Reynold number and make the flow more turbulent. More turbulent flow gives higher Nusselt number and definitely increase the convection heat transfer. Thus, obstacles makes outlet air temperature higher than without any (Handoyo, Ichsani, Prabowo, & Sutardi, 2014). Flow in spacing between obstacles experiences backflow after hitting obstacles and then it reattaches quickly when the ratio $S/H = 2$. When the ratio S/H or spacing between obstacles is smaller, as shown in Fig 6 b) – 6 d), backflow is more dominant than reattached flow in area between the obstacles. When backflow occurs, more air will flow in the gap and contact with absorber plate which is the heat source. It is the reason that smaller obstacles' spacing makes higher air outlet temperature and higher SAH's efficiency. The backflow in space between obstacles contributes pressure drop in the flow. More backflow causes higher pressure drop in air acrossed the v-corrugated absorber plate SAH.

Numerical studies also provide some global properties of the flow, such as the air inlet and outlet temperature, and pressure drop. Air temperature difference is calculated from the change between outlet and inlet air temperature. Comparison of air temperature difference and pressure drop for some ratio S/H from numerical studies is shown in Fig 7. From the air temperature difference and pressure drop data, the following parameters, i.e. SAH's efficiency and friction factor of the air flow in v-corrugated duct with delta-shaped obstacles, are calculated. The efficiency and friction factor are calculated using Equation (8) and (9) according to Duffie & Beckman (1991) and presented in Fig. 8 for three ratio S/H studied.

$$\eta = \frac{q_u}{A_c I} = \frac{\dot{m}_f c_p (T_{fo} - T_{fi})}{A_c I} \quad (8)$$

$$f = \frac{\Delta P}{\frac{L}{D_h} \rho \frac{v^2}{2}} \quad (9)$$

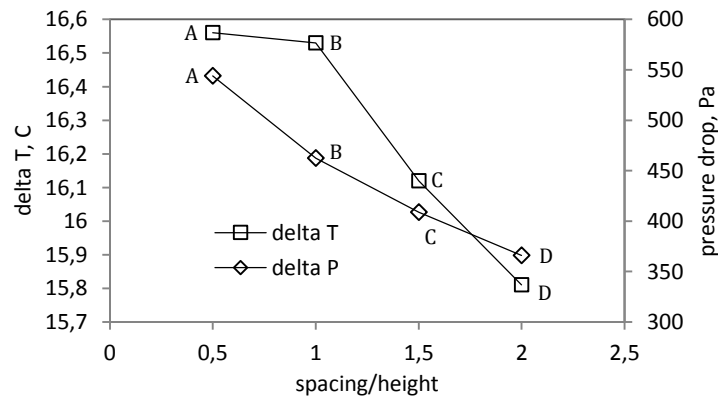


Figure 7. The air temperature difference and pressure drop from numerical studies

Obstacles arranged with ratio $S/H = \frac{1}{2}$ gives the highest air temperature difference and also highest pressure drop for air flowing in a v-corrugated duct, as shown in Fig. 7. This findings are matching with the flow structure discussed above. The obstacles block the air flow and force it to have more contact with absorber plate. Not only forcing the air to the absorber plate, obstacles also causing more backflow. More obstacles produce higher air outlet temperature and higher pressure drop. SAH requires high temperature difference, but low pressure drop. In Fig. 7, considering the temperature difference aspect, point A is the best, but from pressure drop, point D is the best. The gradient of pressure drop in a segment A-B is the steepest among other segments. While the gradient of temperature difference in that segment A-B is the least. Temperature difference in point B (16.53 °C) is slightly less than point A (16.56°C), but pressure drop in point B (462.34 Pa) is much less than point A (544.12 Pa). Sacrifice a little temperature difference but save a lot pressure drop shall be a wise choice.

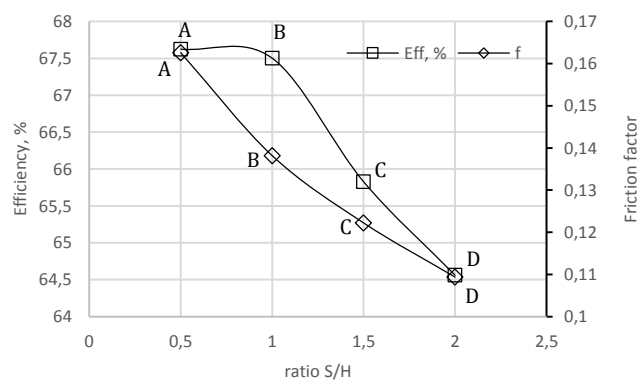


Figure 8. Efficiency of SAH and friction factor of flow with some ratio S/H of obstacles

The thermal efficiency and friction factor are two non-dimensional parameters. Thus, they can be applied to other SAH that has the same geometry and configuration, i.e. corrugated absorber plate and congruent obstacles inserted on bottom plate. Fig. 8 shows those parameters for some ratio S/H studied.

Efficiency of SAH and friction factor are decreasing as ratio S/H is increasing. Gradient of segment A-B of efficiency line is very low compare to other segments. It is rather flat and then getting steepest in segment B-C and CD. When ratio S/H used is 1 instead of 0.5, efficiency of SAH is decreasing 0.18% (from 67.62% to 67.50%) and friction factor is decreasing 15% (from 0.163 to 0.138). So, sacrificing a small amount of efficiency but reducing a significant friction factor is advantageous.

5. Conclusion

From numerical studies in a v-corrugated duct, it is found that backflow between obstacles and high velocity in the gap between obstacles and absorber plate causes the flow became more turbulent and enhanced the convection heat transfer between the air and the absorber plate. Thus, when it is applied in SAH, it will bring improve its efficiency.

Obstacles placed in a small spacing increase air temperature difference and pressure drop. Air temperature difference and pressure drop increase from 15.81°C and 365.89 Pa, to 16.12°C and 408.90 Pa, to 16.53°C and 462.34 Pa, to 16.56°C and 544.12 Pa for ratio S/H decreases from 2 to 1 ½ to 1, and to ½, respectively.

Efficiency of SAH and friction factor are decreasing as ratio S/H is increasing. The best delta-shaped obstacles' spacing inserted in a v-corrugated duct is equal to its height or ratio S/H = 1. When ratio S/H used is 1 instead of 0.5, efficiency of SAH is decreasing 0.18% and friction factor is decreasing 15%. So, sacrificing a small amount of efficiency but reducing a significant friction factor is advantageous.

Acknowledgement

Here, I am very grateful for the support from Kopertis Wilayah VII Jawa Timur, Kementerian Pendidikan dan Kebudayaan by providing Research Grant under contract no: 0004/SP2H/PP/K7/KL/II/2012.

Nomenclature

W	wide of the obstacle (mm)
H	height of the obstacle (mm)
S	spacing between the obstacles (mm)
x, y, z	coordinates
Re	Reynolds number
C_p	specific heat of air (J/kg.K)
\dot{m}_f	mass flow rate of the fluid – air (kg/s)
\dot{Q}_u	useful heat transfer rate (Watt)
I	radiation intensity (W/m ²)
A_c	collector aperture area (m ²)
T_o	collector outlet temperature (K)
T_i	collector air inlet temperature (K)
ϑ	air kinematic viscosity (m ² /s)
ρ	air density (kg/m ³)
α	air thermal diffusion coefficient (m ² /s)
η	efficiency of collector

References

- Abene, A., Dubois, V., Le Ray, M., & Oagued, A. (2004). Study of a solar air flat plate collector: use of obstacle and application for the drying of grape. *J. of Food Engineering*, 65, 15 – 22.
- Akpınar, E. K., & Koçyiğit, F. (2010). Experimental investigation of thermal performance of solar air heater having different obstacles on absorber plates. *Int. Com. in Heat and Mass Transfer*, 37, 416–421.
- ASHRAE. (1986). *Method of Testing to Determine the Thermal Performance of Solar Collectors*. Atlanta: ASHRAE.
- Bekele, A., Mishra, M., & Dutta, S. (2011). Effects of Delta-Shaped Obstacles on the Thermal Performance of Solar Air Heater. *Hindawi Publishing Corporation: Advances in Mechanical Engineering*, 2011, 10 pages.

- Choudhury, C., & Garg, H. P. (1991). Design Analysis of Corrugated and Flat Plate Solar Air Heaters. *Renewable Energy Vol I, No. 5/6*, p. 595 – 607.
- Duffie, J. A., & Beckman, W. A. (1991). *Solar Engineering Of Thermal Processes* (2nd ed. ed.). John Wiley & Sons, Inc.
- Esen, H. (2008). Experimental energy and exergy analysis of a double-flow solar air heater having different obstacles on absorber plates. *Building and Environment*, *43*, 1046–1054.
- FLUENT, I. (2003). *FLUENT User's Guide*.
- Handoyo, E. A., Ichsani, D., Prabowo, & Sutardi. (2014). Experimental Studies on a Solar Air Heater Having V-Corrugated. *Applied Mechanics and Materials*, *493*, 86-92.
- Ho, C.-D., Yeh, H.-M., & Chen, T.-C. (2011). Collector efficiency of upward-type double-pass solar air heaters with fins attached. *Int. Com. in Heat and Mass Transfer*, *38*, 49–56.
- Incropera, F. P., & DeWitt, D. P. (2002). *Fundamentals of Heat and Mass Transfer. 5th edition ed. s.l.:* John Wiley & Sons.
- Islamoglu, Y., & Parmaksizoglu, C. (2003). The effect of channel height on the enhanced heat transfer characteristics in a corrugated heat exchanger channel. *Applied Thermal Engineering* *23*, 979–987.
- Karim, M., & Hawlader, M. (2006). Performance Investigation of Flat Plate, V-Corrugated and Finned Air Collector. *Energy* *31*, 452-470.
- Kurtbas, I., & Turgut, E. (2006). Experimental Investigation of Solar Air Heater with Free and Fixed Fins: Efficiency and Exergy Loss. *Int. J. of Science & Technology, Volume 1*(No 1), 75-82.
- Naphon, P. (2007). Heat transfer characteristics and pressure drop in channel with V corrugated upper and lower plates. *Energy conversion and management* *48*, 1516 – 1524.
- Promvonge, P. (2010). Heat transfer and pressure drop in a channel with multiple 60° V-baffles. *Int. Com. in Heat and Mass Transfer*, *37*, 835–840.
- Romdhane, B. S. (2007). The air solar collectors: Comparative study, introduction of baffles to favor the heat transfer. *Solar Energy*, *81*, 139 – 149.
- Tao, L., Wen, X. L., Wen, F. G., & Chan, X. L. (2007). A Parametric study on the thermal performance of a solar air collector with a V-groove absorber. *Int. J. of Green Energy*, *4*, 601–622.

Your PDF has been built and requires approval

1 message

Solar Energy <se@elsevier.com>

Fri, Oct 9, 2015 at 5:18 PM

To: ekadewi@petra.ac.id, ekadewi@peter.petra.ac.id

Solar Energy

Title: Numerical Studies on the Effect of Delta-Shaped Obstacles' Spacing on the Heat Transfer and Pressure Drop in V-Corrugated Channel of Solar Air Heater
Authors: Ekadewi Anggraini Handoyo, Dr; Ichsani Djatmiko, Prof.; Prabowo Prabowo, Prof.; Sutardi Sutardi, Prof.

Dear Dr. Ekadewi Anggraini Handoyo,

The PDF for your submission, "Numerical Studies on the Effect of Delta-Shaped Obstacles' Spacing on the Heat Transfer and Pressure Drop in V-Corrugated Channel of Solar Air Heater" has now been built and is ready for your approval. Please view the submission before approving it, to be certain that it is free of any errors. If you have already approved the PDF of your submission, this e-mail can be ignored.

To approve the PDF please login to the Elsevier Editorial System as an Author:

<http://ees.elsevier.com/se/>Your username is: ekadewi@petra.ac.id

Then click on the folder 'Submissions Waiting for Author's Approval' to view and approve the PDF of your submission. You may need to click on 'Action Links' to expand your Action Links menu.

You will also need to confirm that you have read and agree with the Elsevier Ethics in Publishing statement before the submission process can be completed. Once all of the above steps are done, you will receive an e-mail confirming receipt of your submission from the Editorial Office. For further information or if you have trouble completing these steps please go to: http://help.elsevier.com/app/answers/detail/a_id/88/p/7923.

Please note that you are required to ensure everything appears appropriately in PDF and no change can be made after approving a submission. If you have any trouble with the generated PDF or completing these steps please go to: http://help.elsevier.com/app/answers/detail/a_id/88/p/7923.

Your submission will be given a reference number once an Editor has been assigned to handle it.

Thank you for your time and patience.

Kind regards,
Editorial Office
Solar Energy

For further assistance, please visit our customer support site at <http://help.elsevier.com/app/answers/list/p/7923>. Here you can search for solutions on a range of topics, find answers to frequently asked questions and learn more about EES via interactive tutorials. You will also find our 24/7 support contact details should you need any further assistance from one of our customer support representatives.



Submission Confirmation

1 message

Solar Energy <se@elsevier.com>

Sun, Oct 11, 2015 at 11:32 PM

To: ekadewi@petra.ac.id, ekadewi@peter.petra.ac.id

Dear Dr. Ekadewi Handoyo,

Your submission entitled "Numerical Studies on the Effect of Delta-Shaped Obstacles' Spacing on the Heat Transfer and Pressure Drop in V-Corrugated Channel of Solar Air Heater" has been received by Solar Energy
Regular Paper

You may check on the progress of your paper by logging on to the Elsevier Editorial System as an author. The URL is <http://ees.elsevier.com/se/>.

Your username is: ekadewi@petra.ac.id

If you can't remember your password please click the "Send Password" link on the Login page.

Your manuscript will be given a reference number once an Editor has been assigned.

Thank you for submitting your work to this journal.

Kind regards,

Elsevier Editorial System
Solar Energy

A manuscript number has been assigned: SE-D-15-01490

1 message

Solar Energy <se@elsevier.com>

Mon, Oct 12, 2015 at 12:09 PM

To: ekadewi@petra.ac.id, ekadewi@peter.petra.ac.id

Ms. Ref. No.: SE-D-15-01490

Title: Numerical Studies on the Effect of Delta-Shaped Obstacles' Spacing on the Heat Transfer and Pressure Drop in V-Corrugated Channel of Solar Air Heater
Solar Energy

Dear Dr. Ekadewi Handoyo,

Your submission entitled "Numerical Studies on the Effect of Delta-Shaped Obstacles' Spacing on the Heat Transfer and Pressure Drop in V-Corrugated Channel of Solar Air Heater" has been assigned the following manuscript number: SE-D-15-01490.

You may check on the progress of your paper by logging on to the Elsevier Editorial System as an author. The URL is <http://ees.elsevier.com/se/>.Your username is: ekadewi@petra.ac.idIf you need to retrieve password details, please go to: http://ees.elsevier.com/se/automail_query.asp

Thank you for submitting your work to this journal.

Kind regards,

Solar Energy



Editor handles SE-D-15-01490

1 message

Solar Energy <se@elsevier.com>

Mon, Oct 12, 2015 at 12:09 PM

To: ekadewi@petra.ac.id, ekadewi@peter.petra.ac.id

Ms. Ref. No.: SE-D-15-01490

Title: Numerical Studies on the Effect of Delta-Shaped Obstacles' Spacing on the Heat Transfer and Pressure Drop in V-Corrugated Channel of Solar Air Heater
Solar Energy

Dear Dr. Ekadewi Handoyo,

Your submission entitled "Numerical Studies on the Effect of Delta-Shaped Obstacles' Spacing on the Heat Transfer and Pressure Drop in V-Corrugated Channel of Solar Air Heater" will be handled by Subject Editor Yanjun DAI.

You may check on the progress of your paper by logging on to the Elsevier Editorial System as an author. The URL is <http://ees.elsevier.com/se/>.

Your username is: ekadewi@petra.ac.id

If you need to retrieve password details, please go to: http://ees.elsevier.com/se/automail_query.asp

Thank you for submitting your work to this journal.

Kind regards,

Solar Energy

Your Submission

1 message

Solar Energy <se@elsevier.com>

Wed, Nov 25, 2015 at 12:22 AM

To: ekadewi@petra.ac.id, ekadewi@peter.petra.ac.id

Cc: bbibek@nic.in, bbibek12@gmail.com, yjdai@hotmail.com

Ms. Ref. No.: SE-D-15-01490

Title: Numerical Studies on the Effect of Delta-Shaped Obstacles' Spacing on the Heat Transfer and Pressure Drop in V-Corrugated Channel of Solar Air Heater
Solar Energy

Dear Dr. Ekadewi Handoyo,

The reviews of your paper are now complete and the overriding opinion of the reviewers is that the paper is not publishable in its present form. Substantial revisions are required and further review is necessary. The reviewers' comments are attached.

Please try to prepare a substantially revised manuscript within the next month (30 days), responsive to the reviewers' comments and criticisms. We will not reject your paper should you take longer than two months to revise, however, we strongly urge you to try to meet that time-frame. Taking longer than two months tends to age the data.

Please be sure to create a master list of revisions/rebuttals, responding to each point raised by the reviewers. If you feel that the reviewers' comment does not warrant a revision, please prepare a reasoned rebuttal to their comment. In this case, please also review your text as it is usually the case that a few small changes or brief additions will prevent other readers from reaching the same 'erroneous' conclusion.

Upon receipt of a suitably revised new paper, I will send it off to the reviewers for their further consideration.

To submit a revision, please go to <http://ees.elsevier.com/se/> and login as an Author.

Your username is: ekadewi@petra.ac.id

If you need to retrieve password details, please go to: http://ees.elsevier.com/se/automail_query.asp

On your Main Menu page is a folder entitled "Submissions Needing Revision". You will find your submission record there.

Please note that this journal offers a new, free service called AudioSlides: brief, webcast-style presentations that are shown next to published articles on ScienceDirect (see also <http://www.elsevier.com/audioslides>). If your paper is accepted for publication, you will automatically receive an invitation to create an AudioSlides presentation.

Solar Energy features the Interactive Plot Viewer, see: <http://www.elsevier.com/interactiveplots>. Interactive Plots provide easy access to the data behind plots. To include one with your article, please prepare a .csv file with your plot data and test it online at <http://authortools.elsevier.com/interactiveplots/verification> before submission as supplementary material.

Thank you for your interest in Solar Energy.

Yours sincerely,

Bibek Bandyopadhyay, PhD
Associate Editor
Solar Energy

Note: While submitting the revised manuscript, please double check the author names provided in the submission so that authorship related changes are made in the revision stage. If your manuscript is accepted, any authorship change will involve approval from co-authors and respective editor handling the submission and this may cause a significant delay in publishing your manuscript.

Reviewers' comments:

Reviewer #1: 1) The objective, methodology, and results should be better described, discussed and justified.

2) The current literature review is not sufficient. For example, please mention (give) following more current studies related to solar air heaters in the sections of Introduction, and References List for completeness of your study and the references:

- Experimental investigation of thermal performance of a double-flow solar air heater having aluminium cans, Renewable Energy, 34(11), 2391-2398 (2009).
- Modelling of a new solar air heater through least-squares support vector machines, Expert Systems with Applications, 36(7), 10673-10682 (2009).
- Artificial neural network and wavelet neural network approaches for modelling of a solar air heater, Expert Systems with Applications, 36(8), 11240-11248 (2009).

3) The results should be expanded significantly and quantitatively.

4) I strongly suggest that authors shall carry out more studies to compare the results from this paper to that from other similar studies.

Reviewer #2: A few minor revisions are suggested to improve the paper. The comments specified below should be addressed to enhance the readability and archival value of the paper:

- The motivation and objective of the study should be more better justified.
- The findings should be enlarged substantially.

- Please compare your findings with results obtained from other works.

Reviewer #3: In this study, v-corrugated absorber with obstacles are investigated, which is interesting. However, following revisions need to be addressed:

1. Highlights should be less than 85 letters including space.
2. Abstract should be more concise.
3. This paper should also investigate the effects of using v-corrugated duct with obstacles on "heat transfer enhancement" compared to conventional duct with/without obstacles and v-corrugated duct without obstacles
4. This paper should also investigate the effects of using v-corrugated duct with obstacles on "pressure drop" compared to conventional duct with/without obstacles and v-corrugated duct without obstacles.
5. The author should give a comprehensive equation to evaluate the relation between heat transfer enhancement and pressure drop.
6. The mesh: the authors are suggested to use "structured hexahedral meshes" which can have very good quality with high accuracy as "Materials and Design, 2012, 33, 284-291", and this reference can be added to extend the introduction part.
7. How to evaluate the thermal stress and thermal strain effects about introducing the "v-corrugated duct with obstacles"? Please illustrate these problem with references.

Reviewer #4: 1) Abstract: While the writers' claim can be trusted that no study has ever been evaluated the effect of the obstacle-spacing; however, due to extensive number of existing literatures in solar air heating, it is possible that writes may have overlooked existing manuscripts. I recommend rewording the sentence in first paragraph of abstract in order to no make a solid statement.

2) Introduction: The literature review of this manuscript (Section 1, Third para.) lists few studies that indicate enhancement in heat transfer characteristics and efficiency of solar air heater, gained from adding fins or obstacles. However, I recommend adding results (values) from those literatures in order to demonstrate whether the increase in efficiency or heat transfer has been significant or not. Often addition of obstacles (if not well designed) may not have significant effects and would not be commercially feasible or cost effective.

3) Results and Discussion: Considering the best case recommended by this manuscript ($\Delta T = 16.53^\circ\text{C}$) and worst case ($\Delta T = 15.81^\circ\text{C}$), the difference between numerical (simulated) best and worst cases are only 0.72°C , which is in fact very small improvement in temperature. In reality (if the experimental values obtained) this difference might be very insignificant and do not make any difference at all. That is, if addition of delta-shaped obstacles enhances absolute outlet temperature; altering S/H ratio has small effect to no effect.

4) Results and Discussion: In the experimental study (to validate numerical model) it is obvious that ΔT in experiment is less than simulation. But it is odd that ΔP in experiment is less than (16%) simulation. In the experiment, many factors such as friction, boundary layers, imperfect geometry, etc. should cause more pressure drop than those seen in the simulation. That said, these writers still believe that experiment has been able to validate the simulation model? Also did other parameters such as actual collector surface temperature, actual radiation on surface, back flow, etc. have been measured and compared to numbers gained from simulation, or they are assumed to be equal? Temperatures (in/out) in Table 2 seems to be in Kelvin not Centigrade.

5) Results and Discussion: Similar to above argument on ΔT , the improvement in efficiency (64.5% to 67.5% from worst case to best case) is only 3%. That is, change in S/H ratio has very small effect in efficiency that cannot be justified by increased complexity and costs.

The reviewer(s) may also have uploaded detailed comments on your manuscript as an attachment. To access these comments, please go to: <http://ees.elsevier.com/se/>. Click on 'Author Login'. Click on 'View Reviewer Attachments' (if present).

Manuscript Number: SE-D-15-01490R1

Title: Numerical Studies on the Effect of Delta-Shaped Obstacles' Spacing on the Heat Transfer and Pressure Drop in V-Corrugated Channel of Solar Air Heater

Article Type: Regular Paper

Section/Category: Solar heating & cooling, buildings, and other applications

Keywords: delta-shaped obstacle; v-corrugated channel; solar air heater; numerical study

Corresponding Author: Dr. Ekadewi Anggraini Handoyo, Dr

Corresponding Author's Institution: Petra Christian University

First Author: Ekadewi Anggraini Handoyo, Dr

Order of Authors: Ekadewi Anggraini Handoyo, Dr; Ichsani Djatmiko, Prof.; Prabowo Prabowo, Prof.; Sutardi Sutardi, Prof.

Abstract: Solar air heater (SAH) is simple in construction compared to solar water heater. Yet, it is very useful for drying or space heating. Unfortunately, the convective heat transfer between the absorber plate and the air inside the solar air heater is rather low. Some researchers reported that obstacles are able to enhance the heat transfer in a flat plate solar air collector and others found that a v-corrugated absorber plate gives better heat transfer than a flat plate. Only a few research combines these two in a SAH. This paper will describe the combination from other point of view, i.e. the spacing between obstacles. Its spacing possibly will effect the heat transfer and pressure drop of the air flowing across the channel.

The first step in numerical study is generating mesh or grid of the air flow inside a v-corrugated channel which was blocked by some delta-shaped obstacles. The mesh was designed three-dimension and not uniform. The mesh are made finer for area near obstacles and walls both for upper and bottom, and then gradually coarser. Grid independency is the next step to be conducted. When the mesh is already independent, the numerical study begins. To validate the numerical model, an indoor experiment was conducted. Turbulent model used was Shear Stress Transport $K-\omega$ (SSTK- ω) standard. Having a valid numerical model, the spacing between obstacles was studied numerically. Ratio spacing to height, S/H of obstacles investigated were 0.5; 1; 1.5; and 2.

From numerical studies in a v-corrugated duct, it is found that backflow between obstacles and high velocity in the gap between obstacles and absorber plate causes the flow became more turbulent and enhanced the convection heat transfer between the air and the absorber plate. Obstacles placed in a small spacing will increase Nusselt number (convection heat transfer) and friction factor (pressure drop). The

Nusselt number enhanced from 27.2 when no obstacle used to 94.2 when obstacles inserted with $S/H = 0.5$. The Nusselt enhanced 3.46 times. The friction factor will increase from 0.0316 at no obstacle to 0.628 at ratio $S/H = 0.5$. The friction factor increased 19.9 times. Efficiency, Nusselt number, and friction factor are decreasing as ratio S/H is increasing. When ratio S/H used is 1 instead of 0.5, Nusselt number enhancement decreased only 1.13%, but friction factor decreased 15.1%. So, sacrificing a small amount of Nusselt number but reducing a significant friction factor is advantageous. The optimal spacing ratio S/H of delta-shaped obstacles inserted in a v-corrugated SAH is one. In other words, the optimal spacing of obstacle equals to its height.

Suggested Reviewers: Ebru Kavak Akpınar

ebruakpinar@firat.edu.tr

He/she write the same topic with me, i.e. obstacles in Solar Air Heater.

Adisu Bekele

addisu2005@yahoo.com

He/she write the same topic with me, i.e. obstacles in Solar Air Heater.

Md Azharul Karim

makarim@mame.mu.oz.au

He/she write the same topic with me, i.e. obstacles in Solar Air Heater.

Response to Reviewers: Response to reviewers:

First, we would like to be grateful to all reviewers. There are many things we did not aware until we got your reviews. All reviewers gave valuable and well-thought comments. Thank you for reviewing our paper.

Reviewer #1:

1. The objective, methodology, and results should be better described, discussed and justified.

Ans: We have revised the objective, methodology, and results of the paper. Hopefully, the revised paper meet your expectation.

2. The current literature review is not sufficient. For example, please mention (give) following more current studies related to solar air heaters in the sections of Introduction, and References List for completeness of your study and the references:

Experimental investigation of thermal performance of a double-flow solar air heater having aluminium cans, Renewable Energy, 34(11), 2391-2398 (2009).

Modelling of a new solar air heater through least-squares support vector machines, Expert Systems with Applications, 36(7), 10673-10682 (2009).

Artificial neural network and wavelet neural network approaches for modelling of a solar air heater, Expert Systems with Applications, 36(8), 11240-11248 (2009).

Ans: Some literature review we wrote in this paper are only related to SAH using v-corrugated absorber plate with and without obstacles. Yet, we have added your suggested literature as in p. 2 - 3.

3. The results should be expanded significantly and quantitatively.

Ans: In this revised paper, we expand the result with discussing the Nusselt number and friction factor of the air flow in a v-corrugated channel with delta-shaped obstacles.

4. I strongly suggest that authors shall carry out more studies to compare the results from this paper to that from other similar studies.

Ans: Yes, we agree with your suggestion. In section 5 of the revised paper, we compared the result of our research with others'.

Reviewer #2:

A few minor revisions are suggested to improve the paper. The comments specified below should be addressed to enhance the readability and archival value of the paper:

1. The motivation and objective of the study should be more better justified.

Ans: We have revised the objective, methodology, and results of the paper. Hopefully, the revised paper meet your expectation.

2. The findings should be enlarged substantially.

Ans: In this revised paper, we expand the result with discussing the Nusselt number and friction factor of the air flow in a v-corrugated channel with some delta-shaped obstacles.

3. Please compare your findings with results obtained from other works.

Ans: Yes, we agree with your suggestion. In section 5 of the revised paper, we compared the result of our research with others'.

Reviewer #3:

In this study, v-corrugated absorber with obstacles are investigated, which is interesting. However, following revisions need to be addressed:

1. Highlights should be less than 85 letters including space.

Ans: We have shortened the highlights.

2. Abstract should be more concise.

Ans: We have revised the Abstract. Hopefully, it is more concise.

3. This paper should also investigate the effects of using v-corrugated duct with obstacles on "heat transfer enhancement" compared to conventional duct with/without obstacles and v-corrugated duct without obstacles

Ans: The revised paper has added the investigation on heat transfer enhancement (Nusselt number) of v-corrugated duct with obstacles compare to without obstacles. We do not compare v-corrugated duct with conventional duct (flat plate), because our focus is on effect of spacing ratio of obstacles in a v-corrugated duct. We might do that in next research/paper.

4. This paper should also investigate the effects of using v-corrugated duct with obstacles on "pressure drop" compared to conventional duct with/without obstacles and v-corrugated duct without obstacles.

Ans: The revised paper has added the investigation on pressure drop increase (friction factor) of v-corrugated duct with obstacles compare to without obstacles. We do not compare v-corrugated duct with conventional duct (flat plate), because our focus is on effect of spacing ratio of obstacles in a v-corrugated duct. We might do that in next research/paper.

5. The author should give a comprehensive equation to evaluate the relation between heat transfer enhancement and pressure drop.

Ans: We have added the equation that relate heat transfer to pressure drop (called Reynolds Analogy) in revised paper p. 4, as follow: According to Incropera [18], in forced convection heat transfer, there are two quantities that are important to be determined. One is friction coefficient, C_f , and the other is Nusselt number, Nu . Friction coefficient, C_f is used to calculate the shear stress at the wall and then to calculate pressure drop. While Nusselt number, Nu is used to calculate convection heat transfer rate. The relation that correlate them is known as Reynolds Analogy: $C_{f,x} Re_{L/2} = Nu_x Pr^{(-1/3)}$ When Nusselt number increases, then friction coefficient will increase, too. In SAH, it is expected that convection heat transfer increases but pressure drop does not. So, many research were conducted to look for increasing in heat transfer at low pressure drop.

6. The mesh: the authors are suggested to use "structured hexahedral meshes" which can have very good quality with high accuracy as "Materials and Design, 2012, 33, 284-291", and this reference can be added to extend the introduction part.

Ans: The mesh used in this research is hexahedral, as shown in the Figure 2, 3, 5, and 6.

We have read the paper which title is "Effects of material selection on the thermal stresses of tube receiver under concentrated solar irradiation". After reading the paper, we think that the paper is not quite related to this research. It described a lot about radial stress on inner surface of tube receiver, temperature & stress profile across the circumference on the tube inner surface at the tube outlet, axial and tangential stress profile on tube inner surface along the length direction at certain angle. So, we really apologize that the paper could not be included as reference.

7. How to evaluate the thermal stress and thermal strain effects about introducing the "v-corrugated duct with obstacles"? Please illustrate these problem with references.

Ans: Tube receiver in Wang, et. al.'s research is installed hanging and supported with parabolic concentrator. The increasing temperature creates thermal strain on the hinge. Thermal strain could create thermal stress. This could cause problem to the tube and the hinge. While v-corrugated duct in this study is supported with board on its side and its bottom. So, the thermal strain and stress have little impact on this study.

Reviewer #4:

1. Abstract: While the writers' claim can be trusted that no study has ever been evaluated the effect of the obstacle-spacing; however, due to extensive number of existing literatures in solar air heating, it is possible that writers may have overlooked existing manuscripts. I recommend rewording the sentence in first paragraph of abstract in order to no make a solid statement.

Ans: Thank you for the suggestion. We have changed the first paragraph of abstract as follow:

Some researchers reported that obstacles are able to enhance the heat transfer in a flat plate solar air collector and others found that a v-corrugated absorber plate gives better heat transfer than a flat plate. Only a few research combines these two in a SAH. This paper will describe the combination from other point of view, i.e. the spacing between obstacles. Its spacing possibly will effect the heat transfer and pressure drop of the air flowing across the channel.

2. Introduction: The literature review of this manuscript (Section 1, Third para.) lists few studies that indicate enhancement in heat transfer characteristics and efficiency of solar air heater, gained from adding fins or obstacles. However, I recommend adding results (values) from those literatures in order to demonstrate whether the increase in efficiency or heat transfer has been significant or not. Often addition of obstacles (if not well designed) may not have significant effects and would not be commercially feasible or cost effective.

Ans: The results (values) of every literature review have been added to each review as in p. 2 - 3 of the revised paper.

3. Results and Discussion: Considering the best case recommended by this manuscript ($\Delta T = 16.53^\circ\text{C}$) and worst case ($\Delta T = 15.81^\circ\text{C}$), the difference between numerical (simulated) best and worst cases are only 0.72°C , which is in fact very small improvement in temperature. In reality (if the experimental values obtained) this difference might be very insignificant and do not make any difference at all. That is, if addition of delta-shaped obstacles enhances absolute outlet temperature; altering S/H ratio has small effect to no effect.

Ans: The data that we presented in the first paper was comparison of result (such as ΔT) between spacing ratio. So, the difference is very small.

In this revised paper, we present and discuss the result (efficiency, Nusselt number, and friction factor) compare to no obstacle. When we altered S/H ratio from 0.5 to 1, the study shows that the efficiency or Nusselt number is not much effected but the friction factor is indeed effected.

4. Results and Discussion: In the experimental study (to validate numerical model) it is obvious that ΔT in experiment is less than simulation. But it is odd that ΔP in experiment is less than (16%) simulation. In the experiment, many factors such as friction, boundary layers, imperfect geometry, etc. should cause more pressure drop than those seen in the simulation. That said, dese writes still believe that experiment has been able to validate the simulation model? Also did other parameters such as actual collector surface temperature, actual radiation on surface, back flow, etc. have been measured and compared to numbers gained from simulation, or they are assumed to be equal? Temperatures (in/out) in Table 2 seems to be in Kelvin not Centigrade.

Ans: Regarding ΔP from simulation that is higher than experiment, we found in a research report titled "Steady-State Evaluation of 'Two-Equation' RANS (Reynolds-averaged Navier-Stokes) Turbulence Models for High-Reynolds Number Hydrodynamic Flow Simulations" by Nicholas J. Mulvany, Li Chen, Jiyuan Y. Tu and Brendon Anderson from Maritime Platforms Division of Australian Government (DSTO-TR-1564) that the pressure coefficient (C_p) distribution at the surface of the hydrofoil predicted with some turbulence model is higher than the experiment as shown in next Figure. In the Figure, the positive C_p means flow above the hydrofoil and negative C_p means flow below the hydrofoil. The distributions predicted by the Realisable $k-\epsilon$ and the SST $k-\omega$ models are very encouraging, however, the Standard $k-\epsilon$ and Standard $k-\omega$ models show significant deviation from the experimental data. The Realisable $k-\epsilon$ turbulence model predicts high-pressure (referenced to the freestream static pressure) below the hydrofoil and low-pressure above, whereas the SST $k-\omega$ model predicts low-pressure both above and below. This indicates that the Realisable $k-\epsilon$ model predicts decreased flow velocity below the pressure surface and increased flow velocity above the suction surface, whereas the SST $k-\omega$ predicts increased flow velocity both above and below the hydrofoil. So, it is possible that numerical simulation give higher pressure drop prediction than experiment.

The collector surface temperature in numerical simulation is defined constant according to data from experiment.

We did not specify radiation on absorber surface, because this study did not include radiation. It focus on convection heat transfer between the surface of absorber plate to air flowing beneath.

Since we could not measure the backflow, we could not do comparison. The backflow from simulation is used to show the flow inside channel.

Yes, you are right. We made mistake with unit of temperature in Table 2. It should be Kelvin. We have corrected it.

5. Results and Discussion: Similar to above argument on ΔT , the improvement in efficiency (64.5% to 67.5% from worst case to best case) is only 3%. That is, change in S/H ratio has very small effect in efficiency that cannot be justified by increased complexity and costs.

Ans: We have changed the Results and Discussion section. Hopefully, the revised paper is able to show the optimal spacing ratio S/H of obstacles inserted in a v-corrugated channel.

Response to reviewers

First, we would like to be grateful to all reviewers. There are many things we did not aware until we got your reviews. All reviewers gave valuable and well-thought comments. Thank you for reviewing our paper.

Reviewer #1:

1. The objective, methodology, and results should be better described, discussed and justified.
We have revised the objective, methodology, and results of the paper. Hopefully, the revised paper meet your expectation.
2. The current literature review is not sufficient. For example, please mention (give) following more current studies related to solar air heaters in the sections of Introduction, and References List for completeness of your study and the references:
 - Experimental investigation of thermal performance of a double-flow solar air heater having aluminium cans, Renewable Energy, 34(11), 2391-2398 (2009).
 - Modelling of a new solar air heater through least-squares support vector machines, Expert Systems with Applications, 36(7), 10673-10682 (2009).
 - Artificial neural network and wavelet neural network approaches for modelling of a solar air heater, Expert Systems with Applications, 36(8), 11240-11248 (2009).

Some literature review we wrote in this paper are only related to SAH using v-corrugated absorber plate with and without obstacles. Yet, we have added your suggested literature as in p. 2 – 3.

3. The results should be expanded significantly and quantitatively.
In this revised paper, we expand the result with discussing the Nusselt number and friction factor of the air flow in a v-corrugated channel with delta-shaped obstacles.
4. I strongly suggest that authors shall carry out more studies to compare the results from this paper to that from other similar studies.
Yes, we agree with your suggestion. In section 5 of the revised paper, we compared the result of our research with others’.

Reviewer #2:

A few minor revisions are suggested to improve the paper. The comments specified below should be addressed to enhance the readability and archival value of the paper:

1. The motivation and objective of the study should be more better justified.
We have revised the objective, methodology, and results of the paper. Hopefully, the revised paper meet your expectation.
2. The findings should be enlarged substantially.
In this revised paper, we expand the result with discussing the Nusselt number and friction factor of the air flow in a v-corrugated channel with some delta-shaped obstacles.
3. Please compare your findings with results obtained from other works.
Yes, we agree with your suggestion. In section 5 of the revised paper, we compared the result of our research with others’.

Reviewer #3:

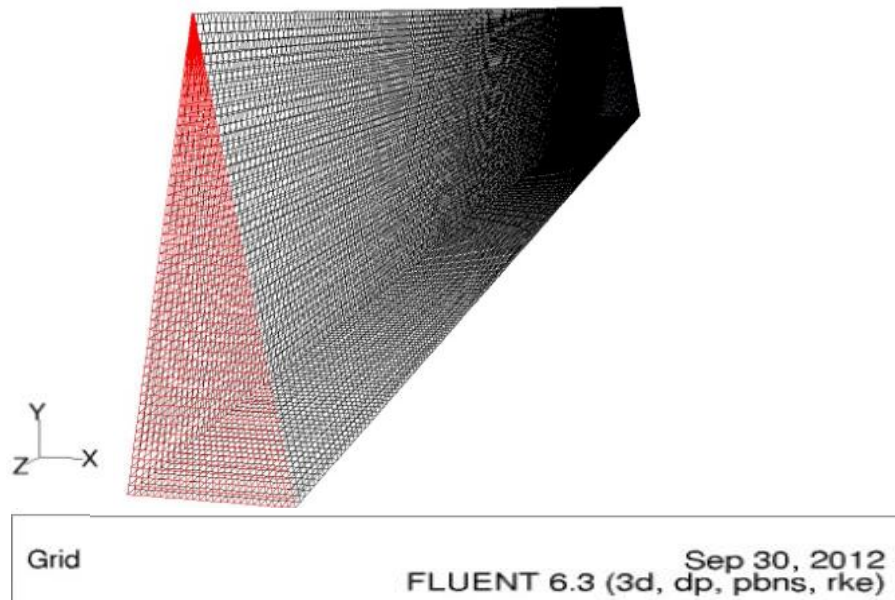
In this study, v-corrugated absorber with obstacles are investigated, which is interesting. However, following revisions need to be addressed:

1. Highlights should be less than 85 letters including space.
We have shortened the highlights.
2. Abstract should be more concise.
We have revised the Abstract. Hopefully, it is more concise.
3. This paper should also investigate the effects of using v-corrugated duct with obstacles on "heat transfer enhancement" compared to conventional duct with/without obstacles and v-corrugated duct without obstacles
The revised paper has added the investigation on heat transfer enhancement (Nusselt number) of v-corrugated duct with obstacles compare to without obstacles. We do not compare v-corrugated duct with conventional duct (flat plate), because our focus is on effect of spacing ratio of obstacles in a v-corrugated duct. We might do that in next research/paper.
4. This paper should also investigate the effects of using v-corrugated duct with obstacles on "pressure drop" compared to conventional duct with/without obstacles and v-corrugated duct without obstacles.
The revised paper has added the investigation on pressure drop increase (friction factor) of v-corrugated duct with obstacles compare to without obstacles. We do not compare v-corrugated duct with conventional duct (flat plate), because our focus is on effect of spacing ratio of obstacles in a v-corrugated duct. We might do that in next research/paper.
5. The author should give a comprehensive equation to evaluate the relation between heat transfer enhancement and pressure drop.
We have added the equation that relate heat transfer to pressure drop (called Reynolds Analogy) in revised paper p. 4, as follow:

According to Incropera [18], in forced convection heat transfer, there are two quantities that are important to be determined. One is friction coefficient, C_f , and the other is Nusselt number, Nu . Friction coefficient, C_f is used to calculate the shear stress at the wall and then to calculate pressure drop. While Nusselt number, Nu is used to calculate convection heat transfer rate. The relation that correlate them is known as Reynolds Analogy: $C_{f,x} \frac{Re_L}{2} = Nu_x Pr^{-1/3}$

When Nusselt number increases, then friction coefficient will increase, too. In SAH, it is expected that convection heat transfer increases but pressure drop does not. So, many research were conducted to look for increasing in heat transfer at low pressure drop.
6. The mesh: the authors are suggested to use "structured hexahedral meshes" which can have very good quality with high accuracy as "Materials and Design, 2012, 33, 284-291", and this reference can be added to extend the introduction part.

The mesh used in this research is hexahedral, as shown in the Figure 2, 3, 5, and 6.



We have read the paper which title is “Effects of material selection on the thermal stresses of tube receiver under concentrated solar irradiation”. After reading the paper, we think that the paper is not quite related to this research. It described a lot about radial stress on inner surface of tube receiver, temperature & stress profile across the circumference on the tube inner surface at the tube outlet, axial and tangential stress profile on tube inner surface along the length direction at certain angle. So, we really apologize that the paper could not be included as reference.

7. How to evaluate the thermal stress and thermal strain effects about introducing the "v-corrugated duct with obstacles"? Please illustrate these problem with references.
Tube receiver in Wang, et. al.'s research is installed hanging and supported with parabolic concentrator. The increasing temperature creates thermal strain on the hinge. Thermal strain could create thermal stress. This could cause problem to the tube and the hinge. While v-corrugated duct in this study is supported with board on its side and its bottom. So, the thermal strain and stress have little impact on this study.

Reviewer #4:

1. Abstract: While the writers' claim can be trusted that no study has ever been evaluated the effect of the obstacle-spacing; however, due to extensive number of existing literatures in solar air heating, it is possible that writers may have overlooked existing manuscripts. I recommend rewording the sentence in first paragraph of abstract in order to not make a solid statement.

Thank you for the suggestion. We have changed the first paragraph of abstract as follow:
Some researchers reported that obstacles are able to enhance the heat transfer in a flat plate solar air collector and others found that a v-corrugated absorber plate gives better heat transfer than a flat plate. Only a few research combines these two in a SAH. This paper will describe the combination from other point of view, i.e. the spacing between obstacles. Its spacing possibly will effect the heat transfer and pressure drop of the air flowing across the channel.

2. Introduction: The literature review of this manuscript (Section 1, Third para.) lists few studies that indicate enhancement in heat transfer characteristics and efficiency of solar air heater, gained from adding fins or obstacles. However, I recommend adding results (values) from those literatures in order to demonstrate whether the increase in efficiency or heat transfer has been significant or not. Often addition of obstacles (if not well designed) may not have significant effects and would not be commercially feasible or cost effective.

The results (values) of every literature review have been added to each review as in p. 2 – 3 of the revised paper.

3. Results and Discussion: Considering the best case recommended by this manuscript ($\Delta T = 16.53^\circ\text{C}$) and worst case ($\Delta T = 15.81^\circ\text{C}$), the difference between numerical (simulated) best and worst cases are only 0.72°C , which is in fact very small improvement in temperature. In reality (if the experimental values obtained) this difference might be very insignificant and do not make any difference at all. That is, if addition of delta-shaped obstacles enhances absolute outlet temperature; altering S/H ratio has small effect to no effect.

The data that we presented in the first paper was comparison of result (such as ΔT) between spacing ratio. So, the difference is very small.

In this revised paper, we present and discuss the result (efficiency, Nusselt number, and friction factor) compare to no obstacle.

When we altered S/H ratio from 0.5 to 1, the study shows that the efficiency or Nusselt number is not much effected but the friction factor is indeed effected.

4. Results and Discussion: In the experimental study (to validate numerical model) it is obvious that ΔT in experiment is less than simulation. But it is odd that ΔP in experiment is less than (16%) simulation. In the experiment, many factors such as friction, boundary layers, imperfect geometry, etc. should cause more pressure drop than those seen in the simulation. That said, dese writes still believe that experiment has been able to validate the simulation model? Also did other parameters such as actual collector surface temperature, actual radiation on surface, back flow, etc. have been measured and compared to numbers gained from simulation, or they are assumed to be equal? Temperatures (in/out) in Table 2 seems to be in Kelvin not Centigrade.

Regarding ΔP from simulation that is higher than experiment, we found in a research report titled "Steady-State Evaluation of 'Two-Equation' RANS (Reynolds-averaged Navier-Stokes) Turbulence Models for High-Reynolds Number Hydrodynamic Flow Simulations" by Nicholas J. Mulvany, Li Chen, Jiyuan Y. Tu and Brendon Anderson from Maritime Platforms Division of Australian Government (DSTO-TR-1564) that the pressure coefficient (C_p) distribution at the surface of the hydrofoil predicted with some turbulence model is higher than the experiment as shown in next Figure. In the Figure, the positive C_p means flow above the hydrofoil and negative C_p means flow below the hydrofoil. The distributions predicted by the Realisable $k-\epsilon$ and the SST $k-\omega$ models are very encouraging, however, the Standard $k-\epsilon$ and Standard $k-\omega$ models show significant deviation from the experimental data. The Realisable $k-\epsilon$ turbulence model predicts high-pressure (referenced to the freestream static pressure) below the hydrofoil and low-pressure above, whereas the SST $k-\omega$ model predicts low-pressure both above and below. This indicates that the Realisable $k-\epsilon$ model predicts decreased flow velocity below the pressure surface and increased flow velocity above the suction surface, whereas the SST $k-\omega$ predicts increased flow velocity both above and below the hydrofoil.

So, it is possible that numerical simulation give higher pressure drop prediction than experiment.

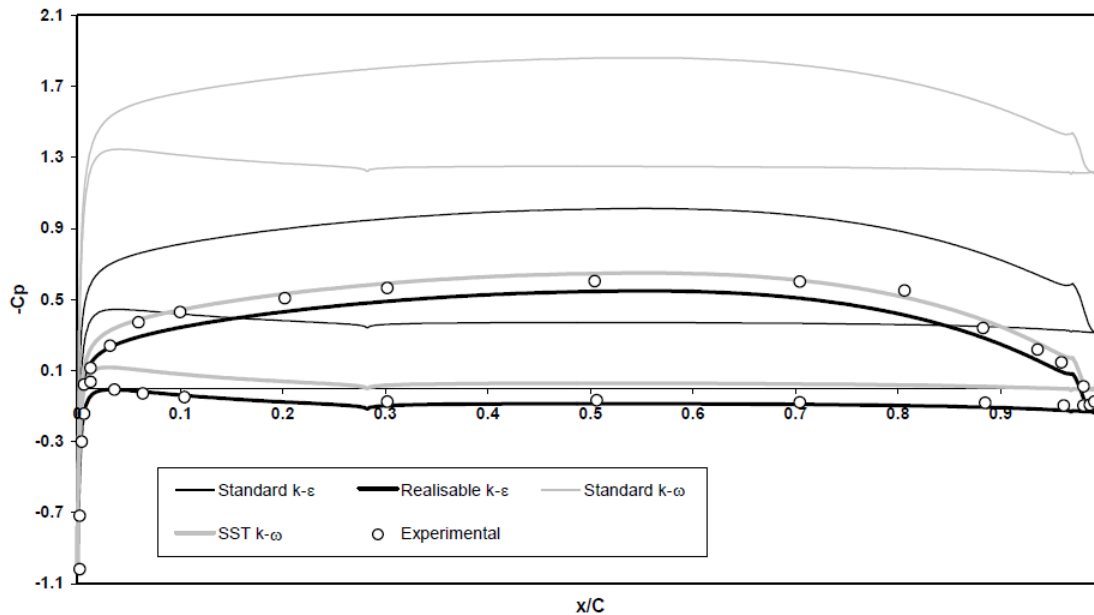


Figure 4. Turbulence Model Performance: Pressure coefficient (C_p) distribution at the surface of the hydrofoil ($U_\infty = 3\text{ m/s}$)

The collector surface temperature in numerical simulation is defined constant according to data from experiment.

We did not specify radiation on absorber surface, because this study did not include radiation. It focus on convection heat transfer between the surface of absorber plate to air flowing beneath.

Since we could not measure the backflow, we could not do comparison. The backflow from simulation is used to show the flow inside channel.

Yes, you are right. We made mistake with unit of temperature in Table 2. It should be Kelvin. We have corrected it.

5. Results and Discussion: Similar to above argument on delta T, the improvement in efficiency (64.5% to 67.5% from worst case to best case) is only 3%. That is, change in S/H ratio has very small effect in efficiency that cannot be justified by increased complexity and costs.

We have changed the Results and Discussion section. Hopefully, the revised paper is able to show the optimal spacing ratio S/H of obstacles inserted in a v-corrugated channel.

Highlights

V-corrugated absorber plate and obstacles improves heat transfer in SAH.

How does the spacing between obstacles effect the convection heat transfer and pressure drop in air flow?

The optimal spacing ratio of obstacles gives optimal Nusselt number (convection) and friction factor (pressure drop).

Numerical Studies on the Effect of Delta-Shaped Obstacles' Spacing on the Heat Transfer and Pressure Drop in V-Corrugated Channel of Solar Air Heater

Ekadewi A. Handoyo¹, Djatmiko Ichsani², Prabowo², Sutardi²

¹Mechanical Engineering Dept, Petra Christian University, Surabaya – Indonesia

²Mechanical Engineering Dept, Institut Teknologi Sepuluh Nopember, Surabaya – Indonesia

Corresponding author: ekadewi@petra.ac.id

Abstract

Solar air heater (SAH) is simple in construction compared to solar water heater. Yet, it is very useful for drying or space heating. Unfortunately, the convective heat transfer between the absorber plate and the air inside the solar air heater is rather low. Some researchers reported that obstacles are able to enhance the heat transfer in a flat plate solar air collector and others found that a v-corrugated absorber plate gives better heat transfer than a flat plate. Only a few research combines these two in a SAH. This paper will describe the combination from other point of view, i.e. the spacing between obstacles. Its spacing possibly will effect the heat transfer and pressure drop of the air flowing across the channel.

The first step in numerical study is generating mesh or grid of the air flow inside a v-corrugated channel which was blocked by some delta-shaped obstacles. The mesh was designed three-dimension and not uniform. The mesh are made finer for area near obstacles and walls both for upper and bottom, and then gradually coarser. Grid independency is the next step to be conducted. When the mesh is already independent, the numerical study begins. To validate the numerical model, an indoor experiment was conducted. Turbulent model used was Shear Stress Transport K- ω (SSTK- ω) standard. Having a valid numerical model, the spacing between obstacles was studied numerically. Ratio spacing to height, S/H of obstacles investigated were 0.5; 1; 1.5; and 2.

From numerical studies in a v-corrugated duct, it is found that backflow between obstacles and high velocity in the gap between obstacles and absorber plate causes the flow became more turbulent and enhanced the convection heat transfer between the air and the absorber plate. Obstacles placed in a small spacing will increase Nusselt number (convection heat transfer) and friction factor (pressure drop). The Nusselt number enhanced from 27.2 when no obstacle used to 94.2 when obstacles inserted with S/H = 0.5. The Nusselt enhanced 3.46 times. The friction factor will increase from 0.0316 at no obstacle to 0.628 at ratio S/H = 0.5. The friction factor increased 19.9 times. Efficiency, Nusselt number, and friction factor are decreasing as ratio S/H is increasing. When ratio S/H used is 1 instead of 0.5, Nusselt number enhancement decreased only 1.13%, but friction factor decreased 15.1%. So, sacrificing a small amount of Nusselt number but reducing a significant friction factor is advantageous. The optimal spacing ratio S/H of delta-shaped obstacles inserted in a v-corrugated SAH is one. In other words, the optimal spacing of obstacle equals to its height.

Keywords: delta-shaped obstacle; v-corrugated channel; solar air heater; numerical study.

1. Introduction

Solar energy can be converted into thermal energy in a solar collector. Solar collector basically is device used to trap solar energy to heat a plate and transfer the heat to a fluid flowing under or above the plate. When sun light falls onto a plate, solar radiation reaches the plate at lower wavelength and heat it up. Then, the heat is carried away by either water or air that flows under or above the plate. Solar collector used to heat up air is called solar air heater (SAH) and solar water heater for water. Generally, the solar air heater is less efficient than the solar water heater, because air has less thermal capacity and less convection heat transfer coefficient. Yet, air is much lighter and less corrosive than water. The other benefit is that heated air can be used for moderate-temperature drying, such as harvested grains or fish. Since the solar air heater has less convective heat transfer coefficient than solar water heater, some researchers tried to increase this convective heat transfer coefficient.

A popular type of solar air heaters is the flat plate SAH, which has a cover glass on the top, insulation on the sides and bottom to prevent heat transferred to the surrounding, a flat absorber plate that makes a passage for the air flowing with sides and bottom plate. Usually, the passage or channel has a rectangular cross-section. The absorber plate will transfer the heat to the air via convection. Unfortunately, the convection coefficient is very low. To increase the convection coefficient from the absorber plate, a v-corrugated plate is used instead of a flat plate. Tao Liu et al. [1] stated that a solar air heater with a v-grooved absorber plate could reach efficiency 18% higher than the flat plate on the same operation condition and dimension or configuration. Karim and Hawlader [2] found that a solar collector with a v-absorber plate gave the highest efficiency and the flat plate gave the least. The results showed that the v-corrugated collector is 10–15% and 5–11% more efficient in single pass and double pass modes, respectively, compared to the flat plate collectors. Choudhury and Garg [3] made a detailed analysis of corrugated and flat plate solar air heaters of five different configurations. For the same length, mass flow rate, and air velocity, it was found out that the corrugated and double cover glass collector gave the highest efficiency. According to Naphon [4] the corrugated surfaces give a significant effect on the enhancement of heat transfer and pressure drop. The Nusselt number of flow in a v-corrugated channel can be 3.2 – 5.0 times higher than in a plane surfaces while the pressure drop 1.96 times higher than on the corresponding plane surface. Islamoglu and Parmaksizoglu [5] reported that the corrugated channel gave the higher Nusselt number than the straight channel and the higher channel height gave higher Nusselt number for the flow with the same Reynolds number.

Besides changing the cross section area of the channel, some also give effort to increase turbulence inside the channel with fins or obstacles. The result of experimental study done by Promvonge [6] in turbulent flow regime (Reynolds number of 5000 to 25,000) showed that multiple 60° V-baffle turbulator fitted on a channel provides the drastic increase in Nusselt number, friction factor, and the thermal enhancement factor values over the smooth wall channel. Promvonge found that Nusselt number was five times higher and friction factor was 30 times than without baffle at Reynolds number = 10000, $e/H = 0.3$, and $P_R = 1$. Kurtbas and Turgut [7] investigated the effect of fins located on the absorber surface in free and fixed manners. They used two kinds of rectangular fins which dimension is different but total area is the same. The first type fin (I) has dimension 810 x 60 mm and the second (II) type 200 x 60 mm. To have the same total area, there are 8 fins and 32 fins for the first and second, respectively. The fins type II, both free and fixed, were more effective than type I and flat-plate

collector. The fixed fin collector was more effective than free fin collector. Kurtbas and Turgut reported that the maximum Instantaneous efficiency of SAH was 0.78 at air mass flow rate 0.08 kg/s when the fixed fins type II were used. While the efficiency of flat plate SAH was only 0.42. So, its efficiency increased 1.86 times. Romdhane [8] created turbulence in the air channel using obstacles or baffles. The efficiency of collector and the air temperature was found increasing with the use of baffles. Baffles should be used to guide the flow toward the absorber plate. Romdhane reported that the efficiency reached 80% for the best type of baffle (chicane) for an air flow rate of 50 m³/h/m². This efficiency was about 1.6 times efficiency without baffle. Ho, et al. [9] inserted fins attached by baffles and external recycling to a solar air heater. The experiment and theoretical investigations gave result that heat transfer was improved by employing baffled double-pass with external recycling and fin attached over and under absorber plate. According to Ho, et al., the highest collector efficiency was 61% in a double-pass flat-plate SAH with recycle when radiation intensity was 1100 W/m², 24 fins attached, and mass flow rate was 0.02 kg/s. It was about 1.35 times its efficiency when there is no recycle. Abene et al. [10] used obstacles on the flat plate of a solar air collector for drying grape. The obstacles ensure a good air flow over the absorber plate, create the turbulence and reduce the dead zones in the collector. The highest efficiency got was 70% when the air flow rate was 50 m³/h/m². It was about 1.9 times its efficiency when no obstacle used. The air pressure drop increased about twice with obstacles. Esen [11] used a double-flow solar air heater to investigate three different type obstacles placed on absorber plates compare with the flat plate. The collector has three absorber plates to make three passages for the air flowing through. From the research done, it was found that all collectors with obstacles gave higher efficiency than the flat plate and type III obstacles with flow in middle passage gave the highest efficiency, i.e. 52.9%, for air flow 0.02 kg/s. It was about 1.13 times higher than its efficiency with no obstacle. Ozgen et al. [12] used aluminum cans as obstacles installed over and under absorber plate. They found that the SAH using double flow passage (over and under absorber plate) gave higher efficiency than just one flow passage (either over or under absorber plate). They also found that SAH with staggered cans (type I) had the highest efficiency compared to aligned cans (type II) and flat plate (type III). The efficiency of SAH type I was 0.73 at air flow rate 0.05 kg/s and it was about 1.4 times of type III. Akpinar and Koçyiğit [13] had experimental investigation on solar air heater with several obstacles (Type I, Type II, and Type III) and without obstacles. The optimal value of efficiency was obtained for the solar air heater with Type II obstacles on absorber plate in flow channel duct for all operating conditions and the collector with obstacles appears significantly better than that without obstacles. The efficiency of Type II was 0.6 at air flow rate 0.0052 kg/s and it was about twice of SAH without obstacle. Bekele et al. [14] investigated experimentally the effect of delta shaped obstacles mounted on the absorber surface of an air heater duct. They found that the obstacle mounted duct enhances the heat transfer to the air. The heat transfer got higher if the obstacle height was taller and its longitudinal pitch was smaller. Nusselt number increased 3.5 times when obstacles inserted with ratio of longitudinal pitch $P_l/e = 3/2$ and height $e/H = 0.75$ at Reynolds number was 10,000. While its friction factor increased 4.7 times than without obstacle. SAH can be modeled through least-squares support vector machines (LS-SVM) method as done by Ezen et al. [15]. The predicted results from LS-SVM model had been compared to experimental results. LS-SVM could be used to predict the efficiency of SAH. They showed that efficiency of type I SAH was the highest. Ezen et al. [16] also proposed Artificial Neural Network and Wavelet Neural Network (ANN and WNN) to predict the efficiency of SAH. They succeeded to show that the method could predict the SAH efficiency.

The combine of those two findings, i.e. obstacles and v-corrugated absorber plate are able to improve SAH are important to be studied. Handoyo et al. [17] reported that the obstacles are able to enhance heat transfer in a v-corrugated SAH but increase the air pressure drop. To reduce the air pressure drop,

the obstacles were bent vertically. The optimal bending angle is 30°. The SAH's efficiency was 5.3% lower when the obstacles bent 30° instead of straight (0°), but the pressure drop was 17.2% lower.

According to Incropera [18], in forced convection heat transfer, there are two quantities that are important to be determined. One is friction coefficient, C_f , and the other is Nusselt number, Nu . Friction coefficient, C_f is used to calculate the shear stress at the wall and then to calculate pressure drop. While Nusselt number, Nu is used to calculate convection heat transfer rate. The relation that correlate them is known as Reynolds Analogy: $C_{f,x} \frac{Re_L}{2} = Nu_x Pr^{-1/3}$

When Nusselt number increases, then friction coefficient will increase, too. In a SAH, it is expected that convection heat transfer increases but pressure drop does not. So, many research were conducted to look for increasing in heat transfer at low pressure drop.

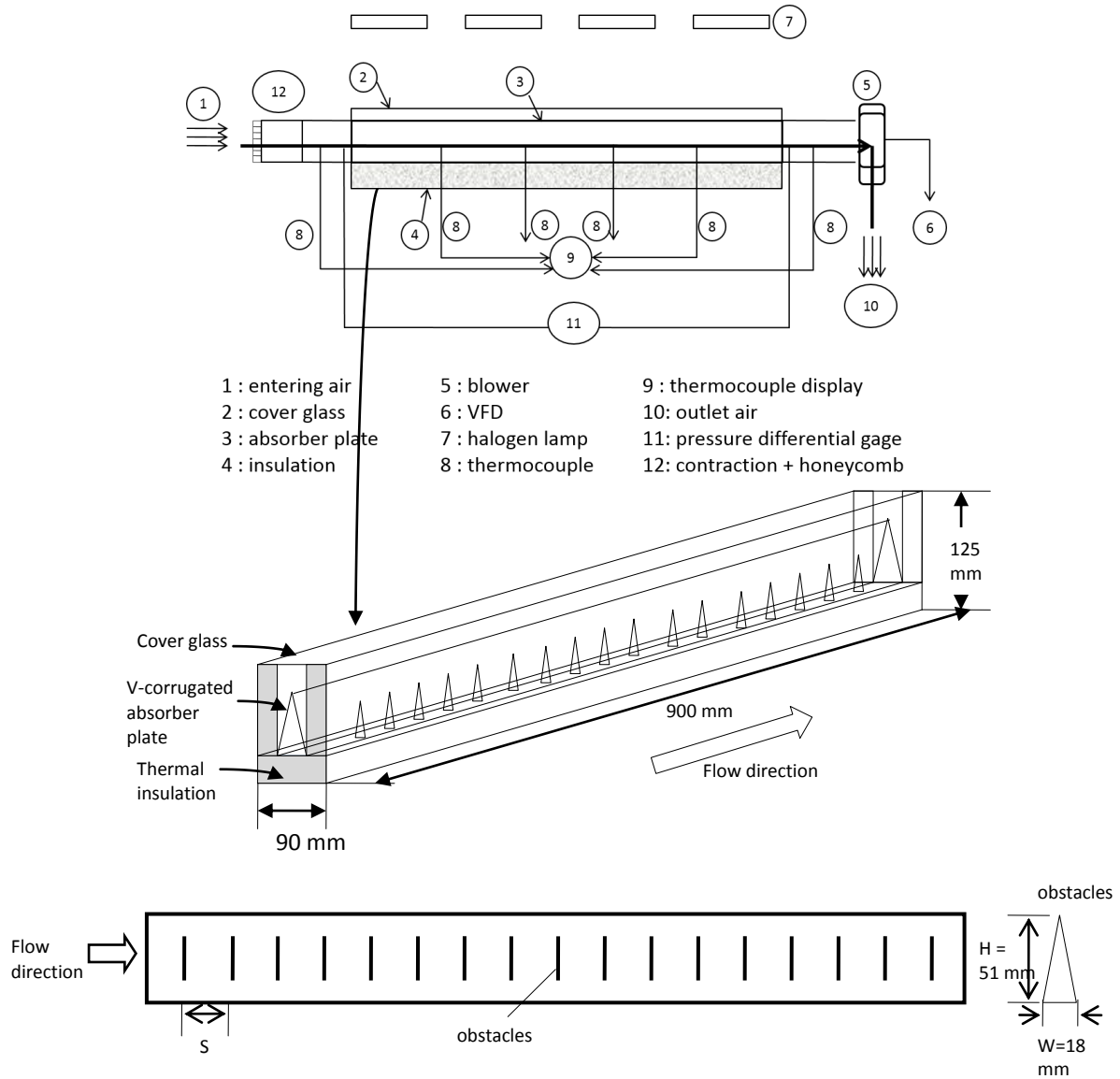
The spacing between obstacles mounted on absorber plate can be varied. A different spacing will give different air pressure drop as the air flows across the collector. Obstacles increase the air pressure drop. When the spacing is large, the obstacles used is less and the air pressure drop will be reduced. What about the heat transfer from the absorber plate to the flowing air? How will the spacing between obstacles effect the heat transfer? To the knowledge of the authors, there is no research investigating the effect of delta-shaped obstacles' spacing on a v-corrugated SAH performance, yet.

This paper describes the result of the numerical studies of obstacles' spacing inserted in a v-corrugated channel of a SAH. The heat transfer from the v-corrugated absorber plate and the air pressure drop flowing the v-corrugated channel is to be discussed. The obstacles are delta-shaped and installed on bottom plate of the channel.

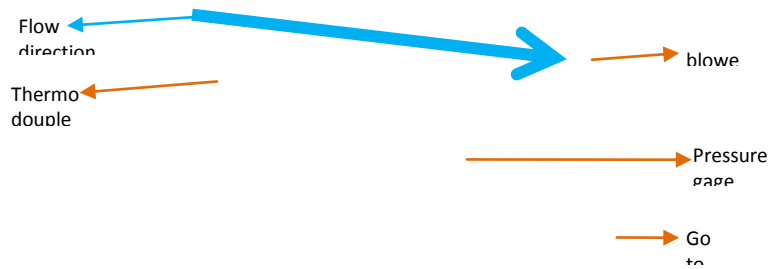
2. Experimental set-up

The studies began with choosing a solar collector model to be studied. The study will be conducted numerically. Thus, a validation is required to prove that the result is true. The validation is accomplished via experiment. An indoor experiment model was constructed to validate numerical result. It is a model of SAH using v-corrugated absorber plate. Its schematic view and photograph are shown in Fig. 1 (a) and (b), respectively. The experiment was conducted in a laboratory of Mechanical Engineering Dept of Petra Christian University, Surabaya, Indonesia.

The collector model's dimension was 900 mm long, 90 mm width, and 125 mm height. A single 3-mm transparent-tempered glass was used as the collector cover. The v-corrugated absorber plate was made of 0.8-mm-thick aluminum and painted black. The apex angle of the v-corrugated plate was 20°. The v-corrugated channel's cross section was 30 mm width and 85 mm height. To prevent heat loss, the left and right walls of collector are insulated with a 25-mm Styrofoam each and a 35-mm Styrofoam for the bottom. The delta-shaped obstacles were made congruent to the channel i.e. triangular and its dimension was 18 mm wide, 51 mm height.



(a) Schematic of the solar collector model



(b) Photograph of experimental set-up.

Figure 1. The SAH model used in experiment

The experiment was conducted indoor to maintain the radiation intensity, wind's velocity and temperature. So, a bias result caused by different outdoor condition could be avoided. The sunlight is replaced with four 500-Watt halogen lamps. The radiation intensity received on the collector was measured using a pyranometer (Kipp & Zonen, type SP Lite2) placed on top of the cover glass. To ensure the homogenous intensity and to generate a certain absorber plate's temperature, these lamps were equipped with adjustable turner individually. The surrounding air condition was controlled by an air conditioner installed in the room. Its temperature, humidity, and wind velocity are well controlled. The collector was equipped with T-type thermocouple which accuracy is 0.1°C for measuring the air temperature at inlet and outlet of the collector, temperature of the absorber plate (at four different locations), and ambient temperature. The pressure drop between inlet and outlet of the flowing air across the collector is also measured with a Magnehelic differential pressure gage which accuracy is ± 2 Pa. A centrifugal blower (1000 m³/h, 580 Pa, 0.2 kW, 380 Volt input) was used to induce the air flowing through the collector. The air flow was adjusted by means of a variable-frequency drive (VFD) to be 5.0 m/s (or Reynolds number = 10,000). The air flow is measured using digital anemometer which accuracy is ± 0.1 m/s. All of the measurement equipments such as pressure gages and thermocouples are installed according to ASHRAE requirement [19].

3. Numerical set up

The discussion in this paper is on the heat transferred to the flowing air and its pressure drop, then the domain of numerical study is focused on the air flow inside the v-corrugated channel. The apex angle of the v-corrugated channel is 20°. Its dimension was 900 mm long, 30 mm width, and 85 mm height. The delta-shaped obstacles were made congruent to the channel i.e. triangular and its dimension was 18 mm wide, 51 mm height. The obstacles were installed in one line only, because there is no much space in the channel. Thus, the spacing to be discussed is also called longitudinal pitch. To specify the obstacles' spacing, a ratio of spacing to height S/H is used. In this study, the ratio S/H used were ½, 1, 1 ½, and 2.

The numerical model for this problem was developed under some assumptions, i.e. as steady three-dimensional turbulent, incompressible flow and constant fluid properties. The space of obstacles was taken equal to height of obstacles, thus ratio is 1. Then, there are 17 obstacles used in this flow. Body force and viscous dissipation are ignored and it was assumed no radiation heat transfer. With these assumptions, [18] give the related governing equations as follow:

$$\frac{\partial u}{\partial x} + \frac{\partial v}{\partial y} + \frac{\partial w}{\partial z} = 0 \quad (1)$$

$$u \frac{\partial u}{\partial x} + v \frac{\partial u}{\partial y} + w \frac{\partial u}{\partial z} = -\frac{1}{\rho} \frac{\partial P}{\partial x} + \nu \left(\frac{\partial^2 u}{\partial x^2} + \frac{\partial^2 u}{\partial y^2} + \frac{\partial^2 u}{\partial z^2} \right) \quad (2)$$

$$u \frac{\partial v}{\partial x} + v \frac{\partial v}{\partial y} + w \frac{\partial v}{\partial z} = -\frac{1}{\rho} \frac{\partial P}{\partial y} + \nu \left(\frac{\partial^2 v}{\partial x^2} + \frac{\partial^2 v}{\partial y^2} + \frac{\partial^2 v}{\partial z^2} \right) \quad (3)$$

$$u \frac{\partial w}{\partial x} + v \frac{\partial w}{\partial y} + w \frac{\partial w}{\partial z} = -\frac{1}{\rho} \frac{\partial P}{\partial z} + \nu \left(\frac{\partial^2 w}{\partial x^2} + \frac{\partial^2 w}{\partial y^2} + \frac{\partial^2 w}{\partial z^2} \right) \quad (4)$$

$$u \frac{\partial T}{\partial x} + v \frac{\partial T}{\partial y} + w \frac{\partial T}{\partial z} = \alpha \left(\frac{\partial^2 T}{\partial x^2} + \frac{\partial^2 T}{\partial y^2} + \frac{\partial^2 T}{\partial z^2} \right) \quad (5)$$

In the above equations, ρ is the density of the air, p is the pressure, ϑ is the kinematic viscosity, α is the thermal diffusivity, and T is the temperature of the fluid. The boundary conditions of this problem were:

At the inlet: $u = 5.0$ m/s, $v = w = 0$, $T = 297.46$ K

At the upper wall which is the absorber plate: $u = v = w = 0$

At the bottom wall: $u = v = w = 0$

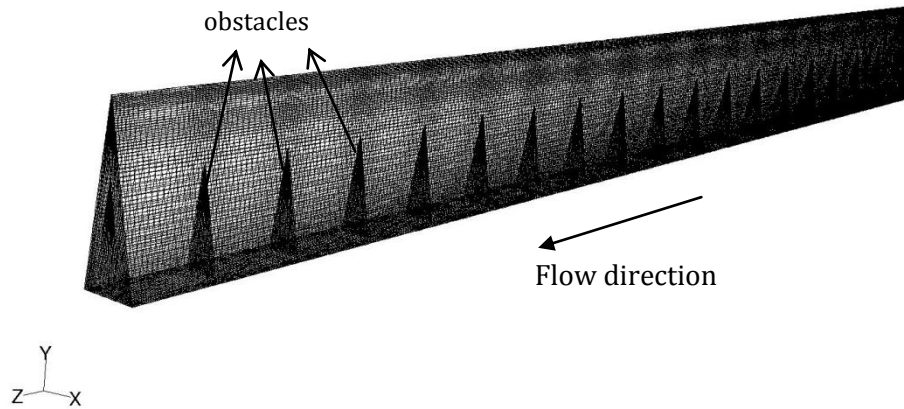
On the 17 obstacles: $u = v = w = 0$

Inlet Reynolds number was calculated with: $Re = \frac{uD_h}{\vartheta}$ (6)

In Eq. (6), D_h is hydraulic diameter and calculated with: $D_h = \frac{4A}{P}$ (7)

The area, A , in Eq. (7) is the channel cross section area, and P , is its perimeter.

The governing equations above with the boundary conditions were solved using a commercial CFD package, FLUENT 6.3.26 [20]. The grids of the domain were generated using Gambit 2.4.6. The domain and meshing used in this numerical study were shown in Fig. 2. Since the geometry is a triangular channel, the numerical study should be conducted in three dimensions and all of the meshes were designed to have quality less than 0.7.

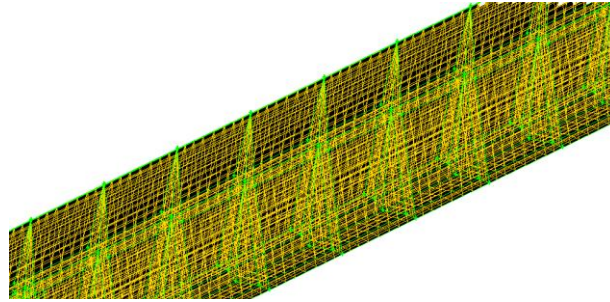


Grid

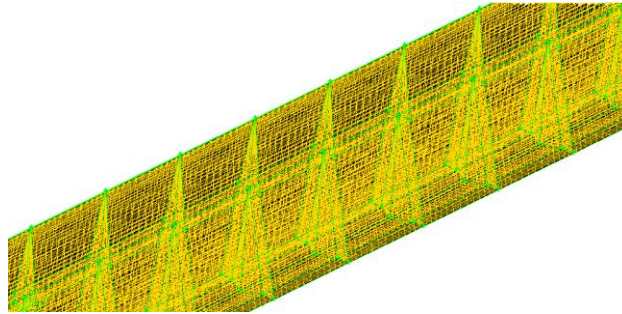
Feb 08, 2013
FLUENT 6.3 (3d, dp, pbns, ske)

Figure 2. The grid used in numerical studies

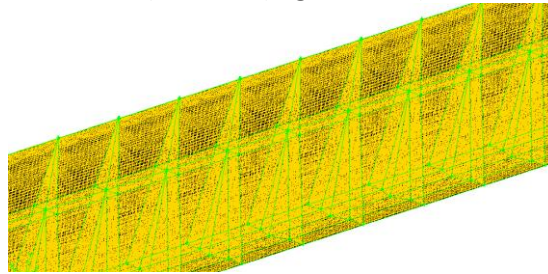
After having a good mesh, the next step is doing grid independency. The grid or mesh is made smaller to get more accurate and detailed result. But, when the mesh is too small, calculation which is done by iteration needs a very long time and might end up with diverge result. Therefore, in this study the mesh or grids were designed not uniform. The finer mesh are used for area near walls both for upper and bottom walls and then gradually the mesh are made coarser as shown in Fig 2. When there are obstacles in the flow, the mesh are designed to be finer not only near the walls but also around the obstacles in Fig 2. There are four meshes designs to be checked for independency as shown in Fig 3a), 3b), 3c), and 3d). The number of cells, faces, and nodes used in each design are shown in Table 1.



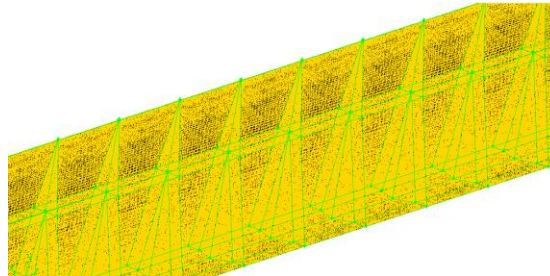
a) Mesh A (most coarse)



b) Mesh B (slight coarse)



c) Mesh C (slight fine)



d) Mesh D (most fine)

Figure 3. Mesh design checked for independency

Table 1. Number of cells, faces, and nodes of the four mesh design

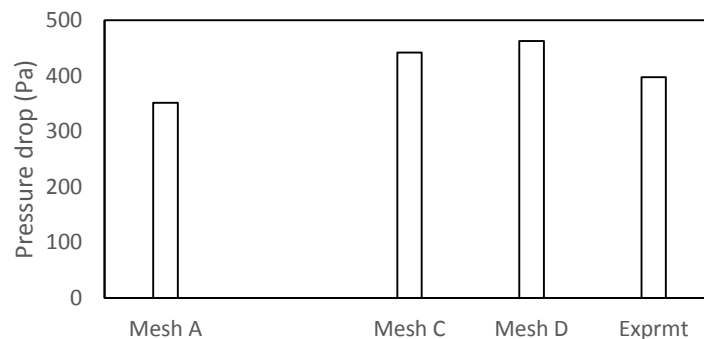
	Mesh A	Mesh B	Mesh C	Mesh D
cell	55,296	338,688	1,092,000	1,980,000
face	173,936	1,043,224	3,335,300	6,026,900
node	63,172	365,480	1,150,798	2,066,248

To check the grid independency, the result from numerical study will be compared to experiment result. The same boundary conditions and setting are used in each numerical study of the four grids design as in Fig 3. The boundary conditions are: inlet air velocity = 5.0 m/s and outflow was employed for the

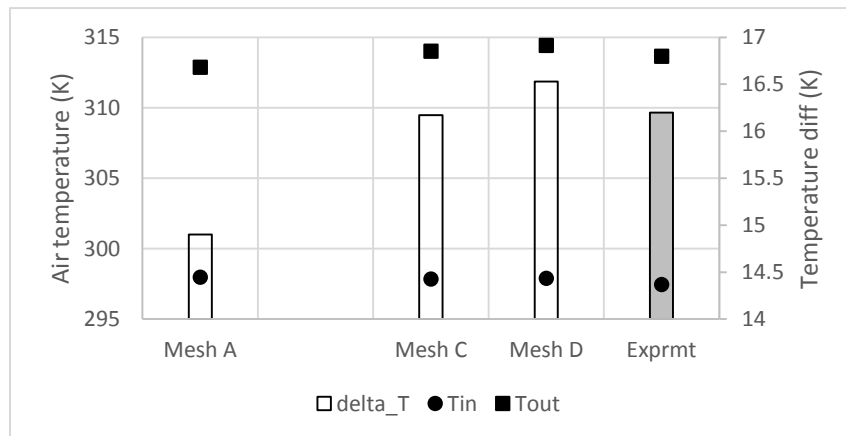
outlet; inlet air temperature = 297.46 K; and absorber plate temperature as obtained during experiments = 320 K. The settings in software used are: three dimension, double precision. Shear Stress Transport K- ω (SSTK- ω) standard turbulent model was chosen to simulate the flow. Zhang and Liu conducted a numerical simulation of the flow inside a diffusing S-duct inlet. Full three-dimensional Navier-Stokes equations are solved and SST turbulence model is employed. Numerical results, include surface static pressure, total pressure recovery at exit, are compared with experiment. A fairly good agreement is apparent [21]. Other researcher, Kirkgoz et. al. reported that numerical modelling using K- ω and SSTK- ω used on the cylinder surface gave reasonably success result [22]. The SIMPLEC algorithm was employed to deal with the problem of velocity and pressure coupling. Second-order upwind scheme were used to discretize the main governing equations. Material of the absorber, bottom plate and the obstacles is aluminum. Fluid was air with inlet pressure 1 atm and its properties, such as density, viscosity, thermal conductivity were function of temperature.

Numerical studies were conducted for each of the four mesh: A, B, C, and D. Fig 4 shows global properties resulted from the numerical studies. They were the inlet and outlet temperature of air flowing through the channel and its pressure drop. Only Mesh B could not converge and the residual could not meet the criteria. So, there was no result of Mesh B in Fig 4.

The experiment result which will be discussed in Section 4 gives pressure drop as much as 397.7 Pa, air temperature outlet 40.7°C when the air inlet velocity is 5.0 m/s and inlet air temperature 24.5°C.



a. The air pressure drop from numerical studies compared to experiment

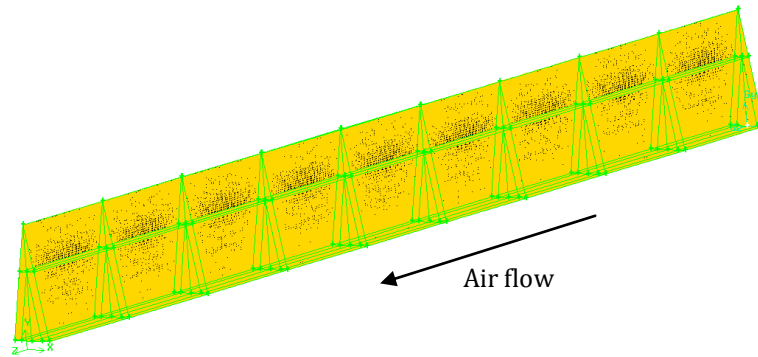


b. The air temperature from numerical studies compared to experiment

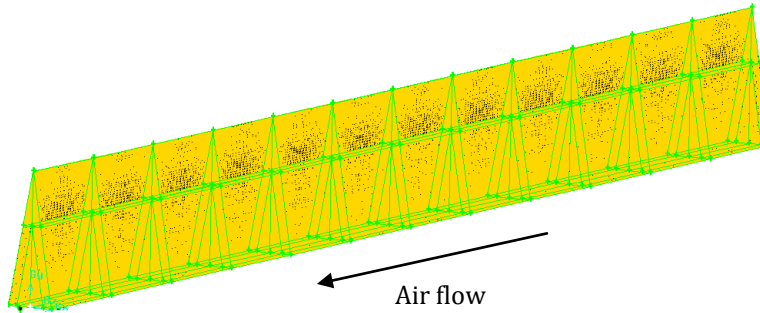
Figure 4. The numerical studies of Mesh A, C, and D compared to the result of experiment for $S/H = 1$

Fig. 4 shows that numerical study with Mesh C and D give better result of air temperature compare to experiment than Mesh A, but mesh D gives too high pressure drop result. Numerical studies using Mesh C give the most closely result to experiments. Thus, Mesh C was chosen for the numerical studies.

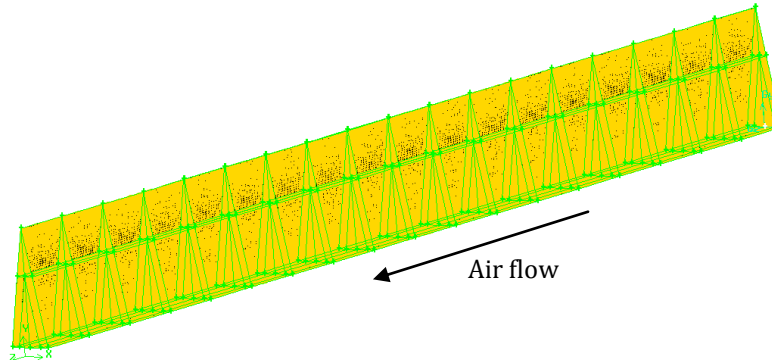
Using Mesh C pattern, some numerical studies were conducted to know the effect of obstacles' spacing. The ratio of spacing to height, S/H , studied numerically were $\frac{1}{2}$, 1, $1\frac{1}{2}$, and 2. The Mesh used in this study are in Fig. 5 a – 5 d. When the ratio S/H is bigger, then the number of obstacle is less. Number of obstacles are 8, 11, 17, and 35 for ratio $S/H = 2, 1\frac{1}{2}, 1$, and $\frac{1}{2}$, respectively.



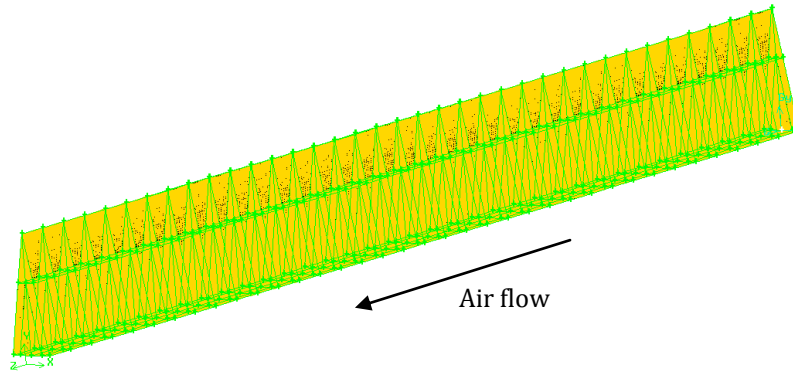
a. Ratio $S/H = 2$



b. Ratio $S/H = 1\frac{1}{2}$



c. Ratio $S/H = 1$



d. Ratio $S/H = \frac{1}{2}$

Figure 5. The Mesh used for numerical studies of each spacing to height ratio, S/H

To give more comprehensive result, numerical study was also conducted for air flow in a v-corrugated channel without obstacle. The domain and mesh used is shown in Fig. 6.

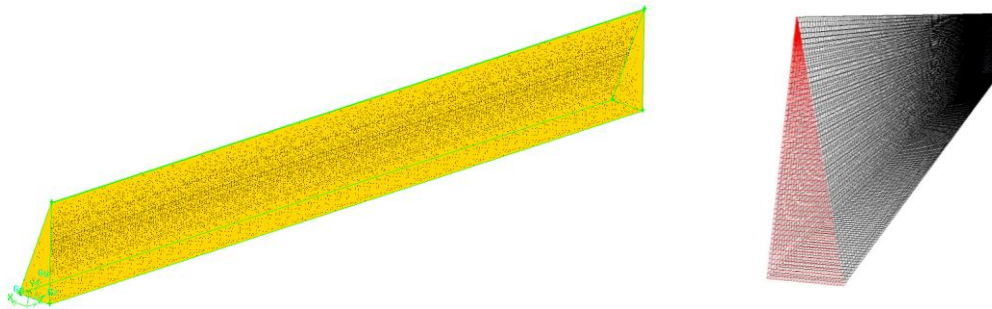


Figure 6. The Mesh used for numerical studies of air flow without obstacle

4. Results and discussion

Since the experiment is conducted to validate the numerical result, then it is not necessary to conduct experiments for all ratio S/H . The ratio S/H used in experiment equals to 1. Thus, there are 17 obstacles inserted and the percentage of air flow blockage in the channel is 36%. The experiment followed the numerical setting. The experiments were conducted at certain inlet air velocity and certain radiation intensity or absorber temperature. A VFD was used to get an inlet air velocity equals to 5.0 m/s. An adjustable turner was used to adjust the radiation intensity that make the absorber's temperature as high as 320 K or 47°C.

When the numerical result is close to the experimental result, then the numerical result is valid. Table 2 shows the comparison between numerical and experimental results at 5.0-m/s-inlet air velocity and 320 K absorber temperature. The air temperature difference and pressure drop of numeric is very close to experiment. Thus, the numerical study using several setting discussed above is acceptable and valid.

Table 2. Comparison between numerical and experimental results

	Numeric	experiment
T_{in} , K	297.9	297.5

T_{out}, K	314.4	313.7
$\Delta T, K$	16.5	16.2
$\Delta P, Pa$	462.3	450.3

To ensure that the model used in numerical study is valid, a comparison between Nusselt number from numerical result and Gnielinski equation for triangular channel without obstacle or smooth duct was conducted. According to Incropera [18], Gnielinski gives more accurate relation to calculate Nusselt number at lower Reynolds number than Dittus – Boelter equation. The relation of Nusselt number is in Equation (8):

$$Nu_D = \frac{(f/8)(Re_D - 1000)Pr}{1 + 12.7(f/8)^{1/2}(Pr^{2/3} - 1)} \quad (8)$$

The friction factor in Equation (8), f , is obtained from Moody diagram. The comparison in Fig. 7 shows that numerical simulation gives pretty accurate results.

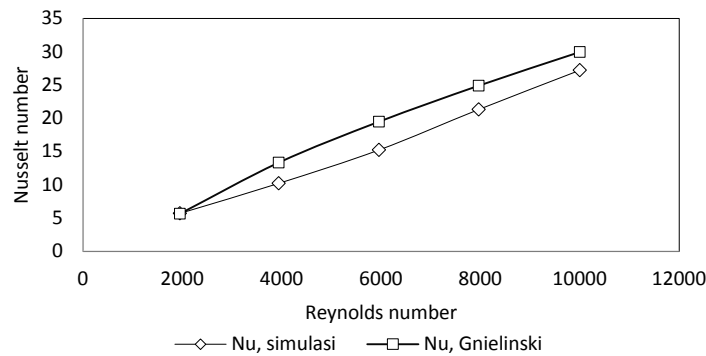
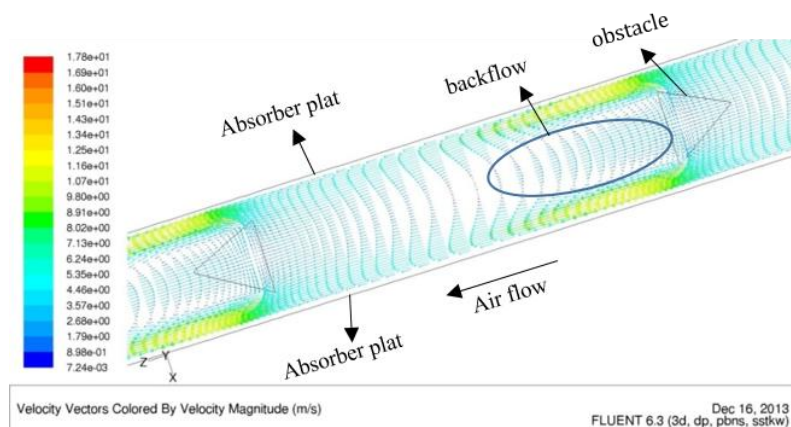


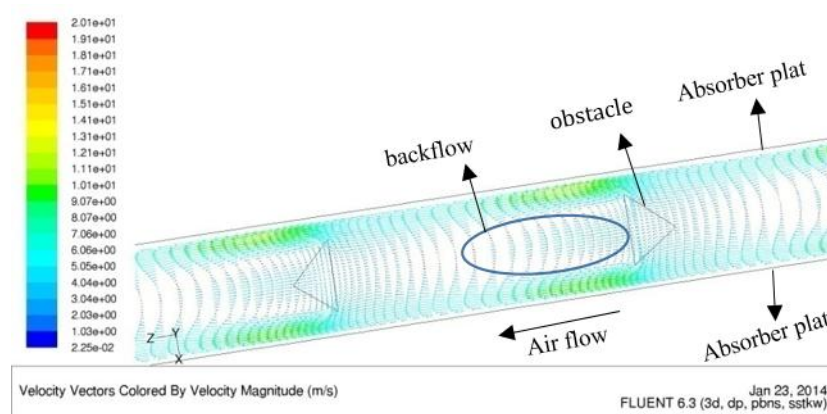
Figure 7. Comparison of Nusselt number for smooth duct (no obstacle) from numerical study and Gnielinski equation.

Having a valid grids, setting, and viscous model, the numerical study was continued to investigate the spacing effect of obstacles on the bottom plate of air duct. Diagrams of velocity vector of air flow around the obstacles inserted at ratio S/H equals to 2, $1 \frac{1}{2}$, 1, and $\frac{1}{2}$ are shown in Figure 8 a), 8 b), 8 c), and 8 d), respectively. All of the velocity vectors were taken at height $y = 10$ mm from the bottom plate. When the ratio $S/H = 2$, the spacing between obstacles = 100 mm. For ratio $S/H = 1 \frac{1}{2}$, the spacing = 75

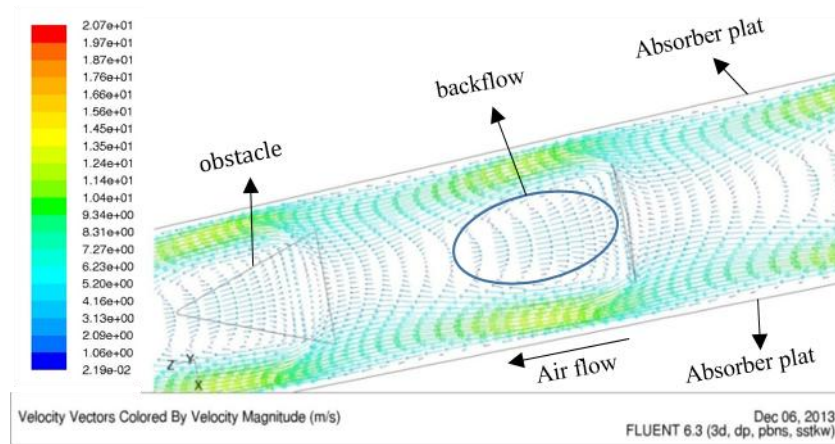


mm, and for ratio $S/H = \frac{1}{2}$, the spacing = 25 mm.

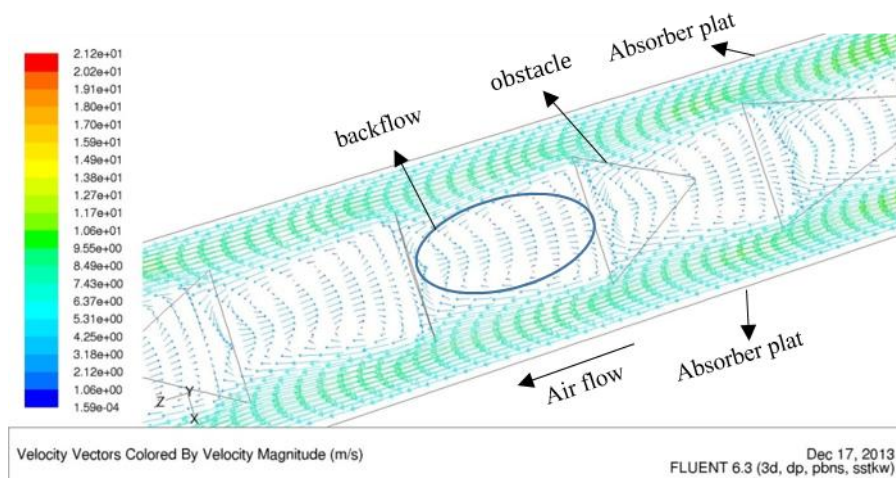
a) Velocity vector of air flow around *obstacle* with ratio $S/H = 2$



b) Velocity vector of air flow around *obstacle* with ratio $S/H = 1 \frac{1}{2}$



c) Velocity vector of air flow around *obstacle* with ratio $S/H = 1$



d) Velocity vector of air flow around obstacle with ratio $S/H = \frac{1}{2}$

Figure 8. Velocity vector of air flow around obstacle with some ratio S/H

Figure 8 a) – 8 d) show how the air flow encounters separation when flow through obstacles. The obstacles cause backflow between two consecutive obstacles in downstream. There are more backflows when the obstacles' spacing are closer and they cause a higher pressure drop. The air velocity looks higher near absorber plate when there is backflow or swirl in the flow. This high air velocity makes flow become more turbulent and more heat transferred from the absorber plate to the air. This convection heat transfer to the air makes outlet air temperature higher. Thus, the closer the obstacles' spacing makes the higher pressure drop and higher convection heat transfer from the absorber plate to the air flow.

When the spacing between obstacles is twice its height (ratio $S/H = 2$), small amount of air flow is blocked by obstacles and causes backflow behind the obstacles. The backflow caused by separation gradually diminish between two obstacles in downstream as shown in Fig 8 a). Since the air is blocked, most of air is forced to flow in the gap between obstacles and absorber plate. It is shown by longer and higher vector of velocity in the gap. More air is heated by absorber plate. Furthermore, higher velocity increases Reynold number and make the flow more turbulent. More turbulent flow gives higher Nusselt number and definitely increase the convection heat transfer. Thus, obstacles makes outlet air temperature higher than without any [17]. Flow in spacing between obstacles experiences backflow after hitting obstacles and then it reattaches quickly when the ratio $S/H = 2$. When the ratio S/H or spacing between obstacles is smaller, as shown in Fig 8 b) – 8 d), backflow is more dominant than reattached flow in area between the obstacles. When backflow occurs, more air will flow in the gap and contact with absorber plate which is the heat source. It is the reason that smaller obstacles' spacing makes higher air outlet temperature and higher SAH's efficiency. The backflow in space between obstacles contributes pressure drop in the flow. More backflow causes higher pressure drop in air acrossed the v-corrugated absorber plate SAH.

Numerical studies also provide some global properties of the flow, such as the air inlet and outlet temperature, and pressure drop. These data were used to acquire the efficiency and friction factor of the air flow in a v-corrugated SAH with delta-shaped obstacles. The efficiency and friction factor are calculated using Equation (9) and (10) according to Duffie & Beckman [23].

$$\eta = \frac{q_u}{A_c I} = \frac{\dot{m}_f c_p (T_{fo} - T_{fi})}{A_c I} \quad (9)$$

$$f = \frac{\Delta P}{\frac{L}{D_h} \rho \frac{v^2}{2}} \quad (10)$$

Comparison of efficiency and friction factor for some ratio S/H from numerical studies is shown in Fig 9. Ratio $S/H = 0$ in Fig. 9 means no obstacle in the air flow. Obstacles arranged with ratio $S/H = \frac{1}{2}$ gives the highest air efficiency, i.e. 68% and also highest fricition factor, i.e. 0.628 for air flowing in a v-corrugated duct, as shown in Fig. 9. For comparison, efficiency when no obstacle is only 49% and friction factor is only 0.0316. This findings are matching with the flow structure discussed above. The obstacles block the air flow and force it to have more contact with absorber plate. Not only forcing the air to the absorber plate, obstacles also causing more backflow. More obstacles produce higher efficiency and higher

friction factor. SAH requires high efficiency or high outlet air temperature, but low friction or pressure drop. Increasing friction factor means increasing pumping power required in SAH.

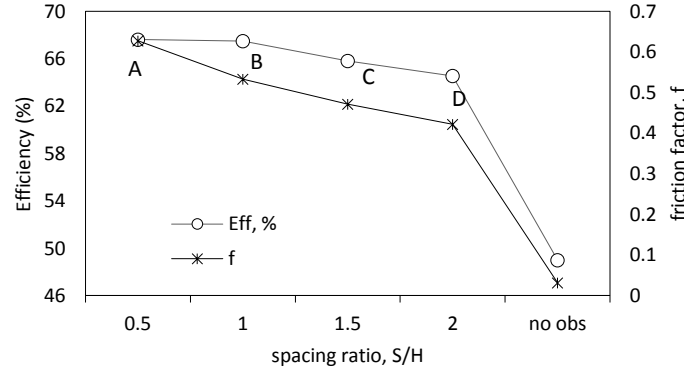


Figure 9. The efficiency of SAH and friction factor of flow with some ratio S/H of obstacles.

Besides efficiency, Nusselt number is interesting to be analyzed. It could be calculated using equation (11).

$$h = \frac{Nu_D k}{D_h} \quad (11)$$

While the convection heat transfer rate and log-mean temperature difference could be calculated using equation (12) and (13).

$$q = h A \Delta T_{lm} \quad (12)$$

$$\Delta T_{lm} = \frac{(T_{abs} - T_o) - (T_{abs} - T_i)}{\ln \frac{(T_{abs} - T_o)}{(T_{abs} - T_i)}} \quad (13)$$

The ratio S/H of obstacles effect the Nusselt number of air flow as shown in Fig. 10. Nusselt number of air flow with obstacles are much higher than without obstacle. The highest Nu number and friction factor are 94.2 and 0.628 at ratio S/H = 0.5 and is only 27.2 and 0.0316 at no obstacle. Fig. 11 shows the enhancement of Nusselt number when obstacles inserted in the flow compare to air flow with no obstacle. Nusselt number enhancement was the Nusselt number with obstacles compare to Nusselt number without obstacle. When obstacles inserted with ratio S/H = 0.5, Nusselt number increases 3.46 times and friction factor increases 19.9 times compare to those without obstacle.

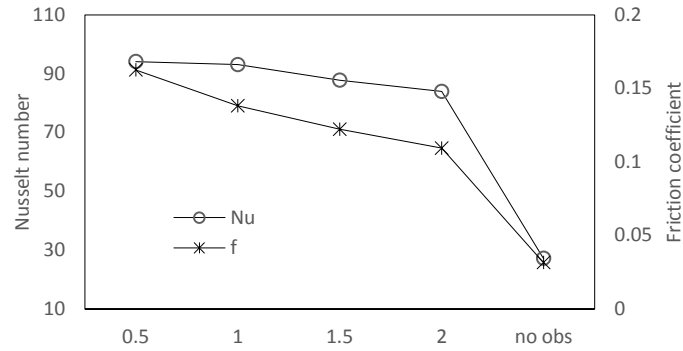


Figure 10. Nusselt number and friction factor of air flow with obstacles inserted at some spacing ratio S/H

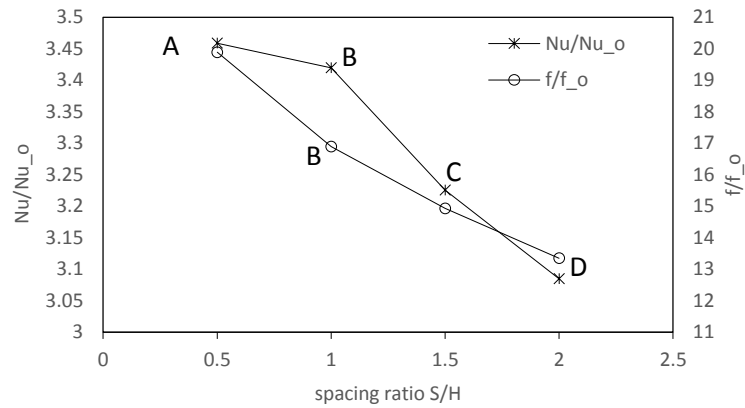


Figure 11. Enhancement Nusselt number and increasing friction factor for some spacing ratio S/H

Fig. 9, 10, and 11 showed the same trend of SAH's efficiency, Nusselt number, and its enhancement. From efficiency and Nusselt number perspective, point A is the best, but from friction factor perspective, point D is the best. The gradient of friction factor in segment A-B is the sharpest among other segments. While the gradient of efficiency and Nusselt number enhancement in segment A-B is the least. The efficiency and Nusselt number in point B is only slightly less than point A. The Nu enhancement in point A is 3.46 and reduce to be 3.42 in point B. Thus, the reduction is only 1.13%. While the reduction of friction factor from point A to point B is 15.1% that is from 19.9 to 16.9. Sacrifice a little efficiency or Nusselt number (convection heat transfer) but save a lot friction factor (pressure drop) shall be a wise choice. So, the optimal spacing ratio, S/H of delta-shaped obstacles attached to a v-corrugated SAH is one. Since the thermal efficiency, Nusselt number, and friction factor are non-dimensional parameters, the result could be applied to other SAH that has different geometry dimension but the same configuration.

5. Comparison to Others' Research

Karim & Hawlader [2] worked on a flat plate solar collector with and without fin and v-corrugated absorber plate solar collector which schema is shown in Fig. 12. Dimension of the collector used is 1.8 m x 0.7 m.

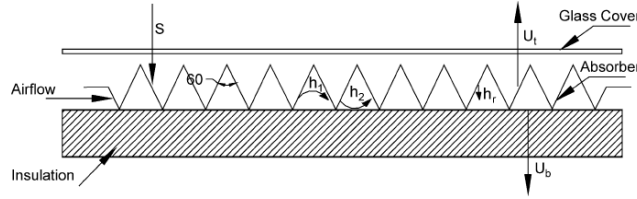


Figure 12. A v-corrugated solar collector used by Karim & Hawlader

The air flow rate generated by the blower in experiment of this paper that is nearest to Karim & Hawlader's SAH is 0.01164 kg/m²s. The comparison of the efficiency of two collectors is shown in Fig. 13.

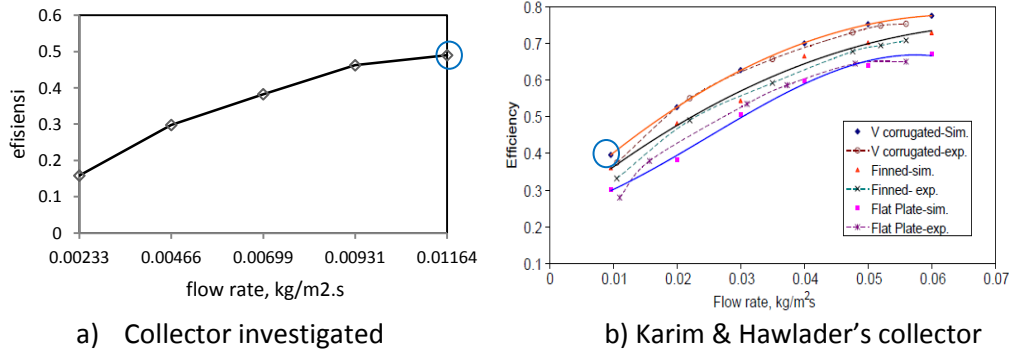


Figure 13. Comparison of the efficiency of collector investigated to Karim & Hawlader's.

The efficiency of SAH investigated is 0.49 and of Karim & Hawlader is 0.4, as in Fig 13. There is a slight difference because the air flow rate is not exactly the same. Therefore, the finding in this paper is look alike with Karim & Hawlader's finding for v-corrugated absorber plate solar collector.

Akpinar & Koçyiğit [13] conducted research on flat plate solar collector with two air mass flow rates, i.e. 0.0074 kg/s and 0.0052 kg/s. There were four collectors used as shown in Fig 14. Three collectors were given obstacles on absorber flat plate. The comparison of Akpinar & Koçyiğit's collector (type II) to investigated collector is shown in Fig. 15. The efficiency of investigated collector is for air mass flow rate 0.00729 kg/s. Parameter $(T_o - T_a) / I$ of the investigated collector is slightly lower, because the air temperature across the investigated collector is lower than Akpinar & Koçyiğit collector. It is because the dimension of investigated collector is smaller than Akpinar & Koçyiğit's. The area of investigated collector was only 900 mm x 87 mm compared to Akpinar & Koçyiğit's that was 1.2 m x 0.7 m. Yet, the difference shown in Fig 15 is not too big. It seems a good conformity between the investigated collector and Akpinar & Koçyiğit's.

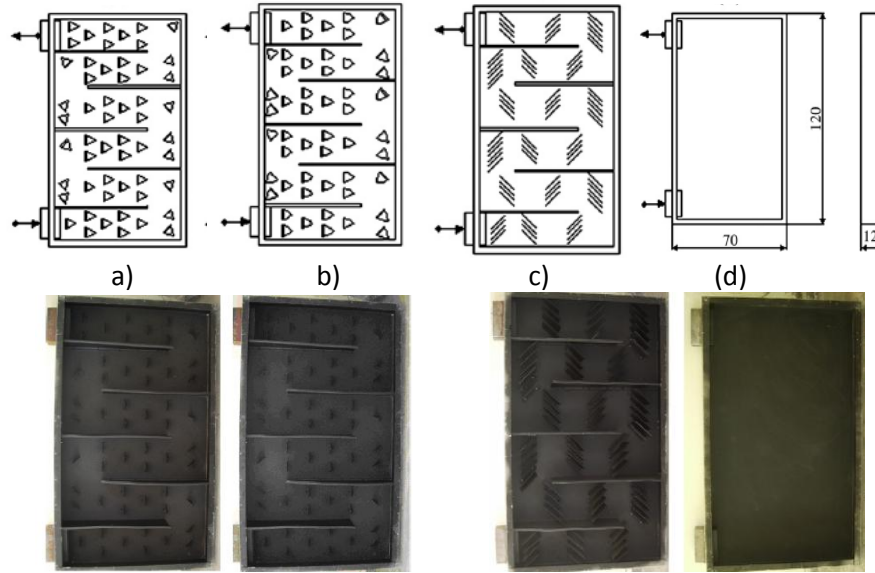
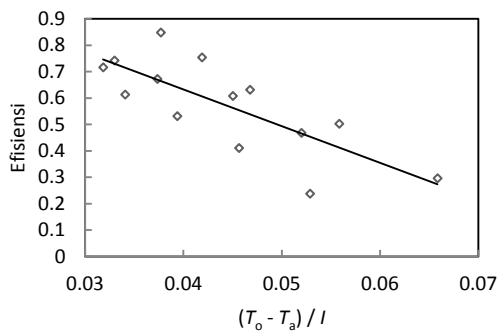
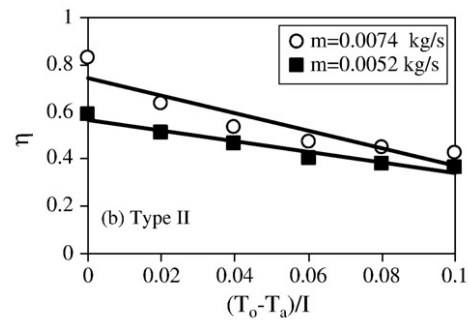


Figure 14. Schematic views of absorber plates: a) with triangular type obstacles, b) with leaf type obstacles, c) with rectangular type obstacles, d) without obstacles [13]



a) collector investigated



b) Akpinar & Koçyiğit's collector

Figure 15. Comparison of efficiency of Akpinar & Koçyiğit's collector and investigated collector

Bekele, et. al. [14] conducted experimental investigation on flat plate SAH with delta-shaped obstacles mounted on the absorber surface as shown in Fig. 16. Some parameter to be investigated by Bekele, et. al. were Reynolds number (from 3400 to 27600), longitudinal pitch of the obstacles P_l/e (from 3/2 to 11/2), and relative obstacle height, e/H (from 0.25 to 0.75). The smaller P_l/e and the higher e/H , the efficiency is higher. The term “e” used by Bekele, et. al. means obstacle's height and “H” means the height of the channel. Bekele, et. al. used P_l/e while the investigated collector used S/H term. The “S” that indicates spacing of obstacles is the same with “ P_l ” that indicates longitudinal pitch (spacing). The comparison of Bekele, et. al.'s collector and collector being investigated (height of obstacle to channel's height, $e/H = 0.6$ and spacing or longitudinal pitch, $P_l/e = 1$ and 3/2) is shown in Fig. 17.

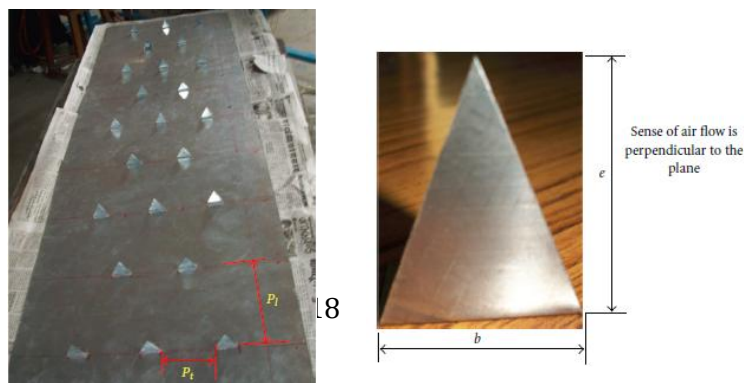
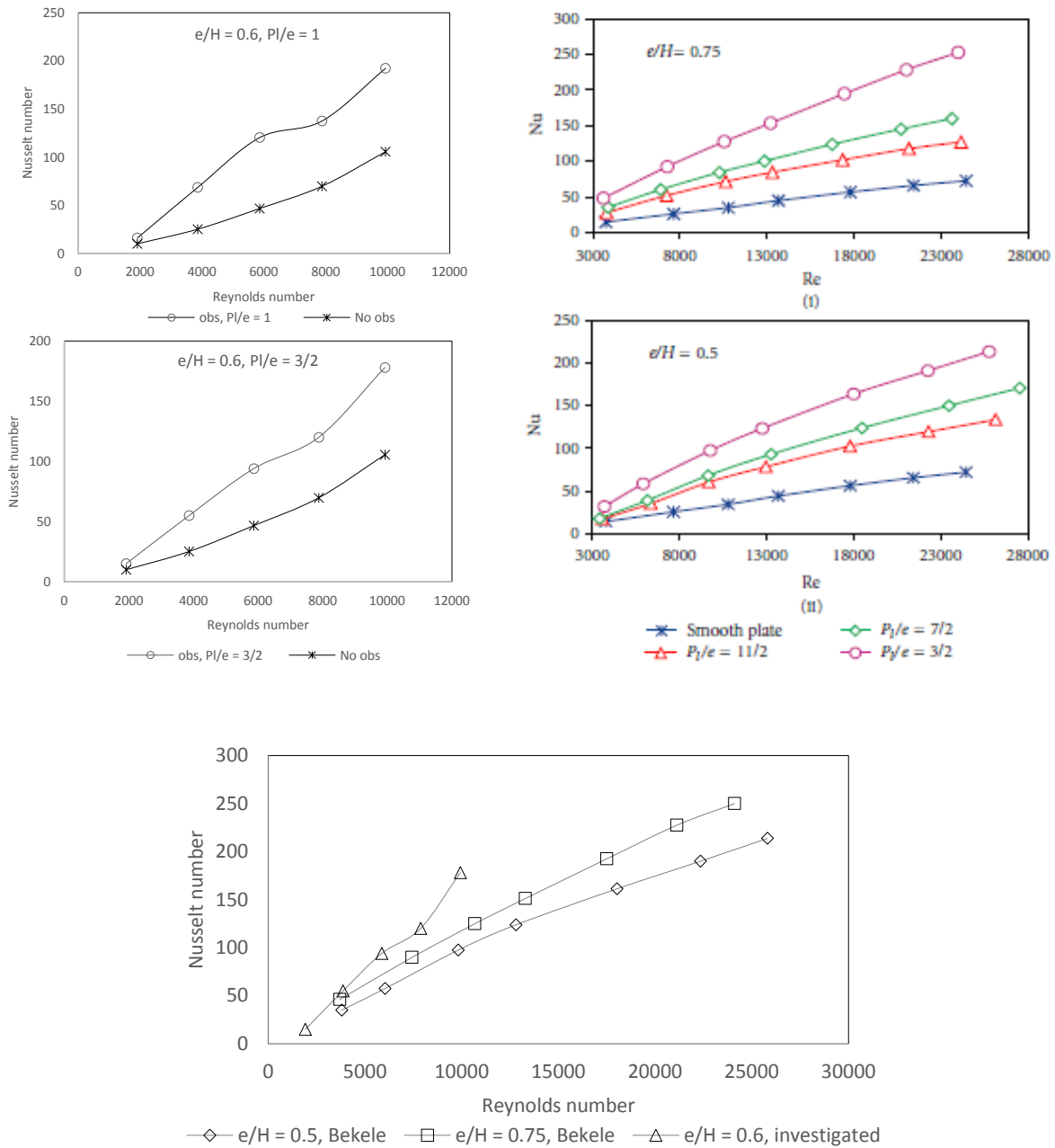


Figure 16. Photographic view of plate with delta-shaped obstacles mounted.



For smooth duct or no obstacle installed, the Nusselt number of investigated collector is higher than Bekele, et. al.'s. It is because the channel of investigated collector is triangular. This is consistent with the finding of Tao Liu, et. al., Karim and Hawlader, Choudhury and Garg, Naphon, Islamoglu and Parmaksizoglu [1] [2] [3] [4] [5]. Yet, the result of Bekele, et. al.'s and the investigated collector show the same trend, i.e. the smaller P_1/e gives higher Nusselt number. It means more obstacles increase heat transfer to the air. The relative obstacle height used in Bekele, et. al.'s collector was 0.5 and 0.75, while

in the investigated collector was 0.6. The comparison of the results is shown in Fig. 18. When Reynolds number around 10,000 and ratio $P/e = 3/2$, Nusselt number of investigated collector was 178 for $e/H = 0.6$ and Nusselt number of Bekele, et. al. was 98 for $e/H = 0.5$ and 125 for $e/H = 0.75$. Like in collector without obstacle, the Nusselt number of investigated collector is also slightly higher than from Bekele, et. al. Yet, the result from this investigated collector is showing the same trend with the finding of Bekele, et. al.

6. Conclusion

From numerical studies in a v-corrugated duct, it is found that backflow between obstacles and high velocity in the gap between obstacles and absorber plate causes the flow became more turbulent and enhanced the convection heat transfer between the air and the absorber plate. Thus, when it is applied to SAH, it will improve its efficiency but increase the air pressure drop.

Obstacles placed in a small spacing will increase Nusselt number (convection heat transfer) and friction factor (pressure drop). The Nusselt number enhanced from 27.2 when no obstacle used to 94.2 when obstacles inserted with $S/H = 0.5$. The Nusselt enhanced 3.46 times. The friction factor will increase from 0.0316 at no obstacle to 0.628 at ratio $S/H = 0.5$. The friction factor increased 19.9 times.

Efficiency, Nusselt number, and friction factor are decreasing as ratio S/H is increasing. When ratio S/H used is 1 instead of 0.5, Nusselt number enhancement decreased only 1.13%, but friction factor decreased 15.1%. So, sacrificing a small amount of Nusselt number but reducing a significant friction factor is advantageous. The optimal spacing ratio S/H of delta-shaped obstacles inserted in a v-corrugated SAH is one. In other words, the optimal spacing of obstacle equals to its height.

Acknowledgement

Here, I am very grateful for the support from Kopertis Wilayah VII Jawa Timur, Kementerian Pendidikan dan Kebudayaan by providing Research Grant under contract no: 0004/SP2H/PP/K7/KL/II/2012.

Nomenclature

W	wide of the obstacle (mm)
H	height of the obstacle (mm)
S	spacing between the obstacles (mm)
x, y, z	coordinates
Re	Reynolds number
C_p	specific heat of air (J/kg.K)
\dot{m}_f	mass flow rate of the fluid – air (kg/s)
\dot{Q}_u	useful heat transfer rate (Watt)
I	radiation intensity (W/m ²)
A_c	collector aperture area (m ²)
T_o	collector outlet temperature (K)
T_i	collector air inlet temperature (K)

T_{abs}	absorber temperature (K)
D_h	hydraulic diameter (m)
Nu_D	Nusselt number
h	convection heat transfer coefficient (W/m ² .K)
f	friction factor
ϑ	air kinematic viscosity (m ² /s)
ρ	air density (kg/m ³)
k	thermal conductivity (W/m.K)
α	air thermal diffusion coefficient (m ² /s)
η	thermal efficiency of SAH

References

- [1] L. Tao, X. L. Wen, F. G. Wen dan X. L. Chan, "A Parametric study on the termal performance of a solar air collector with a V-groove absorber," *Int. J. of Green Energy*, 4, p. 601–622, 2007.
- [2] M. A. Karim dan M. N. A. Hawlader, "Performance Investigation of Flat Plate, V-Corrugated and Finned Air Collector," *Energy* 31, pp. 452–470, 2006.
- [3] C. Choudhury dan H. P. Garg, "Design Analipsis of Corrugated and Flat Plate Solar Air Heaters.," *Renewable Energy Vol I, No. 5/6*, p. p. 595 – 607, 1991.
- [4] P. Naphon, "Heat transfer characteristics and pressure drop in channel with V corrugated upper and lower plates," *Energy conversion and management* 48, p. 1516 – 1524, 2007.
- [5] Y. Islamoglu dan C. Parmaksizoglu, "The effect of channel height on the enhanced heat transfer characteristics in a corrugated heat exchanger channel," *Applied Thermal Engineering* 23, p. 979–987, 2003.
- [6] P. Promvonge, "Heat transfer and pressure drop in a channel with multiple 60° V-baffles," *Int. Com. in Heat and Mass Transfer*, vol. 37, p. 835–840, 2010.
- [7] I. Kurtbas dan E. Turgut, "Experimental Investigation of Solar Air Heater with Free and Fixed Fins: Efficiency and Exergy Loss," *Int. J. of Science & Technology*, vol. Volume 1, no. No 1, pp. 75–82., 2006.
- [8] B. S. Romdhane, "The air solar collectors: Comparative study, introduction of baffles to favor the heat transfer," *Solar Energy*, vol. 81, p. 139 – 149, 2007.
- [9] C.-D. Ho, H.-M. Yeh dan T.-C. Chen, "Collector efficiency of upward-type double-pass solar air heaters with fins attached," *Int. Com. in Heat and Mass Transfer*, vol. 38, p. 49–56, 2011.
- [10] A. Abene, V. Dubois, M. Le Ray dan A. Oagued, "Study of a solar air flat plate collector: use of obstacle and application for the drying of grape," *J. of Food Engineering*, vol. 65, p. 15 – 22, 2004.
- [11] H. Esen, "Experimental energy and exergy analysis of a double-flow solar air heater having different obstacles on absorber plates," *Building and Environment*, vol. 43, p. 1046–1054, 2008.
- [12] F. Ozgen, M. Esen dan H. Esen, "Experimental investigation of thermal performance of a double-flow solar air heater having aluminium cans.," *Renewable Energy, Volume 34*, p. p. 2391–2398., 2009..

- 1
2
3
4
5 [13] E. K. Akpınar dan F. Koçyiğit, "Experimental investigation of thermal performance of solar air heater
6 having different obstacles on absorber plates," *Int. Com. in Heat and Mass Transfer*, vol. 37, p. 416–
7 421, 2010.
8
9 [14] A. Bekele, M. Mishra dan S. Dutta, "Effects of Delta-Shaped Obstacles on the Thermal Performance
10 of Solar Air Heater," *Hindawi Publishing Corporation: Advances in Mechanical Engineering*, vol.
11 2011, p. 10 pages, 2011.
12
13 [15] H. Esen, F. Ozgen, M. Esen dan A. Sengur, "Modelling of a new solar air heater through least-
14 squares support vector machines," *Expert Systems with Applications* 36, pp. 10673-10682, 2009.
15
16 [16] H. Esen, F. Ozgen, M. Esen dan A. Sengur, "Artificial neural network and wavelet neural network
17 approaches for modelling of a solar air heater," *Expert Systems with Applications* 36, pp. 11240-
18 11248, 2009.
19
20 [17] E. A. Handoyo, D. Ichsani, Prabowo dan Sutardi, "Experimental Studies on a Solar Air Heater Having
21 V-Corrugated," *Applied Mechanics and Materials*, vol. 493, pp. 86-92, 2014.
22
23 [18] F. P. Incropera dan D. P. DeWitt, *Fundamentals of Heat and Mass Transfer*. 5th edition ed. s.l.: John
24 Wiley & Sons., 2002.
25
26 [19] ASHRAE, *Method of Testing to Determine the Thermal Performance of Solar Collectors*, Atlanta:
27 ASHRAE, 1986.
28
29 [20] I. FLUENT, *FLUENT User's Guide*, 2003.
30
31 [21] L. Zhang dan Z. Liu, "A Numerical Simulation of the Flow in a Diffusing S-Duct Inlet," *Modern Applied*
32 *Science*, vol. Vol. 3, no. No. 4, pp. 111-116, 2009.
33
34 [22] M. S. Kirkgoz , A. A. Oner dan M. S. Aköz, "Numerical modeling of interaction of a current with a
35 circular cylinder near a rigid bed," *Advances in Engineering Software*, vol. 40, p. 1191–1199, 2009.
36
37 [23] J. A. Duffie dan W. A. Beckman, *Solar Engineering Of Thermal Processes*, 2nd ed. penyunt., John
38 Wiley & Sons, Inc., 1991.
39
40
41
42
43
44
45
46
47
48
49
50
51
52
53
54
55
56
57
58
59
60
61
62
63
64
65

Elsevier Editorial System(tm) for Solar

Energy

Manuscript Draft

Manuscript Number:

Title: Numerical Studies on the Effect of Delta-Shaped Obstacles' Spacing on the Heat Transfer and Pressure Drop in V-Corrugated Channel of Solar Air Heater

Article Type: Regular Paper

Section/Category: Solar heating and cooling, buildings & other applications

Keywords: delta-shaped obstacle; v-corrugated channel; solar air heater; numerical study

Corresponding Author: Dr. Ekadewi Anggraini Handoyo, Dr

Corresponding Author's Institution: Petra Christian University

First Author: Ekadewi Anggraini Handoyo, Dr

Order of Authors: Ekadewi Anggraini Handoyo, Dr; Ichsani Djatmiko, Prof.; Prabowo Prabowo, Prof.; Sutardi Sutardi, Prof.

Abstract: Solar air heater (SAH) is simple in construction compared to solar water heater. Yet, it is very useful for drying or space heating. Unfortunately, the convective heat transfer between the absorber plate and the air inside the solar air heater is rather low. Some researchers reported that obstacles are able to enhance the heat transfer in a flat plate solar air collector and others found that a v-corrugated absorber plate gives better heat transfer than a flat plate. There was research combine these two in a SAH. Yet, the spacing between obstacles was not studied yet. Whereas, its spacing possibly will effect the heat transfer and pressure drop of the air flowing across the channel.

The first step in numerical study is generating mesh or grid of the air flow inside a v-corrugated channel which was blocked by some delta-shaped obstacles. The mesh was designed three-dimension and not uniform. The mesh are made finer for area near obstacles and walls both for upper and bottom, and then gradually coarser. Grid independency is the next step to be conducted. When the mesh is already independent, the numerical study begins. To validate the numerical model, an indoor experiment was conducted. Turbulent model used was Shear Stress Transport K- ω (SSTK- ω) standard. Having a valid numerical model, the spacing between obstacles was studied numerically. Ratio spacing to height, S/H of obstacles investigated were 0.5; 1; 1.5; and 2.

From numerical studies in a v-corrugated duct, it is found that backflow between obstacles and high velocity in the gap between obstacles and absorber plate causes the flow became more turbulent and enhanced the convection heat transfer between the air and the absorber plate. Obstacles placed in a small spacing increase air temperature difference and pressure drop. Air temperature difference and pressure drop increase from 15.81oC and 365.89 Pa, to 16.12oC and 408.90 Pa, to 16.53oC and 462.34 Pa, to 16.56oC and 544.12 Pa for ratio S/H decreases from 2 to 1 ½ to 1, and to ½, respectively. Efficiency of SAH and friction factor are

decreasing as ratio S/H is increasing. The best delta-shaped obstacles' spacing inserted in a v-corrugated duct is equal to its height or ratio $S/H = 1$. When ratio S/H used is 1 instead of 0.5, efficiency of SAH is decreasing 0.18% and friction factor is decreasing 15%. So, sacrificing a small amount of efficiency but reducing a significant friction factor is advantageous.

Suggested Reviewers: Ebru Kavak Akpınar

ebruakpinar@firat.edu.tr

He/she write the same topic with me, i.e. obstacles in Solar Air Heater.

Adisu Bekele

addisu2005@yahoo.com

He/she write the same topic with me, i.e. obstacles in Solar Air Heater.

Md Azharul Karim

makarim@mame.mu.oz.au

He/she write the same topic with me, i.e. v-corrugated air collector.

Numerical Studies on the Effect of Delta-Shaped Obstacles' Spacing on the Heat Transfer and Pressure Drop in V-Corrugated Channel of Solar Air Heater

The research was part of my previous doctoral study. This topic was chosen as an effort to enhance the heat transfer in a solar air heater (SAH) which is usually low. A numerical study was set up to investigate the effect of obstacles' spacing used in a v-corrugated SAH. An indoor model of a SAH was constructed for validation of the numerical study. After generating 3-D mesh or grid of the air flow inside a v-corrugated channel which was blocked by some delta-shaped obstacles, grid independency is the next step to be conducted. When the mesh is already independent, the numerical study begins. Having a valid numerical model, the spacing between obstacles was studied numerically. Ratio spacing to height, S/H of obstacles investigated were 0.5; 1; 1.5; and 2.

From numerical studies in a v-corrugated duct, it is found that backflow between obstacles and high velocity in the gap between obstacles and absorber plate causes the flow became more turbulent and enhanced the convection heat transfer between the air and the absorber plate. Efficiency of SAH and friction factor are decreasing as ratio S/H is increasing. The best delta-shaped obstacles' spacing inserted in a v-corrugated duct is equal to its height or ratio $S/H = 1$. When ratio S/H used is 1 instead of 0.5, efficiency of SAH is decreasing 0.18% and friction factor is decreasing 15%. So, sacrificing a small amount of efficiency but reducing a significant friction factor is advantageous.

The corresponding author is:
Ekadewi A. Handoyo.
Jl. Siwalankerto 121 – 131 Surabaya 60236, Indonesia
Tel.: 62-31-2983465; fax: 62-31-8491215.
E-mail address: ekadewi@petra.ac.id.

This research is certainly original and all of the data are obtained via the experiments done by the authors.

Highlights

This paper explains about how to improve a Solar air heater (SAH) performance. SAH is simple in construction compared to solar water heater. But, it is very useful for drying or space heating. Unfortunately, the convective heat transfer between the absorber plate and the air inside the solar air heater is rather low.

Improving heat transfer in SAH will improve its efficiency, too. Unfortunately, the pressure drop is usually also increasing. Some efforts, such as replacing the flat absorber plate with v-corrugated plate or inserting obstacles in the flow, are using widely. Yet, the spacing between obstacles was not studied yet. Whereas, its spacing possibly will effect the heat transfer and pressure drop of the air flowing across the channel.

This paper shows the velocity vector of the air flow around the obstacles in a v-corrugated channel. Further, it describes how the smaller ratio of spacing to obstacles' height, S/H , more heat is transfered to the air and higher pressure drop. In the end, the paper concludes that sacrificing a small amount of efficiency but reducing a significant friction factor is advantageous.

Numerical Studies on the Effect of Delta-Shaped Obstacles' Spacing on the Heat Transfer and Pressure Drop in V-Corrugated Channel of Solar Air Heater

Ekadewi A. Handoyo¹, Djatmiko Ichsani², Prabowo², Sutardi²

¹Mechanical Engineering Dept, Petra Christian University, Surabaya – Indonesia

²Mechanical Engineering Dept, Institut Teknologi Sepuluh Nopember, Surabaya – Indonesia

Corresponding author: ekadewi@petra.ac.id

Abstract

Solar air heater (SAH) is simple in construction compared to solar water heater. Yet, it is very useful for drying or space heating. Unfortunately, the convective heat transfer between the absorber plate and the air inside the solar air heater is rather low. Some researchers reported that obstacles are able to enhance the heat transfer in a flat plate solar air collector and others found that a v-corrugated absorber plate gives better heat transfer than a flat plate. There was research combine these two in a SAH. Yet, the spacing between obstacles was not studied yet. Whereas, its spacing possibly will effect the heat transfer and pressure drop of the air flowing across the channel.

The first step in numerical study is generating mesh or grid of the air flow inside a v-corrugated channel which was blocked by some delta-shaped obstacles. The mesh was designed three-dimension and not uniform. The mesh are made finer for area near obstacles and walls both for upper and bottom, and then gradually coarser. Grid independency is the next step to be conducted. When the mesh is already independent, the numerical study begins. To validate the numerical model, an indoor experiment was conducted. Turbulent model used was Shear Stress Transport K- ω (SSTK- ω) standard. Having a valid numerical model, the spacing between obstacles was studied numerically. Ratio spacing to height, S/H of obstacles investigated were 0.5; 1; 1.5; and 2.

From numerical studies in a v-corrugated duct, it is found that backflow between obstacles and high velocity in the gap between obstacles and absorber plate causes the flow became more turbulent and enhanced the convection heat transfer between the air and the absorber plate. Obstacles placed in a small spacing increase air temperature difference and pressure drop. Air temperature difference and pressure drop increase from 15.81°C and 365.89 Pa, to 16.12°C and 408.90 Pa, to 16.53°C and 462.34 Pa, to 16.56°C and 544.12 Pa for ratio S/H decreases from 2 to 1 ½ to 1, and to ½, respectively. Efficiency of SAH and friction factor are decreasing as ratio S/H is increasing. The best delta-shaped obstacles' spacing inserted in a v-corrugated duct is equal to its height or ratio S/H = 1. When ratio S/H used is 1 instead of 0.5, efficiency of SAH is decreasing 0.18% and friction factor is decreasing 15%. So, sacrificing a small amount of efficiency but reducing a significant friction factor is advantageous.

Keywords: delta-shaped obstacle; v-corrugated channel, solar air heater; numerical study.

1. Introduction

Solar energy can be converted into thermal energy in a solar collector. Solar collector basically is device used to trap solar energy to heat a plate and transfer the heat to a fluid flowing under or above the plate. When sun light falls onto a plate, solar radiation reaches the plate at lower wavelength and heat it up. Then, the heat is carried away by either water or air that flows under or above the plate. Solar collector used to

heat up air is called solar air heater (SAH) and solar water heater for water. Generally, the solar air heater is less efficient than the solar water heater, because air has less thermal capacity and less convection heat transfer coefficient. Yet, air is much lighter and less corrosive than water. The other benefit is that heated air can be used for moderate-temperature drying, such as harvested grains or fish. Since the solar air heater has less convective heat transfer coefficient than solar water heater, some researchers tried to increase this convective heat transfer coefficient.

A popular type of solar air heaters is the flat plate SAH, which has a cover glass on the top, insulation on the sides and bottom to prevent heat transferred to the surrounding, a flat absorber plate that makes a passage for the air flowing with sides and bottom plate. Usually, the passage or channel has a rectangular cross-section. The absorber plate will transfer the heat to the air via convection. Unfortunately, the convection coefficient is very low. To increase the convection coefficient from the absorber plate, a v-corrugated plate is used instead of a flat plate. Tao Liu et al. (Tao, Wen, Wen, & Chan, 2007) stated that a solar air heater with a v-grooved absorber plate could reach efficiency 18% higher than the flat plate on the same operation condition and dimension or configuration. Karim and Hawlader (Karim & Hawlader, 2006) found that a solar collector with a v-absorber plate gave the highest efficiency and the flat plate gave the least. The results showed that the v-corrugated collector is 10–15% and 5–11% more efficient in single pass and double pass modes, respectively, compared to the flat plate collectors. Choudhury and Garg (Choudhury & Garg, 1991) made a detailed analysis of corrugated and flat plate solar air heaters of five different configurations. For the same length, mass flow rate, and air velocity, it was found out that the corrugated and double cover glass collector gave the highest efficiency. According to Naphon (Naphon, 2007) the corrugated surfaces give a significant effect on the enhancement of heat transfer and pressure drop. The Nusselt number of flow in a v-corrugated channel can be 3.2 – 5.0 times higher than in a plane surfaces while the pressure drop 1.96 times higher than on the corresponding plane surface. Islamoglu and Parmaksizoglu (Islamoglu & Parmaksizoglu, 2003) reported that the corrugated channel gave the higher Nusselt number than the straight channel and the higher channel height gave higher Nusselt number for the flow with the same Reynolds number.

Besides changing the cross section area of the channel, some also give effort to increase turbulence inside the channel with fins or obstacles. The result of experimental study done by Promvonge (Promvonge, 2010) in turbulent flow regime (Reynolds number of 5000 to 25,000) showed that multiple 60° V-baffle turbulator fitted on a channel provides the drastic increase in Nusselt number, friction factor, and the thermal enhancement factor values over the smooth wall channel. Kurtbas and Turgut (Kurtbas & Turgut, 2006) investigated the effect of fins located on the absorber surface in free and fixed manners. They used two kinds of rectangular fins which dimension is different but total area is the same. The first type fin (I) has dimension 810 x 60 mm and the second (II) type 200 x 60 mm. To have the same total area, there are 8 fins and 32 fins for the first and second, respectively. The fins type II, both free and fixed, were more effective than type I and flat-plate collector. The fixed fin collector was more effective than free fin collector. Romdhane (Romdhane, 2007) created turbulence in the air channel using obstacles or baffles. The efficiency of collector and the air temperature was found increasing with the use of baffles. Baffles should be used to guide the flow toward the absorber plate. Ho et al. (Ho, Yeh, & Chen, 2011) inserted fins attached by baffles and external recycling to a solar air heater. The experiment and theoretical investigations gave result that heat transfer was improved by employing baffled double-pass with external recycling and fin attached over and under absorber plate. Abene et al. (Abene, Dubois, Le Ray, & Oagued, 2004) used obstacles on the flat plate of a solar air collector for drying grape. The obstacles ensure a good air flow over

the absorber plate, create the turbulence and reduce the dead zones in the collector. Esen (Esen, 2008) used a double-flow solar air heater to investigate three different type obstacles placed on absorber plates compare with the flat plate. The collector has three absorber plates to make three passages for the air flowing through. From the research done, it was found that type III obstacles with flow in middle passage gave the highest efficiency and all collectors with obstacles gave higher efficiency than the flat plate. Akpınar and Koçyiğit (Akpınar & Koçyiğit, 2010) had experimental investigation on solar air heater with several obstacles (Type I, Type II, and Type III) and without obstacles. The optimal value of efficiency was obtained for the solar air heater with Type II obstacles on absorber plate in flow channel duct for all operating conditions and the collector with obstacles appears significantly better than that without obstacles. Bekele et al. (Bekele, Mishra, & Dutta, 2011) investigated experimentally the effect of delta shaped obstacles mounted on the absorber surface of an air heater duct. They found that the obstacle mounted duct enhances the heat transfer to the air. The heat transfer got higher if the obstacle height was taller and its longitudinal pitch was smaller.

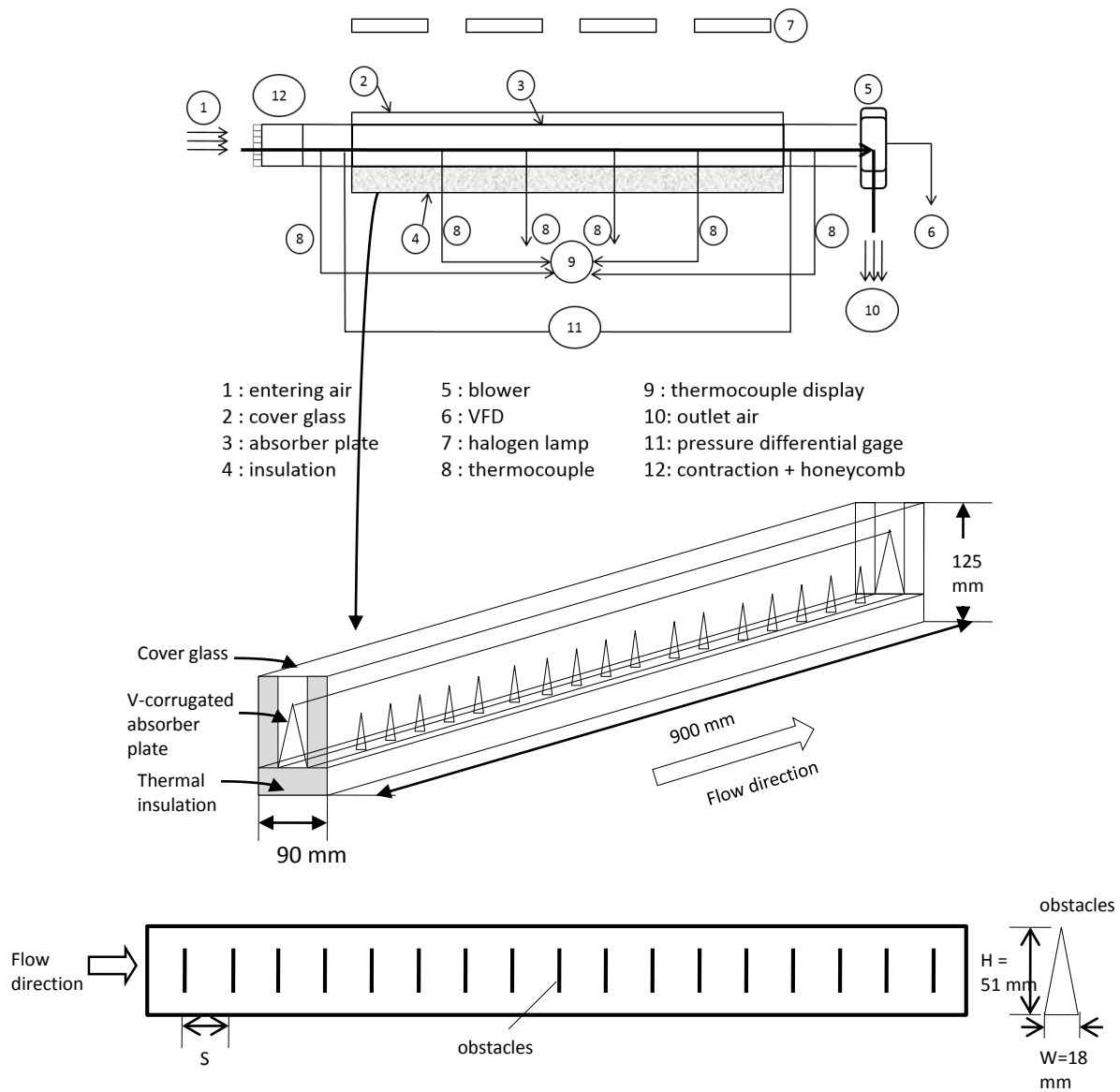
The combine of those two findings, i.e. obstacles and v-corrugated absorber plate are able to improve SAH are important to be studied. Handoyo et al. (Handoyo, Ichsani, Prabowo, & Sutardi, 2014) reported that the obstacles are able to enhance heat transfer in a v-corrugated SAH but increase the air pressure drop. To reduce the air pressure drop, the obstacles were bent vertically. The optimal bending angle is 30° . The SAH's efficiency was 5.3% lower when the obstacles bent 30° instead of straight (0°), but the pressure drop was 17.2% lower. The obstacles' spacing should also give contribution to the air pressure drop. When the spacing is large, the obstacles used is less and the air pressure drop will be reduced. What about the heat transfer? How will the spacing between obstacles effect the heat transfer from the absorber plate to the flowing air? Right now, there is no research investigating the effect of obstacles' spacing on a v-corrugated SAH performance.

This paper describes the result of the numerical studies of obstacles' spacing inserted in a v-corrugated channel of a SAH. The heat transfer from the v-corrugated absorber plate and the air pressure drop flowing the v-corrugated channel is to be discussed. The obstacles are delta-shaped and installed on bottom plate of the channel.

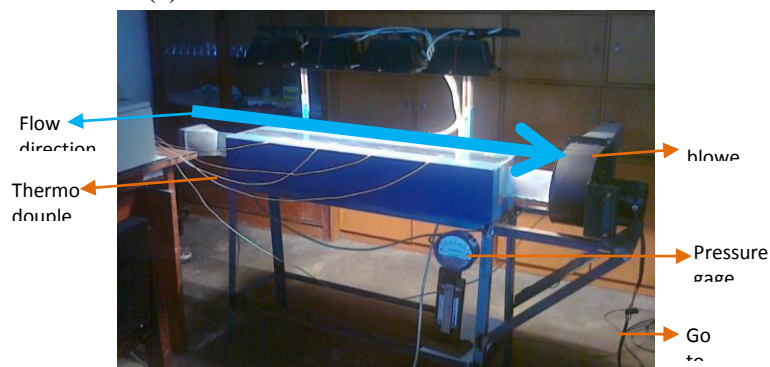
2. Experimental set-up

The studies began with choosing a solar collector model to be studied. The study will be conducted numerically. Thus, a validation is required to prove that the result is true. The validation is accomplished via experiment. An indoor experiment model was constructed to validate numerical result. It is a model of SAH using v-corrugated absorber plate. Its schematic view and photograph are shown in Fig. 1 (a) and (b), respectively. The experiment was conducted in a laboratory of Mechanical Engineering Dept of Petra Christian University, Surabaya, Indonesia.

The collector model's dimension was 900 mm long, 90 mm width, and 125 mm height. A single 3-mm transparent-tempered glass was used as the collector cover. The v-corrugated absorber plate was made of 0.8-mm-thick aluminum and painted black. The apex angle of the v-corrugated plate was 20° . The v-corrugated channel's cross section was 30 mm width and 85 mm height. To prevent heat loss, the left and right walls of collector are insulated with a 25-mm Styrofoam each and a 35-mm Styrofoam for the bottom. The delta-shaped obstacles were made congruent to the channel i.e. triangular and its dimension was 18 mm wide, 51 mm height.



(a) Schematic of the solar collector model



(b) Photograph of experimental set-up.

Fig 1. The SAH model used in experiment

The experiment was conducted indoor to maintain the radiation intensity, wind's velocity and temperature. So, a bias result caused by different outdoor condition could be avoided. The sunlight is replaced with four 500-Watt halogen lamps. The radiation intensity received on the collector was measured using a pyranometer (Kipp & Zonen, type SP Lite2) placed on top of the cover glass. To ensure the homogenous intensity and to generate a certain absorber plate's temperature, these lamps were equipped with adjustable turner individually. The surrounding air condition was controlled by an air conditioner installed in the room. Its temperature, humidity, and wind velocity are well controlled. The collector was equipped with T-type thermocouple which accuracy is 0.1°C for measuring the air temperature at inlet and outlet of the collector, temperature of the absorber plate (at four different locations), and ambient temperature. The pressure drop between inlet and outlet of the flowing air across the collector is also measured with a Magnehelic differential pressure gage which accuracy is ± 2 Pa. A centrifugal blower (1000 m³/h, 580 Pa, 0.2 kW, 380 Volt input) was used to induce the air flowing through the collector. The air flow was adjusted by means of a variable-frequency drive (VFD) to be 5.0 m/s (or Reynolds number = 10,000). The air flow is measured using digital anemometer which accuracy is ± 0.1 m/s. All of the measurement equipments such as pressure gages and thermocouples are installed according to ASHRAE requirement (ASHRAE, 1986).

3. Numerical set up

The discussion in this paper is on the heat transferred to the flowing air and its pressure drop, then the domain of numerical study is focused on the air flow inside the v-corrugated channel. The apex angle of the v-corrugated channel is 20°. Its dimension was 900 mm long, 30 mm width, and 85 mm height. The delta-shaped obstacles were made congruent to the channel i.e. triangular and its dimension was 18 mm wide, 51 mm height. The obstacles were installed in one line only, because there is no much space in the channel. Thus, the spacing to be discussed is actually longitudinal pitch. To specify the obstacles' spacing, a ratio of spacing to height S/H is used. In this study, the ratio S/H used were ½, 1, 1 ½, and 2.

The numerical model for this problem was developed under some assumptions, i.e. as steady three-dimensional turbulent, incompressible flow and constant fluid properties. The space of obstacles was taken equal to height of obstacles, thus ratio is 1. Then, there are 17 obstacles used in this flow. Body force and viscous dissipation are ignored and it was assumed no radiation heat transfer. With these assumptions, (Incropera & DeWitt, 2002) give the related governing equations as follow:

$$\frac{\partial u}{\partial x} + \frac{\partial v}{\partial y} + \frac{\partial w}{\partial z} = 0 \quad (1)$$

$$u \frac{\partial u}{\partial x} + v \frac{\partial u}{\partial y} + w \frac{\partial u}{\partial z} = -\frac{1}{\rho} \frac{\partial P}{\partial x} + \vartheta \left(\frac{\partial^2 u}{\partial x^2} + \frac{\partial^2 u}{\partial y^2} + \frac{\partial^2 u}{\partial z^2} \right) \quad (2)$$

$$u \frac{\partial v}{\partial x} + v \frac{\partial v}{\partial y} + w \frac{\partial v}{\partial z} = -\frac{1}{\rho} \frac{\partial P}{\partial y} + \vartheta \left(\frac{\partial^2 v}{\partial x^2} + \frac{\partial^2 v}{\partial y^2} + \frac{\partial^2 v}{\partial z^2} \right) \quad (3)$$

$$u \frac{\partial w}{\partial x} + v \frac{\partial w}{\partial y} + w \frac{\partial w}{\partial z} = -\frac{1}{\rho} \frac{\partial P}{\partial z} + \vartheta \left(\frac{\partial^2 w}{\partial x^2} + \frac{\partial^2 w}{\partial y^2} + \frac{\partial^2 w}{\partial z^2} \right) \quad (4)$$

$$u \frac{\partial T}{\partial x} + v \frac{\partial T}{\partial y} + w \frac{\partial T}{\partial z} = \alpha \left(\frac{\partial^2 T}{\partial x^2} + \frac{\partial^2 T}{\partial y^2} + \frac{\partial^2 T}{\partial z^2} \right) \quad (5)$$

In the above equations, ρ is the density of the air, p is the pressure, ϑ is the kinematic viscosity, α is the thermal diffusivity, and T is the temperature of the fluid. The boundary conditions of this problem were:

At the inlet: $u = 5.0$ m/s, $v = w = 0$, $T = 297.46$ K

At the upper wall which is the absorber plate: $u = v = w = 0$

At the bottom wall: $u = v = w = 0$

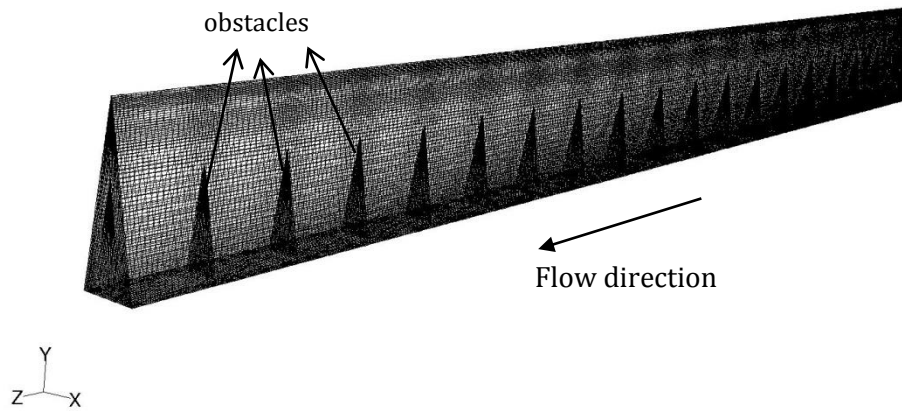
On the 17 obstacles: $u = v = w = 0$

Inlet Reynolds number was calculated with: $Re = \frac{uD_h}{\nu}$ (6)

In Eq. (6), D_h is hydraulic diameter and calculated with: $D_h = \frac{4A}{P}$ (7)

The area, A , in Eq. (7) is the channel cross section area, and P , is its perimeter.

The governing equations above with the boundary conditions were solved using a commercial CFD package, FLUENT 6.3.26 (FLUENT, 2003). The grids of the domain were generated using Gambit 2.4.6. The domain and meshing used in this numerical study were shown in Fig. 2. Since the geometry is a triangular channel, the numerical study should be conducted in three dimensions and all of the meshes were designed to have quality less than 0.7.

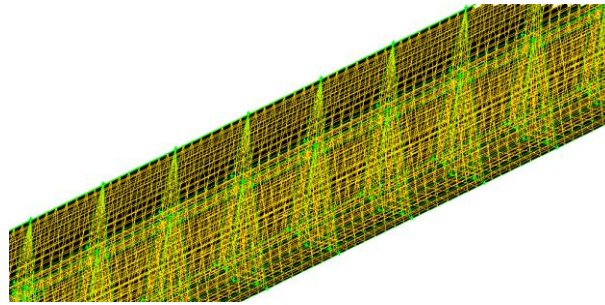


Grid

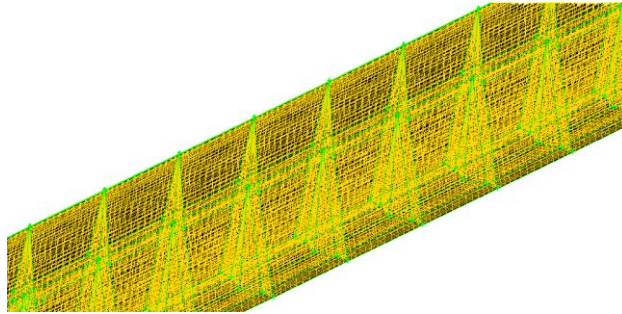
Feb 08, 2013
FLUENT 6.3 (3d, dp, pbns, ske)

Fig 2. The grid used in numerical studies

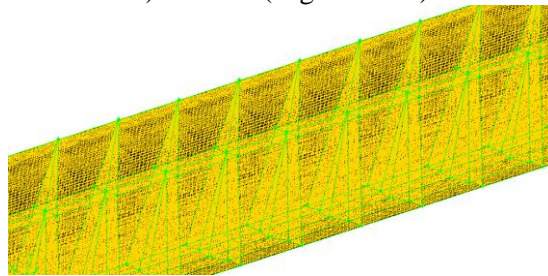
After having a good mesh, the next step is doing grid independency. The grid or mesh is made smaller to get more accurate and detailed result. But, when the mesh is too small, calculation which is done by iteration needs a very long time and might end up with diverge result. Therefore, in this study the mesh or grids were designed not uniform. The finer mesh are used for area near walls both for upper and bottom walls and then gradually the mesh are made coarser as shown in Fig 2. When there are obstacles in the flow, the mesh are designed to be finer not only near the walls but also around the obstacles in Fig 2. There are four meshes designs to be checked for independency as shown in Fig 3a), 3b), 3c), and 3d). The number of cells, faces, and nodes used in each design are shown in Table 1.



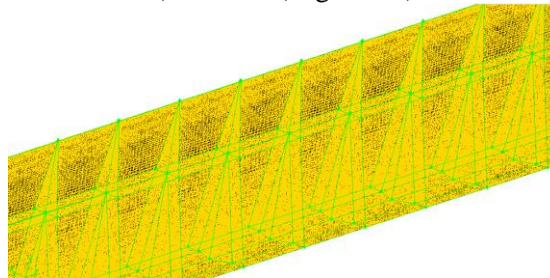
a) Mesh A (most coarse)



b) Mesh B (slight coarse)



c) Mesh C (slight fine)



d) Mesh D (most fine)

Fig 3. Mesh design checked for independency

Table 1. Number of cells, faces, and nodes of the four mesh design

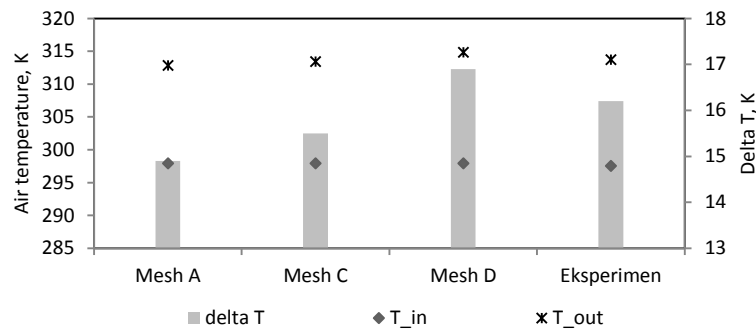
	Mesh A	Mesh B	Mesh C	Mesh D
cell	55,296	338,688	1,092,000	1,980,000
face	173,936	1,043,224	3,335,300	6,026,900
node	63,172	365,480	1,150,798	2,066,248

To check the grid independency, the result from numerical study will be compared to experiment result. The same boundary conditions and setting are used in each numerical study of the four grids design as in Fig 3. The boundary conditions are: inlet air velocity = 5.0 m/s, inlet air temperature = 297.46 K, and constant upper plate temperature. The settings in software used are: three dimension, double precision.

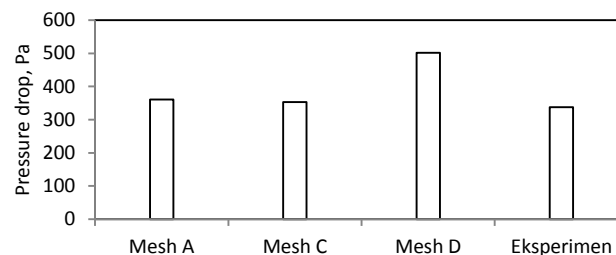
Shear Stress Transport K- ω (SSTK- ω) standard turbulent model was chosen to simulate the flow. The SIMPLEC algorithm was employed to deal with the problem of velocity and pressure coupling. Second-order upwind scheme were used to discretize the main governing equations. Velocity boundary condition was applied at the inlet section while outflow was employed for the outlet. The absorber plate was set to the value as obtained during experiments. Material of the absorber, bottom plate and the obstacles is aluminum. Fluid is air with inlet pressure 1 atm and its properties, such as density, viscosity, thermal conductivity are function of temperature.

Numerical studies were conducted for each of the four mesh: A, B, C, and D. Fig 4 shows global properties resulted from the numerical studies. They are the inlet and outlet temperature of air flowing through the channel and its pressure drop. Only Mesh B could not converge and the residual could not meet the criteria. So, there is no result of Mesh B in Fig 4.

The experiment result which will be discussed in Section 4 gives pressure drop as much as 265 Pa, air temperature outlet 40.5°C when the air inlet velocity is 5.0 m/s and inlet air temperature 24.3°C.



a. The air temperature from numerical studies compared to experiment



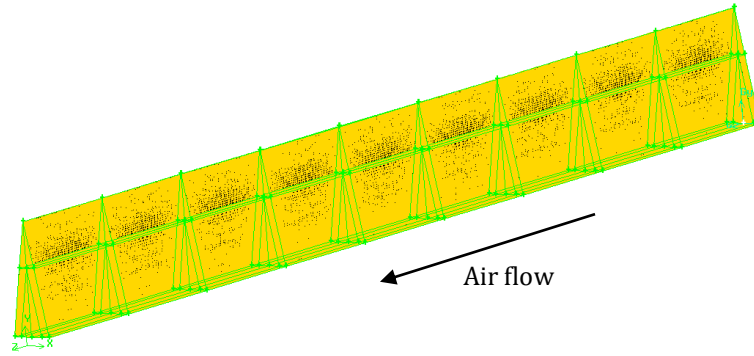
b. The pressure drop from numerical studies compared to experiment

Fig 4. The numerical studies of Mesh A, C, and D compared to the result of experiment

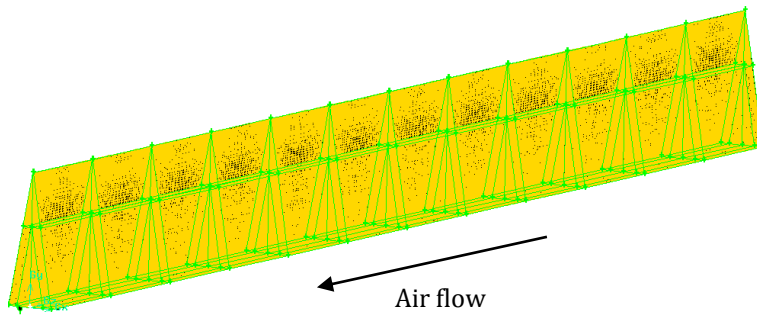
Fig. 4 shows that numerical study with Mesh C and D give better result of air temperature compare to experiment than Mesh A, but mesh D gives too high pressure drop result. Numerical studies using Mesh C give the most closely result to experiments. Thus, Mesh C was chosen for the numerical studies.

Using Mesh C pattern, some numerical studies were conducted to know the effect of obstacles' spacing. The ratio of spacing to height, S/H, studied numerically were 1/2, 1, 1 1/2, and 2. The Mesh used in this study

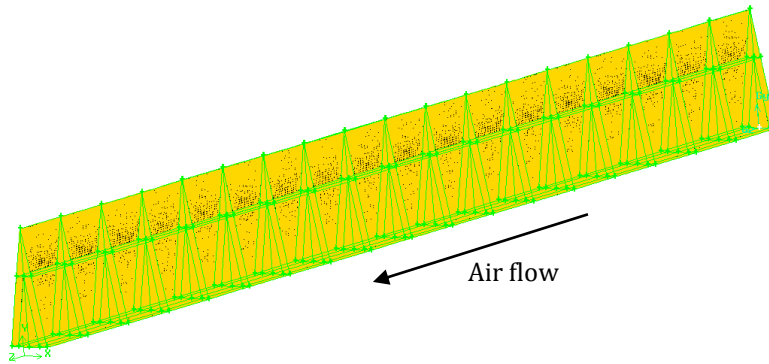
are in Fig. 5 a – 5 d. When the ratio S/H is bigger, then the number of obstacle is less. Number of obstacles are 8, 11, 17, and 35 for ratio S/H 2, $1\frac{1}{2}$, 1, and $\frac{1}{2}$, respectively.



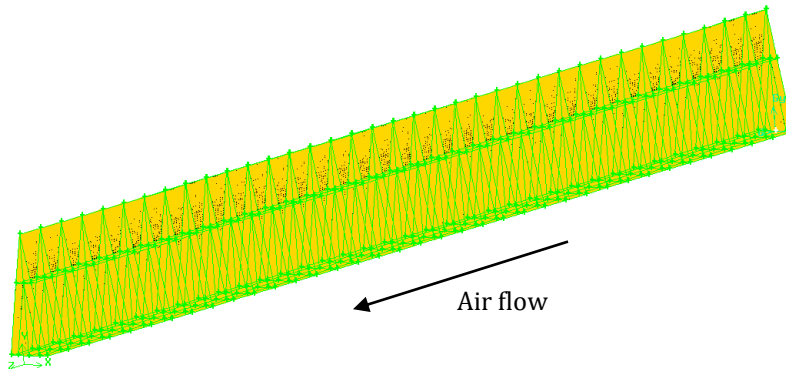
a. Ratio $S/H = 2$



b. Ratio $S/H = 1\frac{1}{2}$



c. Ratio $S/H = 1$



d. Ratio $S/H = \frac{1}{2}$

Fig. 5. The Mesh used for numerical studies of each spacing to height ratio, S/H

4. Results and discussion

Since the experiment is conducted to validate the numerical result, then it is not necessary to conduct experiments for all ratio S/H . The ratio S/H used in experiment equals to 1. Thus, there are 17 obstacles inserted and the percentage of air flow blockage in the channel was 36%. The experiment followed the numerical setting. The experiments were conducted at certain inlet air velocity and certain radiation intensity or absorber temperature. A VFD was used to get an inlet air velocity equals to 5.0 m/s. An adjustable turner was used to adjust the radiation intensity that make the absorber's temperature as high as 320 K or 47°C.

When the numerical result is close to the experimental result, then the numerical result is valid. Table 2 shows the comparison between numerical and experimental results at 5.0-m/s-inlet air velocity and 320 K absorber temperature. Temperature difference of numeric is very close to experiment, while pressure drop is higher about 16% than experiment. Thus, the numerical study using several setting discussed above is acceptable and valid.

Table 2. Comparison between numerical and experimental results

	Numeric	experiment
$T_{in}, ^\circ\text{C}$	297.9	297.5
$T_{out}, ^\circ\text{C}$	314.4	313.7
$\Delta T, ^\circ\text{C}$	16.5	16.2
$\Delta P, \text{Pa}$	462.3	397.7

Having a valid grids, setting, and viscous model, the numerical study was continued to investigate the spacing effect of obstacles on the bottom plate of air duct. Diagrams of velocity vector of air flow around the obstacles inserted at ratio S/H equals to 2, $1\frac{1}{2}$, 1, and $\frac{1}{2}$ are shown in Figure 6 a), 6 b), 6 c) and 6 d), respectively. All of the velocity vectors were taken at height $y = 10 \text{ mm}$ from the bottom plate. When the ratio $S/H = 2$, the spacing between obstacles = 100 mm. For ratio $S/H = 1\frac{1}{2}$, the spacing = 75 mm, and for ratio $S/H = \frac{1}{2}$, the spacing = 25 mm.

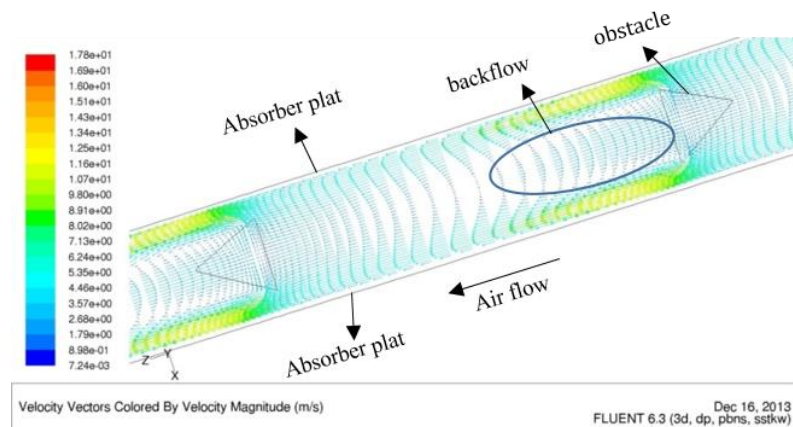


Figure 6 a) Velocity vector of air flow around *obstacle* with ratio $S/H = 2$

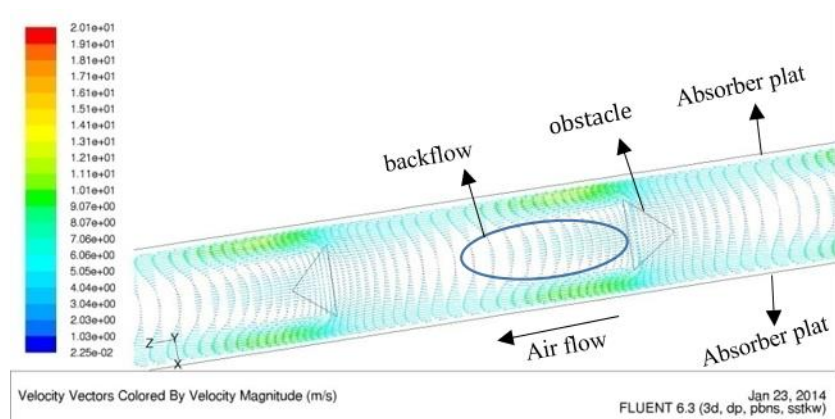


Figure 6 b) Velocity vector of air flow around *obstacle* with ratio $S/H = 1 \frac{1}{2}$

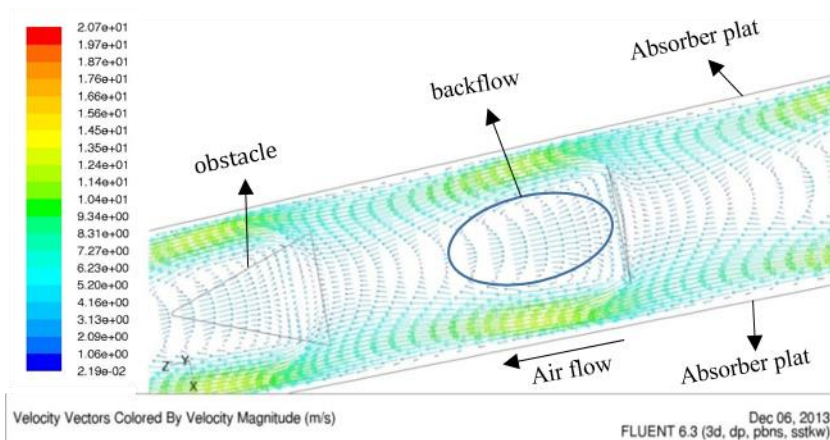


Figure 6 c) Velocity vector of air flow around *obstacle* with ratio $S/H = 1$

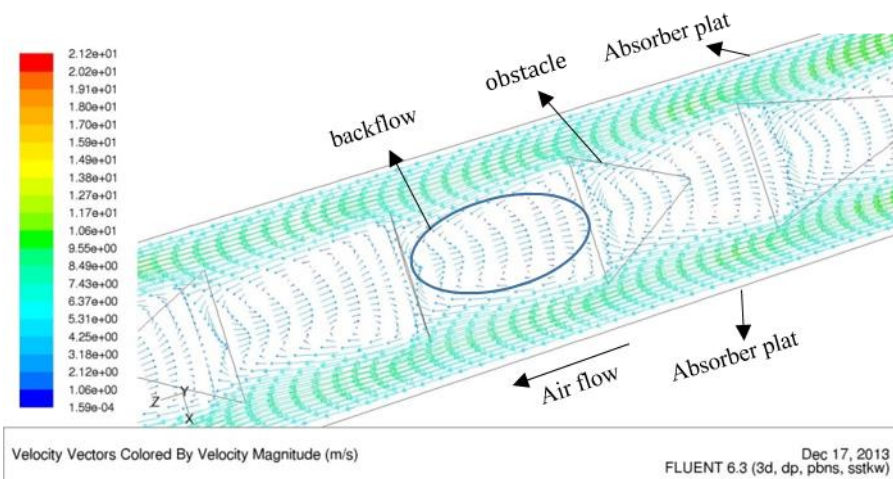


Figure 6 d) Velocity vector of air flow around *obstacle* with ratio $S/H = \frac{1}{2}$

Figure 6 a) – 6 d) show how the air flow encounters separation when flow through obstacles. The obstacles cause backflow between two consecutive obstacles in downstream. There are more backflows when the obstacles' spacing are closer and they cause a higher pressure drop. The air velocity looks higher near

absorber plate when there is backflow or swirl in the flow. This high air velocity makes flow become more turbulent and more heat transferred from the absorber plate to the air. This convection heat transfer to the air makes outlet air temperature higher. Thus, the closer the obstacles' spacing makes the higher pressure drop and higher convection heat transfer from the absorber plate to the air flow.

When the spacing between obstacles is twice its height (ratio $S/H = 2$), air flow is blocked by obstacles and causes backflow behind the obstacles. The backflow caused by separation gradually diminish between two obstacles in downstream as shown in Fig 6 a). Since the air is blocked, most of air is forced to flow in the gap between obstacles and absorber plate. It is shown by longer and higher vector of velocity in the gap. More air is heated by absorber plate. Furthermore, higher velocity increases Reynold number and make the flow more turbulent. More turbulent flow gives higher Nusselt number and definitely increase the convection heat transfer. Thus, obstacles makes outlet air temperature higher than without any (Handoyo, Ichsani, Prabowo, & Sutardi, 2014). Flow in spacing between obstacles experiences backflow after hitting obstacles and then it reattaches quickly when the ratio $S/H = 2$. When the ratio S/H or spacing between obstacles is smaller, as shown in Fig 6 b) – 6 d), backflow is more dominant than reattached flow in area between the obstacles. When backflow occurs, more air will flow in the gap and contact with absorber plate which is the heat source. It is the reason that smaller obstacles' spacing makes higher air outlet temperature and higher SAH's efficiency. The backflow in space between obstacles contributes pressure drop in the flow. More backflow causes higher pressure drop in air acrossed the v-corrugated absorber plate SAH.

Numerical studies also provide some global properties of the flow, such as the air inlet and outlet temperature, and pressure drop. Air temperature difference is calculated from the change between outlet and inlet air temperature. Comparison of air temperature difference and air pressure drop for some ratio S/H from numerical studies is shown in Fig 7. From the air temperature difference and pressure drop data, the following parameters, i.e. SAH's efficiency and friction factor of the air flow in v-corrugated duct with delta-shaped obstacles, are calculated. The efficiency and friction factor are calculated using Equation (8) and (9) according to Duffie & Beckman (1991) and presented in Fig. 8 for three ratio S/H studied.

$$\eta = \frac{q_u}{A_c I} = \frac{\dot{m}_f c_p (T_{fo} - T_{fi})}{A_c I} \quad (8)$$

$$f = \frac{\Delta P}{\frac{L}{D_h} \rho \frac{v^2}{2}} \quad (9)$$

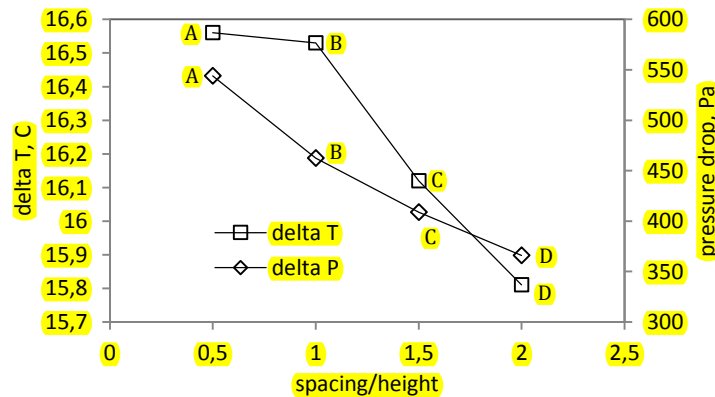


Figure 7. The air temperature difference and pressure drop from numerical studies

Obstacles arranged with ratio $S/H = \frac{1}{2}$ gives the highest air temperature difference and also highest pressure drop for air flowing in a v-corrugated duct, as shown in Fig. 7. This findings are matching with the flow structure discussed above. The obstacles block the air flow and force it to have more contact with absorber plate. Not only forcing the air to the absorber plate, obstacles also causing more backflow. More obstacles produce higher air outlet temperature and higher pressure drop. SAH requires high temperature difference, but low pressure drop. In Fig. 7, considering the temperature difference aspect, point A is the best, but from pressure drop, point D is the best. The gradient of pressure drop in a segment A-B is the steepest among other segments. While the gradient of temperature difference in that segment A-B is the least. Temperature difference in point B (16.53 °C) is slightly less than point A (16.56°C), but pressure drop in point B (462.34 Pa) is much less than point A (544.12 Pa). Sacrifice a little temperature difference but save a lot pressure drop shall be a wise choice.

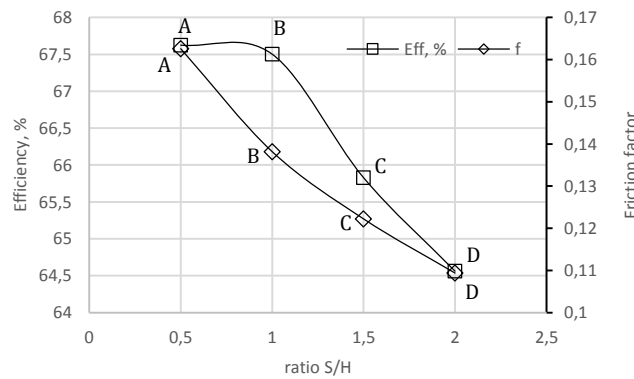


Figure 8. Efficiency of SAH and friction factor of flow with some ratio S/H of obstacles

The thermal efficiency and friction factor are two non-dimensional parameters. Thus, they can be applied to other SAH that has the same geometry and configuration, i.e. corrugated absorber plate and congruent obstacles inserted on bottom plate. Fig. 8 shows those parameters for some ratio S/H studied.

Efficiency of SAH and friction factor are decreasing as ratio S/H is increasing. Gradient of segment A-B of efficiency line is very low compare to other segments. It is rather flat and then getting steepest in segment B-C and CD. When ratio S/H used is 1 instead of 0.5, efficiency of SAH is decreasing 0.18% (from 67.62% to 67.50%) and friction factor is decreasing 15% (from 0.163 to 0.138). So, sacrificing a small amount of efficiency but reducing a significant friction factor is advantageous.

5. Conclusion

From numerical studies in a v-corrugated duct, it is found that backflow between obstacles and high velocity in the gap between obstacles and absorber plate causes the flow became more turbulent and enhanced the convection heat transfer between the air and the absorber plate. Thus, when it is applied in SAH, it will bring improve its efficiency.

Obstacles placed in a small spacing increase air temperature difference and pressure drop. Air temperature difference and pressure drop increase from 15.81°C and 365.89 Pa, to 16.12°C and 408.90 Pa, to 16.53°C and 462.34 Pa, to 16.56°C and 544.12 Pa for ratio S/H decreases from 2 to 1 ½ to 1, and to ½, respectively.

Efficiency of SAH and friction factor are decreasing as ratio S/H is increasing. The best delta-shaped obstacles' spacing inserted in a v-corrugated duct is equal to its height or ratio S/H = 1. When ratio S/H used is 1 instead of 0.5, efficiency of SAH is decreasing 0.18% and friction factor is decreasing 15%. So, sacrificing a small amount of efficiency but reducing a significant friction factor is advantageous.

Acknowledgement

Here, I am very grateful for the support from Kopertis Wilayah VII Jawa Timur, Kementerian Pendidikan dan Kebudayaan by providing Research Grant under contract no: 0004/SP2H/PP/K7/KL/II/2012.

Nomenclature

W	wide of the obstacle (mm)
H	height of the obstacle (mm)
S	spacing between the obstacles (mm)
x, y, z	coordinates
Re	Reynolds number
C_p	specific heat of air (J/kg.K)
\dot{m}_f	mass flow rate of the fluid – air (kg/s)
\dot{Q}_u	useful heat transfer rate (Watt)
I	radiation intensity (W/m ²)
A_c	collector aperture area (m ²)
T_o	collector outlet temperature (K)
T_i	collector air inlet temperature (K)
ϑ	air kinematic viscosity (m ² /s)
ρ	air density (kg/m ³)
α	air thermal diffusion coefficient (m ² /s)
η	efficiency of collector

References

- Abene, A., Dubois, V., Le Ray, M., & Oagued, A. (2004). Study of a solar air flat plate collector: use of obstacle and application for the drying of grape. *J. of Food Engineering*, 65, 15 – 22.
- Akpınar, E. K., & Koçyiğit, F. (2010). Experimental investigation of thermal performance of solar air heater having different obstacles on absorber plates. *Int. Com. in Heat and Mass Transfer*, 37, 416–421.
- ASHRAE. (1986). *Method of Testing to Determine the Thermal Performance of Solar Collectors*. Atlanta: ASHRAE.
- Bekele, A., Mishra, M., & Dutta, S. (2011). Effects of Delta-Shaped Obstacles on the Thermal Performance of Solar Air Heater. *Hindawi Publishing Corporation: Advances in Mechanical Engineering*, 2011, 10 pages.

- Choudhury, C., & Garg, H. P. (1991). Design Analysis of Corrugated and Flat Plate Solar Air Heaters. *Renewable Energy Vol I, No. 5/6*, p. 595 – 607.
- Duffie, J. A., & Beckman, W. A. (1991). *Solar Engineering Of Thermal Processes* (2nd ed. ed.). John Wiley & Sons, Inc.
- Esen, H. (2008). Experimental energy and exergy analysis of a double-flow solar air heater having different obstacles on absorber plates. *Building and Environment*, *43*, 1046–1054.
- FLUENT, I. (2003). *FLUENT User's Guide*.
- Handoyo, E. A., Ichsani, D., Prabowo, & Sutardi. (2014). Experimental Studies on a Solar Air Heater Having V-Corrugated. *Applied Mechanics and Materials*, *493*, 86-92.
- Ho, C.-D., Yeh, H.-M., & Chen, T.-C. (2011). Collector efficiency of upward-type double-pass solar air heaters with fins attached. *Int. Com. in Heat and Mass Transfer*, *38*, 49–56.
- Incropera, F. P., & DeWitt, D. P. (2002). *Fundamentals of Heat and Mass Transfer. 5th edition ed. s.l.:* John Wiley & Sons.
- Islamoglu, Y., & Parmaksizoglu, C. (2003). The effect of channel height on the enhanced heat transfer characteristics in a corrugated heat exchanger channel. *Applied Thermal Engineering* *23*, 979–987.
- Karim, M., & Hawlader, M. (2006). Performance Investigation of Flat Plate, V-Corrugated and Finned Air Collector. *Energy* *31*, 452-470.
- Kurtbas, I., & Turgut, E. (2006). Experimental Investigation of Solar Air Heater with Free and Fixed Fins: Efficiency and Exergy Loss. *Int. J. of Science & Technology, Volume 1*(No 1), 75-82.
- Naphon, P. (2007). Heat transfer characteristics and pressure drop in channel with V corrugated upper and lower plates. *Energy conversion and management* *48*, 1516 – 1524.
- Promvonge, P. (2010). Heat transfer and pressure drop in a channel with multiple 60° V-baffles. *Int. Com. in Heat and Mass Transfer*, *37*, 835–840.
- Romdhane, B. S. (2007). The air solar collectors: Comparative study, introduction of baffles to favor the heat transfer. *Solar Energy*, *81*, 139 – 149.
- Tao, L., Wen, X. L., Wen, F. G., & Chan, X. L. (2007). A Parametric study on the thermal performance of a solar air collector with a V-groove absorber. *Int. J. of Green Energy*, *4*, 601–622.

Your PDF has been built and requires approval

1 message

Solar Energy <se@elsevier.com>

Fri, Jan 22, 2016 at 5:01 PM

To: ekadewi@petra.ac.id, ekadewi@peter.petra.ac.id

Solar Energy

Title: Numerical Studies on the Effect of Delta-Shaped Obstacles' Spacing on the Heat Transfer and Pressure Drop in V-Corrugated Channel of Solar Air Heater
Authors: Ekadewi Anggraini Handoyo, Dr; Ichsani Djatmiko, Prof.; Prabowo Prabowo, Prof.; Sutardi Sutardi, Prof.

Dear Dr. Ekadewi Anggraini Handoyo,

The PDF for your submission, "Numerical Studies on the Effect of Delta-Shaped Obstacles' Spacing on the Heat Transfer and Pressure Drop in V-Corrugated Channel of Solar Air Heater" has now been built and is ready for your approval. Please view the submission before approving it, to be certain that it is free of any errors. If you have already approved the PDF of your submission, this e-mail can be ignored.

To approve the PDF please login to the Elsevier Editorial System as an Author:

<http://ees.elsevier.com/se/>Your username is: ekadewi@petra.ac.id

Then click on the folder 'Submissions Waiting for Author's Approval' to view and approve the PDF of your submission. You may need to click on 'Action Links' to expand your Action Links menu.

You will also need to confirm that you have read and agree with the Elsevier Ethics in Publishing statement before the submission process can be completed. Once all of the above steps are done, you will receive an e-mail confirming receipt of your submission from the Editorial Office. For further information or if you have trouble completing these steps please go to: http://help.elsevier.com/app/answers/detail/a_id/88/p/7923.

Please note that you are required to ensure everything appears appropriately in PDF and no change can be made after approving a submission. If you have any trouble with the generated PDF or completing these steps please go to: http://help.elsevier.com/app/answers/detail/a_id/88/p/7923.

Your submission will be given a reference number once an Editor has been assigned to handle it.

Thank you for your time and patience.

Kind regards,
Editorial Office
Solar Energy

For further assistance, please visit our customer support site at <http://help.elsevier.com/app/answers/list/p/7923>. Here you can search for solutions on a range of topics, find answers to frequently asked questions and learn more about EES via interactive tutorials. You will also find our 24/7 support contact details should you need any further assistance from one of our customer support representatives.

Your Submission

6 messages

Solar Energy <se@elsevier.com>

Sat, Feb 6, 2016 at 9:28 PM

To: ekadewi@petra.ac.id, ekadewi@peter.petra.ac.id
Cc: bbibek@nic.in, bbibek12@gmail.com

Ms. Ref. No.: SE-D-15-01490R1

Title: Numerical Studies on the Effect of Delta-Shaped Obstacles' Spacing on the Heat Transfer and Pressure Drop in V-Corrugated Channel of Solar Air Heater
Solar Energy

Dear Dr. Ekadewi Handoyo,

The reviews of your paper are now complete and I'm happy to tell you that the consensus decision is that the paper should be published, subject to minor revisions which respond to the reviewer's comments. I am attaching the reviewer's comments. Please try to attend to these minor revisions within the next month (30 days).

To submit a revision, please go to <http://ees.elsevier.com/se/> and login as an Author.Your username is: ekadewi@petra.ac.idIf you need to retrieve password details, please go to: http://ees.elsevier.com/se/automail_query.asp

On your Main Menu page is a folder entitled "Submissions Needing Revision". You will find your submission record there.

Please note that this journal offers a new, free service called AudioSlides: brief, webcast-style presentations that are shown next to published articles on ScienceDirect (see also <http://www.elsevier.com/audioslides>). If your paper is accepted for publication, you will automatically receive an invitation to create an AudioSlides presentation.

Solar Energy features the Interactive Plot Viewer, see: <http://www.elsevier.com/interactiveplots>. Interactive Plots provide easy access to the data behind plots. To include one with your article, please prepare a .csv file with your plot data and test it online at <http://authortools.elsevier.com/interactiveplots/verification> before submission as supplementary material.

Thank you for your interest in Solar Energy.

Yours sincerely,

Bibek Bandyopadhyay, PhD
Associate Editor
Solar Energy

Note: While submitting the revised manuscript, please double check the author names provided in the submission so that authorship related changes are made in the revision stage. If your manuscript is accepted, any authorship change will involve approval from co-authors and respective editor handling the submission and this may cause a significant delay in publishing your manuscript.

Reviewers' comments:

Reviewer #1: The authors have well responded to the comments given. The revised paper has been incorporated with the responses suitably. The paper is now acceptable for publication after following some editing revisions:

Please see section of Introduction in page 3. Please correct surname of author for references [15] and [16] as below:

....as done by Esen et al. [15].

Esen et al. [16] also proposed.....

Reviewer #3: Afer Revision, I think this paper can be accepted now!

Reviewer #4: Revised manuscript is acceptable. The authors have addressed my questions.

The reviewer(s) may also have uploaded detailed comments on your manuscript as an attachment. To access these comments, please go to: <http://ees.elsevier.com/se/> . Click on 'Author Login'. Click on 'View Reviewer Attachments' (if present).

Ekadewi Handoyo <ekadewi@petra.ac.id>

Tue, Feb 16, 2016 at 9:49 AM

To: djatmiko@me.its.ac.id, prabowo@me.its.ac.id, sutardi@me.its.ac.id

Yth. Prof. Djatmiko, Prof. Prabowo, dan Prof. Sutardi,

beberapa waktu lalu sy mengirimkan paper yang sy ambil dari disertasi yg dibimbing Bapak-Bapak bertiga ke Solar Energy. Berikut email yang menyatakan paper tsb diterima. Semoga hal ini menggembirakan kita semua...

tnks utk bimbingan Bapak-Bapak,
ekadewi

[Quoted text hidden]

Sutardi <sutardi@me.its.ac.id>
To: Ekadewi Handoyo <ekadewi@petra.ac.id>

Fri, Oct 14, 2016 at 8:06 AM

Bu Eka Yth.,

Kalau boleh mohon kami diemail copy file dari paper yang telah dipublikasikan secara internasional oleh Ibu dan ada nama saya sbg penulis anggota, spt paper di AMM atau di Solar Energy, atau mungkin ada yang lainnya.

Matur nuwun, dan mohon maaf.

Salam,

Sutardi

[Quoted text hidden]

Institut Teknologi Sepuluh Nopember (ITS)

<http://www.its.ac.id>

Ekadewi Handoyo <ekadewi@petra.ac.id>
To: Sutardi <sutardi@me.its.ac.id>

Sat, Oct 15, 2016 at 11:59 PM

Bapak Prof. Sutardi ysh.,

Tentu boleh, Pak...

Berikut sy attach 2 file paper yang dipublikasikan secara internasional dan ada nama Bapak di dalamnya.

semoga berguna,
ekadewi a. handoyo

[Quoted text hidden]

2 attachments



1-s2.0-S0038092X16001389-main termuat di solar energy.pdf

5902K



AMM.493.86.pdf

784K

Sutardi <sutardi@me.its.ac.id>
To: Ekadewi Handoyo <ekadewi@petra.ac.id>

Sun, Oct 16, 2016 at 7:21 AM

Matur nuwun bu Dewi, sangat bermanfaat, kami doakan smg ibu terus produktif dlm publikasi.

Salam.

Sutardi

[Quoted text hidden]

> --

[Quoted text hidden]

Ekadewi Handoyo <ekadewi@petra.ac.id>
To: Sutardi <sutardi@me.its.ac.id>

Sun, Oct 16, 2016 at 9:49 PM

Sami-sami, Prof....

Terima kasih untuk doanya...

Sy doakan Pak Tardi jg produktif terus dlm karya ilmiah....

Hormat sy,

Ekadewi

[Quoted text hidden]



Editor handles your revised submission SE-D-15-01490R1

1 message

Solar Energy <se@elsevier.com>

Sat, Jan 23, 2016 at 12:35 PM

To: ekadewi@petra.ac.id, ekadewi@peter.petra.ac.id

Ref.: Revision of SE-D-15-01490R1

Title: Numerical Studies on the Effect of Delta-Shaped Obstacles' Spacing on the Heat Transfer and Pressure Drop in V-Corrugated Channel of Solar Air Heater

Dear Dr. Handoyo,

Your revised submission "Numerical Studies on the Effect of Delta-Shaped Obstacles' Spacing on the Heat Transfer and Pressure Drop in V-Corrugated Channel of Solar Air Heater" will be handled by Associate Editor Bibek Bandyopadhyay, PhD.

You may check the progress of your revision by logging into the Elsevier Editorial System as an author at <http://ees.elsevier.com/se/>.

Thank you for submitting your revision to this journal.

Kind regards,

Solar Energy

Manuscript Number: SE-D-15-01490R2

Title: Numerical Studies on the Effect of Delta-Shaped Obstacles' Spacing on the Heat Transfer and Pressure Drop in V-Corrugated Channel of Solar Air Heater

Article Type: Regular Paper

Section/Category: Solar heating & cooling, buildings, and other applications

Keywords: delta-shaped obstacle; v-corrugated channel; solar air heater; numerical study

Corresponding Author: Dr. Ekadewi Anggraini Handoyo, Dr

Corresponding Author's Institution: Petra Christian University

First Author: Ekadewi Anggraini Handoyo, Dr

Order of Authors: Ekadewi Anggraini Handoyo, Dr; Ichsani Djatmiko, Prof.; Prabowo Prabowo, Prof.; Sutardi Sutardi, Prof.

Abstract: Solar air heater (SAH) is simple in construction compared to solar water heater. Yet, it is very useful for drying or space heating. Unfortunately, the convective heat transfer between the absorber plate and the air inside the solar air heater is rather low. Some researchers reported that obstacles are able to enhance the heat transfer in a flat plate solar air collector and others found that a v-corrugated absorber plate gives better heat transfer than a flat plate. Only a few research combines these two in a SAH. This paper will describe the combination from other point of view, i.e. the spacing between obstacles. Its spacing possibly will effect the heat transfer and pressure drop of the air flowing across the channel.

The first step in numerical study is generating mesh or grid of the air flow inside a v-corrugated channel which was blocked by some delta-shaped obstacles. The mesh was designed three-dimension and not uniform. The mesh are made finer for area near obstacles and walls both for upper and bottom, and then gradually coarser. Grid independency is the next step to be conducted. When the mesh is already independent, the numerical study begins. To validate the numerical model, an indoor experiment was conducted. Turbulent model used was Shear Stress Transport $K-\omega$ (SSTK- ω) standard. Having a valid numerical model, the spacing between obstacles was studied numerically. Ratio spacing to height, S/H of obstacles investigated were 0.5; 1; 1.5; and 2.

From numerical studies in a v-corrugated duct, it is found that backflow between obstacles and high velocity in the gap between obstacles and absorber plate causes the flow became more turbulent and enhanced the convection heat transfer between the air and the absorber plate. Obstacles placed in a small spacing will increase Nusselt number (convection heat transfer) and friction factor (pressure drop). The

Nusselt number enhanced from 27.2 when no obstacle used to 94.2 when obstacles inserted with $S/H = 0.5$. The Nusselt enhanced 3.46 times. The friction factor will increase from 0.0316 at no obstacle to 0.628 at ratio $S/H = 0.5$. The friction factor increased 19.9 times. Efficiency, Nusselt number, and friction factor are decreasing as ratio S/H is increasing. When ratio S/H used is 1 instead of 0.5, Nusselt number enhancement decreased only 1.13%, but friction factor decreased 15.1%. So, sacrificing a small amount of Nusselt number but reducing a significant friction factor is advantageous. The optimal spacing ratio S/H of delta-shaped obstacles inserted in a v-corrugated SAH is one. In other words, the optimal spacing of obstacle equals to its height.

Suggested Reviewers: Ebru Kavak Akpınar

ebruakpinar@firat.edu.tr

He/she write the same topic with me, i.e. obstacles in Solar Air Heater.

Adisu Bekele

addisu2005@yahoo.com

He/she write the same topic with me, i.e. obstacles in Solar Air Heater.

Md Azharul Karim

makarim@mame.mu.oz.au

He/she write the same topic with me, i.e. obstacles in Solar Air Heater.

Response to Reviewers: Response to reviewers

Ans: Thank you very much for the approval of our paper. It is so delightful. We are very grateful to all reviewers.

Reviewer #1: The authors have well responded to the comments given. The revised paper has been incorporated with the responses suitably. The paper is now acceptable for publication after following some editing revisions:

Please see section of Introduction in page 3. Please correct surname of author for references [15] and [16] as below:

....as done by Esen et al. [15].

Esen et al. [16] also proposed.....

Ans: Thank you for the discreet correction. We are sorry that we wrote the surname mistakenly. We have corrected it. Hopefully, the paper is useful for others.

Reviewer #3: Afer Revision, I think this paper can be accepted now!

Ans: We are really grateful for the approval... Hopefully, the paper is useful for others.

Reviewer #4: Revised manuscript is acceptable. The authors have addressed my questions.

Ans: Thank you very much for the approval... Hopefully, the paper is useful for others.

Highlights

V-corrugated absorber plate and obstacles improves heat transfer in SAH.

How does the spacing between obstacles effect the convection heat transfer and pressure drop in air flow?

The optimal spacing ratio of obstacles gives optimal Nusselt number (convection) and friction factor (pressure drop).

Elsevier Editorial System(tm) for Solar

Energy

Manuscript Draft

Manuscript Number:

Title: Numerical Studies on the Effect of Delta-Shaped Obstacles' Spacing on the Heat Transfer and Pressure Drop in V-Corrugated Channel of Solar Air Heater

Article Type: Regular Paper

Section/Category: Solar heating and cooling, buildings & other applications

Keywords: delta-shaped obstacle; v-corrugated channel; solar air heater; numerical study

Corresponding Author: Dr. Ekadewi Anggraini Handoyo, Dr

Corresponding Author's Institution: Petra Christian University

First Author: Ekadewi Anggraini Handoyo, Dr

Order of Authors: Ekadewi Anggraini Handoyo, Dr; Ichsani Djatmiko, Prof.; Prabowo Prabowo, Prof.; Sutardi Sutardi, Prof.

Abstract: Solar air heater (SAH) is simple in construction compared to solar water heater. Yet, it is very useful for drying or space heating. Unfortunately, the convective heat transfer between the absorber plate and the air inside the solar air heater is rather low. Some researchers reported that obstacles are able to enhance the heat transfer in a flat plate solar air collector and others found that a v-corrugated absorber plate gives better heat transfer than a flat plate. There was research combine these two in a SAH. Yet, the spacing between obstacles was not studied yet. Whereas, its spacing possibly will effect the heat transfer and pressure drop of the air flowing across the channel.

The first step in numerical study is generating mesh or grid of the air flow inside a v-corrugated channel which was blocked by some delta-shaped obstacles. The mesh was designed three-dimension and not uniform. The mesh are made finer for area near obstacles and walls both for upper and bottom, and then gradually coarser. Grid independency is the next step to be conducted. When the mesh is already independent, the numerical study begins. To validate the numerical model, an indoor experiment was conducted. Turbulent model used was Shear Stress Transport K- ω (SSTK- ω) standard. Having a valid numerical model, the spacing between obstacles was studied numerically. Ratio spacing to height, S/H of obstacles investigated were 0.5; 1; 1.5; and 2.

From numerical studies in a v-corrugated duct, it is found that backflow between obstacles and high velocity in the gap between obstacles and absorber plate causes the flow became more turbulent and enhanced the convection heat transfer between the air and the absorber plate. Obstacles placed in a small spacing increase air temperature difference and pressure drop. Air temperature difference and pressure drop increase from 15.81oC and 365.89 Pa, to 16.12oC and 408.90 Pa, to 16.53oC and 462.34 Pa, to 16.56oC and 544.12 Pa for ratio S/H decreases from 2 to 1 ½ to 1, and to ½, respectively. Efficiency of SAH and friction factor are

decreasing as ratio S/H is increasing. The best delta-shaped obstacles' spacing inserted in a v-corrugated duct is equal to its height or ratio $S/H = 1$. When ratio S/H used is 1 instead of 0.5, efficiency of SAH is decreasing 0.18% and friction factor is decreasing 15%. So, sacrificing a small amount of efficiency but reducing a significant friction factor is advantageous.

Suggested Reviewers: Ebru Kavak Akpınar

ebruakpinar@firat.edu.tr

He/she write the same topic with me, i.e. obstacles in Solar Air Heater.

Adisu Bekele

addisu2005@yahoo.com

He/she write the same topic with me, i.e. obstacles in Solar Air Heater.

Md Azharul Karim

makarim@mame.mu.oz.au

He/she write the same topic with me, i.e. v-corrugated air collector.

Numerical Studies on the Effect of Delta-Shaped Obstacles' Spacing on the Heat Transfer and Pressure Drop in V-Corrugated Channel of Solar Air Heater

The research was part of my previous doctoral study. This topic was chosen as an effort to enhance the heat transfer in a solar air heater (SAH) which is usually low. A numerical study was set up to investigate the effect of obstacles' spacing used in a v-corrugated SAH. An indoor model of a SAH was constructed for validation of the numerical study. After generating 3-D mesh or grid of the air flow inside a v-corrugated channel which was blocked by some delta-shaped obstacles, grid independency is the next step to be conducted. When the mesh is already independent, the numerical study begins. Having a valid numerical model, the spacing between obstacles was studied numerically. Ratio spacing to height, S/H of obstacles investigated were 0.5; 1; 1.5; and 2.

From numerical studies in a v-corrugated duct, it is found that backflow between obstacles and high velocity in the gap between obstacles and absorber plate causes the flow became more turbulent and enhanced the convection heat transfer between the air and the absorber plate. Efficiency of SAH and friction factor are decreasing as ratio S/H is increasing. The best delta-shaped obstacles' spacing inserted in a v-corrugated duct is equal to its height or ratio $S/H = 1$. When ratio S/H used is 1 instead of 0.5, efficiency of SAH is decreasing 0.18% and friction factor is decreasing 15%. So, sacrificing a small amount of efficiency but reducing a significant friction factor is advantageous.

The corresponding author is:
Ekadewi A. Handoyo.
Jl. Siwalankerto 121 – 131 Surabaya 60236, Indonesia
Tel.: 62-31-2983465; fax: 62-31-8491215.
E-mail address: ekadewi@petra.ac.id.

This research is certainly original and all of the data are obtained via the experiments done by the authors.

Highlights

This paper explains about how to improve a Solar air heater (SAH) performance. SAH is simple in construction compared to solar water heater. But, it is very useful for drying or space heating. Unfortunately, the convective heat transfer between the absorber plate and the air inside the solar air heater is rather low.

Improving heat transfer in SAH will improve its efficiency, too. Unfortunately, the pressure drop is usually also increasing. Some efforts, such as replacing the flat absorber plate with v-corrugated plate or inserting obstacles in the flow, are using widely. Yet, the spacing between obstacles was not studied yet. Whereas, its spacing possibly will effect the heat transfer and pressure drop of the air flowing across the channel.

This paper shows the velocity vector of the air flow around the obstacles in a v-corrugated channel. Further, it describes how the smaller ratio of spacing to obstacles' height, S/H , more heat is transfered to the air and higher pressure drop. In the end, the paper concludes that sacrificing a small amount of efficiency but reducing a significant friction factor is advantageous.

Numerical Studies on the Effect of Delta-Shaped Obstacles' Spacing on the Heat Transfer and Pressure Drop in V-Corrugated Channel of Solar Air Heater

Ekadewi A. Handoyo¹, Djatmiko Ichسانی², Prabowo², Sutardi²

¹Mechanical Engineering Dept, Petra Christian University, Surabaya – Indonesia

²Mechanical Engineering Dept, Institut Teknologi Sepuluh Nopember, Surabaya – Indonesia

Corresponding author: ekadewi@petra.ac.id

Abstract

Solar air heater (SAH) is simple in construction compared to solar water heater. Yet, it is very useful for drying or space heating. Unfortunately, the convective heat transfer between the absorber plate and the air inside the solar air heater is rather low. Some researchers reported that obstacles are able to enhance the heat transfer in a flat plate solar air collector and others found that a v-corrugated absorber plate gives better heat transfer than a flat plate. There was research combine these two in a SAH. Yet, the spacing between obstacles was not studied yet. Whereas, its spacing possibly will effect the heat transfer and pressure drop of the air flowing across the channel.

The first step in numerical study is generating mesh or grid of the air flow inside a v-corrugated channel which was blocked by some delta-shaped obstacles. The mesh was designed three-dimension and not uniform. The mesh are made finer for area near obstacles and walls both for upper and bottom, and then gradually coarser. Grid independency is the next step to be conducted. When the mesh is already independent, the numerical study begins. To validate the numerical model, an indoor experiment was conducted. Turbulent model used was Shear Stress Transport K- ω (SSTK- ω) standard. Having a valid numerical model, the spacing between obstacles was studied numerically. Ratio spacing to height, S/H of obstacles investigated were 0.5; 1; 1.5; and 2.

From numerical studies in a v-corrugated duct, it is found that backflow between obstacles and high velocity in the gap between obstacles and absorber plate causes the flow became more turbulent and enhanced the convection heat transfer between the air and the absorber plate. Obstacles placed in a small spacing increase air temperature difference and pressure drop. Air temperature difference and pressure drop increase from 15.81°C and 365.89 Pa, to 16.12°C and 408.90 Pa, to 16.53°C and 462.34 Pa, to 16.56°C and 544.12 Pa for ratio S/H decreases from 2 to 1 ½ to 1, and to ½, respectively. Efficiency of SAH and friction factor are decreasing as ratio S/H is increasing. The best delta-shaped obstacles' spacing inserted in a v-corrugated duct is equal to its height or ratio S/H = 1. When ratio S/H used is 1 instead of 0.5, efficiency of SAH is decreasing 0.18% and friction factor is decreasing 15%. So, sacrificing a small amount of efficiency but reducing a significant friction factor is advantageous.

Keywords: delta-shaped obstacle; v-corrugated channel, solar air heater; numerical study.

1. Introduction

Solar energy can be converted into thermal energy in a solar collector. Solar collector basically is device used to trap solar energy to heat a plate and transfer the heat to a fluid flowing under or above the plate. When sun light falls onto a plate, solar radiation reaches the plate at lower wavelength and heat it up. Then, the heat is carried away by either water or air that flows under or above the plate. Solar collector used to

heat up air is called solar air heater (SAH) and solar water heater for water. Generally, the solar air heater is less efficient than the solar water heater, because air has less thermal capacity and less convection heat transfer coefficient. Yet, air is much lighter and less corrosive than water. The other benefit is that heated air can be used for moderate-temperature drying, such as harvested grains or fish. Since the solar air heater has less convective heat transfer coefficient than solar water heater, some researchers tried to increase this convective heat transfer coefficient.

A popular type of solar air heaters is the flat plate SAH, which has a cover glass on the top, insulation on the sides and bottom to prevent heat transferred to the surrounding, a flat absorber plate that makes a passage for the air flowing with sides and bottom plate. Usually, the passage or channel has a rectangular cross-section. The absorber plate will transfer the heat to the air via convection. Unfortunately, the convection coefficient is very low. To increase the convection coefficient from the absorber plate, a v-corrugated plate is used instead of a flat plate. Tao Liu et al. (Tao, Wen, Wen, & Chan, 2007) stated that a solar air heater with a v-grooved absorber plate could reach efficiency 18% higher than the flat plate on the same operation condition and dimension or configuration. Karim and Hawlader (Karim & Hawlader, 2006) found that a solar collector with a v-absorber plate gave the highest efficiency and the flat plate gave the least. The results showed that the v-corrugated collector is 10–15% and 5–11% more efficient in single pass and double pass modes, respectively, compared to the flat plate collectors. Choudhury and Garg (Choudhury & Garg, 1991) made a detailed analysis of corrugated and flat plate solar air heaters of five different configurations. For the same length, mass flow rate, and air velocity, it was found out that the corrugated and double cover glass collector gave the highest efficiency. According to Naphon (Naphon, 2007) the corrugated surfaces give a significant effect on the enhancement of heat transfer and pressure drop. The Nusselt number of flow in a v-corrugated channel can be 3.2 – 5.0 times higher than in a plane surfaces while the pressure drop 1.96 times higher than on the corresponding plane surface. Islamoglu and Parmaksizoglu (Islamoglu & Parmaksizoglu, 2003) reported that the corrugated channel gave the higher Nusselt number than the straight channel and the higher channel height gave higher Nusselt number for the flow with the same Reynolds number.

Besides changing the cross section area of the channel, some also give effort to increase turbulence inside the channel with fins or obstacles. The result of experimental study done by Promvonge (Promvonge, 2010) in turbulent flow regime (Reynolds number of 5000 to 25,000) showed that multiple 60° V-baffle turbulator fitted on a channel provides the drastic increase in Nusselt number, friction factor, and the thermal enhancement factor values over the smooth wall channel. Kurtbas and Turgut (Kurtbas & Turgut, 2006) investigated the effect of fins located on the absorber surface in free and fixed manners. They used two kinds of rectangular fins which dimension is different but total area is the same. The first type fin (I) has dimension 810 x 60 mm and the second (II) type 200 x 60 mm. To have the same total area, there are 8 fins and 32 fins for the first and second, respectively. The fins type II, both free and fixed, were more effective than type I and flat-plate collector. The fixed fin collector was more effective than free fin collector. Romdhane (Romdhane, 2007) created turbulence in the air channel using obstacles or baffles. The efficiency of collector and the air temperature was found increasing with the use of baffles. Baffles should be used to guide the flow toward the absorber plate. Ho et al. (Ho, Yeh, & Chen, 2011) inserted fins attached by baffles and external recycling to a solar air heater. The experiment and theoretical investigations gave result that heat transfer was improved by employing baffled double-pass with external recycling and fin attached over and under absorber plate. Abene et al. (Abene, Dubois, Le Ray, & Oagued, 2004) used obstacles on the flat plate of a solar air collector for drying grape. The obstacles ensure a good air flow over

the absorber plate, create the turbulence and reduce the dead zones in the collector. Esen (Esen, 2008) used a double-flow solar air heater to investigate three different type obstacles placed on absorber plates compare with the flat plate. The collector has three absorber plates to make three passages for the air flowing through. From the research done, it was found that type III obstacles with flow in middle passage gave the highest efficiency and all collectors with obstacles gave higher efficiency than the flat plate. Akpınar and Koçyiğit (Akpınar & Koçyiğit, 2010) had experimental investigation on solar air heater with several obstacles (Type I, Type II, and Type III) and without obstacles. The optimal value of efficiency was obtained for the solar air heater with Type II obstacles on absorber plate in flow channel duct for all operating conditions and the collector with obstacles appears significantly better than that without obstacles. Bekele et al. (Bekele, Mishra, & Dutta, 2011) investigated experimentally the effect of delta shaped obstacles mounted on the absorber surface of an air heater duct. They found that the obstacle mounted duct enhances the heat transfer to the air. The heat transfer got higher if the obstacle height was taller and its longitudinal pitch was smaller.

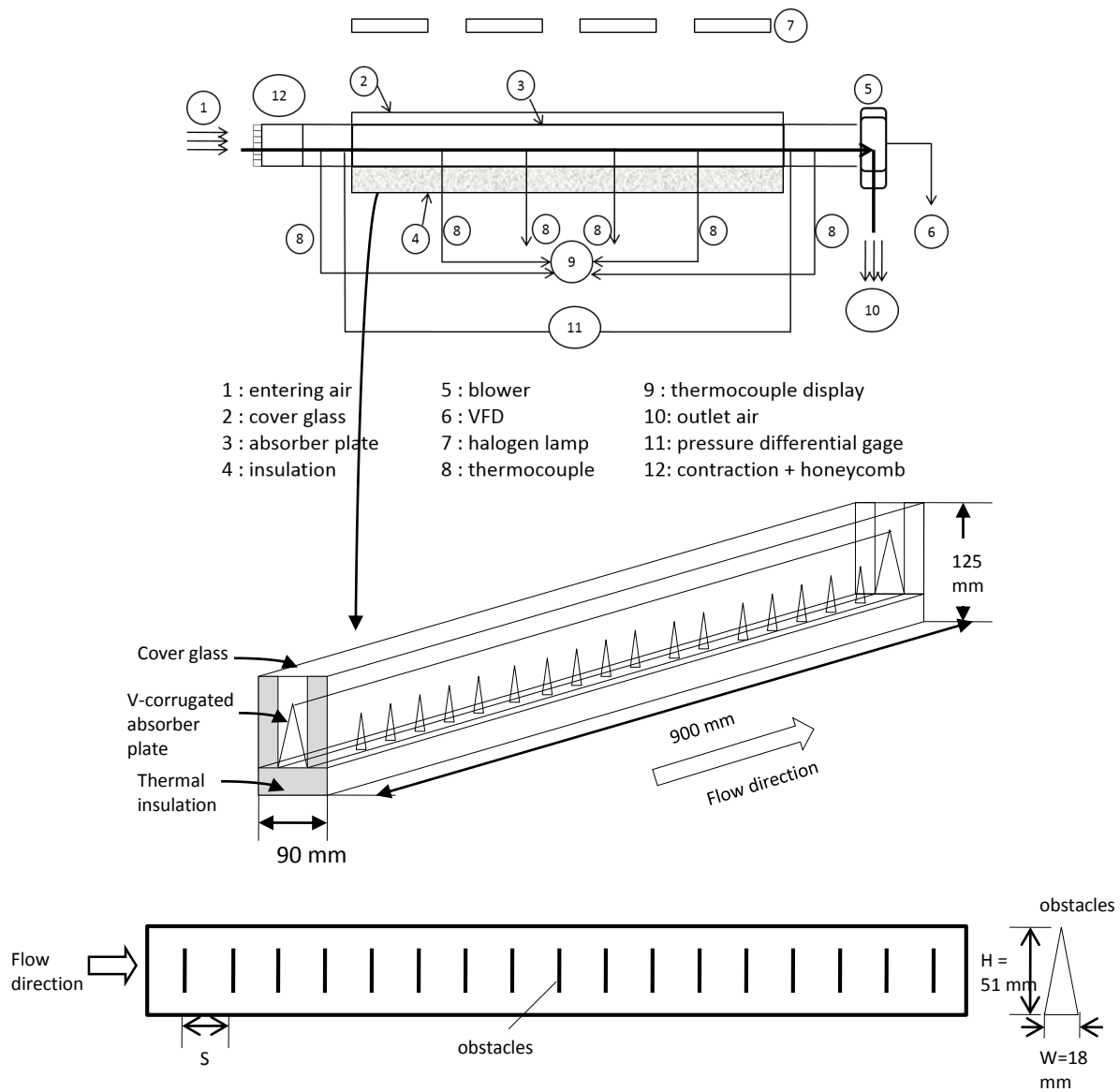
The combine of those two findings, i.e. obstacles and v-corrugated absorber plate are able to improve SAH are important to be studied. Handoyo et al. (Handoyo, Ichsani, Prabowo, & Sutardi, 2014) reported that the obstacles are able to enhance heat transfer in a v-corrugated SAH but increase the air pressure drop. To reduce the air pressure drop, the obstacles were bent vertically. The optimal bending angle is 30° . The SAH's efficiency was 5.3% lower when the obstacles bent 30° instead of straight (0°), but the pressure drop was 17.2% lower. The obstacles' spacing should also give contribution to the air pressure drop. When the spacing is large, the obstacles used is less and the air pressure drop will be reduced. What about the heat transfer? How will the spacing between obstacles effect the heat transfer from the absorber plate to the flowing air? Right now, there is no research investigating the effect of obstacles' spacing on a v-corrugated SAH performance.

This paper describes the result of the numerical studies of obstacles' spacing inserted in a v-corrugated channel of a SAH. The heat transfer from the v-corrugated absorber plate and the air pressure drop flowing the v-corrugated channel is to be discussed. The obstacles are delta-shaped and installed on bottom plate of the channel.

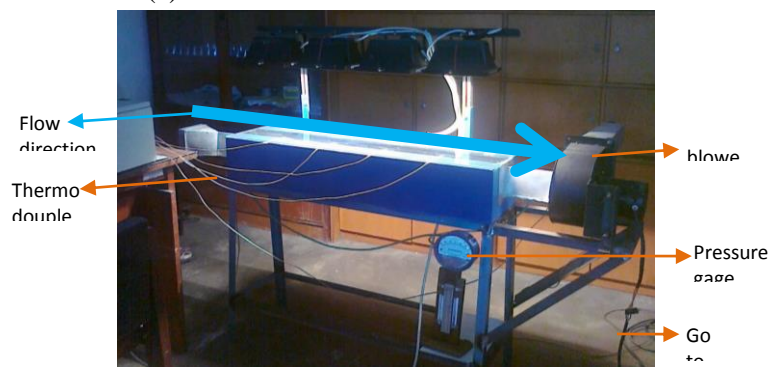
2. Experimental set-up

The studies began with choosing a solar collector model to be studied. The study will be conducted numerically. Thus, a validation is required to prove that the result is true. The validation is accomplished via experiment. An indoor experiment model was constructed to validate numerical result. It is a model of SAH using v-corrugated absorber plate. Its schematic view and photograph are shown in Fig. 1 (a) and (b), respectively. The experiment was conducted in a laboratory of Mechanical Engineering Dept of Petra Christian University, Surabaya, Indonesia.

The collector model's dimension was 900 mm long, 90 mm width, and 125 mm height. A single 3-mm transparent-tempered glass was used as the collector cover. The v-corrugated absorber plate was made of 0.8-mm-thick aluminum and painted black. The apex angle of the v-corrugated plate was 20° . The v-corrugated channel's cross section was 30 mm width and 85 mm height. To prevent heat loss, the left and right walls of collector are insulated with a 25-mm Styrofoam each and a 35-mm Styrofoam for the bottom. The delta-shaped obstacles were made congruent to the channel i.e. triangular and its dimension was 18 mm wide, 51 mm height.



(a) Schematic of the solar collector model



(b) Photograph of experimental set-up.

Fig 1. The SAH model used in experiment

The experiment was conducted indoor to maintain the radiation intensity, wind's velocity and temperature. So, a bias result caused by different outdoor condition could be avoided. The sunlight is replaced with four 500-Watt halogen lamps. The radiation intensity received on the collector was measured using a pyranometer (Kipp & Zonen, type SP Lite2) placed on top of the cover glass. To ensure the homogenous intensity and to generate a certain absorber plate's temperature, these lamps were equipped with adjustable turner individually. The surrounding air condition was controlled by an air conditioner installed in the room. Its temperature, humidity, and wind velocity are well controlled. The collector was equipped with T-type thermocouple which accuracy is 0.1°C for measuring the air temperature at inlet and outlet of the collector, temperature of the absorber plate (at four different locations), and ambient temperature. The pressure drop between inlet and outlet of the flowing air across the collector is also measured with a Magnehelic differential pressure gage which accuracy is ± 2 Pa. A centrifugal blower (1000 m³/h, 580 Pa, 0.2 kW, 380 Volt input) was used to induce the air flowing through the collector. The air flow was adjusted by means of a variable-frequency drive (VFD) to be 5.0 m/s (or Reynolds number = 10,000). The air flow is measured using digital anemometer which accuracy is ± 0.1 m/s. All of the measurement equipments such as pressure gages and thermocouples are installed according to ASHRAE requirement (ASHRAE, 1986).

3. Numerical set up

The discussion in this paper is on the heat transferred to the flowing air and its pressure drop, then the domain of numerical study is focused on the air flow inside the v-corrugated channel. The apex angle of the v-corrugated channel is 20°. Its dimension was 900 mm long, 30 mm width, and 85 mm height. The delta-shaped obstacles were made congruent to the channel i.e. triangular and its dimension was 18 mm wide, 51 mm height. The obstacles were installed in one line only, because there is no much space in the channel. Thus, the spacing to be discussed is actually longitudinal pitch. To specify the obstacles' spacing, a ratio of spacing to height S/H is used. In this study, the ratio S/H used were ½, 1, 1 ½, and 2.

The numerical model for this problem was developed under some assumptions, i.e. as steady three-dimensional turbulent, incompressible flow and constant fluid properties. The space of obstacles was taken equal to height of obstacles, thus ratio is 1. Then, there are 17 obstacles used in this flow. Body force and viscous dissipation are ignored and it was assumed no radiation heat transfer. With these assumptions, (Incropera & DeWitt, 2002) give the related governing equations as follow:

$$\frac{\partial u}{\partial x} + \frac{\partial v}{\partial y} + \frac{\partial w}{\partial z} = 0 \quad (1)$$

$$u \frac{\partial u}{\partial x} + v \frac{\partial u}{\partial y} + w \frac{\partial u}{\partial z} = -\frac{1}{\rho} \frac{\partial P}{\partial x} + \vartheta \left(\frac{\partial^2 u}{\partial x^2} + \frac{\partial^2 u}{\partial y^2} + \frac{\partial^2 u}{\partial z^2} \right) \quad (2)$$

$$u \frac{\partial v}{\partial x} + v \frac{\partial v}{\partial y} + w \frac{\partial v}{\partial z} = -\frac{1}{\rho} \frac{\partial P}{\partial y} + \vartheta \left(\frac{\partial^2 v}{\partial x^2} + \frac{\partial^2 v}{\partial y^2} + \frac{\partial^2 v}{\partial z^2} \right) \quad (3)$$

$$u \frac{\partial w}{\partial x} + v \frac{\partial w}{\partial y} + w \frac{\partial w}{\partial z} = -\frac{1}{\rho} \frac{\partial P}{\partial z} + \vartheta \left(\frac{\partial^2 w}{\partial x^2} + \frac{\partial^2 w}{\partial y^2} + \frac{\partial^2 w}{\partial z^2} \right) \quad (4)$$

$$u \frac{\partial T}{\partial x} + v \frac{\partial T}{\partial y} + w \frac{\partial T}{\partial z} = \alpha \left(\frac{\partial^2 T}{\partial x^2} + \frac{\partial^2 T}{\partial y^2} + \frac{\partial^2 T}{\partial z^2} \right) \quad (5)$$

In the above equations, ρ is the density of the air, p is the pressure, ϑ is the kinematic viscosity, α is the thermal diffusivity, and T is the temperature of the fluid. The boundary conditions of this problem were:

At the inlet: $u = 5.0$ m/s, $v = w = 0$, $T = 297.46$ K

At the upper wall which is the absorber plate: $u = v = w = 0$

At the bottom wall: $u = v = w = 0$

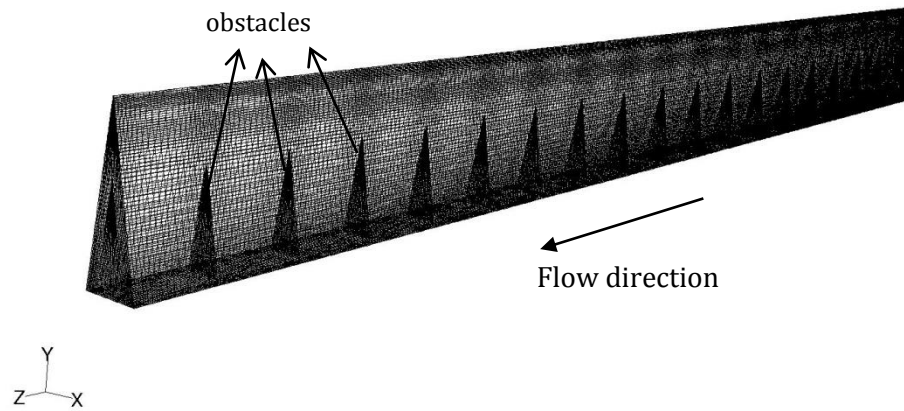
On the 17 obstacles: $u = v = w = 0$

Inlet Reynolds number was calculated with: $Re = \frac{uD_h}{\nu}$ (6)

In Eq. (6), D_h is hydraulic diameter and calculated with: $D_h = \frac{4A}{P}$ (7)

The area, A , in Eq. (7) is the channel cross section area, and P , is its perimeter.

The governing equations above with the boundary conditions were solved using a commercial CFD package, FLUENT 6.3.26 (FLUENT, 2003). The grids of the domain were generated using Gambit 2.4.6. The domain and meshing used in this numerical study were shown in Fig. 2. Since the geometry is a triangular channel, the numerical study should be conducted in three dimensions and all of the meshes were designed to have quality less than 0.7.

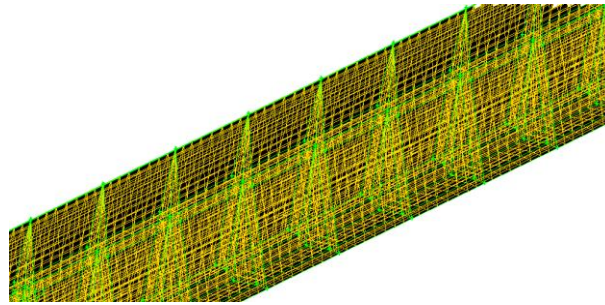


Grid

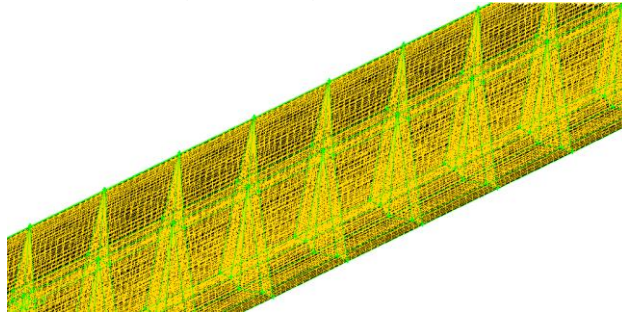
Feb 08, 2013
FLUENT 6.3 (3d, dp, pbns, ske)

Fig 2. The grid used in numerical studies

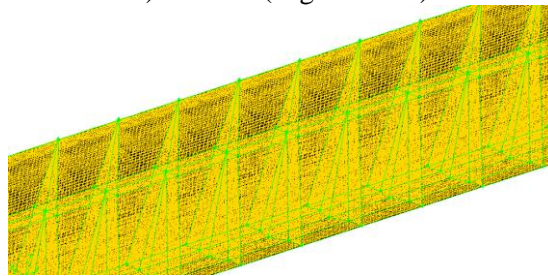
After having a good mesh, the next step is doing grid independency. The grid or mesh is made smaller to get more accurate and detailed result. But, when the mesh is too small, calculation which is done by iteration needs a very long time and might end up with diverge result. Therefore, in this study the mesh or grids were designed not uniform. The finer mesh are used for area near walls both for upper and bottom walls and then gradually the mesh are made coarser as shown in Fig 2. When there are obstacles in the flow, the mesh are designed to be finer not only near the walls but also around the obstacles in Fig 2. There are four meshes designs to be checked for independency as shown in Fig 3a), 3b), 3c), and 3d). The number of cells, faces, and nodes used in each design are shown in Table 1.



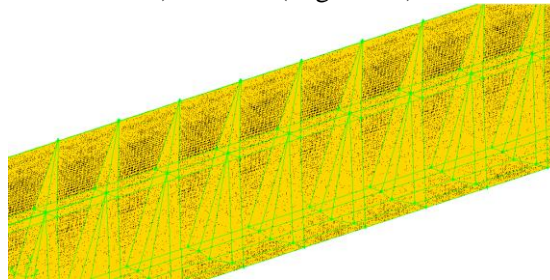
a) Mesh A (most coarse)



b) Mesh B (slight coarse)



c) Mesh C (slight fine)



d) Mesh D (most fine)

Fig 3. Mesh design checked for independency

Table 1. Number of cells, faces, and nodes of the four mesh design

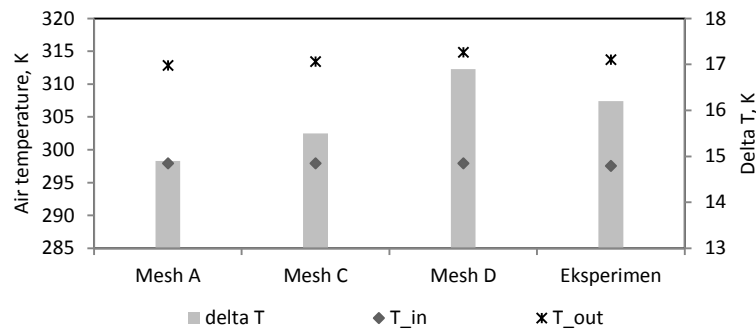
	Mesh A	Mesh B	Mesh C	Mesh D
cell	55,296	338,688	1,092,000	1,980,000
face	173,936	1,043,224	3,335,300	6,026,900
node	63,172	365,480	1,150,798	2,066,248

To check the grid independency, the result from numerical study will be compared to experiment result. The same boundary conditions and setting are used in each numerical study of the four grids design as in Fig 3. The boundary conditions are: inlet air velocity = 5.0 m/s, inlet air temperature = 297.46 K, and constant upper plate temperature. The settings in software used are: three dimension, double precision.

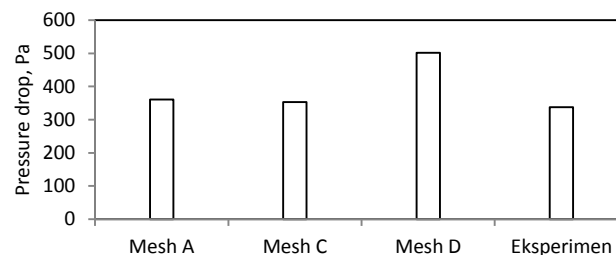
Shear Stress Transport K- ω (SSTK- ω) standard turbulent model was chosen to simulate the flow. The SIMPLEC algorithm was employed to deal with the problem of velocity and pressure coupling. Second-order upwind scheme were used to discretize the main governing equations. Velocity boundary condition was applied at the inlet section while outflow was employed for the outlet. The absorber plate was set to the value as obtained during experiments. Material of the absorber, bottom plate and the obstacles is aluminum. Fluid is air with inlet pressure 1 atm and its properties, such as density, viscosity, thermal conductivity are function of temperature.

Numerical studies were conducted for each of the four mesh: A, B, C, and D. Fig 4 shows global properties resulted from the numerical studies. They are the inlet and outlet temperature of air flowing through the channel and its pressure drop. Only Mesh B could not converge and the residual could not meet the criteria. So, there is no result of Mesh B in Fig 4.

The experiment result which will be discussed in Section 4 gives pressure drop as much as 265 Pa, air temperature outlet 40.5°C when the air inlet velocity is 5.0 m/s and inlet air temperature 24.3°C.



a. The air temperature from numerical studies compared to experiment



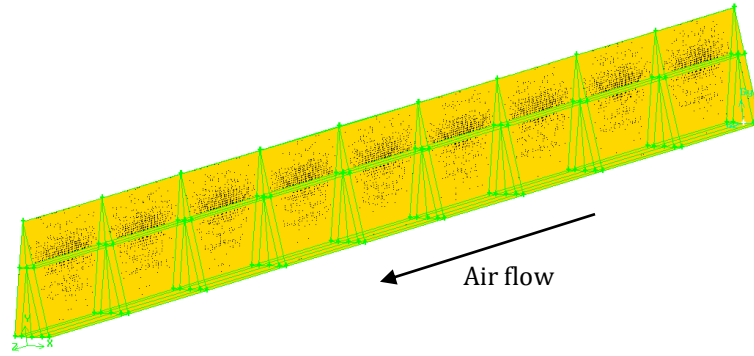
b. The pressure drop from numerical studies compared to experiment

Fig 4. The numerical studies of Mesh A, C, and D compared to the result of experiment

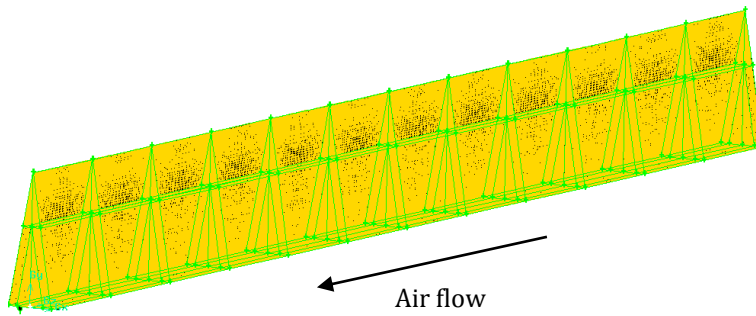
Fig. 4 shows that numerical study with Mesh C and D give better result of air temperature compare to experiment than Mesh A, but mesh D gives too high pressure drop result. Numerical studies using Mesh C give the most closely result to experiments. Thus, Mesh C was chosen for the numerical studies.

Using Mesh C pattern, some numerical studies were conducted to know the effect of obstacles' spacing. The ratio of spacing to height, S/H, studied numerically were 1/2, 1, 1 1/2, and 2. The Mesh used in this study

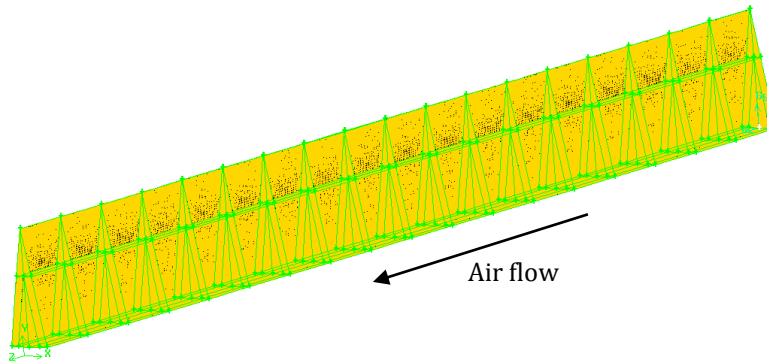
are in Fig. 5 a – 5 d. When the ratio S/H is bigger, then the number of obstacle is less. Number of obstacles are 8, 11, 17, and 35 for ratio S/H 2, $1\frac{1}{2}$, 1, and $\frac{1}{2}$, respectively.



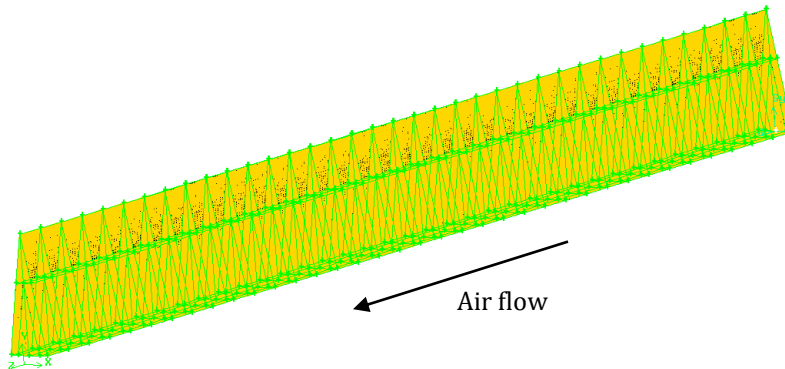
a. Ratio $S/H = 2$



b. Ratio $S/H = 1\frac{1}{2}$



c. Ratio $S/H = 1$



d. Ratio $S/H = \frac{1}{2}$

Fig. 5. The Mesh used for numerical studies of each spacing to height ratio, S/H

4. Results and discussion

Since the experiment is conducted to validate the numerical result, then it is not necessary to conduct experiments for all ratio S/H . The ratio S/H used in experiment equals to 1. Thus, there are 17 obstacles inserted and the percentage of air flow blockage in the channel was 36%. The experiment followed the numerical setting. The experiments were conducted at certain inlet air velocity and certain radiation intensity or absorber temperature. A VFD was used to get an inlet air velocity equals to 5.0 m/s. An adjustable turner was used to adjust the radiation intensity that make the absorber's temperature as high as 320 K or 47°C.

When the numerical result is close to the experimental result, then the numerical result is valid. Table 2 shows the comparison between numerical and experimental results at 5.0-m/s-inlet air velocity and 320 K absorber temperature. Temperature difference of numeric is very close to experiment, while pressure drop is higher about 16% than experiment. Thus, the numerical study using several setting discussed above is acceptable and valid.

Table 2. Comparison between numerical and experimental results

	Numeric	experiment
$T_{in}, ^\circ\text{C}$	297.9	297.5
$T_{out}, ^\circ\text{C}$	314.4	313.7
delta T, $^\circ\text{C}$	16.5	16.2
delta P, Pa	462.3	397.7

Having a valid grids, setting, and viscous model, the numerical study was continued to investigate the spacing effect of obstacles on the bottom plate of air duct. Diagrams of velocity vector of air flow around the obstacles inserted at ratio S/H equals to 2, $1\frac{1}{2}$, 1, and $\frac{1}{2}$ are shown in Figure 6 a), 6 b), 6 c) and 6 d), respectively. All of the velocity vectors were taken at height $y = 10$ mm from the bottom plate. When the ratio $S/H = 2$, the spacing between obstacles = 100 mm. For ratio $S/H = 1\frac{1}{2}$, the spacing = 75 mm, and for ratio $S/H = \frac{1}{2}$, the spacing = 25 mm.

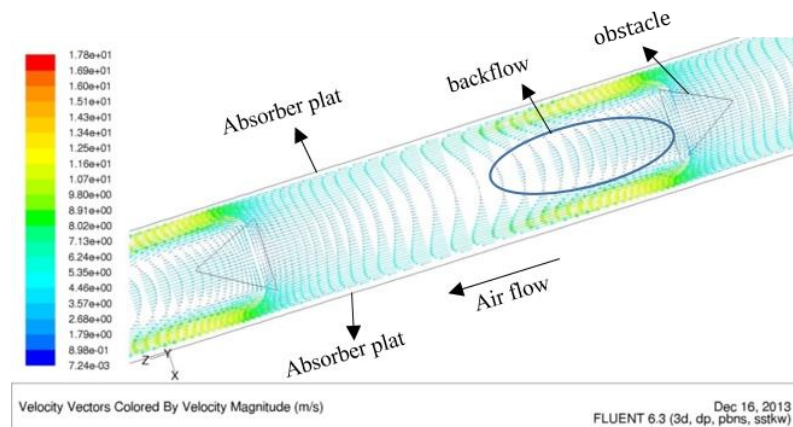


Figure 6 a) Velocity vector of air flow around *obstacle* with ratio $S/H = 2$

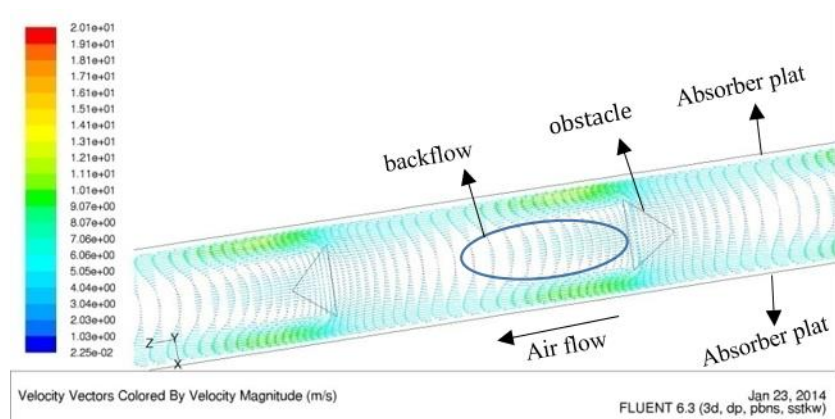


Figure 6 b) Velocity vector of air flow around *obstacle* with ratio $S/H = 1 \frac{1}{2}$

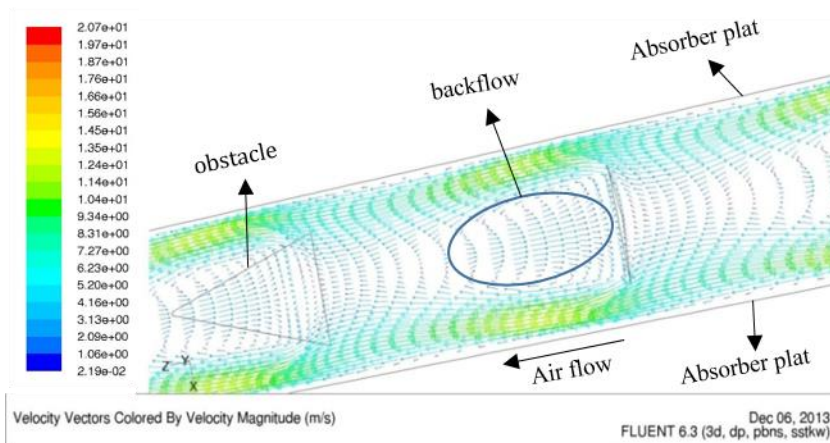


Figure 6 c) Velocity vector of air flow around *obstacle* with ratio $S/H = 1$

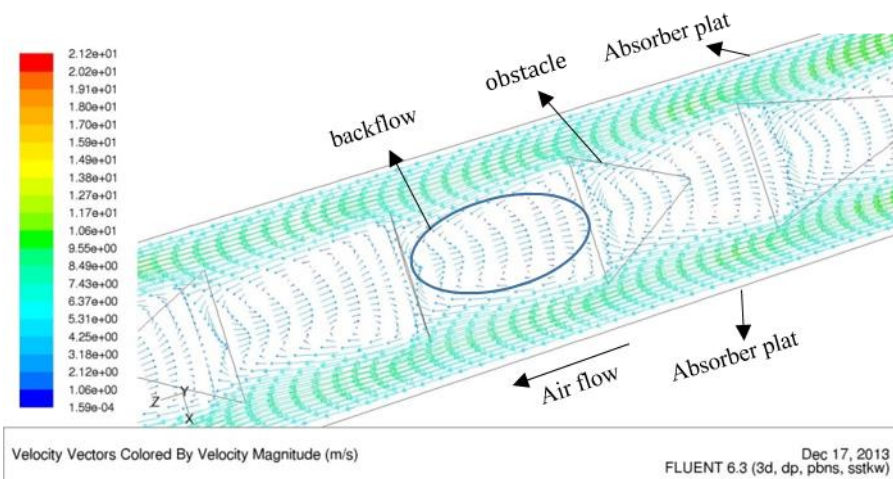


Figure 6 d) Velocity vector of air flow around *obstacle* with ratio $S/H = \frac{1}{2}$

Figure 6 a) – 6 d) show how the air flow encounters separation when flow through obstacles. The obstacles cause backflow between two consecutive obstacles in downstream. There are more backflows when the obstacles' spacing are closer and they cause a higher pressure drop. The air velocity looks higher near

absorber plate when there is backflow or swirl in the flow. This high air velocity makes flow become more turbulent and more heat transferred from the absorber plate to the air. This convection heat transfer to the air makes outlet air temperature higher. Thus, the closer the obstacles' spacing makes the higher pressure drop and higher convection heat transfer from the absorber plate to the air flow.

When the spacing between obstacles is twice its height (ratio $S/H = 2$), air flow is blocked by obstacles and causes backflow behind the obstacles. The backflow caused by separation gradually diminish between two obstacles in downstream as shown in Fig 6 a). Since the air is blocked, most of air is forced to flow in the gap between obstacles and absorber plate. It is shown by longer and higher vector of velocity in the gap. More air is heated by absorber plate. Furthermore, higher velocity increases Reynold number and make the flow more turbulent. More turbulent flow gives higher Nusselt number and definitely increase the convection heat transfer. Thus, obstacles makes outlet air temperature higher than without any (Handoyo, Ichsani, Prabowo, & Sutardi, 2014). Flow in spacing between obstacles experiences backflow after hitting obstacles and then it reattaches quickly when the ratio $S/H = 2$. When the ratio S/H or spacing between obstacles is smaller, as shown in Fig 6 b) – 6 d), backflow is more dominant than reattached flow in area between the obstacles. When backflow occurs, more air will flow in the gap and contact with absorber plate which is the heat source. It is the reason that smaller obstacles' spacing makes higher air outlet temperature and higher SAH's efficiency. The backflow in space between obstacles contributes pressure drop in the flow. More backflow causes higher pressure drop in air acrossed the v-corrugated absorber plate SAH.

Numerical studies also provide some global properties of the flow, such as the air inlet and outlet temperature, and pressure drop. Air temperature difference is calculated from the change between outlet and inlet air temperature. Comparison of air temperature difference and air pressure drop for some ratio S/H from numerical studies is shown in Fig 7. From the air temperature difference and pressure drop data, the following parameters, i.e. SAH's efficiency and friction factor of the air flow in v-corrugated duct with delta-shaped obstacles, are calculated. The efficiency and friction factor are calculated using Equation (8) and (9) according to Duffie & Beckman (1991) and presented in Fig. 8 for three ratio S/H studied.

$$\eta = \frac{q_u}{A_c I} = \frac{\dot{m}_f c_p (T_{fo} - T_{fi})}{A_c I} \quad (8)$$

$$f = \frac{\Delta P}{\frac{L}{D_h} \rho \frac{v^2}{2}} \quad (9)$$

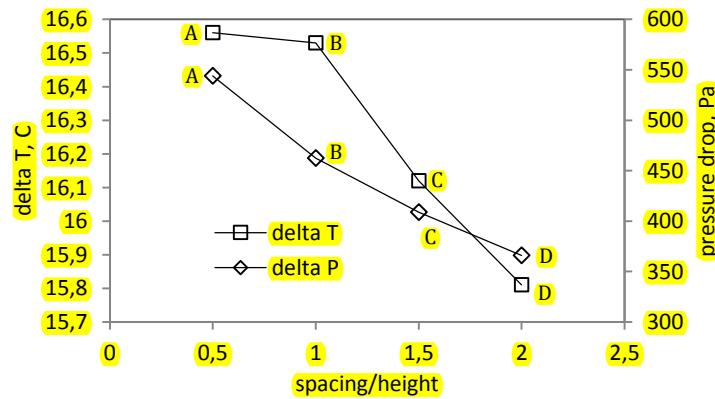


Figure 7. The air temperature difference and pressure drop from numerical studies

Obstacles arranged with ratio $S/H = \frac{1}{2}$ gives the highest air temperature difference and also highest pressure drop for air flowing in a v-corrugated duct, as shown in Fig. 7. This findings are matching with the flow structure discussed above. The obstacles block the air flow and force it to have more contact with absorber plate. Not only forcing the air to the absorber plate, obstacles also causing more backflow. More obstacles produce higher air outlet temperature and higher pressure drop. SAH requires high temperature difference, but low pressure drop. In Fig. 7, considering the temperature difference aspect, point A is the best, but from pressure drop, point D is the best. The gradient of pressure drop in a segment A-B is the steepest among other segments. While the gradient of temperature difference in that segment A-B is the least. Temperature difference in point B (16.53 °C) is slightly less than point A (16.56°C), but pressure drop in point B (462.34 Pa) is much less than point A (544.12 Pa). Sacrifice a little temperature difference but save a lot pressure drop shall be a wise choice.

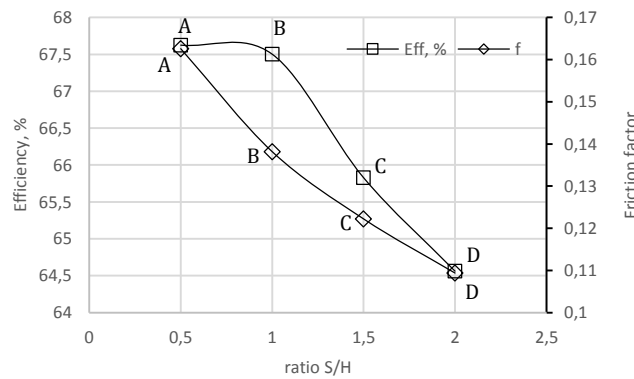


Figure 8. Efficiency of SAH and friction factor of flow with some ratio S/H of obstacles

The thermal efficiency and friction factor are two non-dimensional parameters. Thus, they can be applied to other SAH that has the same geometry and configuration, i.e. corrugated absorber plate and congruent obstacles inserted on bottom plate. Fig. 8 shows those parameters for some ratio S/H studied.

Efficiency of SAH and friction factor are decreasing as ratio S/H is increasing. Gradient of segment A-B of efficiency line is very low compare to other segments. It is rather flat and then getting steepest in segment B-C and CD. When ratio S/H used is 1 instead of 0.5, efficiency of SAH is decreasing 0.18% (from 67.62% to 67.50%) and friction factor is decreasing 15% (from 0.163 to 0.138). So, sacrificing a small amount of efficiency but reducing a significant friction factor is advantageous.

5. Conclusion

From numerical studies in a v-corrugated duct, it is found that backflow between obstacles and high velocity in the gap between obstacles and absorber plate causes the flow became more turbulent and enhanced the convection heat transfer between the air and the absorber plate. Thus, when it is applied in SAH, it will bring improve its efficiency.

Obstacles placed in a small spacing increase air temperature difference and pressure drop. Air temperature difference and pressure drop increase from 15.81°C and 365.89 Pa, to 16.12°C and 408.90 Pa, to 16.53°C and 462.34 Pa, to 16.56°C and 544.12 Pa for ratio S/H decreases from 2 to 1 ½ to 1, and to ½, respectively.

Efficiency of SAH and friction factor are decreasing as ratio S/H is increasing. The best delta-shaped obstacles' spacing inserted in a v-corrugated duct is equal to its height or ratio S/H = 1. When ratio S/H used is 1 instead of 0.5, efficiency of SAH is decreasing 0.18% and friction factor is decreasing 15%. So, sacrificing a small amount of efficiency but reducing a significant friction factor is advantageous.

Acknowledgement

Here, I am very grateful for the support from Kopertis Wilayah VII Jawa Timur, Kementerian Pendidikan dan Kebudayaan by providing Research Grant under contract no: 0004/SP2H/PP/K7/KL/II/2012.

Nomenclature

W	wide of the obstacle (mm)
H	height of the obstacle (mm)
S	spacing between the obstacles (mm)
x, y, z	coordinates
Re	Reynolds number
C_p	specific heat of air (J/kg.K)
\dot{m}_f	mass flow rate of the fluid – air (kg/s)
\dot{Q}_u	useful heat transfer rate (Watt)
I	radiation intensity (W/m ²)
A_c	collector aperture area (m ²)
T_o	collector outlet temperature (K)
T_i	collector air inlet temperature (K)
ϑ	air kinematic viscosity (m ² /s)
ρ	air density (kg/m ³)
α	air thermal diffusion coefficient (m ² /s)
η	efficiency of collector

References

- Abene, A., Dubois, V., Le Ray, M., & Oagued, A. (2004). Study of a solar air flat plate collector: use of obstacle and application for the drying of grape. *J. of Food Engineering*, 65, 15 – 22.
- Akpınar, E. K., & Koçyiğit, F. (2010). Experimental investigation of thermal performance of solar air heater having different obstacles on absorber plates. *Int. Com. in Heat and Mass Transfer*, 37, 416–421.
- ASHRAE. (1986). *Method of Testing to Determine the Thermal Performance of Solar Collectors*. Atlanta: ASHRAE.
- Bekele, A., Mishra, M., & Dutta, S. (2011). Effects of Delta-Shaped Obstacles on the Thermal Performance of Solar Air Heater. *Hindawi Publishing Corporation: Advances in Mechanical Engineering*, 2011, 10 pages.

- Choudhury, C., & Garg, H. P. (1991). Design Analysis of Corrugated and Flat Plate Solar Air Heaters. *Renewable Energy Vol I, No. 5/6*, p. 595 – 607.
- Duffie, J. A., & Beckman, W. A. (1991). *Solar Engineering Of Thermal Processes* (2nd ed. ed.). John Wiley & Sons, Inc.
- Esen, H. (2008). Experimental energy and exergy analysis of a double-flow solar air heater having different obstacles on absorber plates. *Building and Environment*, *43*, 1046–1054.
- FLUENT, I. (2003). *FLUENT User's Guide*.
- Handoyo, E. A., Ichsani, D., Prabowo, & Sutardi. (2014). Experimental Studies on a Solar Air Heater Having V-Corrugated. *Applied Mechanics and Materials*, *493*, 86-92.
- Ho, C.-D., Yeh, H.-M., & Chen, T.-C. (2011). Collector efficiency of upward-type double-pass solar air heaters with fins attached. *Int. Com. in Heat and Mass Transfer*, *38*, 49–56.
- Incropera, F. P., & DeWitt, D. P. (2002). *Fundamentals of Heat and Mass Transfer. 5th edition ed. s.l.:* John Wiley & Sons.
- Islamoglu, Y., & Parmaksizoglu, C. (2003). The effect of channel height on the enhanced heat transfer characteristics in a corrugated heat exchanger channel. *Applied Thermal Engineering* *23*, 979–987.
- Karim, M., & Hawlader, M. (2006). Performance Investigation of Flat Plate, V-Corrugated and Finned Air Collector. *Energy* *31*, 452-470.
- Kurtbas, I., & Turgut, E. (2006). Experimental Investigation of Solar Air Heater with Free and Fixed Fins: Efficiency and Exergy Loss. *Int. J. of Science & Technology, Volume 1*(No 1), 75-82.
- Naphon, P. (2007). Heat transfer characteristics and pressure drop in channel with V corrugated upper and lower plates. *Energy conversion and management* *48*, 1516 – 1524.
- Promvonge, P. (2010). Heat transfer and pressure drop in a channel with multiple 60° V-baffles. *Int. Com. in Heat and Mass Transfer*, *37*, 835–840.
- Romdhane, B. S. (2007). The air solar collectors: Comparative study, introduction of baffles to favor the heat transfer. *Solar Energy*, *81*, 139 – 149.
- Tao, L., Wen, X. L., Wen, F. G., & Chan, X. L. (2007). A Parametric study on the thermal performance of a solar air collector with a V-groove absorber. *Int. J. of Green Energy*, *4*, 601–622.

Response to reviewers

Thank you very much for the approval of our paper. It is so delightful. We are very grateful to all reviewers.

Reviewer #1: The authors have well responded to the comments given. The revised paper has been incorporated with the responses suitably. The paper is now acceptable for publication after following some editing revisions:

Please see section of Introduction in page 3. Please correct surname of author for references [15] and [16] as below:

....as done by Esen et al. [15].

Esen et al. [16] also proposed.....

Thank you for the discreet correction. We are sorry that we wrote the surname mistakenly. We have corrected it. Hopefully, the paper is useful for others.

Reviewer #3: Afer Revision, I think this paper can be accepted now!

We are really grateful for the approval... Hopefully, the paper is useful for others.

Reviewer #4: Revised manuscript is acceptable. The authors have addressed my questions.

Thank you very much for the approval... Hopefully, the paper is useful for others.

Numerical Studies on the Effect of Delta-Shaped Obstacles' Spacing on the Heat Transfer and Pressure Drop in V-Corrugated Channel of Solar Air Heater

Ekadewi A. Handoyo¹, Djatmiko Ichsani², Prabowo², Sutardi²

¹Mechanical Engineering Dept, Petra Christian University, Surabaya – Indonesia

²Mechanical Engineering Dept, Institut Teknologi Sepuluh Nopember, Surabaya – Indonesia

Corresponding author: ekadewi@petra.ac.id

Abstract

Solar air heater (SAH) is simple in construction compared to solar water heater. Yet, it is very useful for drying or space heating. Unfortunately, the convective heat transfer between the absorber plate and the air inside the solar air heater is rather low. Some researchers reported that obstacles are able to enhance the heat transfer in a flat plate solar air collector and others found that a v-corrugated absorber plate gives better heat transfer than a flat plate. Only a few research combines these two in a SAH. This paper will describe the combination from other point of view, i.e. the spacing between obstacles. Its spacing possibly will effect the heat transfer and pressure drop of the air flowing across the channel.

The first step in numerical study is generating mesh or grid of the air flow inside a v-corrugated channel which was blocked by some delta-shaped obstacles. The mesh was designed three-dimension and not uniform. The mesh are made finer for area near obstacles and walls both for upper and bottom, and then gradually coarser. Grid independency is the next step to be conducted. When the mesh is already independent, the numerical study begins. To validate the numerical model, an indoor experiment was conducted. Turbulent model used was Shear Stress Transport K- ω (SSTK- ω) standard. Having a valid numerical model, the spacing between obstacles was studied numerically. Ratio spacing to height, S/H of obstacles investigated were 0.5; 1; 1.5; and 2.

From numerical studies in a v-corrugated duct, it is found that backflow between obstacles and high velocity in the gap between obstacles and absorber plate causes the flow became more turbulent and enhanced the convection heat transfer between the air and the absorber plate. Obstacles placed in a small spacing will increase Nusselt number (convection heat transfer) and friction factor (pressure drop). The Nusselt number enhanced from 27.2 when no obstacle used to 94.2 when obstacles inserted with S/H = 0.5. The Nusselt enhanced 3.46 times. The friction factor will increase from 0.0316 at no obstacle to 0.628 at ratio S/H = 0.5. The friction factor increased 19.9 times. Efficiency, Nusselt number, and friction factor are decreasing as ratio S/H is increasing. When ratio S/H used is 1 instead of 0.5, Nusselt number enhancement decreased only 1.13%, but friction factor decreased 15.1%. So, sacrificing a small amount of Nusselt number but reducing a significant friction factor is advantageous. The optimal spacing ratio S/H of delta-shaped obstacles inserted in a v-corrugated SAH is one. In other words, the optimal spacing of obstacle equals to its height.

Keywords: delta-shaped obstacle; v-corrugated channel; solar air heater; numerical study.

1. Introduction

Solar energy can be converted into thermal energy in a solar collector. Solar collector basically is device used to trap solar energy to heat a plate and transfer the heat to a fluid flowing under or above the plate. When sun light falls onto a plate, solar radiation reaches the plate at lower wavelength and heat it up. Then, the heat is carried away by either water or air that flows under or above the plate. Solar collector used to heat up air is called solar air heater (SAH) and solar water heater for water. Generally, the solar air heater is less efficient than the solar water heater, because air has less thermal capacity and less convection heat transfer coefficient. Yet, air is much lighter and less corrosive than water. The other benefit is that heated air can be used for moderate-temperature drying, such as harvested grains or fish. Since the solar air heater has less convective heat transfer coefficient than solar water heater, some researchers tried to increase this convective heat transfer coefficient.

A popular type of solar air heaters is the flat plate SAH, which has a cover glass on the top, insulation on the sides and bottom to prevent heat transferred to the surrounding, a flat absorber plate that makes a passage for the air flowing with sides and bottom plate. Usually, the passage or channel has a rectangular cross-section. The absorber plate will transfer the heat to the air via convection. Unfortunately, the convection coefficient is very low. To increase the convection coefficient from the absorber plate, a v-corrugated plate is used instead of a flat plate. Tao Liu et al. [1] stated that a solar air heater with a v-grooved absorber plate could reach efficiency 18% higher than the flat plate on the same operation condition and dimension or configuration. Karim and Hawlader [2] found that a solar collector with a v-absorber plate gave the highest efficiency and the flat plate gave the least. The results showed that the v-corrugated collector is 10–15% and 5–11% more efficient in single pass and double pass modes, respectively, compared to the flat plate collectors. Choudhury and Garg [3] made a detailed analysis of corrugated and flat plate solar air heaters of five different configurations. For the same length, mass flow rate, and air velocity, it was found out that the corrugated and double cover glass collector gave the highest efficiency. According to Naphon [4] the corrugated surfaces give a significant effect on the enhancement of heat transfer and pressure drop. The Nusselt number of flow in a v-corrugated channel can be 3.2 – 5.0 times higher than in a plane surfaces while the pressure drop 1.96 times higher than on the corresponding plane surface. Islamoglu and Parmaksizoglu [5] reported that the corrugated channel gave the higher Nusselt number than the straight channel and the higher channel height gave higher Nusselt number for the flow with the same Reynolds number.

Besides changing the cross section area of the channel, some also give effort to increase turbulence inside the channel with fins or obstacles. The result of experimental study done by Promvonge [6] in turbulent flow regime (Reynolds number of 5000 to 25,000) showed that multiple 60° V-baffle turbulator fitted on a channel provides the drastic increase in Nusselt number, friction factor, and the thermal enhancement factor values over the smooth wall channel. Promvonge found that Nusselt number was five times higher and friction factor was 30 times than without baffle at Reynolds number = 10000, $e/H = 0.3$, and $P_R = 1$. Kurtbas and Turgut [7] investigated the effect of fins located on the absorber surface in free and fixed manners. They used two kinds of rectangular fins which dimension is different but total area is the same. The first type fin (I) has dimension 810 x 60 mm and the second (II) type 200 x 60 mm. To have the same total area, there are 8 fins and 32 fins for the first and second, respectively. The fins type II, both free and fixed, were more effective than type I and flat-plate

collector. The fixed fin collector was more effective than free fin collector. Kurtbas and Turgut reported that the maximum Instantaneous efficiency of SAH was 0.78 at air mass flow rate 0.08 kg/s when the fix fins type II were used. While the efficiency of flat plate SAH was only 0.42. So, its efficiency increased 1.86 times. Romdhane [8] created turbulence in the air channel using obstacles or baffles. The efficiency of collector and the air temperature was found increasing with the use of baffles. Baffles should be used to guide the flow toward the absorber plate. Romdhane reported that the efficiency reached 80% for the best type of baffle (chicane) for an air flow rate of 50 m³/h/m². This efficiency was about 1.6 times efficiency without baffle. Ho, et al. [9] inserted fins attached by baffles and external recycling to a solar air heater. The experiment and theoretical investigations gave result that heat transfer was improved by employing baffled double-pass with external recycling and fin attached over and under absorber plate. According to Ho, et al., the highest collector efficiency was 61% in a double-pass flat-plate SAH with recycle when radiation intensity was 1100 W/m², 24 fins attached, and mass flow rate was 0.02 kg/s. It was about 1.35 times its efficiency when there is no recycle. Abene et al. [10] used obstacles on the flat plate of a solar air collector for drying grape. The obstacles ensure a good air flow over the absorber plate, create the turbulence and reduce the dead zones in the collector. The highest efficiency got was 70% when the air flow rate was 50 m³/h/m². It was about 1.9 times its efficiency when no obstacle used. The air pressure drop increased about twice with obstacles. Esen [11] used a double-flow solar air heater to investigate three different type obstacles placed on absorber plates compare with the flat plate. The collector has three absorber plates to make three passages for the air flowing through. From the research done, it was found that all collectors with obstacles gave higher efficiency than the flat plate and type III obstacles with flow in middle passage gave the highest efficiency, i.e. 52.9%, for air flow 0.02 kg/s. It was about 1.13 times higher than its efficiency with no obstacle. Ozgen et al. [12] used aluminum cans as obstacles installed over and under absorber plate. They found that the SAH using double flow passage (over and under absorber plate) gave higher efficiency than just one flow passage (either over or under absorber plate). They also found that SAH with staggered cans (type I) had the highest efficiency compared to aligned cans (type II) and flat plat (type III). The efficiency of SAH type I was 0.73 at air flow rate 0.05 kg/s and it was about 1.4 times of type III. Akpinar and Koçyiğit [13] had experimental investigation on solar air heater with several obstacles (Type I, Type II, and Type III) and without obstacles. The optimal value of efficiency was obtained for the solar air heater with Type II obstacles on absorber plate in flow channel duct for all operating conditions and the collector with obstacles appears significantly better than that without obstacles. The efficiency of Type II was 0.6 at air flow rate 0.0052 kg/s and it was about twice of SAH without obstacle. Bekele et al. [14] investigated experimentally the effect of delta shaped obstacles mounted on the absorber surface of an air heater duct. They found that the obstacle mounted duct enhances the heat transfer to the air. The heat transfer got higher if the obstacle height was taller and its longitudinal pitch was smaller. Nusselt number increased 3.5 times when obstacles inserted with ratio of longitudinal pitch $P_l/e = 3/2$ and height $e/H = 0.75$ at Reynolds number was 10,000. While its friction factor increased 4.7 times than without obstacle. SAH can be modeled through least-squares support vector machines (LS-SVM) method as done by Esen et al. [15]. The predicted results from LS-SVM model had been compared to experimental results. LS-SVM could be used to predict the efficiency of SAH. They showed that efficiency of type I SAH was the highest. Esen et al. [16] also proposed Artificial Neural Network and Wavelet Neural Network (ANN and WNN) to predict the efficiency of SAH. They succeeded to show that the method could predict the SAH efficiency.

The combine of those two findings, i.e. obstacles and v-corrugated absorber plate are able to improve SAH are important to be studied. Handoyo et al. [17] reported that the obstacles are able to enhance heat transfer in a v-corrugated SAH but increase the air pressure drop. To reduce the air pressure drop,

the obstacles were bent vertically. The optimal bending angle is 30°. The SAH's efficiency was 5.3% lower when the obstacles bent 30° instead of straight (0°), but the pressure drop was 17.2% lower.

According to Incropera [18], in forced convection heat transfer, there are two quantities that are important to be determined. One is friction coefficient, C_f , and the other is Nusselt number, Nu . Friction coefficient, C_f is used to calculate the shear stress at the wall and then to calculate pressure drop. While Nusselt number, Nu is used to calculate convection heat transfer rate. The relation that correlate them is known as Reynolds Analogy: $C_{f,x} \frac{Re_L}{2} = Nu_x Pr^{-1/3}$

When Nusselt number increases, then friction coefficient will increase, too. In a SAH, it is expected that convection heat transfer increases but pressure drop does not. So, many research were conducted to look for increasing in heat transfer at low pressure drop.

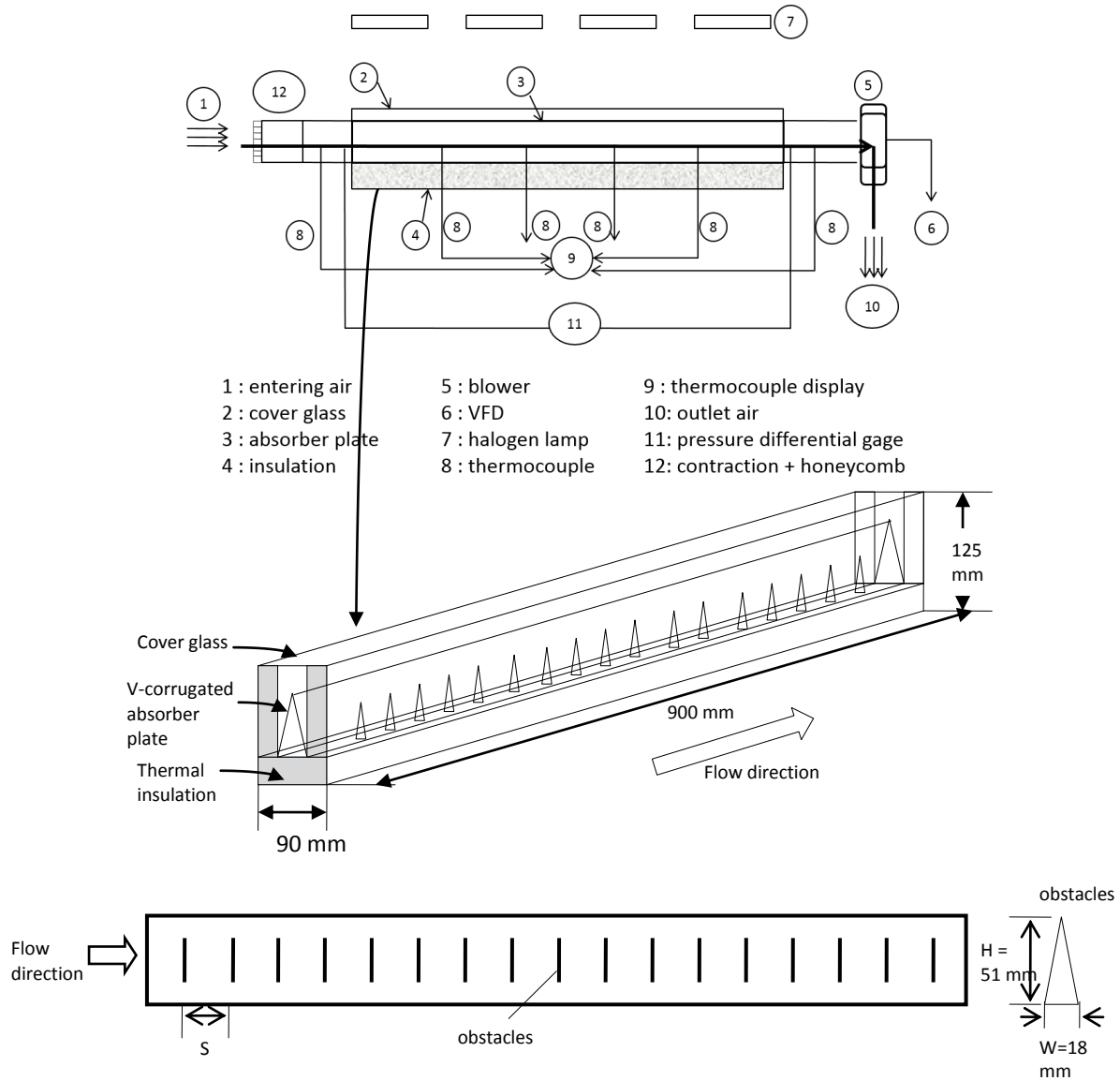
The spacing between obstacles mounted on absorber plate can be varied. A different spacing will give different air pressure drop as the air flows across the collector. Obstacles increase the air pressure drop. When the spacing is large, the obstacles used is less and the air pressure drop will be reduced. What about the heat transfer from the absorber plate to the flowing air? How will the spacing between obstacles effect the heat transfer? To the knowledge of the authors, there is no research investigating the effect of delta-shaped obstacles' spacing on a v-corrugated SAH performance, yet.

This paper describes the result of the numerical studies of obstacles' spacing inserted in a v-corrugated channel of a SAH. The heat transfer from the v-corrugated absorber plate and the air pressure drop flowing the v-corrugated channel is to be discussed. The obstacles are delta-shaped and installed on bottom plate of the channel.

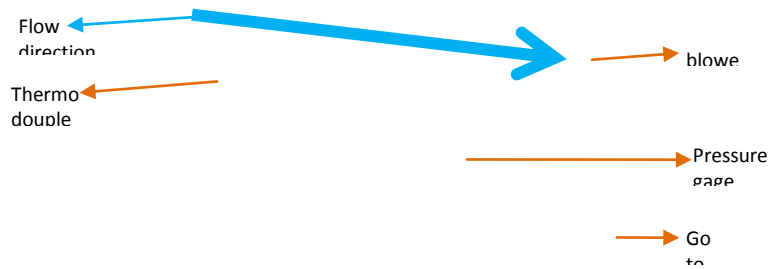
2. Experimental set-up

The studies began with choosing a solar collector model to be studied. The study will be conducted numerically. Thus, a validation is required to prove that the result is true. The validation is accomplished via experiment. An indoor experiment model was constructed to validate numerical result. It is a model of SAH using v-corrugated absorber plate. Its schematic view and photograph are shown in Fig. 1 (a) and (b), respectively. The experiment was conducted in a laboratory of Mechanical Engineering Dept of Petra Christian University, Surabaya, Indonesia.

The collector model's dimension was 900 mm long, 90 mm width, and 125 mm height. A single 3-mm transparent-tempered glass was used as the collector cover. The v-corrugated absorber plate was made of 0.8-mm-thick aluminum and painted black. The apex angle of the v-corrugated plate was 20°. The v-corrugated channel's cross section was 30 mm width and 85 mm height. To prevent heat loss, the left and right walls of collector are insulated with a 25-mm Styrofoam each and a 35-mm Styrofoam for the bottom. The delta-shaped obstacles were made congruent to the channel i.e. triangular and its dimension was 18 mm wide, 51 mm height.



(a) Schematic of the solar collector model



(b) Photograph of experimental set-up.

Figure 1. The SAH model used in experiment

The experiment was conducted indoor to maintain the radiation intensity, wind's velocity and temperature. So, a bias result caused by different outdoor condition could be avoided. The sunlight is replaced with four 500-Watt halogen lamps. The radiation intensity received on the collector was measured using a pyranometer (Kipp & Zonen, type SP Lite2) placed on top of the cover glass. To ensure the homogenous intensity and to generate a certain absorber plate's temperature, these lamps were equipped with adjustable turner individually. The surrounding air condition was controlled by an air conditioner installed in the room. Its temperature, humidity, and wind velocity are well controlled. The collector was equipped with T-type thermocouple which accuracy is 0.1°C for measuring the air temperature at inlet and outlet of the collector, temperature of the absorber plate (at four different locations), and ambient temperature. The pressure drop between inlet and outlet of the flowing air across the collector is also measured with a Magnehelic differential pressure gage which accuracy is ± 2 Pa. A centrifugal blower (1000 m³/h, 580 Pa, 0.2 kW, 380 Volt input) was used to induce the air flowing through the collector. The air flow was adjusted by means of a variable-frequency drive (VFD) to be 5.0 m/s (or Reynolds number = 10,000). The air flow is measured using digital anemometer which accuracy is ± 0.1 m/s. All of the measurement equipments such as pressure gages and thermocouples are installed according to ASHRAE requirement [19].

3. Numerical set up

The discussion in this paper is on the heat transferred to the flowing air and its pressure drop, then the domain of numerical study is focused on the air flow inside the v-corrugated channel. The apex angle of the v-corrugated channel is 20°. Its dimension was 900 mm long, 30 mm width, and 85 mm height. The delta-shaped obstacles were made congruent to the channel i.e. triangular and its dimension was 18 mm wide, 51 mm height. The obstacles were installed in one line only, because there is no much space in the channel. Thus, the spacing to be discussed is also called longitudinal pitch. To specify the obstacles' spacing, a ratio of spacing to height S/H is used. In this study, the ratio S/H used were ½, 1, 1 ½, and 2.

The numerical model for this problem was developed under some assumptions, i.e. as steady three-dimensional turbulent, incompressible flow and constant fluid properties. The space of obstacles was taken equal to height of obstacles, thus ratio is 1. Then, there are 17 obstacles used in this flow. Body force and viscous dissipation are ignored and it was assumed no radiation heat transfer. With these assumptions, [18] give the related governing equations as follow:

$$\frac{\partial u}{\partial x} + \frac{\partial v}{\partial y} + \frac{\partial w}{\partial z} = 0 \quad (1)$$

$$u \frac{\partial u}{\partial x} + v \frac{\partial u}{\partial y} + w \frac{\partial u}{\partial z} = -\frac{1}{\rho} \frac{\partial P}{\partial x} + \nu \left(\frac{\partial^2 u}{\partial x^2} + \frac{\partial^2 u}{\partial y^2} + \frac{\partial^2 u}{\partial z^2} \right) \quad (2)$$

$$u \frac{\partial v}{\partial x} + v \frac{\partial v}{\partial y} + w \frac{\partial v}{\partial z} = -\frac{1}{\rho} \frac{\partial P}{\partial y} + \nu \left(\frac{\partial^2 v}{\partial x^2} + \frac{\partial^2 v}{\partial y^2} + \frac{\partial^2 v}{\partial z^2} \right) \quad (3)$$

$$u \frac{\partial w}{\partial x} + v \frac{\partial w}{\partial y} + w \frac{\partial w}{\partial z} = -\frac{1}{\rho} \frac{\partial P}{\partial z} + \nu \left(\frac{\partial^2 w}{\partial x^2} + \frac{\partial^2 w}{\partial y^2} + \frac{\partial^2 w}{\partial z^2} \right) \quad (4)$$

$$u \frac{\partial T}{\partial x} + v \frac{\partial T}{\partial y} + w \frac{\partial T}{\partial z} = \alpha \left(\frac{\partial^2 T}{\partial x^2} + \frac{\partial^2 T}{\partial y^2} + \frac{\partial^2 T}{\partial z^2} \right) \quad (5)$$

In the above equations, ρ is the density of the air, p is the pressure, ϑ is the kinematic viscosity, α is the thermal diffusivity, and T is the temperature of the fluid. The boundary conditions of this problem were:

At the inlet: $u = 5.0$ m/s, $v = w = 0$, $T = 297.46$ K

At the upper wall which is the absorber plate: $u = v = w = 0$

At the bottom wall: $u = v = w = 0$

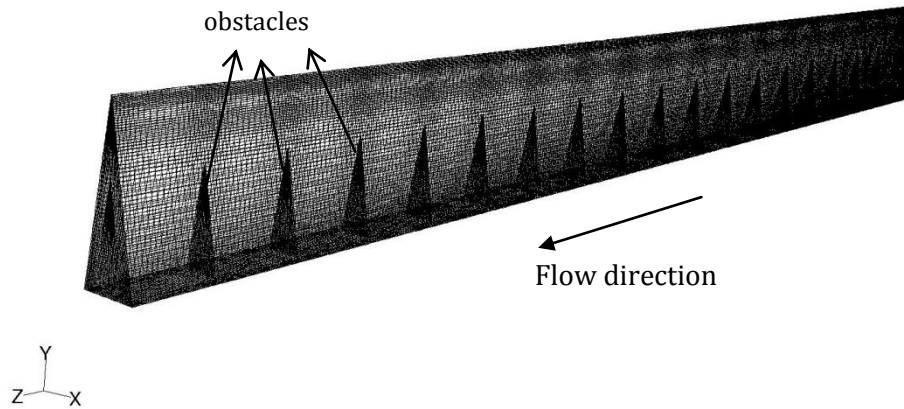
On the 17 obstacles: $u = v = w = 0$

Inlet Reynolds number was calculated with: $Re = \frac{uD_h}{\vartheta}$ (6)

In Eq. (6), D_h is hydraulic diameter and calculated with: $D_h = \frac{4A}{P}$ (7)

The area, A , in Eq. (7) is the channel cross section area, and P , is its perimeter.

The governing equations above with the boundary conditions were solved using a commercial CFD package, FLUENT 6.3.26 [20]. The grids of the domain were generated using Gambit 2.4.6. The domain and meshing used in this numerical study were shown in Fig. 2. Since the geometry is a triangular channel, the numerical study should be conducted in three dimensions and all of the meshes were designed to have quality less than 0.7.

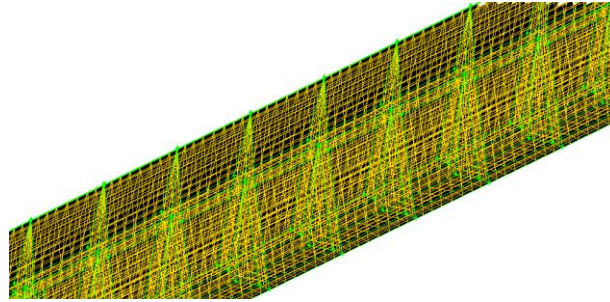


Grid

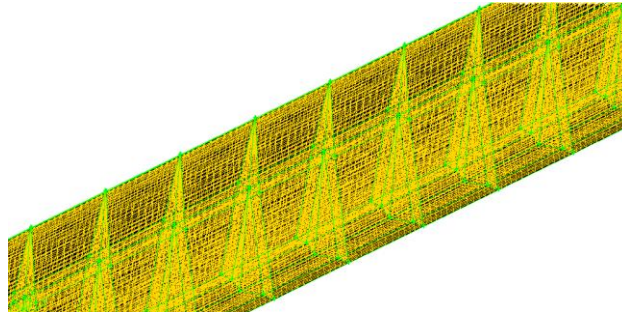
Feb 08, 2013
FLUENT 6.3 (3d, dp, pbns, ske)

Figure 2. The grid used in numerical studies

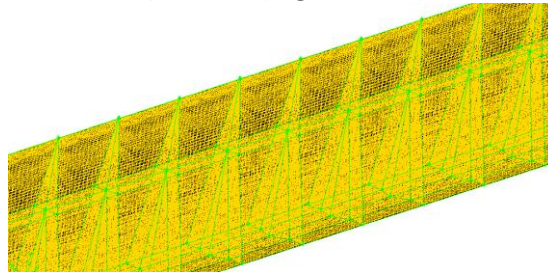
After having a good mesh, the next step is doing grid independency. The grid or mesh is made smaller to get more accurate and detailed result. But, when the mesh is too small, calculation which is done by iteration needs a very long time and might end up with diverge result. Therefore, in this study the mesh or grids were designed not uniform. The finer mesh are used for area near walls both for upper and bottom walls and then gradually the mesh are made coarser as shown in Fig 2. When there are obstacles in the flow, the mesh are designed to be finer not only near the walls but also around the obstacles in Fig 2. There are four meshes designs to be checked for independency as shown in Fig 3a), 3b), 3c), and 3d). The number of cells, faces, and nodes used in each design are shown in Table 1.



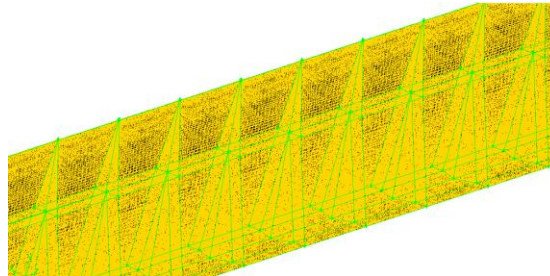
a) Mesh A (most coarse)



b) Mesh B (slight coarse)



c) Mesh C (slight fine)



d) Mesh D (most fine)

Figure 3. Mesh design checked for independency

Table 1. Number of cells, faces, and nodes of the four mesh design

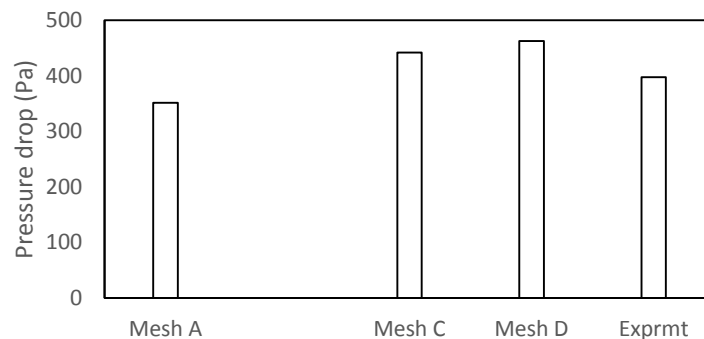
	Mesh A	Mesh B	Mesh C	Mesh D
cell	55,296	338,688	1,092,000	1,980,000
face	173,936	1,043,224	3,335,300	6,026,900
node	63,172	365,480	1,150,798	2,066,248

To check the grid independency, the result from numerical study will be compared to experiment result. The same boundary conditions and setting are used in each numerical study of the four grids design as in Fig 3. The boundary conditions are: inlet air velocity = 5.0 m/s and outflow was employed for the

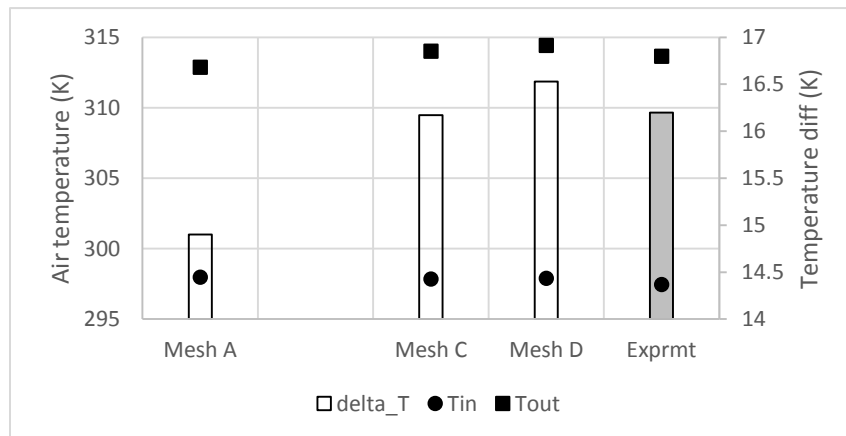
outlet; inlet air temperature = 297.46 K; and absorber plate temperature as obtained during experiments = 320 K. The settings in software used are: three dimension, double precision. Shear Stress Transport K- ω (SSTK- ω) standard turbulent model was chosen to simulate the flow. Zhang and Liu conducted a numerical simulation of the flow inside a diffusing S-duct inlet. Full three-dimensional Navier-Stokes equations are solved and SST turbulence model is employed. Numerical results, include surface static pressure, total pressure recovery at exit, are compared with experiment. A fairly good agreement is apparent [21]. Other researcher, Kirkgoz et. al. reported that numerical modelling using K- ω and SSTK- ω used on the cylinder surface gave reasonably success result [22]. The SIMPLEC algorithm was employed to deal with the problem of velocity and pressure coupling. Second-order upwind scheme were used to discretize the main governing equations. Material of the absorber, bottom plate and the obstacles is aluminum. Fluid was air with inlet pressure 1 atm and its properties, such as density, viscosity, thermal conductivity were function of temperature.

Numerical studies were conducted for each of the four mesh: A, B, C, and D. Fig 4 shows global properties resulted from the numerical studies. They were the inlet and outlet temperature of air flowing through the channel and its pressure drop. Only Mesh B could not converge and the residual could not meet the criteria. So, there was no result of Mesh B in Fig 4.

The experiment result which will be discussed in Section 4 gives pressure drop as much as 397.7 Pa, air temperature outlet 40.7°C when the air inlet velocity is 5.0 m/s and inlet air temperature 24.5°C.



a. The air pressure drop from numerical studies compared to experiment

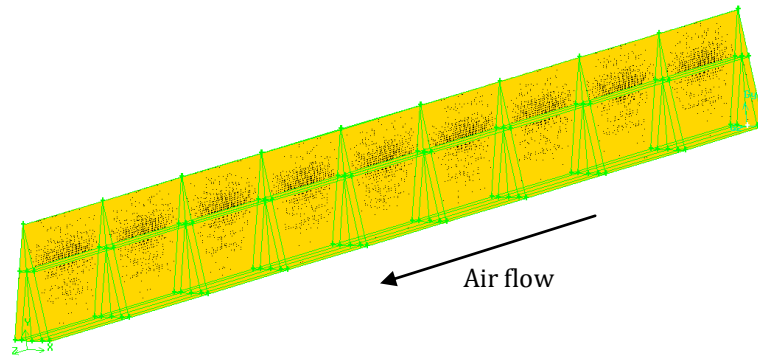


b. The air temperature from numerical studies compared to experiment

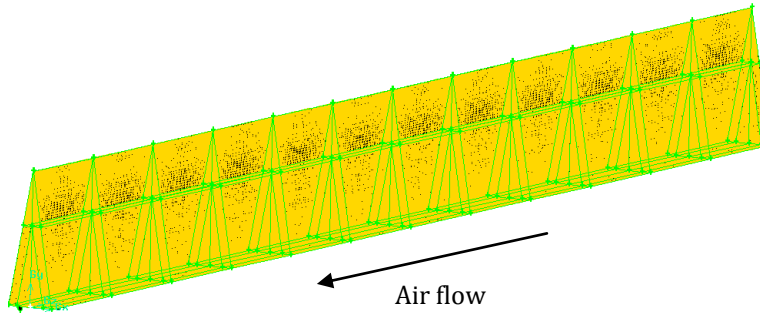
Figure 4. The numerical studies of Mesh A, C, and D compared to the result of experiment for $S/H = 1$

Fig. 4 shows that numerical study with Mesh C and D give better result of air temperature compare to experiment than Mesh A, but mesh D gives too high pressure drop result. Numerical studies using Mesh C give the most closely result to experiments. Thus, Mesh C was chosen for the numerical studies.

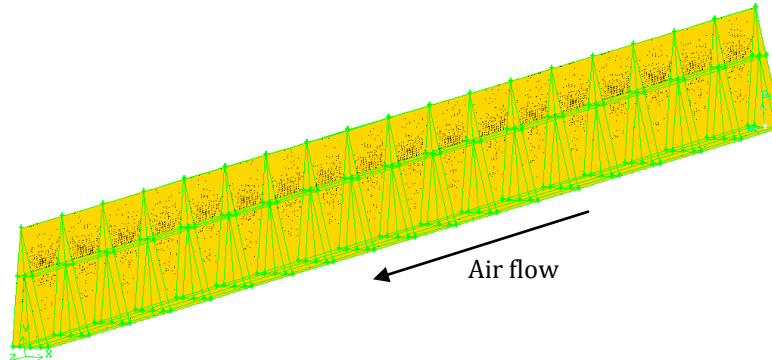
Using Mesh C pattern, some numerical studies were conducted to know the effect of obstacles' spacing. The ratio of spacing to height, S/H , studied numerically were $\frac{1}{2}$, 1, $1\frac{1}{2}$, and 2. The Mesh used in this study are in Fig. 5 a – 5 d. When the ratio S/H is bigger, then the number of obstacle is less. Number of obstacles are 8, 11, 17, and 35 for ratio $S/H = 2, 1\frac{1}{2}, 1$, and $\frac{1}{2}$, respectively.



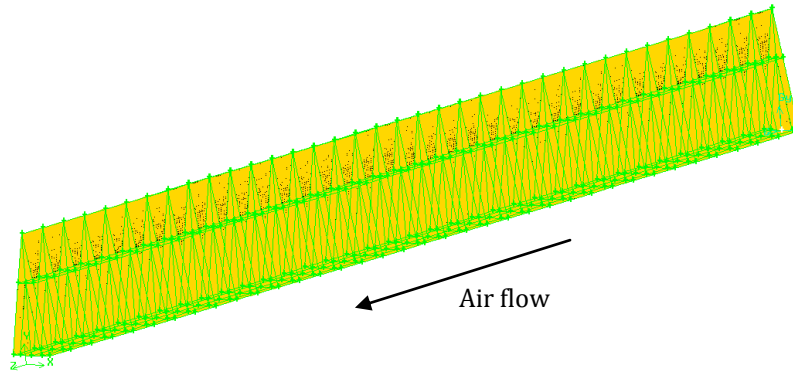
a. Ratio $S/H = 2$



b. Ratio $S/H = 1\frac{1}{2}$



c. Ratio $S/H = 1$



d. Ratio $S/H = \frac{1}{2}$

Figure 5. The Mesh used for numerical studies of each spacing to height ratio, S/H

To give more comprehensive result, numerical study was also conducted for air flow in a v-corrugated channel without obstacle. The domain and mesh used is shown in Fig. 6.

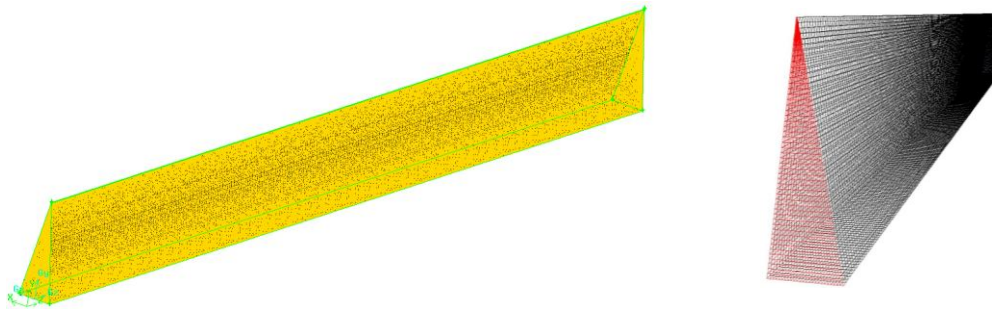


Figure 6. The Mesh used for numerical studies of air flow without obstacle

4. Results and discussion

Since the experiment is conducted to validate the numerical result, then it is not necessary to conduct experiments for all ratio S/H . The ratio S/H used in experiment equals to 1. Thus, there are 17 obstacles inserted and the percentage of air flow blockage in the channel is 36%. The experiment followed the numerical setting. The experiments were conducted at certain inlet air velocity and certain radiation intensity or absorber temperature. A VFD was used to get an inlet air velocity equals to 5.0 m/s. An adjustable turner was used to adjust the radiation intensity that make the absorber's temperature as high as 320 K or 47°C.

When the numerical result is close to the experimental result, then the numerical result is valid. Table 2 shows the comparison between numerical and experimental results at 5.0-m/s-inlet air velocity and 320 K absorber temperature. The air temperature difference and pressure drop of numeric is very close to experiment. Thus, the numerical study using several setting discussed above is acceptable and valid.

Table 2. Comparison between numerical and experimental results

	Numeric	experiment
T_{in} , K	297.9	297.5

T_{out}, K	314.4	313.7
$\Delta T, K$	16.5	16.2
$\Delta P, Pa$	462.3	450.3

To ensure that the model used in numerical study is valid, a comparison between Nusselt number from numerical result and Gnielinski equation for triangular channel without obstacle or smooth duct was conducted. According to Incropera [18], Gnielinski gives more accurate relation to calculate Nusselt number at lower Reynolds number than Dittus – Boelter equation. The relation of Nusselt number is in Equation (8):

$$Nu_D = \frac{(f/8)(Re_D - 1000)Pr}{1 + 12.7(f/8)^{1/2}(Pr^{2/3} - 1)} \quad (8)$$

The friction factor in Equation (8), f , is obtained from Moody diagram. The comparison in Fig. 7 shows that numerical simulation gives pretty accurate results.

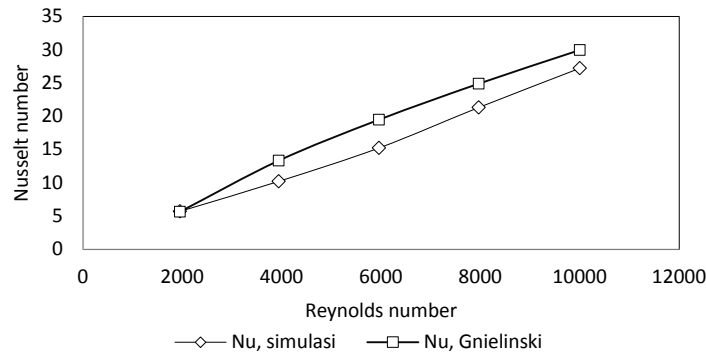
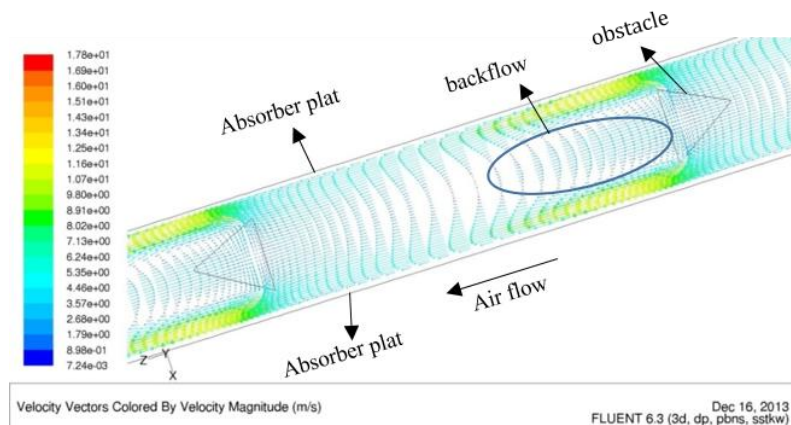


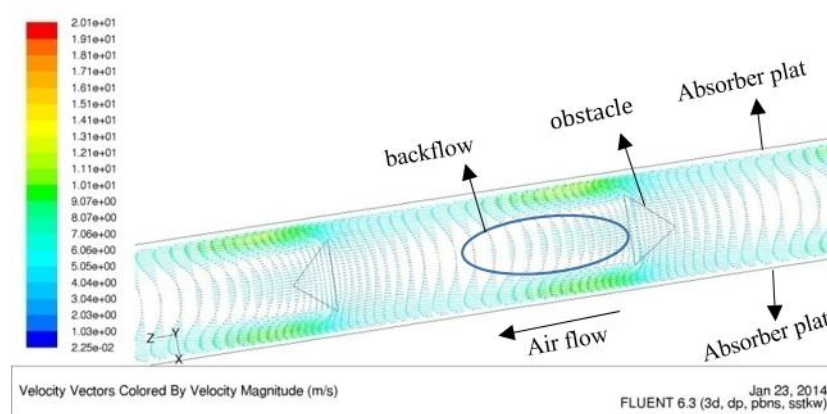
Figure 7. Comparison of Nusselt number for smooth duct (no obstacle) from numerical study and Gnielinski equation.

Having a valid grids, setting, and viscous model, the numerical study was continued to investigate the spacing effect of obstacles on the bottom plate of air duct. Diagrams of velocity vector of air flow around the obstacles inserted at ratio S/H equals to 2, $1 \frac{1}{2}$, 1, and $\frac{1}{2}$ are shown in Figure 8 a), 8 b), 8 c), and 8 d), respectively. All of the velocity vectors were taken at height $y = 10$ mm from the bottom plate. When the ratio $S/H = 2$, the spacing between obstacles = 100 mm. For ratio $S/H = 1 \frac{1}{2}$, the spacing = 75

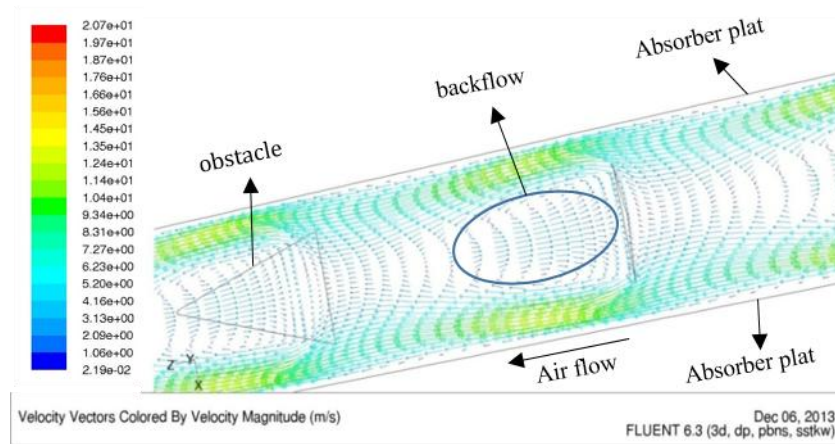


mm, and for ratio $S/H = \frac{1}{2}$, the spacing = 25 mm.

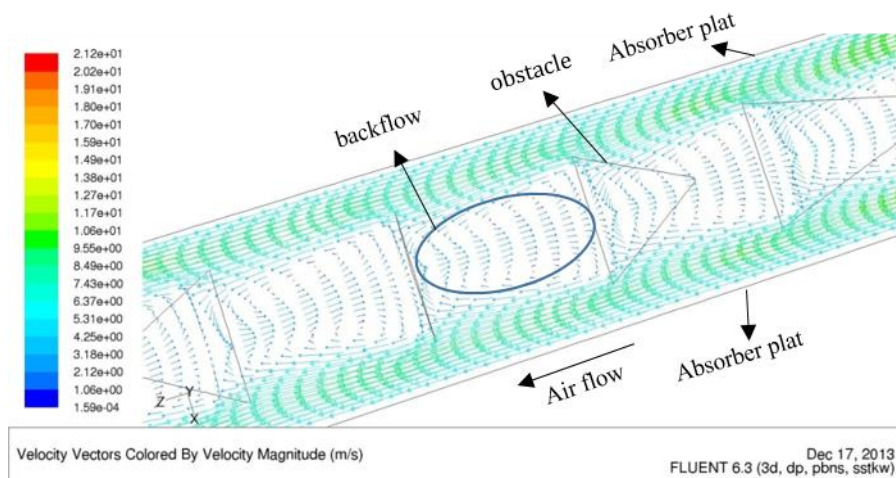
a) Velocity vector of air flow around *obstacle* with ratio $S/H = 2$



b) Velocity vector of air flow around *obstacle* with ratio $S/H = 1 \frac{1}{2}$



c) Velocity vector of air flow around *obstacle* with ratio $S/H = 1$



d) Velocity vector of air flow around obstacle with ratio $S/H = \frac{1}{2}$

Figure 8. Velocity vector of air flow around obstacle with some ratio S/H

Figure 8 a) – 8 d) show how the air flow encounters separation when flow through obstacles. The obstacles cause backflow between two consecutive obstacles in downstream. There are more backflows when the obstacles' spacing are closer and they cause a higher pressure drop. The air velocity looks higher near absorber plate when there is backflow or swirl in the flow. This high air velocity makes flow become more turbulent and more heat transferred from the absorber plate to the air. This convection heat transfer to the air makes outlet air temperature higher. Thus, the closer the obstacles' spacing makes the higher pressure drop and higher convection heat transfer from the absorber plate to the air flow.

When the spacing between obstacles is twice its height (ratio $S/H = 2$), small amount of air flow is blocked by obstacles and causes backflow behind the obstacles. The backflow caused by separation gradually diminish between two obstacles in downstream as shown in Fig 8 a). Since the air is blocked, most of air is forced to flow in the gap between obstacles and absorber plate. It is shown by longer and higher vector of velocity in the gap. More air is heated by absorber plate. Furthermore, higher velocity increases Reynold number and make the flow more turbulent. More turbulent flow gives higher Nusselt number and definitely increase the convection heat transfer. Thus, obstacles makes outlet air temperature higher than without any [17]. Flow in spacing between obstacles experiences backflow after hitting obstacles and then it reattaches quickly when the ratio $S/H = 2$. When the ratio S/H or spacing between obstacles is smaller, as shown in Fig 8 b) – 8 d), backflow is more dominant than reattached flow in area between the obstacles. When backflow occurs, more air will flow in the gap and contact with absorber plate which is the heat source. It is the reason that smaller obstacles' spacing makes higher air outlet temperature and higher SAH's efficiency. The backflow in space between obstacles contributes pressure drop in the flow. More backflow causes higher pressure drop in air acrossed the v-corrugated absorber plate SAH.

Numerical studies also provide some global properties of the flow, such as the air inlet and outlet temperature, and pressure drop. These data were used to acquire the efficiency and friction factor of the air flow in a v-corrugated SAH with delta-shaped obstacles. The efficiency and friction factor are calculated using Equation (9) and (10) according to Duffie & Beckman [23].

$$\eta = \frac{q_u}{A_c I} = \frac{\dot{m}_f c_p (T_{fo} - T_{fi})}{A_c I} \quad (9)$$

$$f = \frac{\Delta P}{\frac{L}{D_h} \rho \frac{v^2}{2}} \quad (10)$$

Comparison of efficiency and friction factor for some ratio S/H from numerical studies is shown in Fig 9. Ratio $S/H = 0$ in Fig. 9 means no obstacle in the air flow. Obstacles arranged with ratio $S/H = \frac{1}{2}$ gives the highest air efficiency, i.e. 68% and also highest fricition factor, i.e. 0.628 for air flowing in a v-corrugated duct, as shown in Fig. 9. For comparison, efficiency when no obstacle is only 49% and friction factor is only 0.0316. This findings are matching with the flow structure discussed above. The obstacles block the air flow and force it to have more contact with absorber plate. Not only forcing the air to the absorber plate, obstacles also causing more backflow. More obstacles produce higher efficiency and higher

friction factor. SAH requires high efficiency or high outlet air temperature, but low friction or pressure drop. Increasing friction factor means increasing pumping power required in SAH.

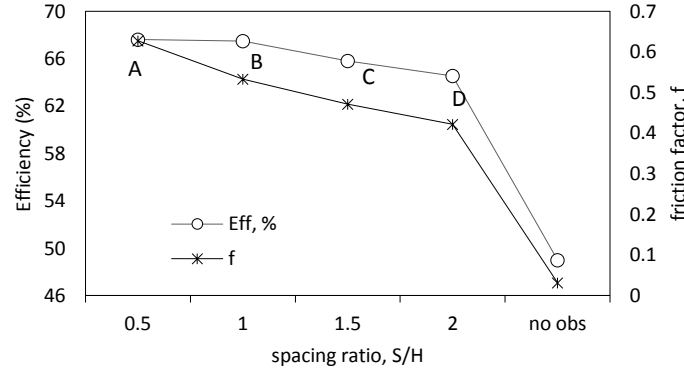


Figure 9. The efficiency of SAH and friction factor of flow with some ratio S/H of obstacles.

Besides efficiency, Nusselt number is interesting to be analyzed. It could be calculated using equation (11).

$$h = \frac{Nu_D k}{D_h} \quad (11)$$

While the convection heat transfer rate and log-mean temperature difference could be calculated using equation (12) and (13).

$$q = h A \Delta T_{lm} \quad (12)$$

$$\Delta T_{lm} = \frac{(T_{abs} - T_o) - (T_{abs} - T_i)}{\ln \frac{(T_{abs} - T_o)}{(T_{abs} - T_i)}} \quad (13)$$

The ratio S/H of obstacles effect the Nusselt number of air flow as shown in Fig. 10. Nusselt number of air flow with obstacles are much higher than without obstacle. The highest Nu number and friction factor are 94.2 and 0.628 at ratio S/H = 0.5 and is only 27.2 and 0.0316 at no obstacle. Fig. 11 shows the enhancement of Nusselt number when obstacles inserted in the flow compare to air flow with no obstacle. Nusselt number enhancement was the Nusselt number with obstacles compare to Nusselt number without obstacle. When obstacles inserted with ratio S/H = 0.5, Nusselt number increases 3.46 times and friction factor increases 19.9 times compare to those without obstacle.

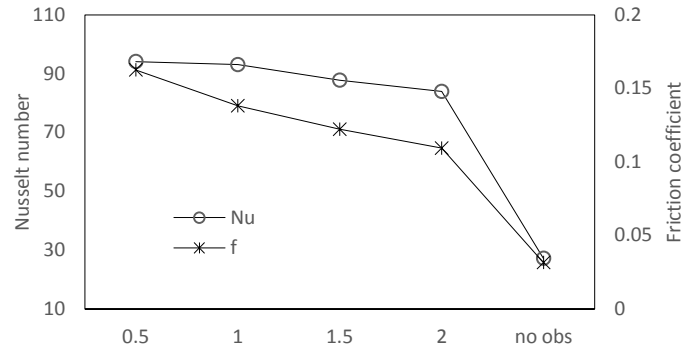


Figure 10. Nusselt number and friction factor of air flow with obstacles inserted at some spacing ratio S/H

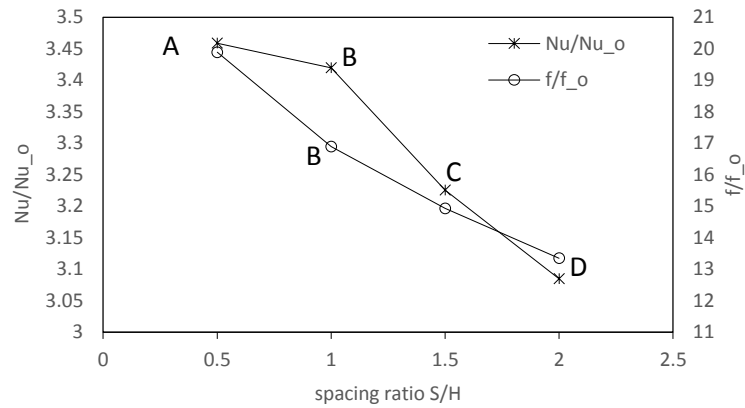


Figure 11. Enhancement Nusselt number and increasing friction factor for some spacing ratio S/H

Fig. 9, 10, and 11 showed the same trend of SAH's efficiency, Nusselt number, and its enhancement. From efficiency and Nusselt number perspective, point A is the best, but from friction factor perspective, point D is the best. The gradient of friction factor in segment A-B is the sharpest among other segments. While the gradient of efficiency and Nusselt number enhancement in segment A-B is the least. The efficiency and Nusselt number in point B is only slightly less than point A. The Nu enhancement in point A is 3.46 and reduce to be 3.42 in point B. Thus, the reduction is only 1.13%. While the reduction of friction factor from point A to point B is 15.1% that is from 19.9 to 16.9. Sacrifice a little efficiency or Nusselt number (convection heat transfer) but save a lot friction factor (pressure drop) shall be a wise choice. So, the optimal spacing ratio, S/H of delta-shaped obstacles attached to a v-corrugated SAH is one. Since the thermal efficiency, Nusselt number, and friction factor are non-dimensional parameters, the result could be applied to other SAH that has different geometry dimension but the same configuration.

5. Comparison to Others' Research

Karim & Hawlader [2] worked on a flat plate solar collector with and without fin and v-corrugated absorber plate solar collector which schema is shown in Fig. 12. Dimension of the collector used is 1.8 m x 0.7 m.

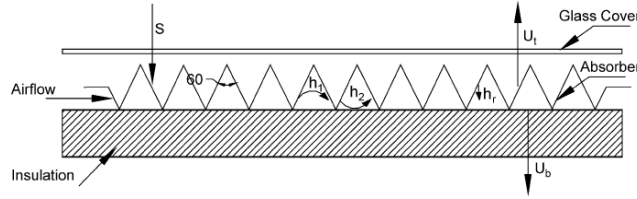


Figure 12. A v-corrugated solar collector used by Karim & Hawlader

The air flow rate generated by the blower in experiment of this paper that is nearest to Karim & Hawlader's SAH is 0.01164 kg/m²s. The comparison of the efficiency of two collectors is shown in Fig. 13.

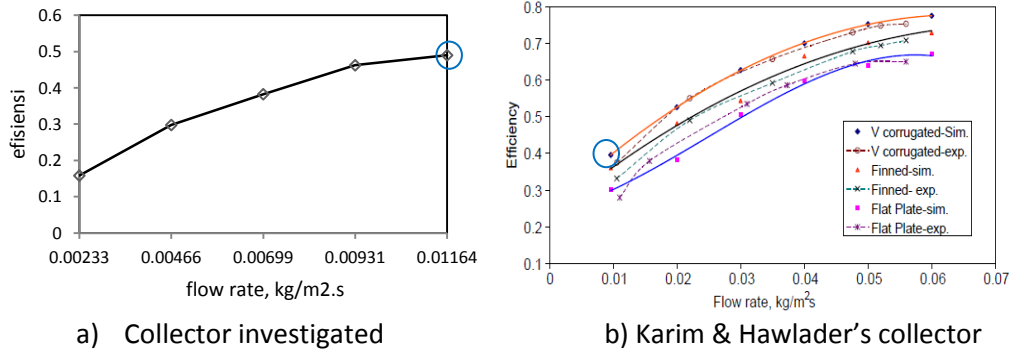


Figure 13. Comparison of the efficiency of collector investigated to Karim & Hawlader's.

The efficiency of SAH investigated is 0.49 and of Karim & Hawlader is 0.4, as in Fig 13. There is a slight difference because the air flow rate is not exactly the same. Therefore, the finding in this paper is look alike with Karim & Hawlader's finding for v-corrugated absorber plate solar collector.

Akpınar & Koçyiğit [13] conducted research on flat plate solar collector with two air mass flow rates, i.e. 0.0074 kg/s and 0.0052 kg/s. There were four collectors used as shown in Fig 14. Three collectors were given obstacles on absorber flat plate. The comparison of Akpınar & Koçyiğit's collector (type II) to investigated collector is shown in Fig. 15. The efficiency of investigated collector is for air mass flow rate 0.00729 kg/s. Parameter $(T_o - T_a) / I$ of the investigated collector is slightly lower, because the air temperature across the investigated collector is lower than Akpınar & Koçyiğit collector. It is because the dimension of investigated collector is smaller than Akpınar & Koçyiğit's. The area of investigated collector was only 900 mm x 87 mm compared to Akpınar & Koçyiğit's that was 1.2 m x 0.7 m. Yet, the difference shown in Fig 15 is not too big. It seems a good conformity between the investigated collector and Akpınar & Koçyiğit's.

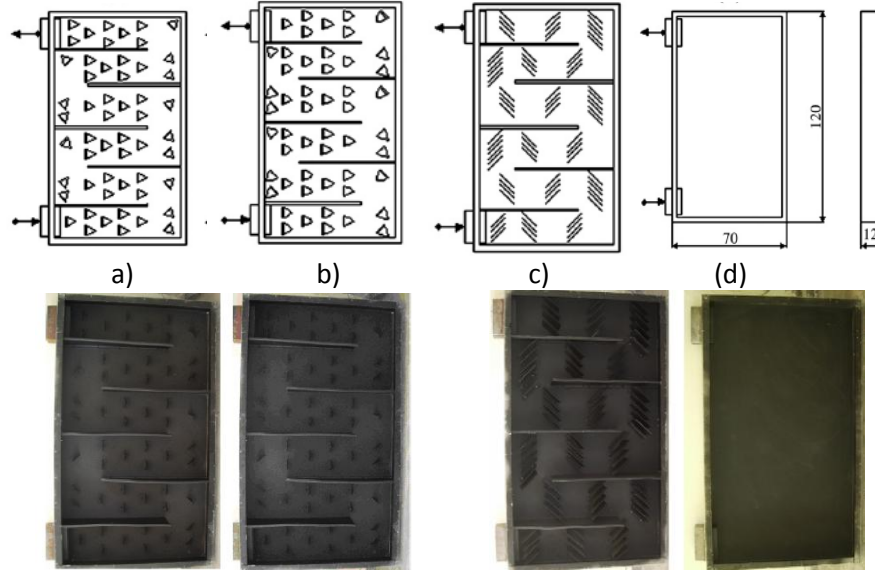
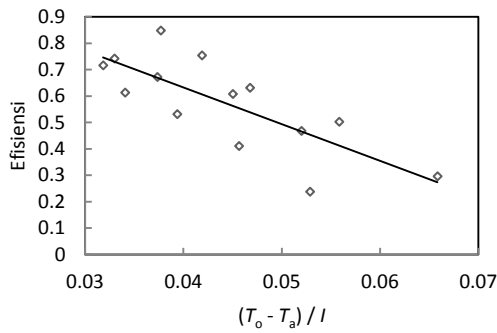
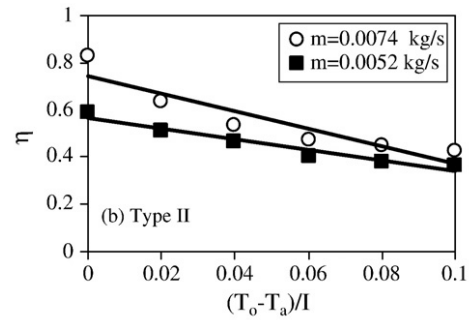


Figure 14. Schematic views of absorber plates: a) with triangular type obstacles, b) with leaf type obstacles, c) with rectangular type obstacles, d) without obstacles [13]



a) collector investigated



b) Akpinar & Koçyiğit's collector

Figure 15. Comparison of efficiency of Akpinar & Koçyiğit's collector and investigated collector

Bekele, et. al. [14] conducted experimental investigation on flat plate SAH with delta-shaped obstacles mounted on the absorber surface as shown in Fig. 16. Some parameter to be investigated by Bekele, et. al. were Reynolds number (from 3400 to 27600), longitudinal pitch of the obstacles P_l/e (from 3/2 to 11/2), and relative obstacle height, e/H (from 0.25 to 0.75). The smaller P_l/e and the higher e/H , the efficiency is higher. The term “e” used by Bekele, et. al. means obstacle's height and “H” means the height of the channel. Bekele, et. al. used P_l/e while the investigated collector used S/H term. The “S” that indicates spacing of obstacles is the same with “ P_l ” that indicates longitudinal pitch (spacing). The comparison of Bekele, et. al.'s collector and collector being investigated (height of obstacle to channel's height, $e/H = 0.6$ and spacing or longitudinal pitch, $P_l/e = 1$ and 3/2) is shown in Fig. 17.

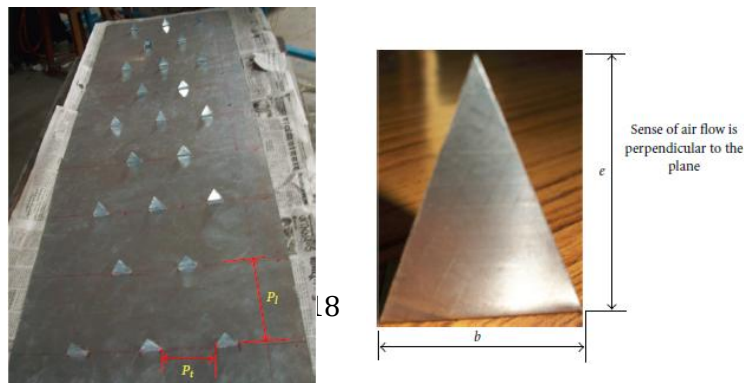


Figure 16. Photographic view of plate with delta-shaped obstacles mounted.

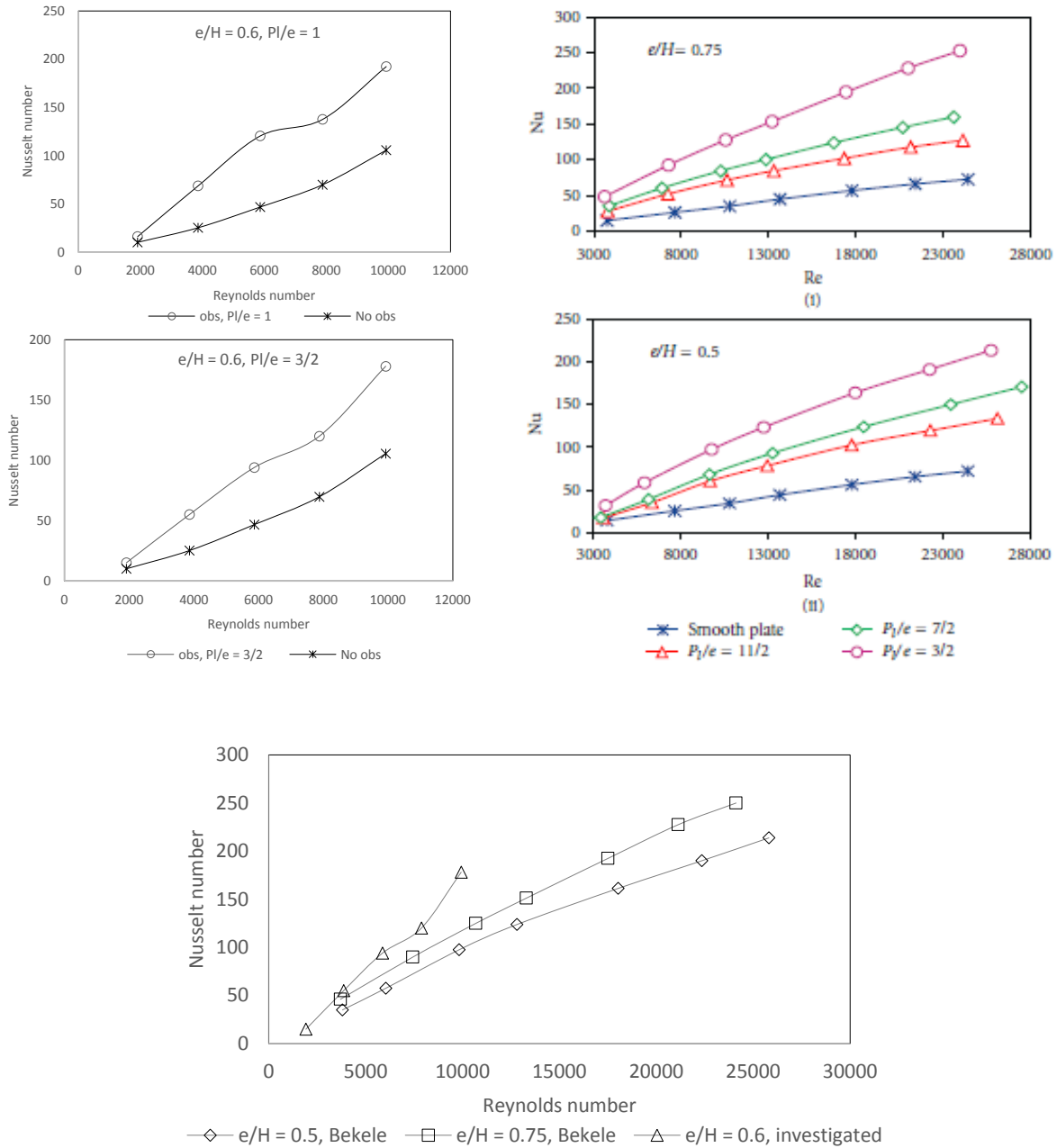


Figure 17. Comparison of Nusselt number of Bekele, et. al.'s collector and investigated collector.

Figure 18. Comparison of Nusselt number of Bekele, et. al.'s and investigated collector for $P_l/e = 3/2$

For smooth duct or no obstacle installed, the Nusselt number of investigated collector is higher than Bekele, et. al.'s. It is because the channel of investigated collector is triangular. This is consistent with the finding of Tao Liu, et. al., Karim and Hawlader, Choudhury and Garg, Naphon, Islamoglu and Parmaksizoglu [1] [2] [3] [4] [5]. Yet, the result of Bekele, et. al.'s and the investigated collector show the same trend, i.e. the smaller P_l/e gives higher Nusselt number. It means more obstacles increase heat transfer to the air. The relative obstacle height used in Bekele, et. al.'s collector was 0.5 and 0.75, while

in the investigated collector was 0.6. The comparison of the results is shown in Fig. 18. When Reynolds number around 10,000 and ratio $P/e = 3/2$, Nusselt number of investigated collector was 178 for $e/H = 0.6$ and Nusselt number of Bekele, et. al. was 98 for $e/H = 0.5$ and 125 for $e/H = 0.75$. Like in collector without obstacle, the Nusselt number of investigated collector is also slightly higher than from Bekele, et. al. Yet, the result from this investigated collector is showing the same trend with the finding of Bekele, et. al.

6. Conclusion

From numerical studies in a v-corrugated duct, it is found that backflow between obstacles and high velocity in the gap between obstacles and absorber plate causes the flow became more turbulent and enhanced the convection heat transfer between the air and the absorber plate. Thus, when it is applied to SAH, it will improve its efficiency but increase the air pressure drop.

Obstacles placed in a small spacing will increase Nusselt number (convection heat transfer) and friction factor (pressure drop). The Nusselt number enhanced from 27.2 when no obstacle used to 94.2 when obstacles inserted with $S/H = 0.5$. The Nusselt enhanced 3.46 times. The friction factor will increase from 0.0316 at no obstacle to 0.628 at ratio $S/H = 0.5$. The friction factor increased 19.9 times.

Efficiency, Nusselt number, and friction factor are decreasing as ratio S/H is increasing. When ratio S/H used is 1 instead of 0.5, Nusselt number enhancement decreased only 1.13%, but friction factor decreased 15.1%. So, sacrificing a small amount of Nusselt number but reducing a significant friction factor is advantageous. The optimal spacing ratio S/H of delta-shaped obstacles inserted in a v-corrugated SAH is one. In other words, the optimal spacing of obstacle equals to its height.

Acknowledgement

Here, I am very grateful for the support from Kopertis Wilayah VII Jawa Timur, Kementerian Pendidikan dan Kebudayaan by providing Research Grant under contract no: 0004/SP2H/PP/K7/KL/II/2012.

Nomenclature

W	wide of the obstacle (mm)
H	height of the obstacle (mm)
S	spacing between the obstacles (mm)
x, y, z	coordinates
Re	Reynolds number
C_p	specific heat of air (J/kg.K)
\dot{m}_f	mass flow rate of the fluid – air (kg/s)
\dot{Q}_u	useful heat transfer rate (Watt)
I	radiation intensity (W/m ²)
A_c	collector aperture area (m ²)
T_o	collector outlet temperature (K)
T_i	collector air inlet temperature (K)

T_{abs}	absorber temperature (K)
D_h	hydraulic diameter (m)
Nu_D	Nusselt number
h	convection heat transfer coefficient (W/m ² .K)
f	friction factor
ϑ	air kinematic viscosity (m ² /s)
ρ	air density (kg/m ³)
k	thermal conductivity (W/m.K)
α	air thermal diffusion coefficient (m ² /s)
η	thermal efficiency of SAH

References

- [1] L. Tao, X. L. Wen, F. G. Wen dan X. L. Chan, "A Parametric study on the termal performance of a solar air collector with a V-groove absorber," *Int. J. of Green Energy*, 4, p. 601–622, 2007.
- [2] M. A. Karim dan M. N. A. Hawlader, "Performance Investigation of Flat Plate, V-Corrugated and Finned Air Collector," *Energy* 31, pp. 452–470, 2006.
- [3] C. Choudhury dan H. P. Garg, "Design Analipsis of Corrugated and Flat Plate Solar Air Heaters.," *Renewable Energy Vol I, No. 5/6*, p. p. 595 – 607, 1991.
- [4] P. Naphon, "Heat transfer characteristics and pressure drop in channel with V corrugated upper and lower plates," *Energy conversion and management* 48, p. 1516 – 1524, 2007.
- [5] Y. Islamoglu dan C. Parmaksizoglu, "The effect of channel height on the enhanced heat transfer characteristics in a corrugated heat exchanger channel," *Applied Thermal Engineering* 23, p. 979–987, 2003.
- [6] P. Promvonge, "Heat transfer and pressure drop in a channel with multiple 60° V-baffles," *Int. Com. in Heat and Mass Transfer*, vol. 37, p. 835–840, 2010.
- [7] I. Kurtbas dan E. Turgut, "Experimental Investigation of Solar Air Heater with Free and Fixed Fins: Efficiency and Exergy Loss," *Int. J. of Science & Technology*, vol. Volume 1, no. No 1, pp. 75–82., 2006.
- [8] B. S. Romdhane, "The air solar collectors: Comparative study, introduction of baffles to favor the heat transfer," *Solar Energy*, vol. 81, p. 139 – 149, 2007.
- [9] C.-D. Ho, H.-M. Yeh dan T.-C. Chen, "Collector efficiency of upward-type double-pass solar air heaters with fins attached," *Int. Com. in Heat and Mass Transfer*, vol. 38, p. 49–56, 2011.
- [10] A. Abene, V. Dubois, M. Le Ray dan A. Oagued, "Study of a solar air flat plate collector: use of obstacle and application for the drying of grape," *J. of Food Engineering*, vol. 65, p. 15 – 22, 2004.
- [11] H. Esen, "Experimental energy and exergy analysis of a double-flow solar air heater having different obstacles on absorber plates," *Building and Environment*, vol. 43, p. 1046–1054, 2008.
- [12] F. Ozgen, M. Esen dan H. Esen, "Experimental investigation of thermal performance of a double-flow solar air heater having aluminium cans.," *Renewable Energy, Volume 34*, p. p. 2391–2398., 2009..

- 1
2
3
4
5 [13] E. K. Akpınar dan F. Koçyiğit, "Experimental investigation of thermal performance of solar air heater
6 having different obstacles on absorber plates," *Int. Com. in Heat and Mass Transfer*, vol. 37, p. 416–
7 421, 2010.
8
9 [14] A. Bekele, M. Mishra dan S. Dutta, "Effects of Delta-Shaped Obstacles on the Thermal Performance
10 of Solar Air Heater," *Hindawi Publishing Corporation: Advances in Mechanical Engineering*, vol.
11 2011, p. 10 pages, 2011.
12
13 [15] H. Esen, F. Ozgen, M. Esen dan A. Sengur, "Modelling of a new solar air heater through least-
14 squares support vector machines," *Expert Systems with Applications* 36, pp. 10673-10682, 2009.
15
16 [16] H. Esen, F. Ozgen, M. Esen dan A. Sengur, "Artificial neural network and wavelet neural network
17 approaches for modelling of a solar air heater," *Expert Systems with Applications* 36, pp. 11240-
18 11248, 2009.
19
20 [17] E. A. Handoyo, D. Ichsani, Prabowo dan Sutardi, "Experimental Studies on a Solar Air Heater Having
21 V-Corrugated," *Applied Mechanics and Materials*, vol. 493, pp. 86-92, 2014.
22
23 [18] F. P. Incropera dan D. P. DeWitt, *Fundamentals of Heat and Mass Transfer*. 5th edition ed. s.l.: John
24 Wiley & Sons., 2002.
25
26 [19] ASHRAE, *Method of Testing to Determine the Thermal Performance of Solar Collectors*, Atlanta:
27 ASHRAE, 1986.
28
29 [20] I. FLUENT, *FLUENT User's Guide*, 2003.
30
31 [21] L. Zhang dan Z. Liu, "A Numerical Simulation of the Flow in a Diffusing S-Duct Inlet," *Modern Applied*
32 *Science*, vol. Vol. 3, no. No. 4, pp. 111-116, 2009.
33
34 [22] M. S. Kirkgoz , A. A. Oner dan M. S. Aköz, "Numerical modeling of interaction of a current with a
35 circular cylinder near a rigid bed," *Advances in Engineering Software*, vol. 40, p. 1191–1199, 2009.
36
37 [23] J. A. Duffie dan W. A. Beckman, *Solar Engineering Of Thermal Processes*, 2nd ed. penyunt., John
38 Wiley & Sons, Inc., 1991.
39
40
41
42
43
44
45
46
47
48
49
50
51
52
53
54
55
56
57
58
59
60
61
62
63
64
65

Your PDF has been built and requires approval

1 message

Solar Energy <se@elsevier.com>

Tue, Feb 9, 2016 at 4:12 PM

To: ekadewi@petra.ac.id, ekadewi@peter.petra.ac.id

Solar Energy

Title: Numerical Studies on the Effect of Delta-Shaped Obstacles' Spacing on the Heat Transfer and Pressure Drop in V-Corrugated Channel of Solar Air Heater
Authors: Ekadewi Anggraini Handoyo, Dr; Ichsani Djatmiko, Prof.; Prabowo Prabowo, Prof.; Sutardi Sutardi, Prof.

Dear Dr. Ekadewi Anggraini Handoyo,

The PDF for your submission, "Numerical Studies on the Effect of Delta-Shaped Obstacles' Spacing on the Heat Transfer and Pressure Drop in V-Corrugated Channel of Solar Air Heater" has now been built and is ready for your approval. Please view the submission before approving it, to be certain that it is free of any errors. If you have already approved the PDF of your submission, this e-mail can be ignored.

To approve the PDF please login to the Elsevier Editorial System as an Author:

<http://ees.elsevier.com/se/>Your username is: ekadewi@petra.ac.id

Then click on the folder 'Submissions Waiting for Author's Approval' to view and approve the PDF of your submission. You may need to click on 'Action Links' to expand your Action Links menu.

You will also need to confirm that you have read and agree with the Elsevier Ethics in Publishing statement before the submission process can be completed. Once all of the above steps are done, you will receive an e-mail confirming receipt of your submission from the Editorial Office. For further information or if you have trouble completing these steps please go to: http://help.elsevier.com/app/answers/detail/a_id/88/p/7923.

Please note that you are required to ensure everything appears appropriately in PDF and no change can be made after approving a submission. If you have any trouble with the generated PDF or completing these steps please go to: http://help.elsevier.com/app/answers/detail/a_id/88/p/7923.

Your submission will be given a reference number once an Editor has been assigned to handle it.

Thank you for your time and patience.

Kind regards,
Editorial Office
Solar Energy

For further assistance, please visit our customer support site at <http://help.elsevier.com/app/answers/list/p/7923>. Here you can search for solutions on a range of topics, find answers to frequently asked questions and learn more about EES via interactive tutorials. You will also find our 24/7 support contact details should you need any further assistance from one of our customer support representatives.



Submission Confirmation for SE-D-15-01490R2

1 message

Solar Energy <se@elsevier.com>

Tue, Feb 9, 2016 at 4:14 PM

To: ekadewi@petra.ac.id, ekadewi@peter.petra.ac.id

Ms. Ref. No.: SE-D-15-01490R2

Title: Numerical Studies on the Effect of Delta-Shaped Obstacles' Spacing on the Heat Transfer and Pressure Drop in V-Corrugated Channel of Solar Air Heater
Solar Energy

Dear Dr. Ekadewi Handoyo,

Your revised manuscript was received for reconsideration for publication in Solar Energy.

You may check the status of your manuscript by logging onto the Elsevier Editorial System as an Author at <http://ees.elsevier.com/se/>.

Your username is: ekadewi@petra.ac.id

If you can't remember your password please click the "Send Password" link on the Login page.

Kind regards,

Elsevier Editorial System
Solar Energy

Your Submission

1 message

Solar Energy <se@elsevier.com>

Tue, Feb 16, 2016 at 1:53 PM

To: ekadewi@petra.ac.id, ekadewi@peter.petra.ac.id
Cc: bbibek@nic.in, bbibek12@gmail.com

Ms. Ref. No.: SE-D-15-01490R2

Title: Numerical Studies on the Effect of Delta-Shaped Obstacles' Spacing on the Heat Transfer and Pressure Drop in V-Corrugated Channel of Solar Air Heater
Solar Energy

Dear Dr. Ekadewi Handoyo,

I am happy to inform you that your paper is now recommended for publication.

When your paper is published on ScienceDirect, you want to make sure it gets the attention it deserves. To help you get your message across, Elsevier has developed a new, free service called AudioSlides: brief, webcast-style presentations that are shown (publicly available) next to your published article. This format gives you the opportunity to explain your research in your own words and attract interest. You will receive an invitation email to create an AudioSlides presentation shortly. For more information and examples, please visit <http://www.elsevier.com/audioslides>.

Thank you for submitting your work to this journal.

With best regards,

Bibek Bandyopadhyay, PhD
Associate Editor
Solar Energy

Note from the International Solar Energy Society

Dear Dr. Ekadewi Handoyo,

The International Solar Energy Society, ISES, would especially like to thank you for your research in the field of solar energy. ISES believes that scientists play a key role in the transformation to a 100% renewable energy future. We are a member-based society and are very happy to invite you to join our community. As a special thank you for your scientific contribution, you are entitled to a 20% discount off the membership fee. To join ISES, simply visit <https://join.ises.org> and select "Individual Membership". After entering your details, select your membership category and enter the code "JOURNAL". Please visit join.ises.org to find more about ISES membership.

If you are already an ISES member, we are very grateful that you contribute to the Solar Energy Journal and invite you to use the discount code "JOURNAL" for a 20% discount when you renew your membership.

We would also like to invite you to write a short message to the Solar Energy Journal subscribers as to why your research is important for the development of solar energy. We may use this message to highlight your research paper in our members newsletter, our website (www.ises.org) and our social media channels (Facebook, Twitter, Google+). Please send your message directly to public.relations@ises.org.

If you have any questions about ISES or about membership, please do not hesitate to contact us members@ises.org.

The International Solar Energy Society



Your Submission

2 messages

Solar Energy <se@elsevier.com>

Wed, Feb 17, 2016 at 2:36 PM

To: ekadewi@petra.ac.id, ekadewi@peter.petra.ac.id

Ms. Ref. No.: SE-D-15-01490R2

Title: Numerical Studies on the Effect of Delta-Shaped Obstacles' Spacing on the Heat Transfer and Pressure Drop in V-Corrugated Channel of Solar Air Heater
Solar Energy

Dear Dr. Ekadewi Handoyo,

A final disposition of "Accept" has been registered for the above-mentioned manuscript.

Kind regards,

Solar Energy

Ekadewi Handoyo <ekadewi@petra.ac.id>

Wed, Feb 17, 2016 at 3:28 PM

To: Solar Energy <se@elsevier.com>

Thank you very much for this beautiful notification...

ekadewi a. handoyo

[Quoted text hidden]

Corrections received

1 message

optteam@elsevierproofcentral.com <optteam@elsevierproofcentral.com>

Thu, Feb 25, 2016 at 11:38 AM

To: ekadewi@petra.ac.id

This is an automatically generated message. Please do not reply because this mailbox is not monitored.

Dear Dr. Ekadewi A. Handoyo,

Thank you very much for using the Proof Central application for your article "Numerical studies on the effect of delta-shaped obstacles' spacing on the heat transfer and pressure drop in v-corrugated channel of solar air heater" in the title "SE"

All your corrections have been saved in our system. Please find attached the PDF summary of your corrections generated from the Proof Central application for your immediate reference.

To track the status of your article throughout the publication process, please use our article tracking service:

http://authors.elsevier.com/TrackPaper.html?trk_article=SE4927&trk_surname=Handoyo

For help with article tracking:

http://support.elsevier.com/app/answers/detail/a_id/90


Kindly note that now we have received your corrections, your article is considered finalised and further amendments are no longer possible.

For further assistance, please visit our customer support site at <http://support.elsevier.com>. Here you can search for solutions on a range of topics. You will also find our 24/7 support contact details should you need any further assistance from one of our customer support representatives.

Yours sincerely,
Elsevier Proof Central team

When you publish in an Elsevier journal/book your article is widely accessible. All Elsevier journal articles and book chapters are automatically added to Elsevier's SciVerse ScienceDirect which is used by 16 million researchers. This means that Elsevier helps your research get discovered and ensures that you have the greatest impact with your new article.

www.sciencedirect.com

 **SE_4927_edit_report.pdf**
827K

Numerical Studies on the Effect of Delta-Shaped Obstacles' Spacing on the Heat Transfer and Pressure Drop in V-Corrugated Channel of Solar Air Heater

Ekadewi A. Handoyo^{a,*}
ekadewi@petra.ac.id

Djatismiko Ichsani^b

Prabowo^b

Sutardi^b

^aMechanical Engineering Dept, Petra Christian University, Surabaya, Indonesia

^bMechanical Engineering Dept, Institut Teknologi Sepuluh Nopember, Surabaya, Indonesia

*Corresponding author.

Communicated by: Associate Editor Bibek Bandyopadhyay

Abstract

Solar air heater (SAH) is simple in construction compared to solar water heater. Yet, it is very useful for drying or space heating. Unfortunately, the convective heat transfer between the absorber plate and the air inside the solar air heater is rather low. Some researchers reported that obstacles are able to enhance the heat transfer in a flat plate solar air collector and others found that a v-corrugated absorber plate gives better heat transfer than a flat plate. Only a few research combines these two in a SAH. This paper will describe the combination from other point of view, i.e. the spacing between obstacles. Its spacing possibly will effect the heat transfer and pressure drop of the air flowing across the channel.

The first step in numerical study is generating mesh or grid of the air flow inside a v-corrugated channel which was blocked by some delta-shaped obstacles. The mesh was designed three-dimension and not uniform. The mesh are made finer for area near obstacles and walls both for upper and bottom, and then gradually coarser. Grid independency is the next step to be conducted. When the mesh is already independent, the numerical study begins. To validate the numerical model, an indoor experiment was conducted. Turbulent model used was Shear Stress Transport K- ω (SSTK- ω) standard. Having a valid numerical model, the spacing between obstacles was studied numerically. Ratio spacing to height, S/H of obstacles investigated were 0.5; 1; 1.5; and 2.

From numerical studies in a v-corrugated duct, it is found that backflow between obstacles and high velocity in the gap between obstacles and absorber plate causes the flow became more turbulent and enhanced the convection heat transfer between the air and the absorber plate. Obstacles placed in a small spacing will increase Nusselt number (convection heat transfer) and friction factor (pressure drop). The Nusselt number enhanced from 27.2 when no obstacle used to 94.2 when obstacles inserted with $S/H = 0.5$. The Nusselt enhanced 3.46 times. The friction factor will increase from 0.0316 at no obstacle to 0.628 at ratio $S/H = 0.5$. The friction factor increased 19.9 times. Efficiency, Nusselt number, and friction factor are decreasing as ratio S/H is increasing. When ratio S/H used is 1 instead of 0.5, Nusselt number enhancement decreased only 1.13%, but friction factor decreased 15.1%. So, sacrificing a small amount of Nusselt number but reducing a significant friction factor is advantageous. The optimal spacing ratio S/H of delta-shaped obstacles inserted in a v-corrugated SAH is one. In other words, the optimal spacing of obstacle equals to its height.

Keywords: Delta-shaped obstacle; v-corrugated channel; Solar air heater; Numerical study

Nomenclature

W

wide of the obstacle (mm)

H

height of the obstacle (mm)

S

spacing between the obstacles (mm)

x, y, z

coordinates

Re

Reynolds number

C_p

specific heat of air (J/kg K)

\dot{m}_f

mass flow rate of the fluid–air (kg/s)

\dot{Q}_u

useful heat transfer rate (~~Watt~~W)

I

radiation intensity (W/m²)

A_c

collector aperture area (m²)

T_o

collector outlet temperature (K)

T_i

collector air inlet temperature (K)

T_{abs}

absorber temperature (K)

D_h

hydraulic diameter (m)

Nu_D

Nusselt number

h

convection heat transfer coefficient (W/m²~~°~~K)

f

friction factor

ν

air kinematic viscosity (m²/s)

ρ

air density (kg/m³)

k

thermal conductivity (W/m²·K)

α

air thermal diffusion coefficient (m²/s)

η

thermal efficiency of SAH

1 Introduction

Solar energy can be converted into thermal energy in a solar collector. Solar collector basically is device used to trap solar energy to heat a plate and transfer the heat to a fluid flowing under or above the plate. When sun light falls onto a plate, solar radiation reaches the plate at lower wavelength and heat it up. Then, the heat is carried away by either water or air that flows under or above the plate. Solar collector used to heat up air is called solar air heater (SAH) and solar water heater for water. Generally, the solar air heater is less efficient than the solar water heater, because air has less thermal capacity and less convection heat transfer coefficient. Yet, air is much lighter and less corrosive than water. The other benefit is that heated air can be used for moderate-temperature drying, such as harvested grains or fish. Since the solar air heater has less convective heat transfer coefficient than solar water heater, some researchers tried to increase this convective heat transfer coefficient.

A popular type of solar air heaters is the flat plate SAH, which has a cover glass on the top, insulation on the sides and bottom to prevent heat transferred to the surrounding, a flat absorber plate that makes a passage for the air flowing with sides and bottom plate. Usually, the passage or channel has a rectangular cross-section. The absorber plate will transfer the heat to the air via convection. Unfortunately, the convection coefficient is very low. To increase the convection coefficient from the absorber plate, a v-corrugated plate is used instead of a flat plate. [Tao et al. \(2007\)](#) stated that a solar air heater with a v-grooved absorber plate could reach efficiency 18% higher than the flat plate on the same operation condition and dimension or configuration. [Karim dan and Hawlader \(2006\)](#) found that a solar collector with a v-absorber plate gave the highest efficiency and the flat plate gave the least. The results showed that the v-corrugated collector is 10–15% and 5–11% more efficient in single pass and double pass modes, respectively, compared to the flat plate collectors. [Choudhury dan and Garg \(1991\)](#) made a detailed analysis of corrugated and flat plate solar air heaters of five different configurations. For the same length, mass flow rate, and air velocity, it was found out that the corrugated and double cover glass collector gave the highest efficiency. According to [Naphon \(2007\)](#) the corrugated surfaces give a significant effect on the enhancement of heat transfer and pressure drop. The Nusselt number of flow in a v-corrugated channel can be 3.2–5.0 times higher than in a plane surfaces while the pressure drop 1.96 times higher than on the ~~corresending~~[corresponding](#) plane surface. [Islamoglu dan and Parmaksizoglu \(2003\)](#) reported that the corrugated channel gave the higher Nusselt number than the straight channel and the higher channel height gave higher Nusselt number for the flow with the same Reynolds number.

Besides changing the cross section area of the channel, some also give effort to increase turbulence inside the channel with fins or obstacles. The result of experimental study done by [Promvonge \(2010\)](#) in turbulent flow regime (Reynolds number of 5000~~to~~[to](#) 25,000) showed that multiple 60° V-baffle turbulator fitted on a channel provides the drastic increase in Nusselt number, friction factor, and the thermal enhancement factor values over the smooth wall channel. Promvonge found that Nusselt number was five times higher and friction factor was 30 times than without baffle at Reynolds number = 10000, $e/H = 0.3$, and $P_R = 1$. [Kurtbas dan and Turgut \(2006\)](#) investigated the effect of fins located on the absorber surface in free and fixed manners. They used two kinds of rectangular fins which dimension is different but total area is the same. The first type fin (I) has dimension 810~~x~~[x](#)60 mm and the second (II) type 200~~x~~[x](#)60 mm. To have the same total area, there are 8 fins and 32 fins for the first and second, respectively. The fins type II, both free and fixed, were more effective than type I and flat-plate collector. The fixed fin collector was more effective than free fin collector. Kurtbas and Turgut reported that the maximum Instantaneous efficiency of SAH was 0.78 at air mass flow rate 0.08 kg/s when the fix fins type II were used. While the efficiency of flat plate SAH was only 0.42. So, its efficiency increased 1.86

times. Romdhane (2007) created turbulence in the air channel using obstacles or baffles. The efficiency of collector and the air temperature was found increasing with the use of baffles. Baffles should be used to guide the flow toward the absorber plate. Romdhane reported that the efficiency reached 80% for the best type of baffle (chicane) for an air flow rate of 50 m³/h/m². This efficiency was about 1.6 times efficiency without baffle. Ho et al. (2011) inserted fins attached by baffles and external recycling to a solar air heater. The experiment and theoretical investigations gave result that heat transfer was improved by employing baffled double-pass with external recycling and fin attached over and under absorber plate. According to Ho et al., the highest collector efficiency was 61% in a double-pass flat-plate SAH with recycle when radiation intensity was 1100 W/m², 24 fins attached, and mass flow rate was 0.02 kg/s. It was about 1.35 times its efficiency when there is no recycle. Abene et al. (2004) used obstacles on the flat plate of a solar air collector for drying grape. The obstacles ensure a good air flow over the absorber plate, create the turbulence and reduce the dead zones in the collector. The highest efficiency got was 70% when the air flow rate was 50 m³/h/m². It was about 1.9 times its efficiency when no obstacle used. The air pressure drop increased about twice with obstacles. Esen (2008) used a double-flow solar air heater to investigate three different type obstacles placed on absorber plates compare with the flat plate. The collector has three absorber plates to make three passages for the air flowing through. From the research done, it was found that all collectors with obstacles gave higher efficiency than the flat plate and type III obstacles with flow in middle passage gave the highest efficiency, i.e. 52.9%, for air flow 0.02 kg/s. It was about 1.13 times higher than its effieencyefficiency with no obstacle. Ozgen et al. (2009) used aluminum cans as obstacles installed over and under absorber plate. They found that the SAH using double flow passage (over and under absorber plate) gave higher efficiency than just one flow passage (either over or under absorber plate). They also found that SAH with staggered cans (type I) had the highest efficiency compared to aligned cans (type II) and flat plat (type III). The efficiency of SAH type I was 0.73 at air flow rate 0.05 kg/s and it was about 1.4 times of type III. Akpinar dan and Koçyiğit (2010) had experimental investigation on solar air heater with several obstacles (Types I, Type II, and Type III) and without obstacles. The optimal value of efficiency was obtained for the solar air heater with Type II obstacles on absorber plate in flow channel duct for all operating conditions and the collector with obstacles appears significantly better than that without obstacles. The efficiency of Type II was 0.6 at air flow rate 0.0052 kg/s and it was about twice of SAH without obstacle. Bekele et al. (2011) investigated experimentally the effect of delta shaped obstacles mounted on the absorber surface of an air heater duct. They found that the obstacle mounted duct enhances the heat transfer to the air. The heat transfer got higher if the obstacle height was taller and its longitudinal pitch was smaller. Nusselt number increased 3.5 times when obstacles inserted with ratio of longitudinal pitch $P/e = 3/2$ and height $e/H = 0.75$ at Reynolds number was 10,000. While its friction factor increased 4.7 times than without obstacle. SAH can be modeled through least-squares support vector machines (LS-SVM) method as done by Esen et al. (2009a). The predicted results from LS-SVM model had been compared to experimental results. LS-SVM could be used to predict the efficiency of SAH. They ashowed that efficiency of type I SAH was the highest. Esen et al. (2009b) also proposed Artificial Neural Network and Wavelet Neural Network (ANN and WNN) to predict the efficiency of SAH. They succeeded to show that the method could predict the SAH efficiency.

The combine of those two findings, i.e. obstacles and v-corrugated absorber plate are able to improve SAH are important to be studied. Handoyo et al. (2014) reported that the obstacles are able to enhance heat transfer in a v-corrugated SAH but increase the air pressure drop. To reduce the air pressure drop, the obstacles were bent vertically. The optimal bending angle is 30°. The SAH's efficiency was 5.3% lower when the obstacles bent 30° instead of straight (0°), but the pressure drop was 17.2% lower.

According to Incropera dan and DeWitt (2002), in forced convection heat transfer, there are two quantities that are important to be determined. One is friction coefficient, C_f , and the other is Nusselt number, Nu. Friction coefficient, C_f , is used to calculate the shear stress at the wall and then to calculate pressure drop. While Nusselt number, Nu is used to calculate convection heat transfer rate. The relation that correlate them is known as Reynolds Analogy:

$$C_{f,x} \frac{Re_x}{2} = Nu_x Pr^{-1/3}$$

When Nusselt number increases, then friction coefficient will increase, too. In a SAH, it is expected that convection heat transfer increases but pressure drop does not. So, many research were conducted to look for increasing in heat transfer at low pressure drop.

The spacing between obstacles mounted on absorber plate can be varied. A different spacing will give different air pressure drop as the air flows across the collector. Obstacles increase the air pressure drop. When the spacing is large, the obstacles used is less and the air pressure drop will be reduced. What about the heat transfer from the absorber plate to the flowing air? How will the spacing between obstacles effect the heat transfer? To the knowledge of the authors, there is no research investigating the effect of delta-shaped obstacles' spacing on a v-corrugated SAH performance, yet.

This paper describes the result of the numerical studies of obstacles' spacing inserted in a v-corrugated channel of a SAH. The heat transfer from the v-corrugated absorber plate and the air pressure drop flowing the v-corrugated channel is to be discussed. The obstacles are delta-shaped and installed on bottom plate of the channel.

2 Experimental set-up

The studies began with choosing a solar collector model to be studied. The study will be conducted numerically. Thus, a validation is required to prove that the result is true. The validation is accomplished via experiment. An indoor experiment model was constructed to validate numerical result. It is a model of SAH using v-corrugated absorber plate. Its schematic view and photograph are shown in Fig. 1(a) and (b), respectively. The experiment was conducted in a laboratory of Mechanical Engineering Dept of Petra Christian University, Surabaya, Indonesia.

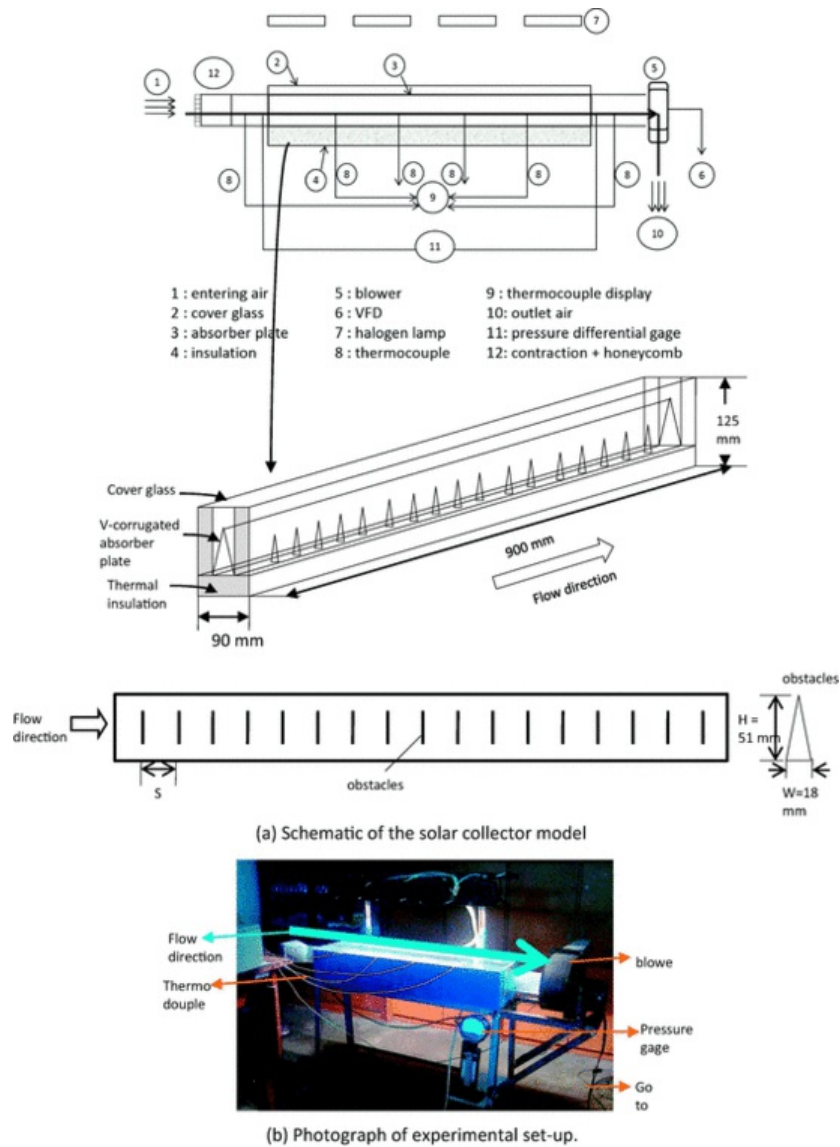


Fig. 1 The SAH model used in experiment.

The collector model's dimension was 900 mm long, 90 mm width, and 125 mm height. A single 3-mm transparent-tempered glass was used as the collector cover. The v-corrugated absorber plate was made of 0.8-mm-thick aluminum and painted black. The apex angle of the v-corrugated plate was 20°. The v-corrugated channel's cross section was 30 mm width and 85 mm height. To prevent heat loss, the left and right walls of collector are insulated with a 25-mm Styrofoam each and a 35-mm Styrofoam for the bottom. The delta-shaped obstacles were made congruent to the channel i.e. triangular and its dimension was 18 mm wide, 51 mm height.

The experiment was conducted indoor to maintain the radiation intensity, wind's velocity and temperature. So, a bias result caused by different outdoor condition could be avoided. The sunlight is replaced with four 500-Watt halogen lamps. The radiation intensity received on the collector was measured using a pyranometer (Kipp & Zonen, type SP Lite2) placed on top of the cover glass. To ensure the homogenous intensity and to generate a certain absorber plate's temperature, these lamps were equipped with adjustable turner individually. The surrounding air condition was controlled by an air conditioner installed in the room. Its temperature, humidity, and wind velocity are well controlled. The collector was

equipped with T-type thermocouple which accuracy is 0.1 °C for measuring the air temperature at inlet and outlet of the collector, temperature of the absorber plate (at four different locations), and ambient temperature. The pressure drop between inlet and outlet of the flowing air across the collector is also measured with a Magnehelic differential pressure gage which accuracy is ±2 Pa. A centrifugal blower (1000 m³/h, 580 Pa, 0.2 kW, 380 V_{eff} input) was used to induce the air flowing through the collector. The air flow was adjusted by means of a variable-frequency drive (VFD) to be 5.0 m/s (or Reynolds number = 10,000). The air flow is measured using digital anemometer which accuracy is ±0.1 m/s. All of the measurement equipments such as pressure gages and thermocouples are installed according to ASHRAE requirement ([ASHRAE, 1986](#)).

3 Numerical set up

The discussion in this paper is on the heat transferred to the flowing air and its pressure drop, then the domain of numerical study is focused on the air flow inside the v-corrugated channel. The apex angle of the v-corrugated channel is 20°. Its dimension was 900 mm long, 30 mm width, and 85 mm height. The delta-shaped obstacles were made congruent to the channel i.e. triangular and its dimension was 18 mm wide, 51 mm height. The obstacles were installed in one line only, because there is no much space in the channel. Thus, the spacing to be discussed is also called longitudinal pitch. To specify the obstacles' spacing, a ratio of spacing to height *S/H* is used. In this study, the ratio *S/H* used were ½, 1, 1½, and 2.

The numerical model for this problem was developed under some assumptions, i.e. as steady three-dimensional turbulent, incompressible flow and constant fluid properties. The space of obstacles was taken equal to height of obstacles, thus ratio is 1. Then, there are 17 obstacles used in this flow. Body force and viscous dissipation are ignored and it was assumed no radiation heat transfer. With these assumptions, ([Incropera dan and DeWitt, 2002](#)) give the related governing equations as follow:

$$\frac{\partial u}{\partial x}+\frac{\partial v}{\partial y}+\frac{\partial w}{\partial z}=0 \tag{1}$$

$$u\frac{\partial u}{\partial x}+v\frac{\partial u}{\partial y}+w\frac{\partial u}{\partial z}=-\frac{1}{\rho}\frac{\partial P}{\partial x}+\vartheta\left(\frac{\partial^2 u}{\partial x^2}+\frac{\partial^2 u}{\partial y^2}+\frac{\partial^2 u}{\partial z^2}\right) \tag{2}$$

$$u\frac{\partial v}{\partial x}+v\frac{\partial v}{\partial y}+w\frac{\partial v}{\partial z}=-\frac{1}{\rho}\frac{\partial P}{\partial y}+\vartheta\left(\frac{\partial^2 v}{\partial x^2}+\frac{\partial^2 v}{\partial y^2}+\frac{\partial^2 v}{\partial z^2}\right) \tag{3}$$

$$u\frac{\partial w}{\partial x}+v\frac{\partial w}{\partial y}+w\frac{\partial w}{\partial z}=-\frac{1}{\rho}\frac{\partial P}{\partial z}+\vartheta\left(\frac{\partial^2 w}{\partial x^2}+\frac{\partial^2 w}{\partial y^2}+\frac{\partial^2 w}{\partial z^2}\right) \tag{4}$$

$$u\frac{\partial T}{\partial x}+v\frac{\partial T}{\partial y}+w\frac{\partial T}{\partial z}=\alpha\left(\frac{\partial^2 T}{\partial x^2}+\frac{\partial^2 T}{\partial y^2}+\frac{\partial^2 T}{\partial z^2}\right) \tag{5}$$

In the above equations, ρ is the density of the air, P is the pressure, ϑ is the kinematic viscosity, α is the thermal diffusivity, and T is the temperature of the fluid. The boundary conditions of this problem were:	
At the inlet: $u = 5.0$ m/s, $v = w = 0$, $T = 297.46$ K	
At the upper wall which is the absorber plate: $u = v = w = 0$	
At the bottom wall: $u = v = w = 0$	
On the 17 obstacles: $u = v = w = 0$	

Inlet Reynolds number was calculated with : $Re = \frac{uD_h}{\vartheta}$ (6)

In Eq. (6), D_h is hydraulic diameter and calculated with:

$$D_h = \frac{4A}{P}$$
(7)

The area, A , in Eq. (7) is the channel cross section area, and P , is its perimeter.

The governing equations above with the boundary conditions were solved using a commercial CFD package, FLUENT 6.3.26 ([FLUENT, 2003](#)). The grids of the domain were generated using Gambit 2.4.6. The domain and meshing used

in this numerical study were shown in Fig. 2. Since the geometry is a triangular channel, the numerical study should be conducted in three dimensions and all of the meshes were designed to have quality less than 0.7.

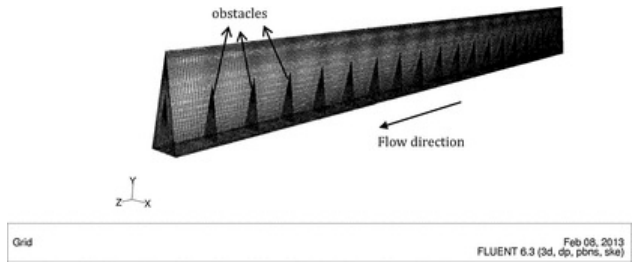
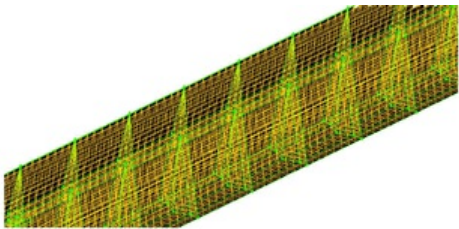
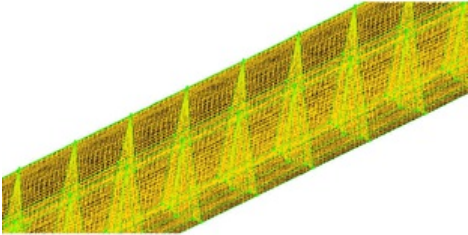


Fig. 2 The grid used in numerical studies.

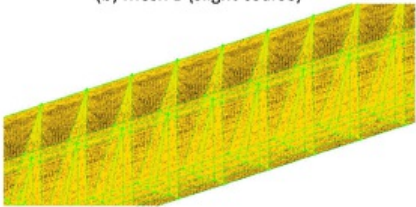
After having a good mesh, the next step is doing grid independency. The grid or mesh is made smaller to get more accurate and detailed result. But, when the mesh is too small, calculation which is done by iteration needs a very long time and might end up with diverge result. Therefore, in this study the mesh or grids were designed not uniform. The finer mesh are used for area near walls both for upper and bottom walls and then gradually the mesh are made coarser as shown in Fig. 2. When there are obstacles in the flow, the mesh are designed to be finer not only near the walls but also around the obstacles in Fig. 2. There are four meshes designs to be checked for independency as shown in Fig. 3(a), (b), (c), and (d). The number of cells, faces, and nodes used in each design are shown in Table 1.



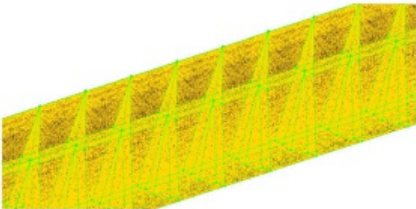
(a) Mesh A (most coarse)



(b) Mesh B (slight coarse)



(c) Mesh C (slight fine)



(d) Mesh D (most fine)

Fig. 3 Mesh design checked for independency.

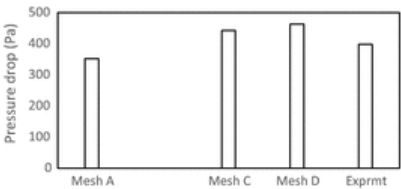
Table 1 Number of cells, faces, and nodes of the four mesh design.

	Mesh A	Mesh B	Mesh C	Mesh D
Cell	55,296	338,688	1,092,000	1,980,000
Face	173,936	1,043,224	3,335,300	6,026,900
Node	63,172	365,480	1,150,798	2,066,248

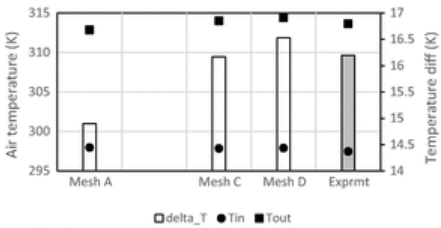
To check the grid independency, the result from numerical study will be compared to experiment result. The same boundary conditions and setting are used in each numerical study of the four grids design as in Fig. 3. The boundary conditions are: inlet air velocity = 5.0 m/s and outflow was employed for the outlet; inlet air temperature = 297.46 K; and absorber plate temperature as obtained during experiments = 320 K. The settings in software used are: three dimension,

double precision. Shear Stress Transport K- ω (SSTK- ω) standard turbulent model was chosen to simulate the flow. Zhang and Liu conducted a numerical simulation of the flow inside a diffusing S-duct inlet. Full three-dimensional Navier-Stokes equations are solved and SST turbulence model is employed. Numerical results, include surface static pressure, total pressure recovery at exit, are compared with experiment. A fairly good agreement is apparent (Zhangdan and Liu, 2009). Other researcher, Kirkgoz et al. reported that numerical modeling using K- ω and SSTK- ω used on the cylinder surface gave reasonably success result (Kirkgoz et al., 2009). The SIMPLC algorithm was employed to deal with the problem of velocity and pressure coupling. Second-order upwind scheme were used to discretize the main governing equations. Material of the absorber, bottom plate and the obstacles is aluminum. Fluid was air with inlet pressure 1 atm and its properties, such as density, viscosity, thermal conductivity were function of temperature.

Numerical studies were conducted for each of the four Mesh: A, B, C, and D. Fig. 4 shows global properties resulted from the numerical studies. They were the inlet and outlet temperature of air flowing through the channel and its pressure drop. Only Mesh B could not converge and the residual could not meet the criteria. So, there was no result of Mesh B in Fig. 4.



(a) The air pressure drop from numerical studies compared to experiment



(b) The air temperature from numerical studies compared to experiment

Fig. 4 The numerical studies of Mesh A, C, and D compared to the result of experiment for $S/H = 1$.

The experiment result which will be discussed in Section 4 gives pressure drop as much as 397.7 Pa, air temperature outlet 40.7 °C when the air inlet velocity is 5.0 m/s and inlet air temperature 24.5 °C. Fig. 4 shows that numerical study with Mesh C and D give better result of air temperature compare to experiment than Mesh A, but mesh-Mesh D gives too high pressure drop result. Numerical studies using Mesh C give the most closely result to experiments. Thus, Mesh C was chosen for the numerical studies.

Using Mesh C pattern, some numerical studies were conducted to know the effect of obstacles' spacing. The ratio of spacing to height, S/H , studied numerically were $\frac{1}{2}$, 1, 1 $\frac{1}{2}$, and 2. The Mesh used in this study are in Fig. 5a-d. When the ratio S/H is bigger, then the number of obstacle is less. Number of obstacles are 8, 11, 17, and 35 for ratio $S/H = 2, 1 \frac{1}{2}, 1,$ and $\frac{1}{2}$, respectively.

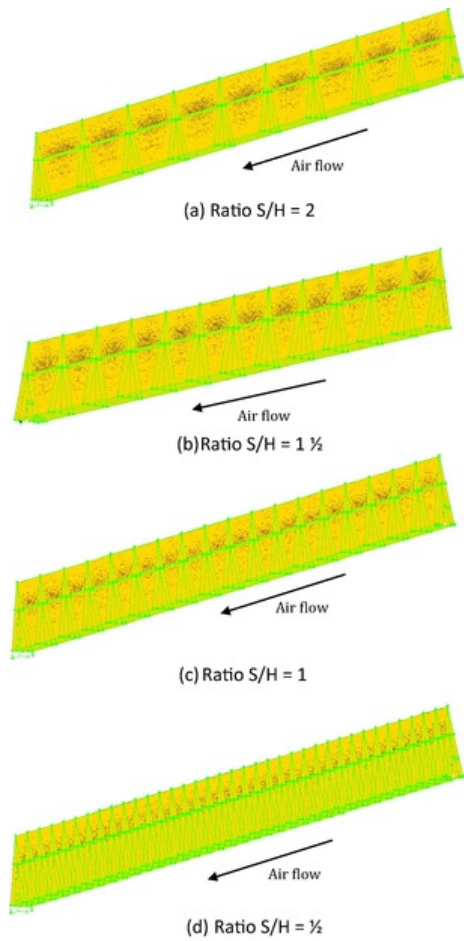


Fig. 5 The Mesh used for numerical studies of each spacing to height ratio, S/H .

To give more comprehensive result, numerical study was also conducted for air flow in a v-corrugated channel without obstacle. The domain and mesh used is shown in [Fig. 6](#).

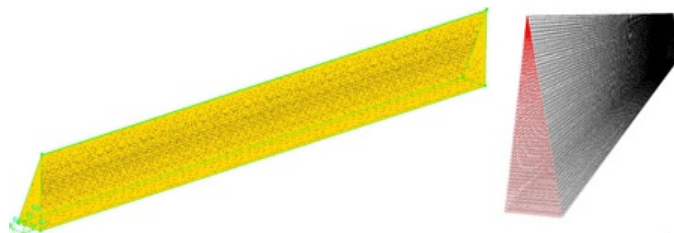


Fig. 6 The Mesh used for numerical studies of air flow without obstacle.

4 Results and discussion

Since the experiment is conducted to validate the numerical result, then it is not necessary to conduct experiments for all ratio S/H . The ratio S/H used in experiment equals to 1. Thus, there are 17 obstacles inserted and the percentage

of air flow blockage in the channel is 36%. The experiment followed the numerical setting. The experiments were conducted at certain inlet air velocity and certain radiation intensity or absorber temperature. A VFD was used to get an inlet air velocity equals to 5.0 m/s. An adjustable turner was used to adjust the radiation intensity that make the absorber's temperature as high as 320 K or 47 °C.

When the numerical result is close to the experimental result, then the numerical result is valid. Table 2 shows the comparison between numerical and experimental results at 5.0-m/s-inlet air velocity and 320 K absorber temperature. The air temperature difference and pressure drop of numeric is very close to experiment. Thus, the numerical study using several setting discussed above is acceptable and valid.

Table 2 Comparison between numerical and experimental results.

	Numeric	Experiment
T_{in} (K)	297.9	297.5
T_{out} (K)	314.4	313.7
delta T (K)	16.5	16.2
delta P (Pa)	462.3	450.3

To ensure that the model used in numerical study is valid, a comparison between Nusselt number from numerical result and Gnielinski equation for triangular channel without obstacle or smooth duct was conducted. According to Incropera dan DeWitt (2002), Gnielinski gives more accurate relation to calculate Nusselt number at lower Reynolds number than Dittus–Boelter equation. The relation of Nusselt number is in Eq. (8):

$$Nu_D = \frac{(f/8)(Re_D - 1000)Pr}{1 + 12.7(f/8)^{1/2}(Pr^{2/3} - 1)}$$

(8)

The friction factor in Eq. (8), f , is obtained from Moody diagram. The comparison in Fig. 7 shows that numerical simulation gives pretty accurate results.

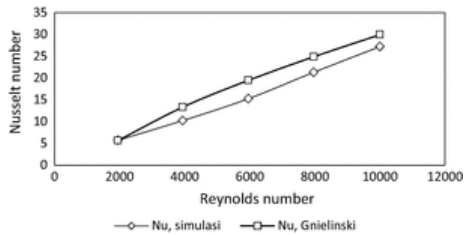
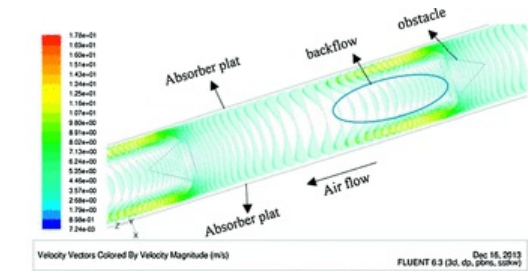
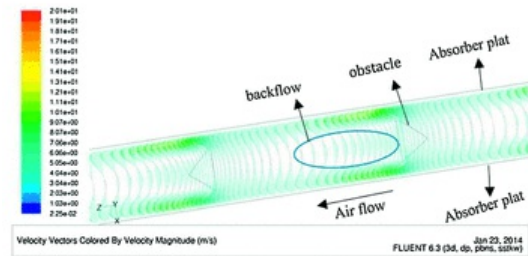


Fig. 7 Comparison of Nusselt number for smooth duct (no obstacle) from numerical study and Gnielinski equation.

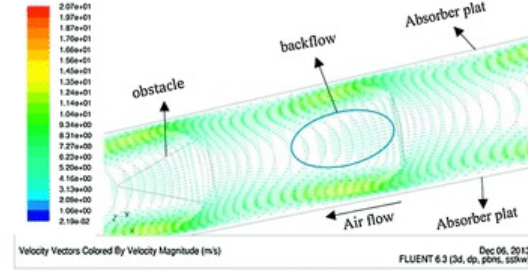
Having a valid grids, setting, and viscous model, the numerical study was continued to investigate the spacing effect of obstacles on the bottom plate of air duct. Diagrams of velocity vector of air flow around the obstacles inserted at ratio S/H equals to 2, 1 ½, 1, and ½ are shown in Fig. 8(a), (b), (c), and (d), respectively. All of the velocity vectors were taken at height $y = 10$ mm from the bottom plate. When the ratio $S/H = 2$, the spacing between obstacles = 100 mm. For ratio $S/H = 1$ ½, the spacing = 75 mm, and for ratio $S/H = ½$, the spacing = 25 mm.



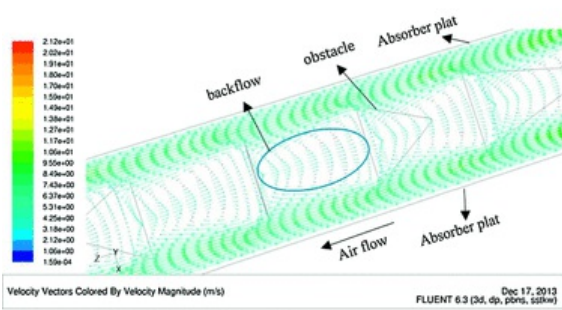
(a) Velocity vector of air flow around *obstacle* with ratio $S/H = 2$



(b) Velocity vector of air flow around *obstacle* with ratio $S/H = 1 \frac{1}{2}$



(c) Velocity vector of air flow around *obstacle* with ratio $S/H = 1$



(d) Velocity vector of air flow around *obstacle* with ratio $S/H = \frac{1}{2}$

Fig. 8 Velocity vector of air flow around obstacle with some ratio S/H .

Fig. 8(a)–(d) shows how the air flow encounters separation when flow through obstacles. The obstacles cause backflow between two consecutive obstacles in downstream. There are more backflows when the obstacles' spacing are closer and they cause a higher pressure drop. The air velocity looks higher near absorber plate when there is backflow or swirl in the flow. This high air velocity makes flow become more turbulent and more heat transferred from the absorber plate to the air. This convection heat transfer to the air makes outlet air temperature higher. Thus, the closer the obstacles' spacing makes the higher pressure drop and higher convection heat transfer from the absorber plate to the air

flow.

When the spacing between obstacles is twice its height (ratio $S/H = 2$), small amount of air flow is blocked by obstacles and causes backflow behind the obstacles. The backflow caused by separation gradually diminish between two obstacles in downstream as shown in Fig. 8(a). Since the air is blocked, most of air is forced to flow in the gap between obstacles and absorber plate. It is shown by longer and higher vector of velocity in the gap. More air is heated by absorber plate. Furthermore, higher velocity increases Reynolds number and make the flow more turbulent. More turbulent flow gives higher Nusselt number and definitely increase the convection heat transfer. Thus, obstacles makes outlet air temperature higher than without any (Handoyo et al., 2014). Flow in spacing between obstacles experiences backflow after hitting obstacles and then it reattaches quickly when the ratio $S/H = 2$. When the ratio S/H or spacing between obstacles is smaller, as shown in Fig. 8(b)–(d), backflow is more dominant than reattached flow in area between the obstacles. When backflow occurs, more air will flow in the gap and contact with absorber plate which is the heat source. It is the reason that smaller obstacles' spacing makes higher air outlet temperature and higher SAH's efficiency. The backflow in space between obstacles contributes pressure drop in the flow. More backflow causes higher pressure drop in air acrossed the v-corrugated absorber plate SAH.

Numerical studies also provide some global properties of the flow, such as the air inlet and outlet temperature, and pressure drop. These data were used to acquire the efficiency and friction factor of the air flow in a v-corrugated SAH with delta-shaped obstacles. The efficiency and friction factor are calculated using Eqs. (9) and (10) according to Duffie dan Beckman (1991).

$$\eta = \frac{q_u}{A_e I} = \frac{\dot{m}_f c_p (T_{fo} - T_{fi})}{A_e I} \quad (9)$$

$$f = \frac{\Delta P}{\frac{L}{D_h} \rho \frac{v^2}{2}} \quad (10)$$

Comparison of efficiency and friction factor for some ratio S/H from numerical studies is shown in Fig. 9. Ratio $S/H = 0$ in Fig. 9 means no obstacle in the air flow. Obstacles arranged with ratio $S/H = 1/2$ gives the highest air efficiency, i.e. 68% and also highest friction factor, i.e. 0.628 for air flowing in a v-corrugated duct, as shown in Fig. 9. For comparison, efficiency when no obstacle is only 49% and friction factor is only 0.0316. This findings are matching with the flow structure discussed above. The obstacles block the air flow and force it to have more contact with absorber plate. Not only forcing the air to the absorber plate, obstacles also causing more backflow. More obstacles produce higher efficiency and higher friction factor. SAH requires high efficiency or high outlet air temperature, but low friction or pressure drop. Increasing friction factor means increasing pumping power required in SAH.

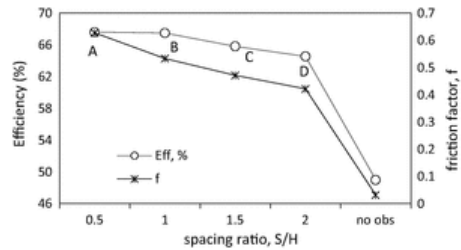


Fig. 9 The efficiency of SAH and friction factor of flow with some ratio S/H of obstacles.

Besides efficiency, Nusselt number is interesting to be analyzed. It could be calculated using Eq. (11).

$$h = \frac{Nu_D k}{D_h} \quad (11)$$

While the convection heat transfer rate and log-mean temperature difference could be calculated using Eqs. (12) and (13).

$$q = h A \Delta T_{lm} \quad (12)$$

$$\Delta T_{lm} = \frac{(T_{abs} - T_o) - (T_{abs} - T_i)}{\ln \frac{(T_{abs} - T_o)}{(T_{abs} - T_i)}} \quad (13)$$

The ratio S/H of obstacles effect the Nusselt number of air flow as shown in Fig. 10. Nusselt number of air flow with obstacles are much higher than without obstacle. The highest Nu number and friction factor are 94.2 and 0.628 at ratio $S/H = 0.5$ and is only 27.2 and 0.0316 at no obstacle. Fig. 11 shows the enhancement of Nusselt number when obstacles inserted in the flow compare to air flow with no obstacle. Nusselt number enhancement was the Nusselt number with

obstacles compare to Nusselt number without obstacle. When obstacles inserted with ratio $S/H = 0.5$, Nusselt number increases 3.46 times and friction factor increases 19.9 times compare to those without obstacle.

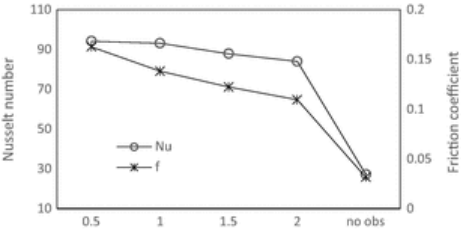


Fig. 10 Nusselt number and friction factor of air flow with obstacles inserted at some spacing ratio S/H .

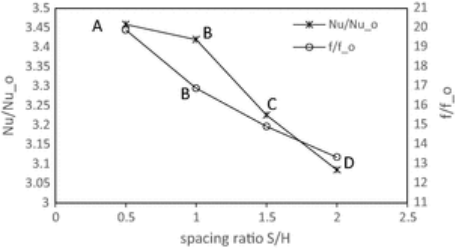


Fig. 11 Enhancement Nusselt number and increasing friction factor for some spacing ratio S/H .

Figs. 9–11 showed the same trend of SAH’s efficiency, Nusselt number, and its enhancement. From efficiency and Nusselt number perspective, point A is the best, but from friction factor perspective, point D is the best. The gradient of friction factor in segment A–B is the sharpest among other segments. While the gradient of efficiency and Nusselt number enhancement in segment A–B is the least. The efficiency and Nusselt number in point B is only slightly less than point A. The Nu enhancement in point A is 3.46 and reduce to be 3.42 in point B. Thus, the reduction is only 1.13%. While the reduction of friction factor from point A to point B is 15.1% that is from 19.9 to 16.9. Sacrifice a little efficiency or Nusselt number (convection heat transfer) but save a lot friction factor (pressure drop) shall be a wise choice. So, the optimal spacing ratio, S/H of delta-shaped obstacles attached to a v-corrugated SAH is one. Since the thermal efficiency, Nusselt number, and friction factor are non-dimensional parameters, the result could be applied to other SAH that has different geometry dimension but the same configuration.

5 Comparison to Others’ Research

Karim dan and Hawlader (2006) worked on a flat plate solar collector with and without fin and v-corrugated absorber plate solar collector which schema is shown in Fig. 12. Dimension of the collector used is 1.8 m \times 0.7 m.

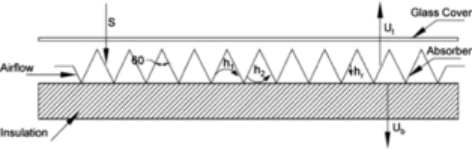


Fig. 12 A v-corrugated solar collector used by Karim & Hawlader.

The air flow rate generated by the blower in experiment of this paper that is nearest to Karim & Hawlader’s SAH is 0.01164 kg/m²s. The comparison of the efficiency of two collectors is shown in Fig. 13.

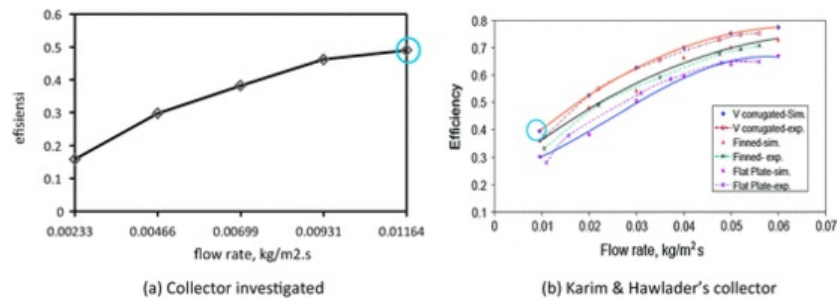


Fig. 13 Comparison of the efficiency of collector investigated to Karim & Hawlader's.

The efficiency of SAH investigated is 0.49 and of Karim & Hawlader is 0.4, as in Fig. 13. There is a slight difference because the air flow rate is not exactly the same. Therefore, the finding in this paper is look alike with Karim & Hawlader's finding for v-corrugated absorber plate solar collector.

Akpınar dan and Koçyiğit (2010) conducted research on flat plate solar collector with two air mass flow rates, i.e. 0.0074 kg/s and 0.0052 kg/s. There were four collectors used as shown in Fig. 14. Three collectors were given obstacles on absorber flat plate. The comparison of Akpınar & Koçyiğit's collector (type II) to investigated collector is shown in Fig. 15. The efficiency of investigated collector is for air mass flow rate 0.00729 kg/s. Parameter $(T_o - T_a)/I$ of the investigated collector is slightly lower, because the air temperature across the investigated collector is lower than Akpınar & Koçyiğit collector. It is because the dimension of investigated collector is smaller than Akpınar & Koçyiğit's. The area of investigated collector was only 900 mm \times 87 mm compared to Akpınar & Koçyiğit's that was 1.2 m \times 0.7 m. Yet, the difference shown in Fig. 15 is not too big. It seems a good conformity between the investigated collector and Akpınar & Koçyiğit's.

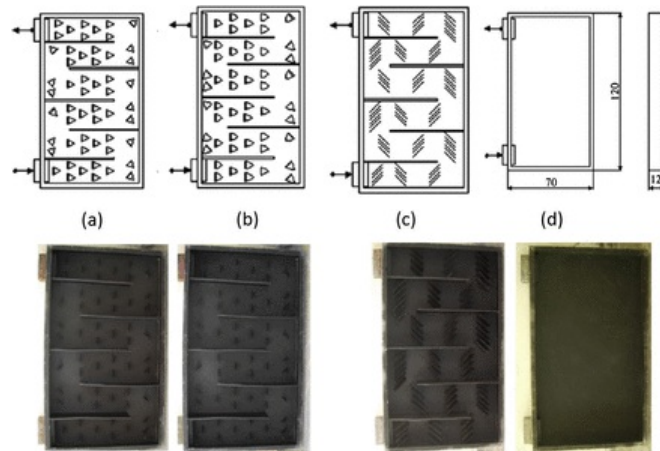


Fig. 14 Schematic views of absorber plates: (a) with triangular type obstacles, (b) with leaf type obstacles, (c) with rectangular type obstacles, and (d) without obstacles (Akpınar dan and Koçyiğit, 2010).

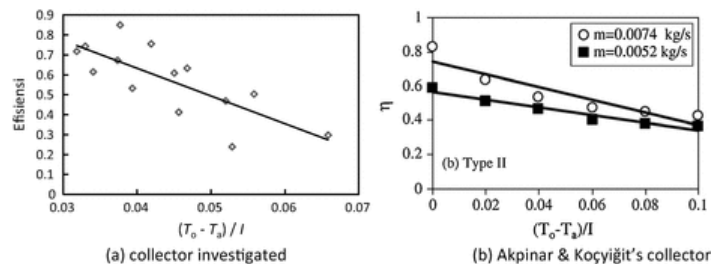


Fig. 15 Comparison of efficiency of Akpınar & Koçyiğit's collector and investigated collector.

Bekele et al. (2011) conducted experimental investigation on flat plate SAH with delta-shaped obstacles mounted on the absorber surface as shown in Fig. 16. Some parameter to be investigated by Bekele et al. were Reynolds number (from 3400 to 27,600), longitudinal pitch of the obstacles P/e (from 3/2 to 11/2), and relative obstacle height, e/H (from 0.25 to 0.75). The smaller P/e and the higher e/H , the efficiency is higher. The term “ e ” used by Bekele et al. means obstacle’s height and “ H ” means the height of the channel. Bekele et al. used P/e while the investigated collector used S/H term. The “ S ” that indicates spacing of obstacles is the same with “ P ” that indicates longitudinal pitch (spacing). The comparison of Bekele et al.’s collector and collector being investigated (height of obstacle to channel’s height, $e/H = 0.6$ and spacing or longitudinal pitch, $P/e = 1$ and 3/2) is shown in Fig. 17.

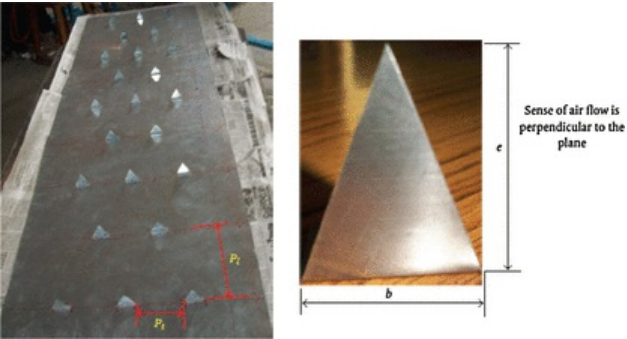


Fig. 16 Photographic view of plate with delta-shaped obstacles mounted.

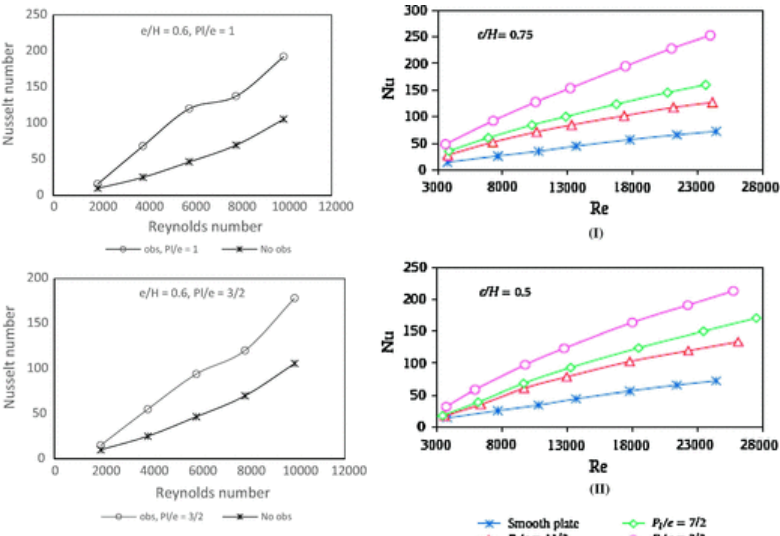


Fig. 17 Comparison of Nusselt number of Bekele et al.’s collector and investigated collector.

For smooth duct or no obstacle installed, the Nusselt number of investigated collector is higher than Bekele et al.’s. It is because the channel of investigated collector is triangular. This is consistent with the finding of Tao et al. (2007), Karim dan and Hawlader (2006), Choudhury dan and Garg (1991), Naphon (2007), Islamoglu dan and Parmaksizoglu (2003). Yet, the result of Bekele et al.’s and the investigated collector show the same trend, i.e. the smaller P/e gives higher Nusselt number. It means more obstacles increase heat transfer to the air. The relative obstacle height used in Bekele et al.’s collector was 0.5 and 0.75, while in the investigated collector was 0.6. The comparison of the results is shown in Fig. 18. When Reynolds number around 10,000 and ratio $P/e = 3/2$, Nusselt number of investigated collector was 178 for $e/H = 0.6$ and Nusselt number of Bekele et al. was 98 for $e/H = 0.5$ and 125 for $e/H = 0.75$. Like in collector without obstacle, the Nusselt number of investigated collector is also slightly higher than from Bekele et al. Yet, the result from this investigated collector is showing the same trend with the finding of Bekele et al.

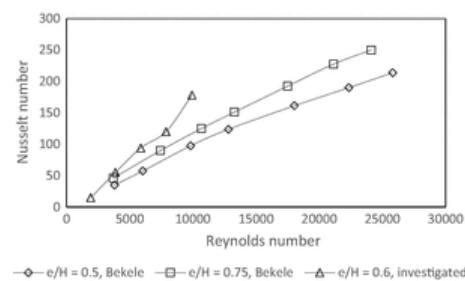


Fig. 18 Comparison of Nusselt number of Bekele et al.'s and investigated collector for $P/e = 3/2$.

6 Conclusion

From numerical studies in a v-corrugated duct, it is found that backflow between obstacles and high velocity in the gap between obstacles and absorber plate causes the flow became more turbulent and enhanced the convection heat transfer between the air and the absorber plate. Thus, when it is applied to SAH, it will improve its efficiency but increase the air pressure drop.

Obstacles placed in a small spacing will increase Nusselt number (convection heat transfer) and friction factor (pressure drop). The Nusselt number enhanced from 27.2 when no obstacle used to 94.2 when obstacles inserted with $S/H = 0.5$. The Nusselt enhanced 3.46 times. The friction factor will increase from 0.0316 at no obstacle to 0.628 at ratio $S/H = 0.5$. The friction factor increased 19.9 times.

Efficiency, Nusselt number, and friction factor are decreasing as ratio S/H is increasing. When ratio S/H used is 1 instead of 0.5, Nusselt number enhancement decreased only 1.13%, but friction factor decreased 15.1%. So, sacrificing a small amount of Nusselt number but reducing a significant friction factor is advantageous. The optimal spacing ratio S/H of delta-shaped obstacles inserted in a v-corrugated SAH is one. In other words, the optimal spacing of obstacle equals to its height.

Acknowledgements

Here, I am very grateful for the support from [Kopertis Wilayah VII Jawa Timur, Kementerian Pendidikan dan Kebudayaan](#) by providing Research Grant under contract No: [0004/SP2H/PP/K7/KL/II/2012](#).

References

Tao L., Wen X.L., Wen dan F.G. and Chan X.L., A Parametric study on the termal performance of a solar air collector with a V-groove absorber, *Int. J. Green Energy* **4**, 2007, 601–622.

Karim dan M.A. and Hawlader M.N.A., Performance investigation of flat plate, V-corrugated and finned air collector, *Energy* **31**, 2006, 452–470.

Choudhury dan C. and Garg H.P., Design analiysis of corrugated and flat plate solar air heaters, *Renew. Energy* **1** (5/6), 1991, 595–607.

Naphon P., Heat transfer characteristics and pressure drop in channel with V corrugated upper and lower plates, *Energy Convers. Manage.* **48**, 2007, 1516–1524.

Islamoglu dan Y. and Parmaksizoglu C., The effect of channel height on the enhanced heat transfer characteristics in a corrugated heat exchanger channel, *Appl. Therm. Eng.* **23**, 2003, 979–987.

Promvonge P., Heat transfer and pressure drop in a channel with multiple 60° V-baffles, *Int. Commun. Heat Mass Transfer* **37**, 2010, 835–840.

Kurtbas dan I. and Turgut E., Experimental investigation of solar air heater with free and fixed fins: efficiency and exergy loss, *Int. J. Sci. Technol.* **1** (1), 2006, 75–82.

Romdhane B.S., The air solar collectors: comparative study, introduction of baffles to favor the heat transfer, *Sol. Energy* **81**, 2007, 139–149.

Ho C.-D., Yeh dan H.-M. and Chen T.-C., Collector efficiency of upward-type double-pass solar air heaters with fins attached, *Int. Commun. Heat Mass Transfer* **38**, 2011, 49–56.

Abene A., Dubois V., Le Ray dan M. and Oagued A., Study of a solar air flat plate collector: use of obstacle and application for the drying of grape, *J. Food Eng.* **65**, 2004, 15–22.

Esen H., Experimental energy and exergy analysis of a double-flow solar air heater having different obstacles on absorber plates, *Build. Environ.* **43**, 2008, 1046–1054.

Ozgen F., Esen dan M. and Esen H., Experimental investigation of thermal performance of a double-flow solar air heater having aluminium cans, *Renew. Energy* **34**, 2009, 2391–2398.

Akpinar dan E.K. and Koçyiğit F., Experimental investigation of thermal performance of solar air heater having different obstacles on absorber plates, *Int. Commun. Heat Mass Transfer* **37**, 2010, 416–421.

Bekele A., Mishra dan M. and Dutta S., Effects of delta-shaped obstacles on the thermal performance of solar air heater, *Hindawi Publishing Corporation: Advances in Mechanical Engineering* **2011**, 2011, 10 pages.

Esen H., Ozgen F., Esen dan M. and Sengur A., Modelling of a new solar air heater through least-squares support vector machines, *Expert Syst. Appl.* **36**, 2009a, 10673–10682.

Esen H., Ozgen F., Esen dan M. and Sengur A., Artificial neural network and wavelet neural network approaches for modelling of a solar air heater, *Expert Syst. Appl.* **36**, 2009b, 11240–11248.

Handoyo E.A., Ichsan D. and Sutardi Prabowo dan, Experimental studies on a solar air heater having V-corrugated, *Appl. Mech. Mater.* **493**, 2014, 86–92.

Incropera dan F.P. and DeWitt D.P., Fundamentals of Heat and Mass Transfer, fifth ed., 2002, John Wiley & Sons; s.l..

ASHRAE, Method of Testing to Determine the Thermal Performance of Solar Collectors, 1986, ASHRAE; Atlanta.

I. FLUENT, Fluent User's Guide, 2003.

Zhangdan L. and Liu Z., A numerical simulation of the flow in a diffusing S-duct inlet, *Mod. Appl. Sci.* **3** (4), 2009, 111–116.

Kirkgoz M.S., Onerdan A.A. and Akoz M.S., Numerical modeling of interaction of a current with a circular cylinder near a rigid bed, *Adv. Eng. Softw.* **40**, 2009, 1191–1199.

Duffie dan J.A. and Beckman W.A., Solar Engineering of Thermal Processes, second ed., 1991, John Wiley & Sons Inc, penyunt.



Highlights

- v-corrugated absorber plate and obstacles improves heat transfer in SAH.
- How does the spacing between obstacles effect the convection heat transfer and pressure drop in air flow?
- The optimal spacing ratio of obstacles gives optimal Nusselt number (convection) and friction factor (pressure drop).

Queries and Answers

Query: Please check the edits made in article title, and correct if necessary.

Answer: Yes

Query: Your article is registered as a regular item and is being processed for inclusion in a regular issue of the journal. If this is NOT correct and your article belongs to a Special Issue/Collection please contact santhoshi.bs@elsevier.com immediately prior to returning your corrections.

Answer: Yes, it is correct.

Query: The author names have been tagged as given names and surnames (surnames are highlighted in teal color). Please confirm if they have been identified correctly.

Answer: Yes, they are correct.

Query: Please check whether the designated corresponding author is correct, and amend if necessary.

Answer: Yes

Query: Please note that the reference style has been changed from a Numbered style to a Name–Date style as per the journal specifications.

Answer: Yes

Numerical studies on the effect of delta-shaped obstacles' spacing on the heat transfer and pressure drop in v-corrugated channel of solar air heater

Ekadewi A. Handoyo^{a,*}, Djatmiko Ichsani^b, Prabowo^b, Sutardi^b

^a Mechanical Engineering Dept, Petra Christian University, Surabaya, Indonesia

^b Mechanical Engineering Dept, Institut Teknologi Sepuluh Nopember, Surabaya, Indonesia

Received 11 October 2015; received in revised form 9 February 2016; accepted 16 February 2016

Communicated by: Associate Editor Bibek Bandyopadhyay

Abstract

Solar air heater (SAH) is simple in construction compared to solar water heater. Yet, it is very useful for drying or space heating. Unfortunately, the convective heat transfer between the absorber plate and the air inside the solar air heater is rather low. Some researchers reported that obstacles are able to enhance the heat transfer in a flat plate solar air collector and others found that a v-corrugated absorber plate gives better heat transfer than a flat plate. Only a few research combines these two in a SAH. This paper will describe the combination from other point of view, i.e. the spacing between obstacles. Its spacing possibly will effect the heat transfer and pressure drop of the air flowing across the channel.

The first step in numerical study is generating mesh or grid of the air flow inside a v-corrugated channel which was blocked by some delta-shaped obstacles. The mesh was designed three-dimension and not uniform. The mesh are made finer for area near obstacles and walls both for upper and bottom, and then gradually coarser. Grid independency is the next step to be conducted. When the mesh is already independent, the numerical study begins. To validate the numerical model, an indoor experiment was conducted. Turbulent model used was Shear Stress Transport $K-\omega$ (SSTK- ω) standard. Having a valid numerical model, the spacing between obstacles was studied numerically. Ratio spacing to height, S/H of obstacles investigated were 0.5; 1; 1.5; and 2.

From numerical studies in a v-corrugated duct, it is found that backflow between obstacles and high velocity in the gap between obstacles and absorber plate causes the flow became more turbulent and enhanced the convection heat transfer between the air and the absorber plate. Obstacles placed in a small spacing will increase Nusselt number (convection heat transfer) and friction factor (pressure drop). The Nusselt number enhanced from 27.2 when no obstacle used to 94.2 when obstacles inserted with $S/H = 0.5$. The Nusselt enhanced 3.46 times. The friction factor will increase from 0.0316 at no obstacle to 0.628 at ratio $S/H = 0.5$. The friction factor increased 19.9 times. Efficiency, Nusselt number, and friction factor are decreasing as ratio S/H is increasing. When ratio S/H used is 1 instead of 0.5, Nusselt number enhancement decreased only 1.13%, but friction factor decreased 15.1%. So, sacrificing a small amount of Nusselt number but reducing a significant friction factor is advantageous. The optimal spacing ratio S/H of delta-shaped obstacles inserted in a v-corrugated SAH is one. In other words, the optimal spacing of obstacle equals to its height.

© 2016 Elsevier Ltd. All rights reserved.

Keywords: Delta-shaped obstacle; v-corrugated channel; Solar air heater; Numerical study

* Corresponding author.

E-mail address: ekadewi@petra.ac.id (E.A. Handoyo).

Nomenclature

W	wide of the obstacle (mm)	T_{abs}	absorber temperature (K)
H	height of the obstacle (mm)	D_h	hydraulic diameter (m)
S	spacing between the obstacles (mm)	Nu_D	Nusselt number
x, y, z	coordinates	h	convection heat transfer coefficient (W/m ² K)
Re	Reynolds number	f	friction factor
C_p	specific heat of air (J/kg K)	ν	air kinematic viscosity (m ² /s)
\dot{m}_f	mass flow rate of the fluid–air (kg/s)	ρ	air density (kg/m ³)
\dot{Q}_u	useful heat transfer rate (W)	k	thermal conductivity (W/m K)
I	radiation intensity (W/m ²)	α	air thermal diffusion coefficient (m ² /s)
A_c	collector aperture area (m ²)	η	thermal efficiency of SAH
T_o	collector outlet temperature (K)		
T_i	collector air inlet temperature (K)		

1. Introduction

Solar energy can be converted into thermal energy in a solar collector. Solar collector basically is device used to trap solar energy to heat a plate and transfer the heat to a fluid flowing under or above the plate. When sun light falls onto a plate, solar radiation reaches the plate at lower wavelength and heat it up. Then, the heat is carried away by either water or air that flows under or above the plate. Solar collector used to heat up air is called solar air heater (SAH) and solar water heater for water. Generally, the solar air heater is less efficient than the solar water heater, because air has less thermal capacity and less convection heat transfer coefficient. Yet, air is much lighter and less corrosive than water. The other benefit is that heated air can be used for moderate-temperature drying, such as harvested grains or fish. Since the solar air heater has less convective heat transfer coefficient than solar water heater, some researchers tried to increase this convective heat transfer coefficient.

A popular type of solar air heaters is the flat plate SAH, which has a cover glass on the top, insulation on the sides and bottom to prevent heat transferred to the surrounding, a flat absorber plate that makes a passage for the air flowing with sides and bottom plate. Usually, the passage or channel has a rectangular cross-section. The absorber plate will transfer the heat to the air via convection. Unfortunately, the convection coefficient is very low. To increase the convection coefficient from the absorber plate, a v-corrugated plate is used instead of a flat plate. Tao et al. (2007) stated that a solar air heater with a v-grooved absorber plate could reach efficiency 18% higher than the flat plate on the same operation condition and dimension or configuration. Karim dan and Hawlader (2006) found that a solar collector with a v-absorber plate gave the highest efficiency and the flat plate gave the least. The results showed that the v-corrugated collector is 10–15% and 5–11% more efficient in single pass and double pass modes, respectively, compared to the flat plate collectors.

Choudhury dan and Garg (1991) made a detailed analysis of corrugated and flat plate solar air heaters of five different configurations. For the same length, mass flow rate, and air velocity, it was found out that the corrugated and double cover glass collector gave the highest efficiency. According to Naphon (2007) the corrugated surfaces give a significant effect on the enhancement of heat transfer and pressure drop. The Nusselt number of flow in a v-corrugated channel can be 3.2–5.0 times higher than in a plane surfaces while the pressure drop 1.96 times higher than on the corresponding plane surface. Islamoglu dan and Parmaksizoglu (2003) reported that the corrugated channel gave the higher Nusselt number than the straight channel and the higher channel height gave higher Nusselt number for the flow with the same Reynolds number.

Besides changing the cross section area of the channel, some also give effort to increase turbulence inside the channel with fins or obstacles. The result of experimental study done by Promvong (2010) in turbulent flow regime (Reynolds number of 5000–25,000) showed that multiple 60° V-baffle turbulator fitted on a channel provides the drastic increase in Nusselt number, friction factor, and the thermal enhancement factor values over the smooth wall channel. Promvong found that Nusselt number was five times higher and friction factor was 30 times than without baffle at Reynolds number = 10000, $e/H = 0.3$, and $P_R = 1$. Kurtbas dan and Turgut (2006) investigated the effect of fins located on the absorber surface in free and fixed manners. They used two kinds of rectangular fins which dimension is different but total area is the same. The first type fin (I) has dimension 810 × 60 mm and the second (II) type 200 × 60 mm. To have the same total area, there are 8 fins and 32 fins for the first and second, respectively. The fins type II, both free and fixed, were more effective than type I and flat-plate collector. The fixed fin collector was more effective than free fin collector. Kurtbas and Turgut reported that the maximum Instantaneous efficiency of SAH was 0.78 at air mass flow rate 0.08 kg/s when the fix fins type II were used. While the efficiency of flat plate

SAH was only 0.42. So, its efficiency increased 1.86 times. Romdhane (2007) created turbulence in the air channel using obstacles or baffles. The efficiency of collector and the air temperature was found increasing with the use of baffles. Baffles should be used to guide the flow toward the absorber plate. Romdhane reported that the efficiency reached 80% for the best type of baffle (chicane) for an air flow rate of $50 \text{ m}^3/\text{h}/\text{m}^2$. This efficiency was about 1.6 times efficiency without baffle. Ho et al. (2011) inserted fins attached by baffles and external recycling to a solar air heater. The experiment and theoretical investigations gave result that heat transfer was improved by employing baffled double-pass with external recycling and fin attached over and under absorber plate. According to Ho et al., the highest collector efficiency was 61% in a double-pass flat-plate SAH with recycle when radiation intensity was $1100 \text{ W}/\text{m}^2$, 24 fins attached, and mass flow rate was $0.02 \text{ kg}/\text{s}$. It was about 1.35 times its efficiency when there is no recycle. Abene et al. (2004) used obstacles on the flat plate of a solar air collector for drying grape. The obstacles ensure a good air flow over the absorber plate, create the turbulence and reduce the dead zones in the collector. The highest efficiency got was 70% when the air flow rate was $50 \text{ m}^3/\text{h}/\text{m}^2$. It was about 1.9 times its efficiency when no obstacle used. The air pressure drop increased about twice with obstacles. Esen (2008) used a double-flow solar air heater to investigate three different type obstacles placed on absorber plates compare with the flat plate. The collector has three absorber plates to make three passages for the air flowing through. From the research done, it was found that all collectors with obstacles gave higher efficiency than the flat plate and type III obstacles with flow in middle passage gave the highest efficiency, i.e. 52.9%, for air flow $0.02 \text{ kg}/\text{s}$. It was about 1.13 times higher than its efficiency with no obstacle. Ozgen et al. (2009) used aluminum cans as obstacles installed over and under absorber plate. They found that the SAH using double flow passage (over and under absorber plate) gave higher efficiency than just one flow passage (either over or under absorber plate). They also found that SAH with staggered cans (type I) had the highest efficiency compared to aligned cans (type II) and flat plat (type III). The efficiency of SAH type I was 0.73 at air flow rate $0.05 \text{ kg}/\text{s}$ and it was about 1.4 times of type III. Akpınar dan and Koçyiğit (2010) had experimental investigation on solar air heater with several obstacles (Types I–III) and without obstacles. The optimal value of efficiency was obtained for the solar air heater with Type II obstacles on absorber plate in flow channel duct for all operating conditions and the collector with obstacles appears significantly better than that without obstacles. The efficiency of Type II was 0.6 at air flow rate $0.0052 \text{ kg}/\text{s}$ and it was about twice of SAH without obstacle. Bekele et al. (2011) investigated experimentally the effect of delta shaped obstacles mounted on the absorber surface of an air heater duct. They found that the obstacle mounted duct enhances the heat transfer to the air. The

heat transfer got higher if the obstacle height was taller and its longitudinal pitch was smaller. Nusselt number increased 3.5 times when obstacles inserted with ratio of longitudinal pitch $P_l/e = 3/2$ and height $e/H = 0.75$ at Reynolds number was 10,000. While its friction factor increased 4.7 times than without obstacle. SAH can be modeled through least-squares support vector machines (LS-SVM) method as done by Esen et al. (2009a). The predicted results from LS-SVM model had been compared to experimental results. LS-SVM could be used to predict the efficiency of SAH. They showed that efficiency of type I SAH was the highest. Esen et al. (2009b) also proposed Artificial Neural Network and Wavelet Neural Network (ANN and WNN) to predict the efficiency of SAH. They succeeded to show that the method could predict the SAH efficiency.

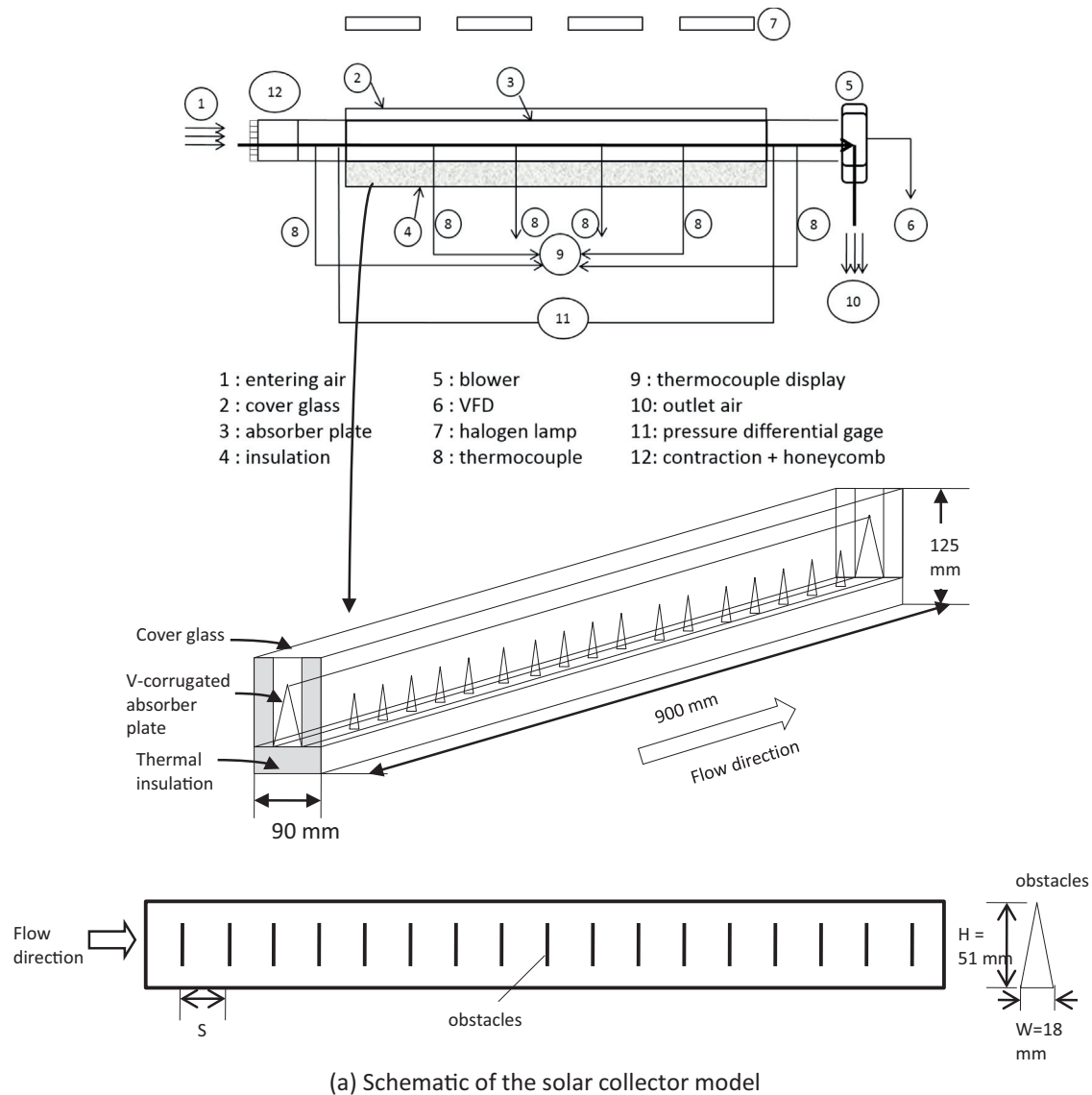
The combine of those two findings, i.e. obstacles and v-corrugated absorber plate are able to improve SAH are important to be studied. Handoyo et al. (2014) reported that the obstacles are able to enhance heat transfer in a v-corrugated SAH but increase the air pressure drop. To reduce the air pressure drop, the obstacles were bent vertically. The optimal bending angle is 30° . The SAH's efficiency was 5.3% lower when the obstacles bent 30° instead of straight (0°), but the pressure drop was 17.2% lower.

According to Incropera dan and DeWitt (2002), in forced convection heat transfer, there are two quantities that are important to be determined. One is friction coefficient, C_f , and the other is Nusselt number, Nu. Friction coefficient, C_f is used to calculate the shear stress at the wall and then to calculate pressure drop. While Nusselt number, Nu is used to calculate convection heat transfer rate. The relation that correlate them is known as Reynolds Analogy: $C_{f,x} \frac{Re_L}{2} = Nu_x Pr^{-1/3}$

When Nusselt number increases, then friction coefficient will increase, too. In a SAH, it is expected that convection heat transfer increases but pressure drop does not. So, many research were conducted to look for increasing in heat transfer at low pressure drop.

The spacing between obstacles mounted on absorber plate can be varied. A different spacing will give different air pressure drop as the air flows across the collector. Obstacles increase the air pressure drop. When the spacing is large, the obstacles used is less and the air pressure drop will be reduced. What about the heat transfer from the absorber plate to the flowing air? How will the spacing between obstacles effect the heat transfer? To the knowledge of the authors, there is no research investigating the effect of delta-shaped obstacles' spacing on a v-corrugated SAH performance, yet.

This paper describes the result of the numerical studies of obstacles' spacing inserted in a v-corrugated channel of a SAH. The heat transfer from the v-corrugated absorber plate and the air pressure drop flowing the v-corrugated channel is to be discussed. The obstacles are delta-shaped and installed on bottom plate of the channel.



(a) Schematic of the solar collector model

(b) Photograph of experimental set-up.

Fig. 1. The SAH model used in experiment.

2. Experimental set-up

The studies began with choosing a solar collector model to be studied. The study will be conducted numerically. Thus, a validation is required to prove that the result is

true. The validation is accomplished via experiment. An indoor experiment model was constructed to validate numerical result. It is a model of SAH using v-corrugated absorber plate. Its schematic view and photograph are shown in Fig. 1(a) and (b), respectively. The experiment

was conducted in a laboratory of Mechanical Engineering Dept of Petra Christian University, Surabaya, Indonesia.

The collector model's dimension was 900 mm long, 90 mm width, and 125 mm height. A single 3-mm transparent-tempered glass was used as the collector cover. The v-corrugated absorber plate was made of 0.8-mm-thick aluminum and painted black. The apex angle of the v-corrugated plate was 20°. The v-corrugated channel's cross section was 30 mm width and 85 mm height. To prevent heat loss, the left and right walls of collector are insulated with a 25-mm Styrofoam each and a 35-mm Styrofoam for the bottom. The delta-shaped obstacles were made congruent to the channel i.e. triangular and its dimension was 18 mm wide, 51 mm height.

The experiment was conducted indoor to maintain the radiation intensity, wind's velocity and temperature. So, a bias result caused by different outdoor condition could be avoided. The sunlight is replaced with four 500-W halogen lamps. The radiation intensity received on the collector was measured using a pyranometer (Kipp & Zonen, type SP Lite2) placed on top of the cover glass. To ensure the homogenous intensity and to generate a certain absorber plate's temperature, these lamps were equipped with adjustable turner individually. The surrounding air condition was controlled by an air conditioner installed in the room. Its temperature, humidity, and wind velocity are well controlled. The collector was equipped with T-type thermocouple which accuracy is 0.1 °C for measuring the air temperature at inlet and outlet of the collector, temperature of the absorber plate (at four different locations), and ambient temperature. The pressure drop between inlet and outlet of the flowing air across the collector is also measured with a Magnehelic differential pressure gage which accuracy is ± 2 Pa. A centrifugal blower (1000 m³/h, 580 Pa, 0.2 kW, 380 V input) was used to induce the air flowing through the collector. The air flow was adjusted by means of a variable-frequency drive (VFD) to be 5.0 m/s (or Reynolds number = 10,000). The air flow is measured using digital anemometer which accuracy is ± 0.1 m/s. All of the measurement equipments such as pressure gages and thermocouples are installed according to ASHRAE requirement (ASHRAE, 1986).

3. Numerical set up

The discussion in this paper is on the heat transferred to the flowing air and its pressure drop, then the domain of numerical study is focused on the air flow inside the v-corrugated channel. The apex angle of the v-corrugated channel is 20°. Its dimension was 900 mm long, 30 mm width, and 85 mm height. The delta-shaped obstacles were made congruent to the channel i.e. triangular and its dimension was 18 mm wide, 51 mm height. The obstacles were installed in one line only, because there is no much space in the channel. Thus, the spacing to be discussed is also called longitudinal pitch. To specify the obstacles'

spacing, a ratio of spacing to height S/H is used. In this study, the ratio S/H used were \emptyset , 1, 1 \emptyset , and 2.

The numerical model for this problem was developed under some assumptions, i.e. as steady three-dimensional turbulent, incompressible flow and constant fluid properties. The space of obstacles was taken equal to height of obstacles, thus ratio is 1. Then, there are 17 obstacles used in this flow. Body force and viscous dissipation are ignored and it was assumed no radiation heat transfer. With these assumptions, (Incropera dan and DeWitt, 2002) give the related governing equations as follow:

$$\frac{\partial u}{\partial x} + \frac{\partial v}{\partial y} + \frac{\partial w}{\partial z} = 0 \quad (1)$$

$$u \frac{\partial u}{\partial x} + v \frac{\partial u}{\partial y} + w \frac{\partial u}{\partial z} = -\frac{1}{\rho} \frac{\partial P}{\partial x} + \nu \left(\frac{\partial^2 u}{\partial x^2} + \frac{\partial^2 u}{\partial y^2} + \frac{\partial^2 u}{\partial z^2} \right) \quad (2)$$

$$u \frac{\partial v}{\partial x} + v \frac{\partial v}{\partial y} + w \frac{\partial v}{\partial z} = -\frac{1}{\rho} \frac{\partial P}{\partial y} + \nu \left(\frac{\partial^2 v}{\partial x^2} + \frac{\partial^2 v}{\partial y^2} + \frac{\partial^2 v}{\partial z^2} \right) \quad (3)$$

$$u \frac{\partial w}{\partial x} + v \frac{\partial w}{\partial y} + w \frac{\partial w}{\partial z} = -\frac{1}{\rho} \frac{\partial P}{\partial z} + \nu \left(\frac{\partial^2 w}{\partial x^2} + \frac{\partial^2 w}{\partial y^2} + \frac{\partial^2 w}{\partial z^2} \right) \quad (4)$$

$$u \frac{\partial T}{\partial x} + v \frac{\partial T}{\partial y} + w \frac{\partial T}{\partial z} = \alpha \left(\frac{\partial^2 T}{\partial x^2} + \frac{\partial^2 T}{\partial y^2} + \frac{\partial^2 T}{\partial z^2} \right) \quad (5)$$

In the above equations, ρ is the density of the air, p is the pressure, ν is the kinematic viscosity, α is the thermal diffusivity, and T is the temperature of the fluid. The boundary conditions of this problem were:

At the inlet: $u = 5.0$ m/s, $v = w = 0$, $T = 297.46$ K

At the upper wall which is the absorber plate:
 $u = v = w = 0$

At the bottom wall: $u = v = w = 0$

On the 17 obstacles: $u = v = w = 0$

Inlet Reynolds number was calculated with : Re

$$= \frac{uD_h}{\nu} \quad (6)$$

In Eq. (6), D_h is hydraulic diameter and calculated with:

$$D_h = \frac{4A}{P} \quad (7)$$

The area, A , in Eq. (7) is the channel cross section area, and P , is its perimeter.

The governing equations above with the boundary conditions were solved using a commercial CFD package, FLUENT 6.3.26 (FLUENT, 2003). The grids of the domain were generated using Gambit 2.4.6. The domain and meshing used in this numerical study were shown in Fig. 2. Since the geometry is a triangular channel, the numerical study should be conducted in three dimensions and all of the meshes were designed to have quality less than 0.7.

After having a good mesh, the next step is doing grid independency. The grid or mesh is made smaller to get more accurate and detailed result. But, when the mesh is

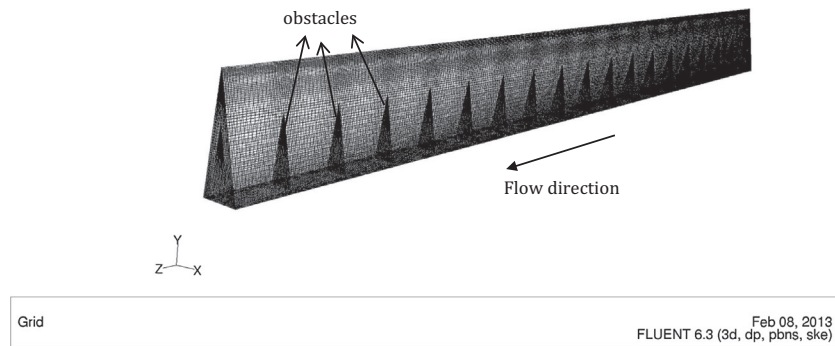


Fig. 2. The grid used in numerical studies.

too small, calculation which is done by iteration needs a very long time and might end up with diverge result. Therefore, in this study the mesh or grids were designed not uniform. The finer mesh are used for area near walls both for upper and bottom walls and then gradually the mesh are made coarser as shown in Fig. 2. When there are obstacles in the flow, the mesh are designed to be finer not only near the walls but also around the obstacles in Fig. 2. There are four meshes designs to be checked for independency as shown in Fig. 3(a)–(d). The number of cells, faces, and nodes used in each design are shown in Table 1.

To check the grid independency, the result from numerical study will be compared to experiment result. The same boundary conditions and setting are used in each numerical study of the four grids design as in Fig. 3. The boundary conditions are: inlet air velocity = 5.0 m/s and outflow was employed for the outlet; inlet air temperature = 297.46 K; and absorber plate temperature as obtained during experiments = 320 K. The settings in software used are: three dimension, double precision. Shear Stress Transport $K-\omega$ (SSTK- ω) standard turbulent model was chosen to simulate the flow. Zhang and Liu conducted a numerical simulation of the flow inside a diffusing S-duct inlet. Full three-dimensional Navier–Stokes equations are solved and SST turbulence model is employed. Numerical results, include surface static pressure, total pressure recovery at exit, are compared with experiment. A fairly good agreement is apparent (Zhangdan and Liu, 2009). Other researcher, Kirkgoz et al. reported that numerical modeling using $K-\omega$ and SSTK- ω used on the cylinder surface gave reasonably success result (Kirkgoz et al., 2009). The SIM-PLEC algorithm was employed to deal with the problem of velocity and pressure coupling. Second-order upwind scheme were used to discretize the main governing equations. Material of the absorber, bottom plate and the obstacles is aluminum. Fluid was air with inlet pressure 1 atm and its properties, such as density, viscosity, thermal conductivity were function of temperature.

Numerical studies were conducted for each of the four Mesh: A, B, C, and D. Fig. 4 shows global properties resulted from the numerical studies. They were the inlet and outlet temperature of air flowing through the channel and its pressure drop. Only Mesh B could not converge and

the residual could not meet the criteria. So, there was no result of Mesh B in Fig. 4.

The experiment result which will be discussed in Section 4 gives pressure drop as much as 397.7 Pa, air temperature outlet 40.7 °C when the air inlet velocity is 5.0 m/s and inlet air temperature 24.5 °C.

Fig. 4 shows that numerical study with Mesh C and D give better result of air temperature compare to experiment than Mesh A, but Mesh D gives too high pressure drop result. Numerical studies using Mesh C give the most closely result to experiments. Thus, Mesh C was chosen for the numerical studies.

Using Mesh C pattern, some numerical studies were conducted to know the effect of obstacles' spacing. The ratio of spacing to height, S/H , studied numerically were \emptyset , 1, 1 \emptyset , and 2. The Mesh used in this study are in Fig. 5a–d. When the ratio S/H is bigger, then the number of obstacle is less. Number of obstacles are 8, 11, 17, and 35 for ratio $S/H = 2, 1 \emptyset, 1$, and \emptyset , respectively.

To give more comprehensive result, numerical study was also conducted for air flow in a v-corrugated channel without obstacle. The domain and mesh used is shown in Fig. 6.

4. Results and discussion

Since the experiment is conducted to validate the numerical result, then it is not necessary to conduct experiments for all ratio S/H . The ratio S/H used in experiment equals to 1. Thus, there are 17 obstacles inserted and the percentage of air flow blockage in the channel is 36%. The experiment followed the numerical setting. The experiments were conducted at certain inlet air velocity and certain radiation intensity or absorber temperature. A VFD was used to get an inlet air velocity equals to 5.0 m/s. An adjustable turner was used to adjust the radiation intensity that make the absorber's temperature as high as 320 K or 47 °C.

When the numerical result is close to the experimental result, then the numerical result is valid. Table 2 shows the comparison between numerical and experimental results at 5.0-m/s-inlet air velocity and 320 K absorber temperature. The air temperature difference and pressure drop

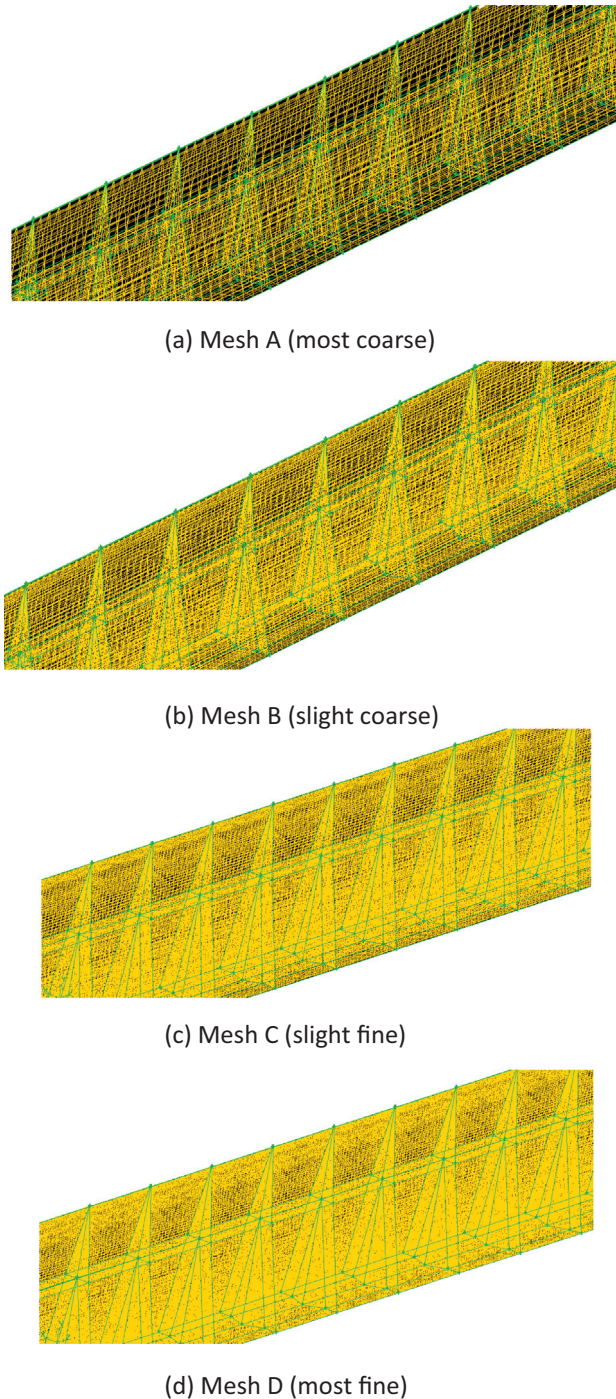
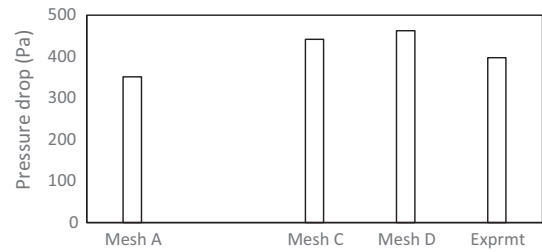


Fig. 3. Mesh design checked for independency.

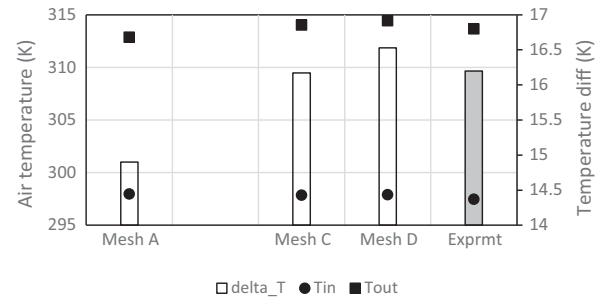
Table 1
Number of cells, faces, and nodes of the four mesh design.

	Mesh A	Mesh B	Mesh C	Mesh D
Cell	55,296	338,688	1,092,000	1,980,000
Face	173,936	1,043,224	3,335,300	6,026,900
Node	63,172	365,480	1,150,798	2,066,248

of numeric is very close to experiment. Thus, the numerical study using several setting discussed above is acceptable and valid.



(a) The air pressure drop from numerical studies compared to experiment



(b) The air temperature from numerical studies compared to experiment

Fig. 4. The numerical studies of Mesh A, C, and D compared to the result of experiment for $S/H = 1$.

To ensure that the model used in numerical study is valid, a comparison between Nusselt number from numerical result and Gnielinski equation for triangular channel without obstacle or smooth duct was conducted. According to Incropera dan and DeWitt (2002), Gnielinski gives more accurate relation to calculate Nusselt number at lower Reynolds number than Dittus–Boelter equation. The relation of Nusselt number is in Eq. (8):

$$Nu_D = \frac{(f/8)(Re_D - 1000)Pr}{1 + 12.7(f/8)^{1/2}(Pr^{2/3} - 1)} \quad (8)$$

The friction factor in Eq. (8), f , is obtained from Moody diagram. The comparison in Fig. 7 shows that numerical simulation gives pretty accurate results.

Having a valid grids, setting, and viscous model, the numerical study was continued to investigate the spacing effect of obstacles on the bottom plate of air duct. Diagrams of velocity vector of air flow around the obstacles inserted at ratio S/H equals to 2, 1, 0, 1, and 0 are shown in Fig. 8(a)–(d), respectively. All of the velocity vectors were taken at height $y = 10$ mm from the bottom plate. When the ratio $S/H = 2$, the spacing between obstacles = 100 mm. For ratio $S/H = 1$, the spacing = 75 mm, and for ratio $S/H = 0$, the spacing = 25 mm.

Fig. 8(a)–(d) shows how the air flow encounters separation when flow through obstacles. The obstacles cause backflow when flow through obstacles. There are more backflows when the obstacles' spacing are closer and they cause a higher pressure drop. The air velocity looks higher near absorber plate when

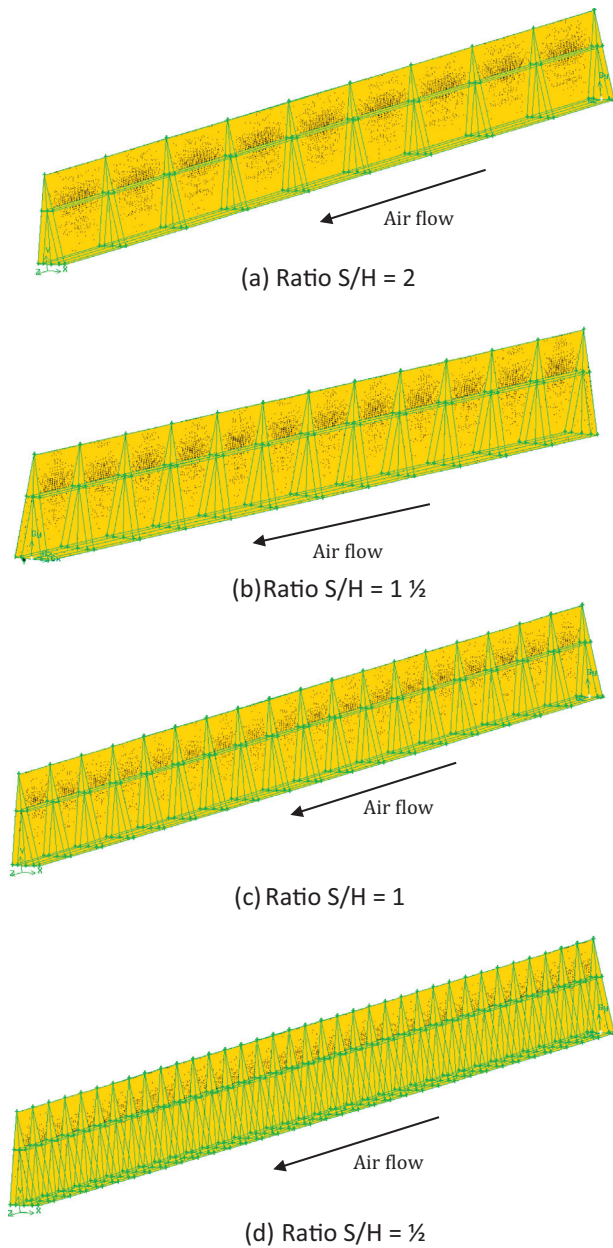


Fig. 5. The Mesh used for numerical studies of each spacing to height ratio, S/H .

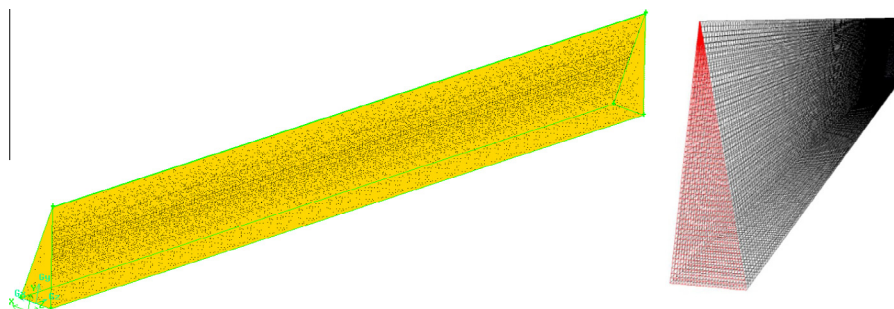


Fig. 6. The Mesh used for numerical studies of air flow without obstacle.

Table 2

Comparison between numerical and experimental results.

	Numeric	Experiment
T_{in} (K)	297.9	297.5
T_{out} (K)	314.4	313.7
ΔT (K)	16.5	16.2
ΔP (Pa)	462.3	450.3

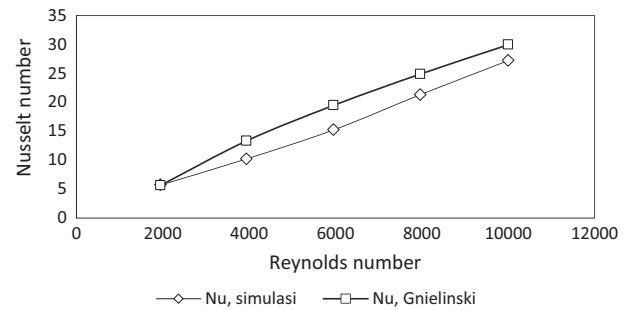
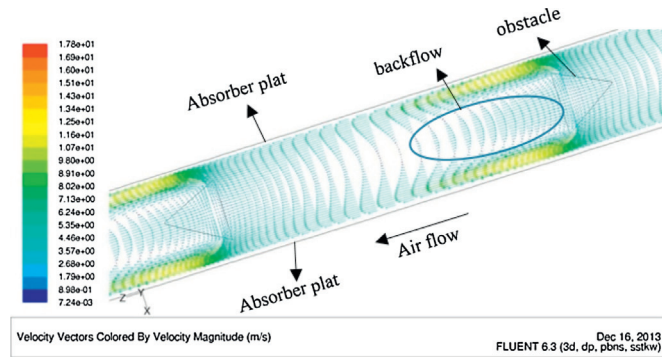
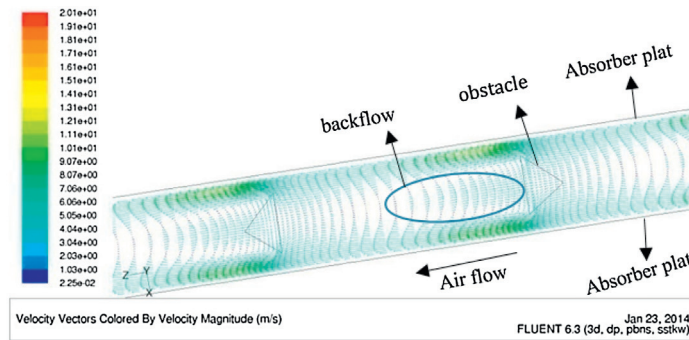
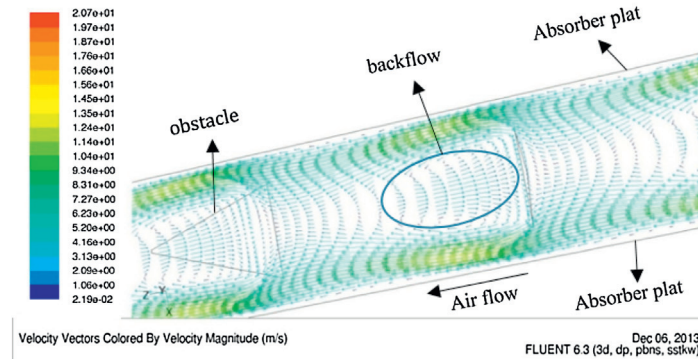
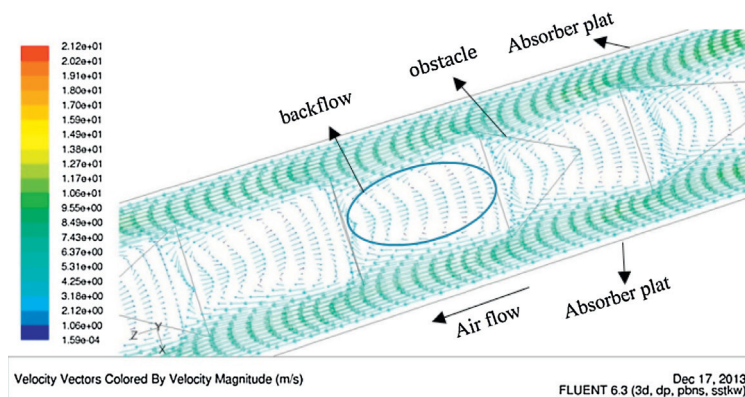


Fig. 7. Comparison of Nusselt number for smooth duct (no obstacle) from numerical study and Gnielinski equation.

there is backflow or swirl in the flow. This high air velocity makes flow become more turbulent and more heat transferred from the absorber plate to the air. This convection heat transfer to the air makes outlet air temperature higher. Thus, the closer the obstacles' spacing makes the higher pressure drop and higher convection heat transfer from the absorber plate to the air flow.

When the spacing between obstacles is twice its height (ratio $S/H = 2$), small amount of air flow is blocked by obstacles and causes backflow behind the obstacles. The backflow caused by separation gradually diminish between two obstacles in downstream as shown in Fig. 8(a). Since the air is blocked, most of air is forced to flow in the gap between obstacles and absorber plate. It is shown by longer and higher vector of velocity in the gap. More air is heated by absorber plate. Furthermore, higher velocity increases Reynolds number and make the flow more turbulent. More turbulent flow gives higher Nusselt number and definitely increase the convection heat transfer. Thus, obstacles makes outlet air temperature higher than without any

(a) Velocity vector of air flow around *obstacle* with ratio $S/H = 2$ (b) Velocity vector of air flow around *obstacle* with ratio $S/H = 1 \frac{1}{2}$ (c) Velocity vector of air flow around *obstacle* with ratio $S/H = 1$ (d) Velocity vector of air flow around *obstacle* with ratio $S/H = \frac{1}{2}$ Fig. 8. Velocity vector of air flow around *obstacle* with some ratio S/H .

(Handoyo et al., 2014). Flow in spacing between obstacles experiences backflow after hitting obstacles and then it reattaches quickly when the ratio $S/H = 2$. When the ratio S/H or spacing between obstacles is smaller, as shown in Fig. 8(b)–(d), backflow is more dominant than reattached flow in area between the obstacles. When backflow occurs, more air will flow in the gap and contact with absorber plate which is the heat source. It is the reason that smaller obstacles' spacing makes higher air outlet temperature and higher SAH's efficiency. The backflow in space between obstacles contributes pressure drop in the flow. More backflow causes higher pressure drop in air acrossed the v-corrugated absorber plate SAH.

Numerical studies also provide some global properties of the flow, such as the air inlet and outlet temperature, and pressure drop. These data were used to acquire the efficiency and friction factor of the air flow in a v-corrugated SAH with delta-shaped obstacles. The efficiency and friction factor are calculated using Eqs. (9) and (10) according to Duffie dan and Beckman (1991).

$$\eta = \frac{q_u}{A_c I} = \frac{\dot{m}_f c_p (T_{fo} - T_{fi})}{A_c I} \quad (9)$$

$$f = \frac{\Delta P}{\frac{L}{D_h} \rho \frac{v^2}{2}} \quad (10)$$

Comparison of efficiency and friction factor for some ratio S/H from numerical studies is shown in Fig. 9. Ratio $S/H = 0$ in Fig. 9 means no obstacle in the air flow. Obstacles arranged with ratio $S/H = \infty$ gives the highest air efficiency, i.e. 68% and also highest friction factor, i.e. 0.628 for air flowing in a v-corrugated duct, as shown in Fig. 9. For comparison, efficiency when no obstacle is only 49% and friction factor is only 0.0316. This findings are matching with the flow structure discussed above. The obstacles block the air flow and force it to have more contact with absorber plate. Not only forcing the air to the absorber plate, obstacles also causing more backflow. More obstacles produce higher efficiency and higher friction factor. SAH requires high efficiency or high outlet air temperature, but low friction or pressure drop. Increasing friction factor means increasing pumping power required in SAH.

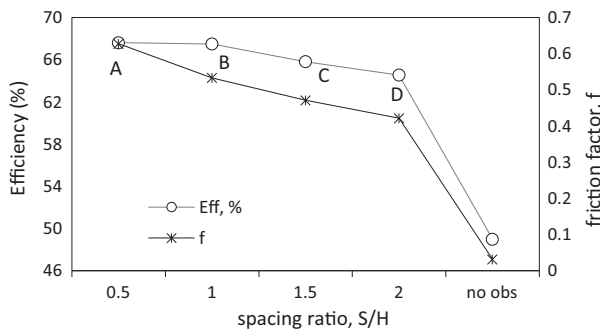


Fig. 9. The efficiency of SAH and friction factor of flow with some ratio S/H of obstacles.

Besides efficiency, Nusselt number is interesting to be analyzed. It could be calculated using Eq. (11).

$$h = \frac{Nu_D k}{D_h} \quad (11)$$

While the convection heat transfer rate and log-mean temperature difference could be calculated using Eqs. (12) and (13).

$$q = h A \Delta T_{lm} \quad (12)$$

$$\Delta T_{lm} = \frac{(T_{abs} - T_o) - (T_{abs} - T_i)}{\ln \left(\frac{T_{abs} - T_o}{T_{abs} - T_i} \right)} \quad (13)$$

The ratio S/H of obstacles effect the Nusselt number of air flow as shown in Fig. 10. Nusselt number of air flow with obstacles are much higher than without obstacle. The highest Nu number and friction factor are 94.2 and 0.628 at ratio $S/H = 0.5$ and is only 27.2 and 0.0316 at no obstacle. Fig. 11 shows the enhancement of Nusselt number when obstacles inserted in the flow compare to air flow with no obstacle. Nusselt number enhancement was the Nusselt number with obstacles compare to Nusselt number without obstacle. When obstacles inserted with ratio $S/H = 0.5$, Nusselt number increases 3.46 times and friction factor increases 19.9 times compare to those without obstacle.

Figs. 9–11 showed the same trend of SAH's efficiency, Nusselt number, and its enhancement. From efficiency and Nusselt number perspective, point A is the best, but from friction factor perspective, point D is the best. The gradient of friction factor in segment A–B is the sharpest among other segments. While the gradient of efficiency and Nusselt number enhancement in segment A–B is the least. The efficiency and Nusselt number in point B is only slightly less than point A. The Nu enhancement in point A is 3.46 and reduce to be 3.42 in point B. Thus, the reduction is only 1.13%. While the reduction of friction factor from point A to point B is 15.1% that is from 19.9 to 16.9. Sacrifice a little efficiency or Nusselt number (convection heat transfer) but save a lot friction factor (pressure drop) shall be a wise choice. So, the optimal spacing ratio, S/H of delta-shaped obstacles attached to a v-corrugated SAH is one. Since the thermal efficiency, Nusselt number, and friction factor are non-dimensional parameters, the result

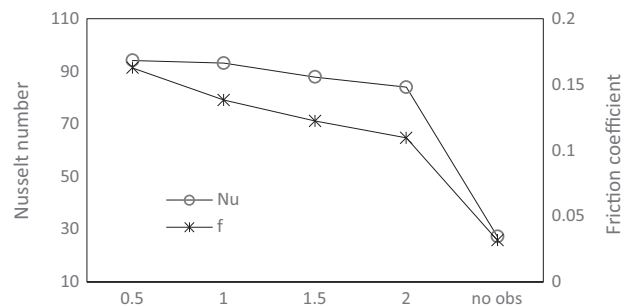


Fig. 10. Nusselt number and friction factor of air flow with obstacles inserted at some spacing ratio S/H .

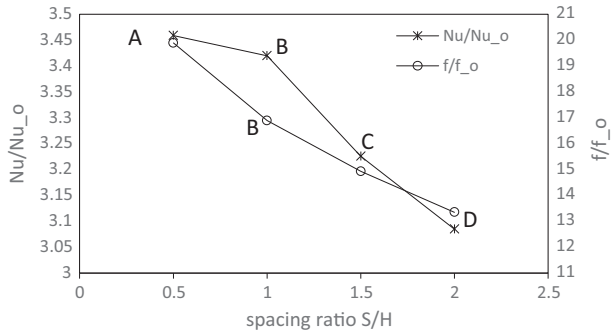


Fig. 11. Enhancement Nusselt number and increasing friction factor for some spacing ratio S/H .

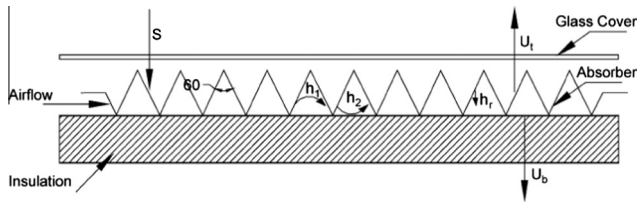


Fig. 12. A v-corrugated solar collector used by Karim & Hawlader.

could be applied to other SAH that has different geometry dimension but the same configuration.

5. Comparison to others' research

Karim dan and Hawlader (2006) worked on a flat plate solar collector with and without fin and v-corrugated absorber plate solar collector which schema is shown in Fig. 12. Dimension of the collector used is $1.8 \text{ m} \times 0.7 \text{ m}$.

The air flow rate generated by the blower in experiment of this paper that is nearest to Karim & Hawlader's SAH is $0.01164 \text{ kg/m}^2 \text{ s}$. The comparison of the efficiency of two collectors is shown in Fig. 13.

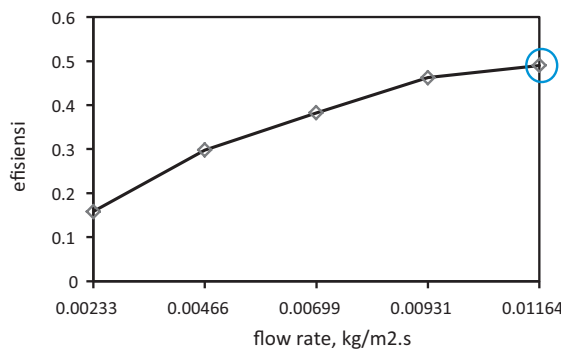
The efficiency of SAH investigated is 0.49 and of Karim & Hawlader is 0.4, as in Fig. 13. There is a slight difference because the air flow rate is not exactly the same. Therefore, the finding in this paper is look alike with Karim & Haw-

lader's finding for v-corrugated absorber plate solar collector.

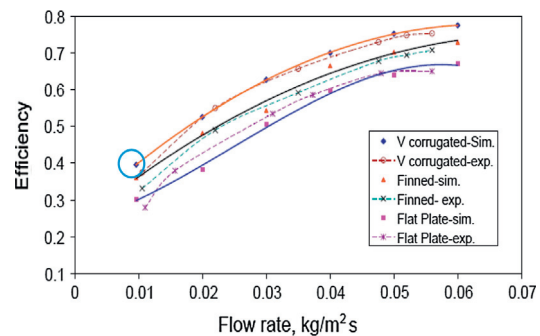
Akpinar dan and Koçyiğit (2010) conducted research on flat plate solar collector with two air mass flow rates, i.e. 0.0074 kg/s and 0.0052 kg/s . There were four collectors used as shown in Fig. 14. Three collectors were given obstacles on absorber flat plate. The comparison of Akpinar & Koçyiğit's collector (type II) to investigated collector is shown in Fig. 15. The efficiency of investigated collector is for air mass flow rate 0.00729 kg/s . Parameter $(T_o - T_a)/I$ of the investigated collector is slightly lower, because the air temperature across the investigated collector is lower than Akpinar & Koçyiğit collector. It is because the dimension of investigated collector is smaller than Akpinar & Koçyiğit's. The area of investigated collector was only $900 \text{ mm} \times 87 \text{ mm}$ compared to Akpinar & Koçyiğit's that was $1.2 \text{ m} \times 0.7 \text{ m}$. Yet, the difference shown in Fig. 15 is not too big. It seems a good conformity between the investigated collector and Akpinar & Koçyiğit's.

Bekele et al. (2011) conducted experimental investigation on flat plate SAH with delta-shaped obstacles mounted on the absorber surface as shown in Fig. 16. Some parameter to be investigated by Bekele et al. were Reynolds number (from 3400 to 27,600), longitudinal pitch of the obstacles P_l/e (from $3/2$ to $11/2$), and relative obstacle height, e/H (from 0.25 to 0.75). The smaller P_l/e and the higher e/H , the efficiency is higher. The term "e" used by Bekele et al., means obstacle's height and "H" means the height of the channel. Bekele et al. used P_l/e while the investigated collector used S/H term. The "S" that indicates spacing of obstacles is the same with " P_l " that indicates longitudinal pitch (spacing). The comparison of Bekele et al.'s collector and collector being investigated (height of obstacle to channel's height, $e/H = 0.6$ and spacing or longitudinal pitch, $P_l/e = 1$ and $3/2$) is shown in Fig. 17.

For smooth duct or no obstacle installed, the Nusselt number of investigated collector is higher than Bekele et al.'s. It is because the channel of investigated collector is triangular. This is consistent with the finding of Tao et al. (2007), Karim dan and Hawlader (2006),



(a) Collector investigated



(b) Karim & Hawlader's collector

Fig. 13. Comparison of the efficiency of collector investigated to Karim & Hawlader's.

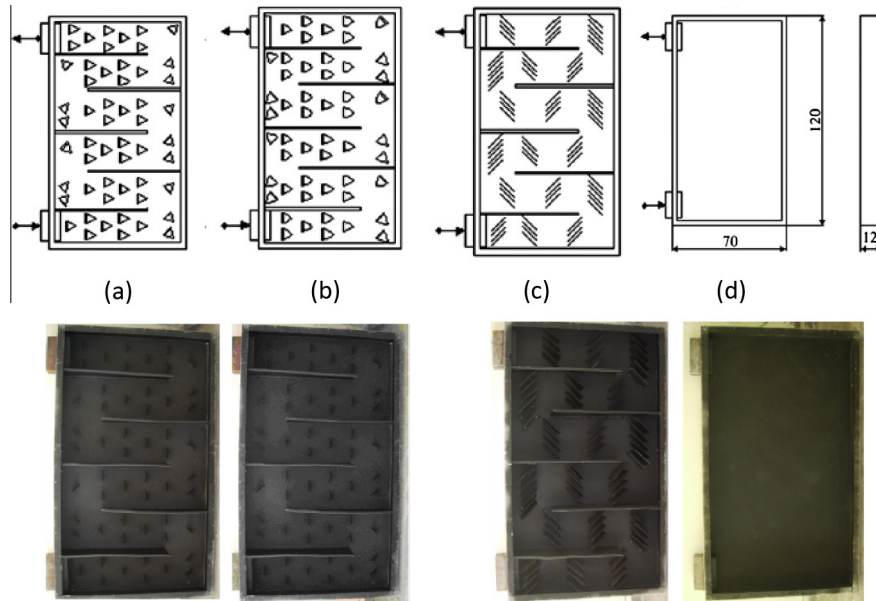


Fig. 14. Schematic views of absorber plates: (a) with triangular type obstacles, (b) with leaf type obstacles, (c) with rectangular type obstacles, and (d) without obstacles (Akpınar dan and Koçyiğit, 2010).

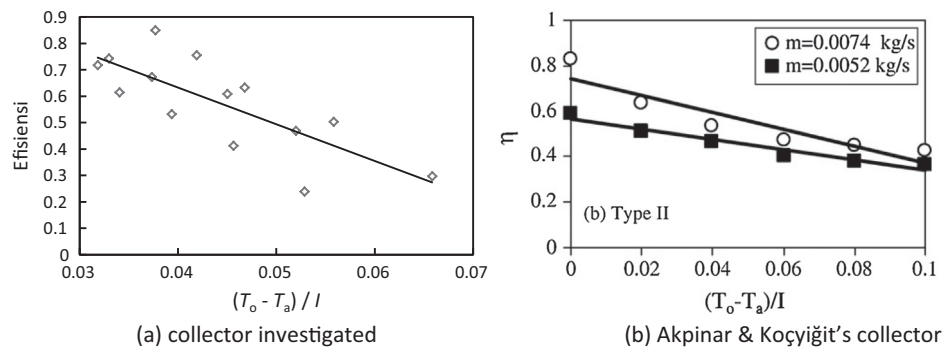


Fig. 15. Comparison of efficiency of Akpınar & Koçyiğit's collector and investigated collector.

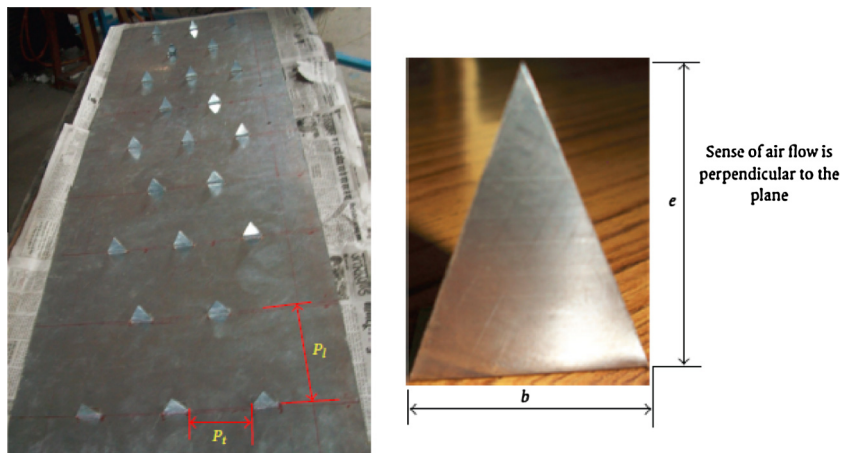


Fig. 16. Photographic view of plate with delta-shaped obstacles mounted.

Choudhury dan and Garg (1991), Naphon (2007), Islamoglu dan and Parmaksizoglu (2003). Yet, the result of Bekele et al.'s and the investigated collector show the

same trend, i.e. the smaller P_l/e gives higher Nusselt number. It means more obstacles increase heat transfer to the air. The relative obstacle height used in Bekele et al.'s

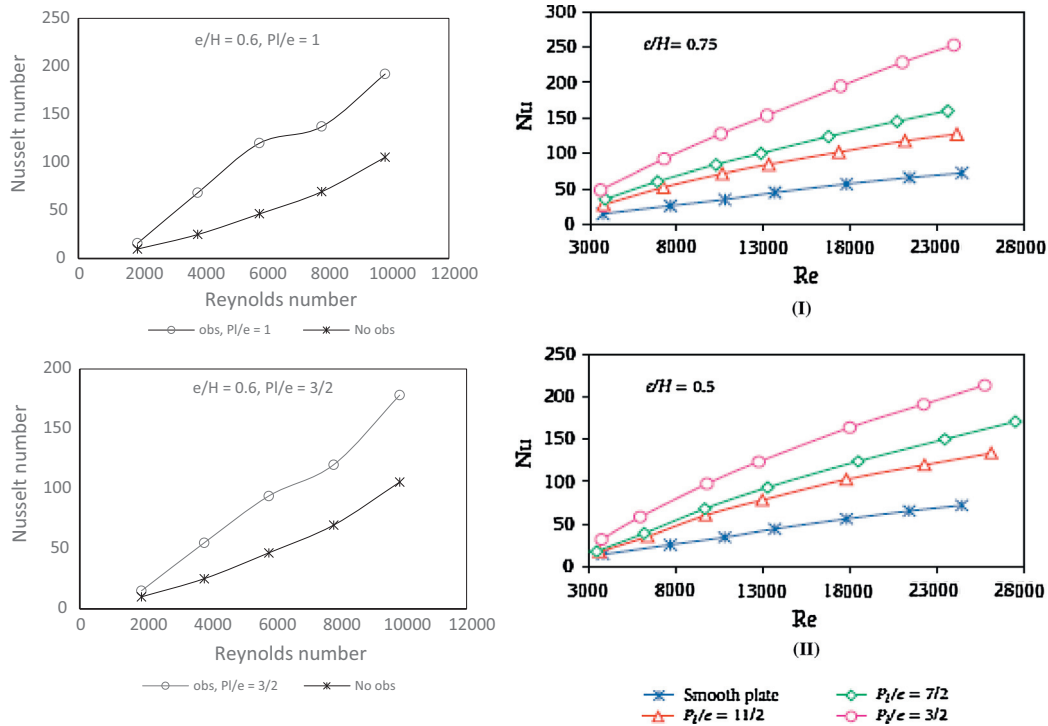


Fig. 17. Comparison of Nusselt number of Bekele et al.'s collector and investigated collector.

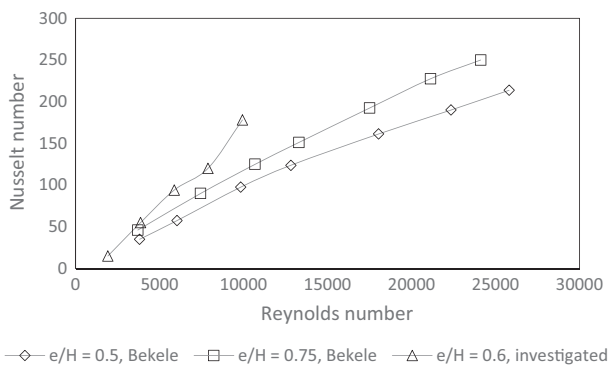


Fig. 18. Comparison of Nusselt number of Bekele et al.'s and investigated collector for $P_l/e = 3/2$.

collector was 0.5 and 0.75, while in the investigated collector was 0.6. The comparison of the results is shown in Fig. 18. When Reynolds number around 10,000 and ratio $P_l/e = 3/2$, Nusselt number of investigated collector was 178 for $e/H = 0.6$ and Nusselt number of Bekele et al. was 98 for $e/H = 0.5$ and 125 for $e/H = 0.75$. Like in collector without obstacle, the Nusselt number of investigated collector is also slightly higher than from Bekele et al. Yet, the result from this investigated collector is showing the same trend with the finding of Bekele et al.

6. Conclusion

From numerical studies in a v-corrugated duct, it is found that backflow between obstacles and high velocity

in the gap between obstacles and absorber plate causes the flow became more turbulent and enhanced the convection heat transfer between the air and the absorber plate. Thus, when it is applied to SAH, it will improve its efficiency but increase the air pressure drop.

Obstacles placed in a small spacing will increase Nusselt number (convection heat transfer) and friction factor (pressure drop). The Nusselt number enhanced from 27.2 when no obstacle used to 94.2 when obstacles inserted with $S/H = 0.5$. The Nusselt enhanced 3.46 times. The friction factor will increase from 0.0316 at no obstacle to 0.628 at ratio $S/H = 0.5$. The friction factor increased 19.9 times.

Efficiency, Nusselt number, and friction factor are decreasing as ratio S/H is increasing. When ratio S/H used is 1 instead of 0.5, Nusselt number enhancement decreased only 1.13%, but friction factor decreased 15.1%. So, sacrificing a small amount of Nusselt number but reducing a significant friction factor is advantageous. The optimal spacing ratio S/H of delta-shaped obstacles inserted in a v-corrugated SAH is one. In other words, the optimal spacing of obstacle equals to its height.

Acknowledgements

Here, I am very grateful for the support from Kopertis Wilayah VII Jawa Timur, Kementerian Pendidikan dan Kebudayaan by providing Research Grant under contract No: 0004/SP2H/PP/K7/KL/II/2012.

References

- Tao, L., Wen, X.L., Wen dan, F.G., Chan, X.L., 2007. A Parametric study on the thermal performance of a solar air collector with a V-groove absorber. *Int. J. Green Energy* 4, 601–622.
- Karim dan, M.A., Hawlader, M.N.A., 2006. Performance investigation of flat plate, V-corrugated and finned air collector. *Energy* 31, 452–470.
- Choudhury dan, C., Garg, H.P., 1991. Design analysis of corrugated and flat plate solar air heaters. *Renew. Energy* 1 (5/6), 595–607.
- Naphon, P., 2007. Heat transfer characteristics and pressure drop in channel with V corrugated upper and lower plates. *Energy Convers. Manage.* 48, 1516–1524.
- Islamoglu dan, Y., Parmaksizoglu, C., 2003. The effect of channel height on the enhanced heat transfer characteristics in a corrugated heat exchanger channel. *Appl. Therm. Eng.* 23, 979–987.
- Promvonge, P., 2010. Heat transfer and pressure drop in a channel with multiple 60° V-baffles. *Int. Commun. Heat Mass Transfer* 37, 835–840.
- Kurtbas dan, I., Turgut, E., 2006. Experimental investigation of solar air heater with free and fixed fins: efficiency and exergy loss. *Int. J. Sci. Technol.* 1 (1), 75–82.
- Romdhane, B.S., 2007. The air solar collectors: comparative study, introduction of baffles to favor the heat transfer. *Sol. Energy* 81, 139–149.
- Ho, C.-D., Yeh dan, H.-M., Chen, T.-C., 2011. Collector efficiency of upward-type double-pass solar air heaters with fins attached. *Int. Commun. Heat Mass Transfer* 38, 49–56.
- Abene, A., Dubois, V., Le Ray dan, M., Oagued, A., 2004. Study of a solar air flat plate collector: use of obstacle and application for the drying of grape. *J. Food Eng.* 65, 15–22.
- Esen, H., 2008. Experimental energy and exergy analysis of a double-flow solar air heater having different obstacles on absorber plates. *Build. Environ.* 43, 1046–1054.
- Ozgen, F., Esen dan, M., Esen, H., 2009. Experimental investigation of thermal performance of a double-flow solar air heater having aluminium cans. *Renew. Energy* 34, 2391–2398.
- Akpınar dan, E.K., Koçyiğit, F., 2010. Experimental investigation of thermal performance of solar air heater having different obstacles on absorber plates. *Int. Commun. Heat Mass Transfer* 37, 416–421.
- Bekele, A., Mishra dan, M., Dutta, S., 2011. Effects of delta-shaped obstacles on the thermal performance of solar air heater. Hindawi Publishing Corporation: *Advances in Mechanical Engineering* 2011, 10 pages.
- Esen, H., Ozgen, F., Esen dan, M., Sengur, A., 2009a. Modelling of a new solar air heater through least-squares support vector machines. *Expert Syst. Appl.* 36, 10673–10682.
- Esen, H., Ozgen, F., Esen dan, M., Sengur, A., 2009b. Artificial neural network and wavelet neural network approaches for modelling of a solar air heater. *Expert Syst. Appl.* 36, 11240–11248.
- Handoyo, E.A., Ichsani, D., Sutardi, Prabowo dan, 2014. Experimental studies on a solar air heater having V-corrugated. *Appl. Mech. Mater.* 493, 86–92.
- Incropera dan, F.P., DeWitt, D.P., 2002. *Fundamentals of Heat and Mass Transfer*, fifth ed. John Wiley & Sons, s.l..
- ASHRAE, 1986. *Method of Testing to Determine the Thermal Performance of Solar Collectors*. ASHRAE, Atlanta.
- I. FLUENT, *Fluent User's Guide*, 2003.
- Zhangdan, L., Liu, Z., 2009. A numerical simulation of the flow in a diffusing S-duct inlet. *Mod. Appl. Sci.* 3 (4), 111–116.
- Kirkgoz, M.S., Onerdan, A.A., Aköz, M.S., 2009. Numerical modeling of interaction of a current with a circular cylinder near a rigid bed. *Adv. Eng. Softw.* 40, 1191–1199.
- Duffie dan, J.A., Beckman, W.A., 1991. *Solar Engineering of Thermal Processes*, second ed. John Wiley & Sons Inc, penyunt.